AEROJET
GENERAL TIRE
GENERAL

REPORT NO. RN-S-0290

FINAL REPORT
GTR-16 RADIATION EFFECTS TEST ON STRUCTURAL MATERIALS AT -423°F

NERVA PROGRAM

CONTRACT SNP-1

ROCKET ENGINE OPERATIONS – NUCLEAR

NOVEMBER 1966

CLASSIFICATION CATEGORY

UNCLASSIFIED

W. Welff — CLASSIFYING OFFICER

12-6-1966 — DATE

AEROJET-GENERAL CORPORATION
A SUBSIDIARY OF THE GENERAL TIRE & RUBBER COMPANY

REPORT NO. RN-S-0290

FINAL REPORT
GTR-16 RADIATION EFFECTS TEST ON STRUCTURAL MATERIALS AT -423°F

W. Weleff
C. Dixon
J. Bauer
P. Dessau
R. Matt

C. M. Rice
Program Manager
Rocket Engine Operations - Nuclear

ABSTRACT

This report summarizes the results of the second radiation test on structural materials conducted for the NERVA Program under Contract SNP 1. The report contains the following detailed data pertaining to structural materials; ultimate and yield tensile strength, reduction of area, elongation, stress-strain curves, notched tensile strength, notched-to-unnotched strength ratio, and shear strength.

The report includes micrographs of representative specimens of each material in strained and unstrained region, as well as X-ray diffraction and electron fractographs.

Radiation effects were evaluated by comparing the mechanical and metalurgical properties with and without radiation.

All materials used were alloys and were irradiated and tested at liquid hydrogen environment without warm up. The average dose level obtained was 5×10^{16} nvt ($E > 1.0$ Mev).

The report also contains detailed control and irradiated data for three types of bearing retainers. These retainers were made of Armalon containing FEP Teflon, or TFE Teflon. The irradiated specimens received a maximum integrated fast neutron exposure of 6×10^{16} nvt ($E > 1.0$ Mev) and 1 x 10" ergs/gr(C) while immersed in LH_2. Both control and irradiated specimens were tested at room temperature.

TABLE OF CONTENTS

Table of Contents (cont.)

Table of Contents (cont.)

LIST OF TABLES

List of Tables (cont.)

LIST OF FIGURES

List of Figures (cont.)

List of Figures (cont.)

List of Figures (cont.)

PART 1

Radiation Effects Test on
STRUCTURAL MATERIALS

BLANK PAGE

I. INTRODUCTION

This report summarizes the results of the second irradiation effects test on structural materials. The test was designated as GTR-16 and was one in a series of tests being conducted by Aerojet-General Corporation in conjunction with the NERVA Program on materials submerged in liquid hydrogen while being irradiated. This summary report is submitted in partial fulfillment of the contractual objectives of Subtasks 1.9 and 2.8 on Contract SNP-1.

The purpose of the test was to investigate changes in mechanical properties of materials used in the various NERVA engine components under this unusual cryogenic and nuclear environment and to provide design allowables for this environment. Previous test results are reported in References 1, 2 and

Six individual tests were scheduled for the 400-hour radiation run: three were sponsored by Aerojet and three by WANL. The Aerojet sponsored tests, described in Reference 4, consisted of a tensile test on eleven alloys (37/A002), shear test on 10 alloys (37/A003) and thermal conductivity test on five alloys (37/A004). The latter test was cancelled during the pre-irradiation control test because of a malfunction of the test equipment. All Aerojet tests were performed at liquid hydrogen temperatures. The WANL-sponsored test, performed at liquid nitrogen temperature, consisted of metal and graphite tensile test, wire resistivity and spring test (37/W401), "O" ring seal test (15/W401) and unfueled segments with cemented orifices (37/W202). The results of the WANL test are reported independently.

Detailed data presented in this report on the irradiated materials includes ultimate and yield tensile strength, reduction of area, elongation, stress-strain curves and notched tensile and shear strength. Micrographs of representative specimens for each material in the strained and unstrained region, X-ray diffraction and electron microscopy are included for each type of material. The radiation effect is evaluated by comparing the mechanical and metallurgical properties of the materials before and after radiation. For comparison, the report includes the

BLANK PAGE

average values of these properties at room temperature and liquid hydrogen temperature, without radiation. Detailed data on control specimens are presented in Reference 2. Each material and each property is individually discussed. Test procedures and a description of the test specimens, test fixtures and test equipment are included.

II. SUMMARY

The test described in this report (and designated as GTR-16) was designed by Aerojet-General Corporation and conducted at the General Dynamics, Fort Worth Radiation Facilities. The objective of the test was to determine the effects of nuclear radiation at liquid hydrogen environment on the mechanical properties of several materials considered for structural application in the NERVA and other nuclear propulsion systems. The three access areas to the ground test reactor were utilized. Liquid hydrogen was used for the east and west pulling assemblies and liquid nitrogen for the north pallet. The north pallet, having the highest flux rate, was used by WANL (Run 37/W102) and the results are reported independently. The test consisted of two consecutive 200-hour radiation runs.

Tensile and shear tests were performed in accordance with the test specifications outlined in REON Report RN-S-0184. The third scheduled type of test (thermal conductivity) was cancelled since problems during the control run were encountered with the test equipment.

The following materials were tested:

Aluminum alloys: A-356-T6, 6061-T6, 7075-T6
Steels: 347SS, A-286, 440C, 410SS
Nickel Alloys: Hastelloy C, Inconel X-750, Inconel 713-C
Titanium Alloy: A-110AT -ELI

Data were obtained for ultimate and yield tensile strength, elongation, reduction of area, hardness, notched tensile and shear strength properties. Summaries of these data are presented in Tables 1, 2 and 3. Data acquisition systems performed satisfactorily including remotely-operated extensometers.

TABLE 1

COMPARISON OF TENSILE PROPERTIES: CONTROL VS IRRADIATED

Material	Ultimate Tensile Strength					Notched Strength					Notched/Unnotched Ratio			Shear Strength				
	Control	Irrad.	Variance	Damage %	Threshold	Control	Irrad.	Variance	Damage %	Threshold	Control	Irrad.	Damage %	Control	Irrad.	Variance	Damage %	Threshold
347*	259.9	227.1	- 32.8	- 12.65	T	139.4	135.1	- 4.3	- 3.1		0.54	0.595	+ 10.2	152.4	150.2	- 2.2	- 1.4	
347W	224.2	226.7	+ 2.5	+ 1.1		136.5	126.9	- 9.6	- 7.0	T	0.61	0.55	- 10.0					
Inco 750	253.3	227.7	- 25.6	- 10.1		191.6	197.2	+ 5.6	+ 2.9		0.76	0.87	+ 14.5	152.8	162.0	+ 9.2	+ 6.0	T
A-286	223.7	219.8	- 3.9	- 1.7		185.8	188.6	+ 2.8	+ 1.5		0.83	0.86	+ 3.6	168.2	157.1	-11.1	- 6.6	
A110-AT-T***	216.4	226.5	+ 10.1	+ 4.7		171.0	153.7	-17.3	-10.1		0.79	0.68	- 14.0	130.6	142.5	+11.9	+ 9.1	
A-110-AT-TW	214.6	217.1	+ 2.5	+ 1.17		118.1	121.2	+ 3.1	+ 2.6		0.55	0.56	+ 1.8					
Hastelloy C	185.7	187.3	+ 1.6	+ .86			156.3					0.835		153.40●	139.2	14.2	- 9.2	T
713-C	111.6	133.4	+ 21.8	+ 19.5	T	127.7	135.4	+ 7.7	+ 6.0		1.14	0.99	- 13.1	144.5				
347-C	117.3	115.4	- 1.9	- 1.62		99.2	102.3	+ 3.1	+ 3.1		0.85	0.885	+ 4.1	163.4				
440-C	204.0	213.0	+ 9.0	+ 4.40			50.7					0.24						
7075-T6	110.4	113.4	+ 3.0	+ 2.7		70.6	75.5	+ 4.9	+ 6.9		0.64	0.67	+ 4.7	95.2	80.3	-14.9	-15.7	T
6061-T6	64.7	69.0	+ 4.3	+ 6.65		61.4	65.8	+ 4.4	+ 7.2		0.95	0.95	0	49.8	52.3	+ 2.5	+ 5.0	
6061-TWU	67.3	71.7	+ 4.4	+ 6.5		56.5	65.1	+ 8.6	+15.2	T	0.84	0.91	+ 8.3					
6061-LWU	68.9	70.7	+ 1.8	+ 2.6		57.3	67.60	+10.3	+18.0	T	0.83	0.96	+ 16.0					
*6061-LWU**	61.5	44.1	- 17.4	- 28.3	T	42.1	41.0	- 1.1	- 2.6		0.68	0.93	+ 36.8					
*6061-TWU**	54.9	45.9	- 9.0	- 16.4	T	31.8	38.0	+ 6.2	+19.5		0.58	0.83	+ 43.0					
A356	44.7	52.8	+ 8.1	+ 18.1	T	39.7	43.2	+ 3.5	+8.9		0.89	.82	- 7.9	50.4	45.6	- 4.8	- 9.3	T
410 SS														149.3	160.7	+11.4	+ 8	

* Different Batches
** As welded
*** K_t = 17.0

● Calculated from Instron Data

TABLE 2

COMPARISON OF ELONGATIONS CONTROL VS IRRADIATED

MATERIAL	TYPE OF SPECIMEN	EXTENSOMETER IRRAD.%	EXTENSOMETER STD. DEV.	ROD CROSS HEAD TRAVEL IRRAD.%	ROD CROSS HEAD TRAVEL STD. DEV.	BENCH MEASUREMENT CONTROL%	BENCH MEASUREMENT STD. DEV.	BENCH MEASUREMENT IRRAD.%	BENCH MEASUREMENT STD. DEV.	VARIANCE %	DAMAGE %	THRESHOLD
Hastelloy C	LU	40.6	8.6	41.6	8.45	39.2	1.8	42.5	10.2	+ 3.3	+ 8.5	
347SS**	LU	36.5	3.68	39.8	1.17	40.2	2.25	40.9	3.0	+ 0.7	+ 1.7	
A-286	LU	28.0	6.95	29.5	5.9	37.5	1.2	32.25	7.8	- 5.25	-13.1	
Inconel X-750	LU	27.9	1.38	30.3	1.02	31.2	2.1	33.1	1.85	+ 1.9	+ 6.1	
347 S.S.	LWU	28.2	1.45	31.8	2.68	27.1	4.2	36.3	3.06	+ 9.2	+ 34	T
6061-T6	LU	19.9	1.55	20.6	1.48	24.1	2.4	24.1	3.5	0	-	
A-110AT	TU	14.9	0.95	18.6	0.6	17.1	1.4	18.6	0.45	+ 1.7	+ 8.8	
6061-T6	LWU	7.6	3.0	9.3	3.46	6.0	2.4	10.1	3.4	+ 4.1	+ 68	
347-C	LU	6.15	1.7	7.35	2.08	7.7	1.4	8.5	Δ	+ 0.8	+10.4	
7075-T6	LU	6.1	1.45	8.0	0.74	6.4	1.1	5.8	1.1	- 0.6	- 9.4	
6061-T6	TWU	9.01	Δ	8.62	1.81	9.0	2.6	9.05	3.8	+ 0.05	+ 0.55	
A-110-AT	TWU	5.1	0.95	7.64	0.42	5.9	1.4	5.95	1.8	+ 0.05	+ 0.85	
6061-T6**	LWU*	3.5	1.77	3.7	1.87	13.8	2.2	4.8	2.1	- 9.0	- 65	T
6061-T6**	TWU*	5.5	0.33	7.6	1.56	6.7	3.2	7.75	1.4	+ 1.05	+16.4	
A-356-T6	LU	1.59	0.34	2.20	0.34	1.5	0.9	1.95	0.05	+ 0.45	+ 30	
713-C	LU	0.85	0.14	2.70	0.75	3.0	0.9	1.8	1.3	- 1.2	- 39	

* As welded
** Different batches
Δ One specimen

TABLE 3

GTR-16 HARDNESS DATA (ALUMINUM ALLOYS) POST IRRADIATION

Material	Specimen Cond.	Specimen No.	Depression Measurements 1	2	3	4	5	Avg. (mm.)	Weight kg.	BHN	Specification BHN at Room Temp.
6061-T6	LWN	727	2.75	2.70	2.72	2.70	2.66	2.71	500	85	95 Normal
6061-T6	TWN	721	3.20	3.25	3.28	3.20	3.01	3.19	500	61.0	95 Normal
6061-T6	LWN	3-90	2.40	2.42	2.48	2.43	2.46	2.44	500	105	95 Alcoa HB
6061-T6	TWN	3-46	2.40	2.41	2.42	2.40	--	2.41	500	108	95 Normal
6061-T6	LN	2-89	2.51	2.56	2.52	2.51	2.50	2.52	500	99	95 Normal
A356-T6	LN	2-18	2.80	2.90	2.75	2.91	2.80	2.83	500	78	72 - 78 Range
7075 T6	LN	113	4.55	4.50	4.51	4.50	4.55	4.51	3000	187	168 - 200 Range

GTR-16 HARDNESS DATA (STEEL & TITANIUM)

Material	Specimen Cond.	Specimen No.	Hardness Measurements 1	2	3	4	5	Avg.	Scale	Specification at Room Temp.
SS 347 C	LN	185	83.0	83.2	83.5	84.5	84.1	84	RB	80 - 88
SS 347	LN	705	84.0	83.7	85.0	84.0	84.2	84	RB	80 - 88
SS 347	LWN	210	89.1	88.1	87.0	88.0	87.2	88	RB	80 - 88
SS A-286	LN	221	47.0	47.8	47.6	48.0	48.5	48	RD	47 - 50
SS 440 C	LN	604	58.0	59.3	59.7	59.5	59.5	59	RC	57 - 60
Inc X-750	LN	389	52.5	53.0	52.2	51.5	51.6	52	RD	49 min
Inc 713-C	LN	413	51.6	53.3	53.7	54.2	53.2	53	RD	47 - 60
Hastelloy C	LN	365	95.2	96.2	95.2	96.5	96.5	96	RB	90 - 96
A-110-AT	TN	330	47.3	52.3	48.0	50.4	50.8	50	RD	47 - 51
A-110-AT	TWN	342	49.0	50.5	50.1	48.8	47.7	49	RD	47 - 51

Sufficient back up instrumentation was built into the system to permit data acquisition in the event some of the systems became inoperable after the prolonged radiation exposure. The load applied to break the specimens was measured with two devices - the Instron load cell and strain gage load cell (ram) - on each pull rod.

Elongation was measured by extensometer, rod movement, bench measurement and cross-head travel of the Instron. Several specimens also had strain gages attached. The accuracy of the Instron cross-head travel was found inadequate as a measuring device for elongation caused by the effects of the hydraulic system, and these data for this type of elongation, are not reported. Area reduction was measured by planimeter from photographic enlargements of the fractured specimens.

The radiation damage is evaluated by comparison of the mechanical properties data obtained before and after radiation, including X-ray diffraction and electron microscopic examination.

As defined herein, material has reached the threshold of damage from radiation when the average change of one of the investigated properties has exceeded the sum of the standard deviation for both control and irradiated specimens. Average dose level for all materials was 5×10^{16} nvt ($E > 1.0$ Mev). Threshold level of damage was obtained for one or more properties of most materials tested.

III. CONCLUSIONS

A. At the temperature of liquid hydrogen nuclear radiation damage is more severe to weldments and cast material than to wrought alloys.

B. Threshold level for radiation damage for one or more properties was exceeded for most of the materials tested in GTR-16.

C. The tensile and shear strength for all materials did not consistently increase after radiation.

D. The notched strength was not significantly affected by this dose level.

E. Results on certain alloys are in doubt because of differences in the batch of materials between control and irradiated specimens.

IV. TEST RESULTS AND TECHNICAL DISCUSSION

A. GENERAL

All specimens were fabricated from $\frac{1}{4}$-in. thick sheet material. The castings were procured in 0.25-in. cast slabs. For most of the alloys sufficient material was procured to enable fabrication of all room temperature, liquid hydrogen control, radiation, and shear specimens from the same heat and batch of material, thus eliminating batch-to-batch variations in the evaluation of the test results. However, later procurements (347 and 6061-T6) introduced batch-to-batch variation.

Type of material, material condition, specification, type of test and test specimens are listed in Table 4. Chemical analysis of each material as certified by the vendor and independently obtained by Aerojet or commercial laboratories are shown in Table 5.

1. Specimens Design

The dimensions of both notched and unnotched specimens are shown in Figures 1 and 2. Dimensions of the unnotched specimens are similar to those shown in ASTM-E8-57T and Federal Test Method Standard No. 151A as modified to permit pin-loading and a standard 2-in. gage length. Notable difference is the reduction from 0.25 to 0.125-in. thickness in the test section.

Dimensions of the notched specimens are those of the NASA edge notch type specimen with a stress concentration factor of $K_t = 6.3$, with the exception of the specimen for titanium parent metal. The notched strength of this material for $K_t = 6.3$ was previously evaluated (Reference 1). Since titanium is a serious contender for flight-type pressure vessel, this alloy was subjected to more rigorous notch criteria than the remaining alloys.

Specimens are designed with slotted holes on one side to permit individual and sequential testing Slots were determined on total elongation at cryogenic temperature using available or extrapolated information.

TABLE 4

MATERIAL, CONDITION, TYPE OF SPECIMEN AND TYPE OF TEST SPECIFICATION FOR GTR-16

MATERIAL	TYPE OF SPECIMEN	SPECIFICATION	TYPE OF TEST
AL 6061-T6	U, N, TWU*, LWU* TWN*, TWU, LWU, LWN, TWN	QQA 327B Cond. T	Tension, Shear
A 286	U, N,	AMS 5525	Tension, Shear
SS 347	U, N, WU, WN	MIL-S-6721B	Tension, Shear
440-C	U, N	AMS 5630 R_c = 58-60	Tension
Hastelloy C	U, N	AMS 5530C	Tension, Shear
Allo-AT	U, N, WU, WN	MIL-T-9046C Class 3, ELI	Tension, Shear
A356-T6	U, N	QQA 601	Tension, Shear
7075-T6	U, N	QQA 283A Cond. T	Tension, Shear
Inconel X-750	U, N	AMS 5542F	Tension, Shear
SS 347C	U, N	AMS 5363B	Tension
Inconel 713C	U, N	AMS 5391	Tension
410 S.S.		AMS 5504	Shear
D 979		AMS 5746	Shear

U = Unnotched
N = Notched
T = Transverse
W = Welded - heat treated
W* = As welded

BLANK PAGE

MATERIAL			Ni	C	Cr	Mo	Mn	Si	Sn	S	P	$C_b - T_a$	Al	Ti	Cu	Co	Fe	B	W	Mg	Zn	Zr	V	N_2	H_2	O_2
ALUMINUM A 356-T6		MIN					-	6.5												0.20						
1/4" CAST PLATE	SPECIFICATION LIMIT	MAX					0.35	7.5						0.25	0.25		0.60			0.40	0.35					
QQA-601	VENDOR ANALYSIS						NIL	7.23						0.14	0.02		0.12			0.36	NIL					
(HEAT TREATED)	AGC ANALYSIS							7.34						0.16	0.02		0.15			0.30						
ALUMINUM 6061-T6		MIN			0.15		-	0.4						-	0.15		-			0.8	-					
1/4" PLATE,	SPECIFICATION LIMIT	MAX			0.35		0.15	0.8						0.15	0.40		0.70			1.2	0.25					
QQA-327B,	VENDOR ANALYSIS				-		-	-						-	-		-			-	-					
COND. T-6	AGC ANALYSIS				0.20		0.03	0.54						0.09	0.24		0.50			0.90	0.03					
ALUMINUM 7075-T651		MIN			0.18		-	-						-	1.2		-			2.1	5.1					
1/4" PLATE,	SPECIFICATION LIMIT	MAX			0.40		0.30	0.50						0.20	2.0		0.70			2.9	6.1					
QQA-283A,	VENDOR ANALYSIS				-		-	-						-	-		-			-	-					
COND. T651	AGC ANALYSIS				0.20		0.03	0.04						0.13	1.4		0.04			2.54	5.78					
A110-AT-, ELI		MIN		-			-		2.0				4.7	BAL			-									
1/4" PLATE, MIL-T-9046C	SPECIFICATION LIMIT	MAX		0.05			0.01		3.0				5.6				0.25							0.04	0.018	0.12
CLASS 3 GRADE ELI	VENDOR ANALYSIS			0.022			0.006		2.5				5.1	BAL			0.08							01014	0.011	0.08
(HOT ROLLED, ANNEALED)	AGC ANALYSIS			-			-		-				4.53				-							0.0045	0.0055	0.08
TYPE 347		MIN	9.0	-	17.0	-	-	0.05		-		10XC			-		BAL									
MIL-S-6721-B	SPECIFICATION LIMIT	MAX	13.0	0.008	19.0	1.5	2.0	1.00		.03	0.040	1.25			0.50											
(HOT ROLLED, ANNEALED AND PICKLED)	VENDOR ANALYSIS		11.2	0.062	17.17	0.35	1.75	0.67		.008	0.031	0.87			0.24		BAL									
	AGC ANALYSIS		10.5	0.06	17.57	0.37	1.7	0.69		.004	0.016	0.80												0.0214	0.0004	0.0016
TYPE 347-C		MIN	9.00	-	17.0	-	-	-		-	-	10XC														
SAND CASTING	SPECIFICATION LIMIT	MAX	12.00	0.10	20.0	0.50	2.00	1.50		0.040	0.040	1.35			0.50		BAL									
AMS 53638	VENDOR ANALYSIS			-		-	-	-		-	-															
(ANNEALED)	AGC ANALYSIS		9.35	0.08	19.3	0.28	1.09	1.00		0.018	0.014	1.26												0.011	0.0015	0.069
440-C, 1/4" x 2" FORGED BAR		MIN		0.95	16.00	0.40	-	-		-				0.75	0.31		BAL									
AMS 5630-C	SPECIFICATION LIMIT	MAX	0.75	1.20	18.00	0.60	1.00	1.00		0.030	0.040						BAL									
(HEAT TREATED TO ROCKWELL C-58-60)	VENDOR ANALYSIS		0.16	1.05	17.09	0.47	0.35	0.23		0.008	0.016						BAL									
	AGC ANALYSIS		0.24	0.99	16.50	0.51	0.39	0.25		0.010	0.013						BAL							0.010	0.0006	0.060
410 S.S.		MIN			11.5	-	-	-		-	-		-				BAL									
AMS-5613	SPECIFICATION LIMIT	MAX	0.75	0.15	13.5	0.5	1.0	1.0	0.50	0.03	0.04		0.05		0.50									0.080		
(HEAT TREATED AT 1800°F OIL QUENCHED AND TEMPERED AT 1050°F	VENDOR ANALYSIS		-	-	-	-	-	-	-	-	-		-		-		-									
	AGC ANALYSIS		0.29	0.09	12.5	0.11	0.33	0.37	0.04	0.19	0.018		0.03		0.06		BAL							0.019	0.00015	0.014
A-286; 1/4" PLATE		MIN	24.00	-	13.50	1.00	1.00	0.40		-	-		-	1.90				0.003			0.10					
AMS-5525	SPECIFICATION LIMIT	MAX	27.00	0.08	16.00	1.50	2.00	1.00		0.03	0.04		0.35	2.30				0.01			0.50					
(SOLUTION TREATED AND AGED AT 1350°F FOR 16 HOURS)	VENDOR ANALYSIS		25.04	0.061	14.92	1.24	1.29	0.63		0.003	0.019		0.23	2.05				0.005			0.20					
	AGC ANALYSIS		25.65	0.061	14.87	1.15	1.11	0.70		0.003	0.010		0.19	2.03				-			0.28			0.0007		0.0005
INCONEL X-750		MIN	70.00	-	14.00		-	-				.70	0.40	2.25			5.00									
1/4" PLATE	SPECIFICATION LIMIT	MAX	-	0.08	17.00		1.0	0.50				1.20	1.00	2.75	0.50		9.00									
AMS 5542G (AGED AT 1350°F FOR 16 HOURS)	VENDOR ANALYSIS		73.44	0.04	14.98		0.5	0.34		0.007		0.92	0.61	2.45	0.05		6.64									
	AGC ANALYSIS		-	0.02	-		-	0.34		0.002			0.71											0.0003	0.0083	0.0001
INCONEL 713 C		MIN	BAL	0.08	12.00	3.80	-	-		-		1.8	5.50	0.50	-			0.005				0.05				
1/4" INVESTMENT CASTING	SPECIFICATION LIMIT	MAX		0.20	14.00	5.20	0.20	0.50		0.015		2.8	6.50	1.00	0.50	1.00	2.50	0.015				0115				
AMS 5391	VENDOR ANALYSIS		BAL	0.13	12.86	4.51	0.02	0.16		0.007		2.31	6.22	0.73	0.03	0.73	0.85	0.010				0.14				
AS CAST	AGC ANALYSIS		BAL	0.10	11.99	3.50	-	0.15		-		2.47	5.50	0.77			1.13									
HASTELLOY C, 1/4"		MIN		-	14.50	15.00	-	-		-	-					-	4.00		3.00							
PLATE AMS 5530 C	SPECIFICATION	MAX		0.08	16.50	17.00	1.00	1.00		0.03	0.040					2.50	7.00		4.50		0.35					
(SOLUTION TREATED)	VENDOR ANALYSIS		BAL	0.05	15.75	15.78	0.55	0.63		0.012	0.008					1.44	5.46		3.40		0.26					
	AGC ANALYSIS			0.03				0.69		0.009	0.021										0.22			0.012	0.0003	0.028
D 979	SPECIFICATION LIMIT	MIN	42.0		14.0	3.00	-						0.75	2.70			BAL	0.008	3.0							
AMS 5746		MAX	48.0	0.080	16.0	4.50	0.75	0.75		0.040	0.040		1.30	3.30				0.016	4.5							
FORGING	VENDOR ANALYSIS AGC ANALYSIS		45.15	0.054	14.8	3.97	0.04	0.06		0.005	0.001		1.17	3.23			27.31	0.012	4.2							

TABLE 5

CHEMICAL ANALYSIS

P	C_b - T_a	Al	Ti	Cu	Co	Fe	B	W	Mg	Zn	Zr	V	N_2	H_2	O_2
									0.20						
			0.25	0.25		0.60			0.40	0.35					
			0.14	0.02		0.12			0.36	NIL					
			0.16	0.02		0.15			0.30						
			-	0.15		-			0.8	-					
			0.15	0.40		0.70			1.2	0.25					
			-	-		-			-	-					
			0.09	0.24		0.50			0.90	0.03					
			-	1.2		-			2.1	5.1					
			0.20	2.0		0.70			2.9	6.1					
			-	-		-			-	-					
			0.13	1.4		0.04			2.54	5.78					
		4.7	BAL			-									
		5.6				0.25							0.04	0.018	0.12
		5.1	BAL			0.08							01014	0.011	0.08
		4.53				-							0.0045	0.0055	0.08
	10XC			-		BAL									
0.040	1.25			0.50											
0.031	0.87			0.24		BAL									
0.016	0.80												0.0214	0.0004	0.0016
-	10XC														
0.040	1.35			0.50		BAL									
-															
0.014	1.26		0.75	0.31		BAL							0.011	0.0015	0.069
0.040						BAL									
0.016						BAL									
0.013						BAL							0.010	0.0006	0.060
-		-				BAL									
0.04		0.05		0.50									0.080		
-		-		-		-									
0.018		0.03		0.06		BAL							0.019	0.00015	0.014
-		-	1.90				0.003			0.10					
0.04		0.35	2.30				0.01			0.50					
0.019		0.23	2.05				0.005			0.20					
0.010		0.19	2.03				-			0.28			0.0007		0.0005
	.70	0.40	2.25			5.00									
	1.20	1.00	2.75	0.50		9.00									
	0.92	0.61	2.45	0.05		6.64									
		0.71											0.0003	0.0083	0.0001
	1.8	5.50	0.50	-			0.005				0.05				
	2.8	6.50	1.00	0.50	1.00	2.50	0.015				0115				
	2.31	6.22	0.73	0.03	0.73	0.85	0.010				0.14				
	2.47	5.50	0.77			1.13									
-					-	4.00		3.00							
0.049					2.50	7.00		4.50		0.35					
0.008					1.44	5.46		3.40		0.26					
0.021										0.22			0.012	0.0003	0.028
		0.75	2.70			BAL	0.008	3.0							
0.040		1.30	3.30				0.016	4.5							
0.001		1.17	3.23			27.31	0.012	4.2							

TABLE 5

CHEMICAL ANALYSIS

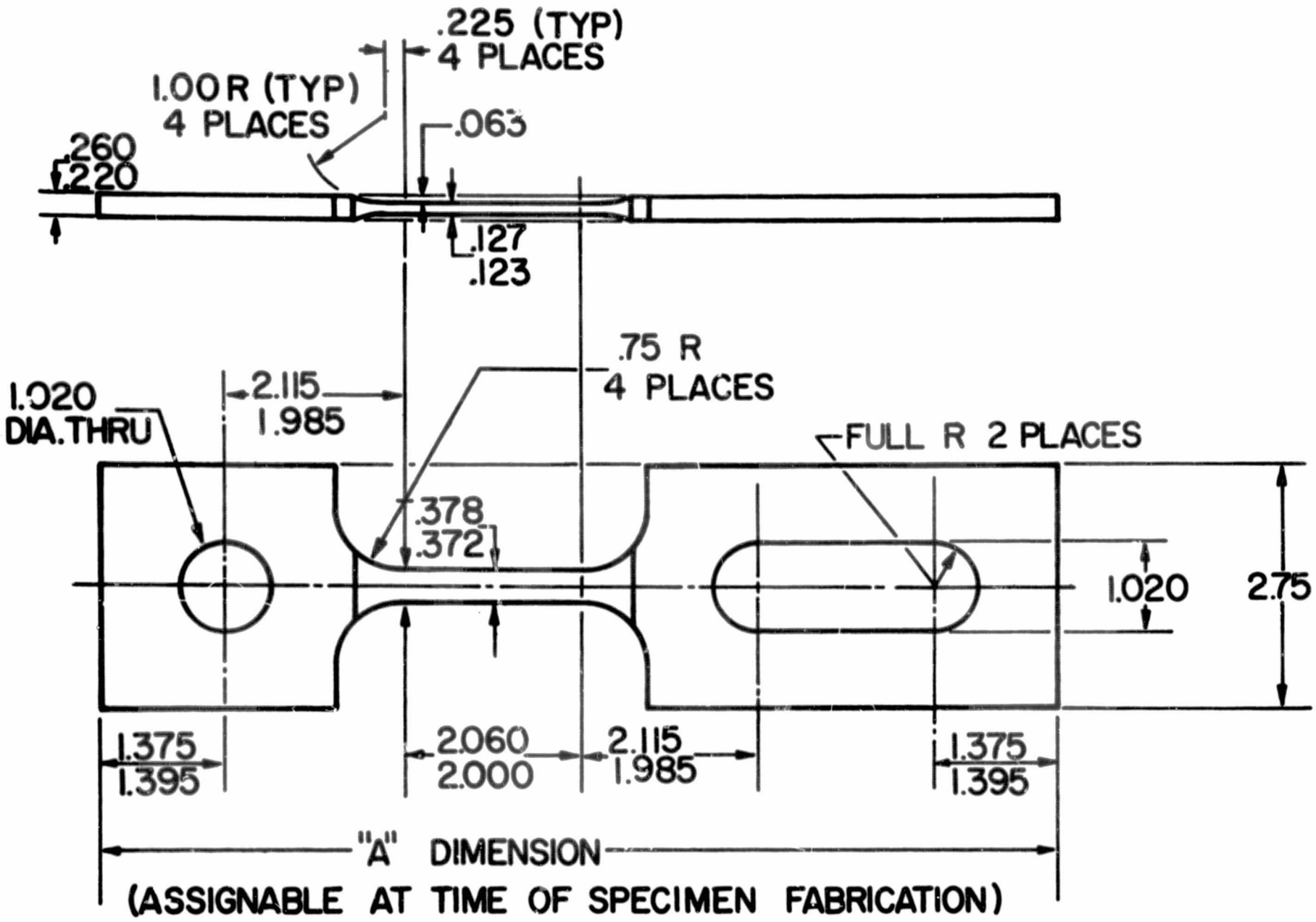

Figure 1

Unnotched Tensile Specimen for Sheet and Plate

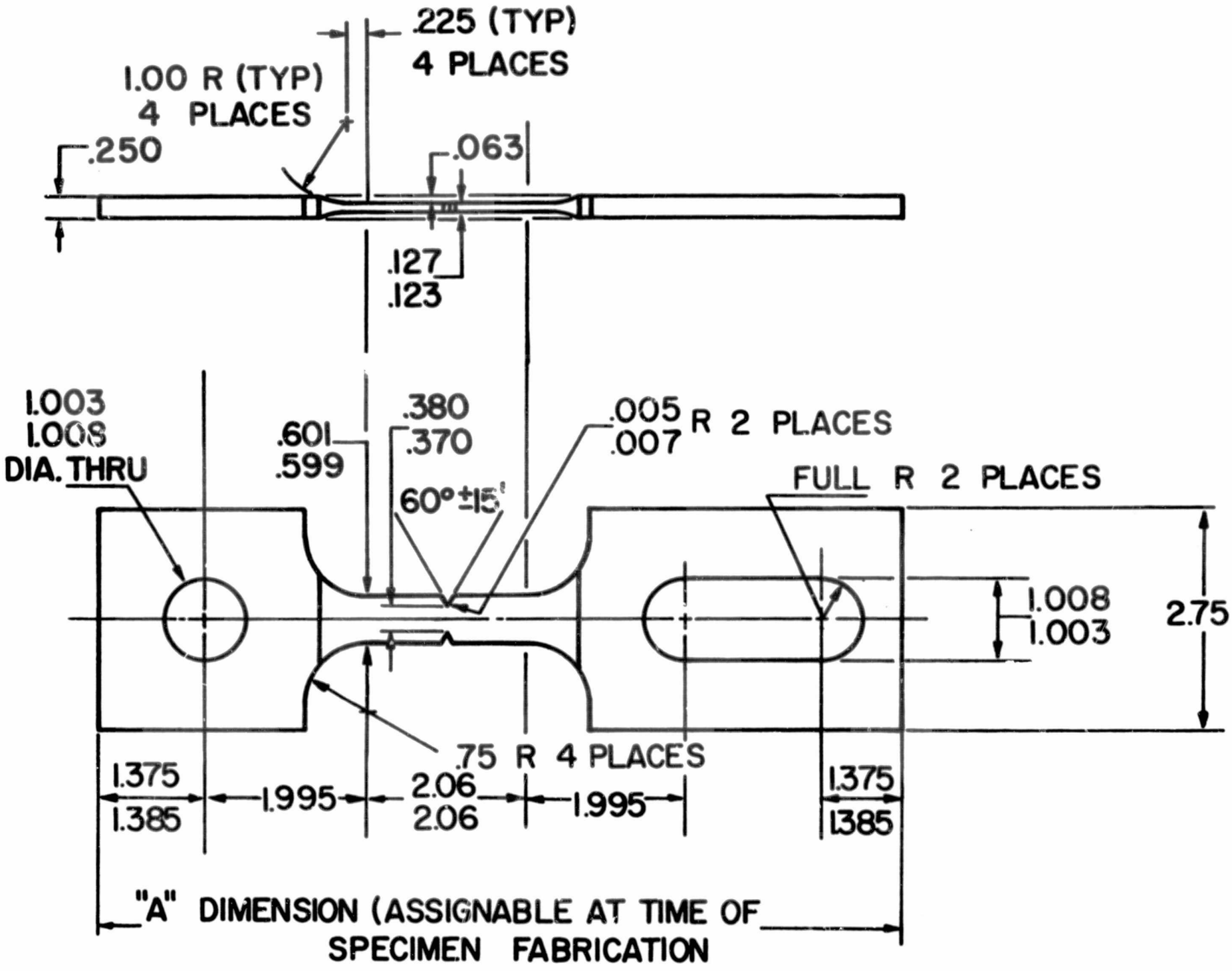

Figure 2

Notched Tensile Specimen for Sheet and Plate

2. Chemical Composition

Chemical analyses as obtained from the vendor and sample analyses by AGC or an independent laboratory (including X-ray Fluorescent analysis), were made to determine acceptability to specifications and provide possible basis for comparison of the radiation effects associated with the alloy constituents. Impurities and percent content of each element are included in these analyses. This analysis was performed by wet chemical methods or combustion technique.

Table 5 contains the chemical composition as compared to the specifications requirements.

3. Mechanical Properties

The evaluation of the damaging effect of nuclear radiation and liquid hydrogen environment on the structural materials tested in GTR-16 is based primarily on comparing their mechanical properties with and without radiation. Average mechanical properties, including standard deviations for both irradiated and non-irradiated material, are compared. Increase or decrease of these properties because of radiation is presented as variance, and in percent, and is tabulated as nuclear damage to this property. When the variance (difference between average data of control and average data of irradiated samples) exceeds the standard deviation for the control and irradiated specimen the threshold limit for this material has been reached.

Properties obtained and evaluated for most of the materials include: ultimate and yield tensile strength, elongation, reduction of area and notched-tensile and shear strength.

4. Metallography of Materials

Specimens for study of control and irradiated conditions of the materials were taken from two areas on a tensile coupon. One specimen was taken adjacent to the failure zone in the gage length area and showed the effects of

straining. A second specimen was taken from the grip area to show unstrained microstructure. Comparisons were made with the as-received material and the strained and unstrained areas.

Typical photographs were taken at magnifications of 100X and 1000X.

5. Electron Microscopy

Electron microscopic examinations, at ultra-high magnifications, were performed on all metallic specimens on which metallographic studies had been performed. Specimens were repolished and etched suitably for replication techniques.

A Hitachi HS-6 electron microscope was used for examination of the replicas. Several grids from each replica were examined in order to obtain representative microstructures. Representative electron photographs were taken at 15,000X.

Electron microscopic fractography studies (the examination of fracture surfaces at high magnification using the electron microscope) were performed. To accomplish this, replication techniques were used on the fracture surface itself. Areas of the fracture zone were examined from the center to the edge of the specimen. Representative photomicrographs were shown from edge and center positions. Mode of failure was evaluated for correlation with mechanical properties. Studies were not performed on room temperature tensile specimens.

A problem existed in that the control specimens were examined at 15,000X while the fracture surface of the irradiated samples were viewed at 4200X. The 4200X fractographs were considered of greater value because they indicated a general mode of failure while the more refined 15,000X fractographs exhibited primarily a failure texture.

6. X-Ray Diffraction Analysis

In order to follow crystallographic changes (that is, transformations, lattice distortions) the X-ray diffraction technique was used. Lattice-parameter measurements and "half-height-width" micro-stress comparisons were made.

North American Phillips (Norelco) X-ray diffraction equipment was used for these studies in the control specimens. For ferrous materials, filtered chromium radiation (35 Kvp-11ma) was used for the control and cobalt for the radiated specimen. The non-ferrous metals were examined with filtered copper radiation at 50 Kvp-20 ma. Comparative X-ray fluorescence analyses were made with a tungsten target tube operated at 50 Kvp-40 ma. A lithium fluoride analyzing crystal was used at all times.

Complete X-ray diffraction patterns were obtained from each specimen (as-received, control, and irradiated). This information provided a semi-quantitative analysis of phases present, identified certain aspects of texture and provided for crystal imperfection.

Lattice parameter measurements were made in all conditions. The absolute accuracy of the lattice parameter measurements varied for different alloys. In general, it is estimated to be in the range of $\pm$ 0.004°A to $\pm$ 0.003°A The accuracy of lattice parameter differences between the strained and unstrained region are estimated to be somewhat better than the absolute accuracy in most cases. The diffraction patterns provide information about preferred orientations normal to the surface. Comparative residual stresses were determined by measurement of the width at half height of high-angle diffraction lines in all conditions of the materials. This width (in 2θ) at half-height of a diffraction line is presented in the data as "microstress". Comparison of microstress levels for the ferrous materials obtained by use of two reference X-ray sources makes the data interpretation more difficult. Interpretations of the meaning of this line broadening in a particular alloy requires more extensive studies than were justified at this stage of the investigation. It may represent either localized stresses or may be attributed, in some instances, to defects such as stacking faults.

B. ALUMINUM ALLOYS

1. A 356-T6 Casting (Al-Si-Alloy)

a. Mechanical Properties

Average values and standard deviations of mechanical properties obtained at room temperature, at liquid hydrogen temperature without radiation (control), and at liquid hydrogen temperature with nuclear radiation are presented in Table 6. Detailed test results for the irradiated specimens (tested without warm up) are shown in Table 7. A general increase in ultimate tensile and yield strength from room to liquid hydrogen temperature was followed by additional increase from the radiation exposure. A 45.7% increase in ultimate strength from room to liquid hydrogen temperature was followed by 18.1% increase because of radiation. A rather small percentage increase in yield strength from room temperature (14%) was followed by a larger (38%) increase in this property because of radiation. The low ductility of this material at room temperature shows decrease in both elongation and reduction of area because of the liquid hydrogen environment. This event is then reversed, an increase in ductility for both parameters (elongation and area reduction) followed as a result of radiation. An initial 99.5% increase in shear strength because of the liquid hydrogen environment was followed by a 9% decrease. This is a typical example of a material showing increase in some mechanical properties and decrease in others as a result of the radiation environment. Notched strength increased continuously from room temperature; however, notched-to-unnotched ratio decreased for both control and irradiated material. A decrease of notched-to-unnotched yield strength ratio of 21% should be noted as a result of radiation. Stress-strain curves obtained with the extensometer are shown in Figure 3. For comparison reasons, average stress-strain curves at room and liquid hydrogen temperatures are included. The threshold level of damage was obtained for the ultimate and yield tensile and shear strength of this alloy.

TABLE 6

AVERAGE MECHANICAL PROPERTIES TEST DATA

A-356-T6

	Room Temp.	Control -423°F	Change- Room Temp. vs Control in Percent	Irrad. -423°F	Change- Control vs Irradiated in Percent	Threshold
UNNOTCHED						
Ultimate Strength-PSI	30,700	44,700	+45.7	52,800	+18.1	T
Std. Deviation-PSI	2,100	1,700		2,100		
0.2% Yield Strength-PSI	27,200	31,000	+13.95	42,800	+38	T
Std. Deviation-PSI	2,060	850		2,400		
% Elongation	3.25	1.5	-53.2	1.95	+30	
Std. Deviation-%	.87	0.9		0.05		
% Reduction in Area	7.9	6.3	-20.3	6.8	+8.0	
Std. Deviation-%	2.2	0.4		1.6		
Ult. Shear Strength-PSI	25,500	50,400	+99.5	45,600	-9.3	T
Std. Deviation-PSI	700	2,300		630		
NOTCHED Kt = 6.3						
Ultimate Strength-PSI	29,200	39,700	+36	43,200	+8.9	
Std. Deviation-PSI	600	3,300		2,600		
Ratio $\frac{\text{Notched Ult.}}{\text{Unnotched Ult.}}$	0.95	0.89	-6.3	0.82	-7.9	
Ratio $\frac{\text{Notched Ult.}}{\text{Unnotched Yield}}$	1.07	1.28	+19.6	1.01	-21	

TABLE 7

DETAILED MECHANICAL PROPERTIES DATA
A-356-T6

Specimen Number	Specimen Condition	Ultimate Strength: Instron Cell (ksi)	Ultimate Strength: Ram Cell (ksi)	Yield Strength 0.2% Offset(ksi)	Percent Reduction in Area	Percent Elongation
17	LN	42.23	39.78			
18	LN	46.05	43.38			
21	LN	49.08	46.22			
22	LN	48.29	43.49			
5	LU	54.88	51.70	42.5	6.3	2.0
6	LU	56.02	55.49		9.2	
9	LU	53.80	50.68	41.0	5.5	1.9
10	LU	60.06	53.37	45.0	6.4	

ELONGATION DATA

Specimen Number	Specimen Condition	Extensometer: Post Irradiation (Mills)	Pull Rod: Post Irradiation (Mills)	Pull Rod: Control (Mills)	Bench Measurement: Post Irradiation (Mills)	Bench Measurement: Control (Mills)
5	LU	41	59		40	
6	LU	-	52		-	
9	LU	38	56		38	
10	LU	56	74		-	
Average		45	60	75.8	39	30
% Elongation		1.59	2.2	2.68	1.95	1.5
% Damage			-17.9		+30	

Ultimate Shear Strength (ksi)

46.3
45.2
45.4

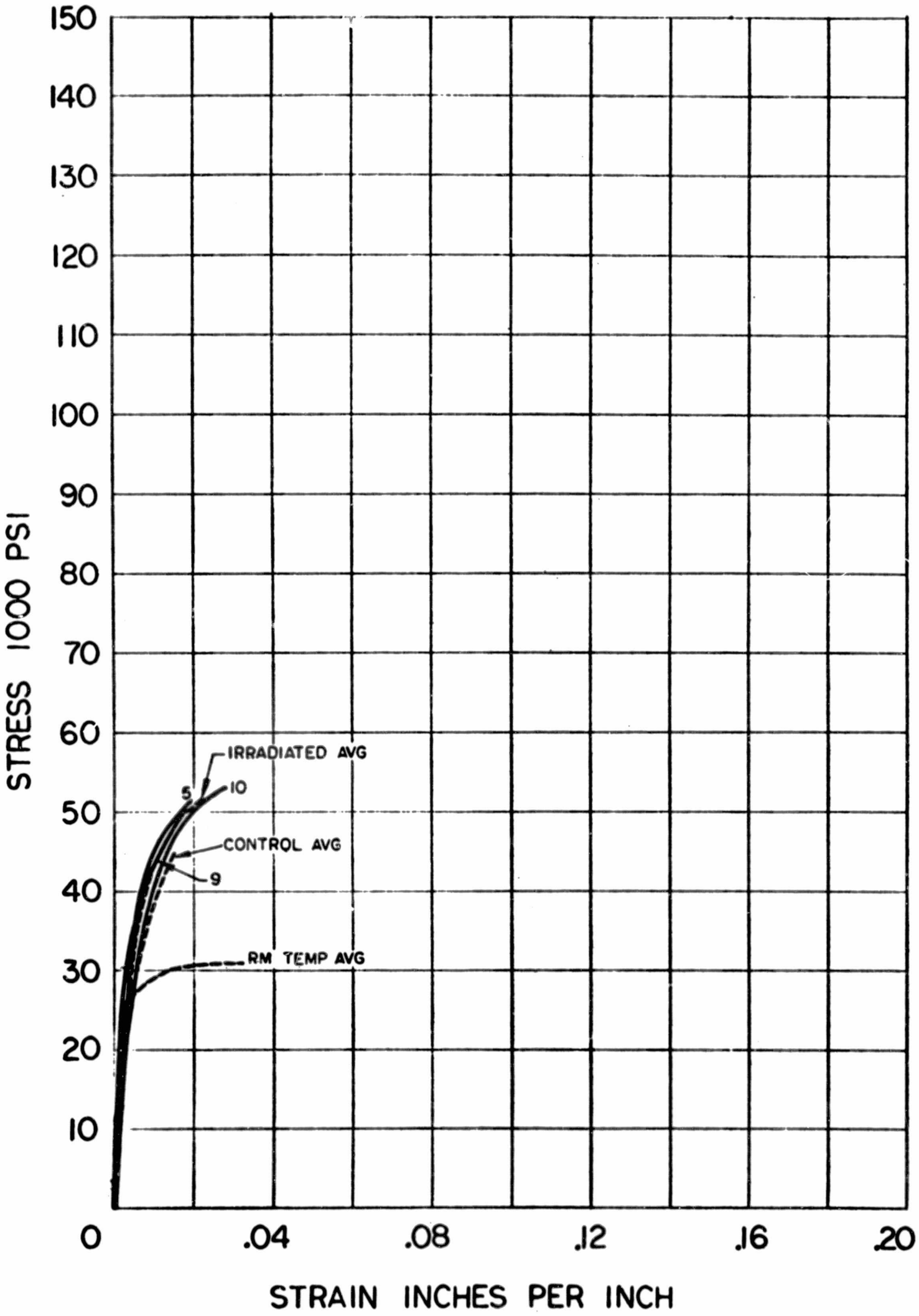

Figure 3

Stress - Strain Curves for A-356 Aluminum

b. Metallography

Photomicrographs of control and irradiated specimen were made to illustrate the main features of the microstructures observed during examination of the strained, fractured area and an unstrained area.

The microstructure shown in Figure 4 at 1000X magnification is typical for A356 in the strained condition. Very little change in microstructure was observed after the material had been irradiated. Microstructure of the control specimens is available in Reference 1. Fragments of the Al-Si eutectic appear to justify the conclusion that a significant amount of fracturing occurred along these constituents in the microstructure. The microstructure of the unstrained area did not show any changes from radiation, and photographs are not presented.

Material: Aluminum A356-T6

Form: 1/4" Cast Plate

Specimen No.: LU 10

Specification: QQA 601

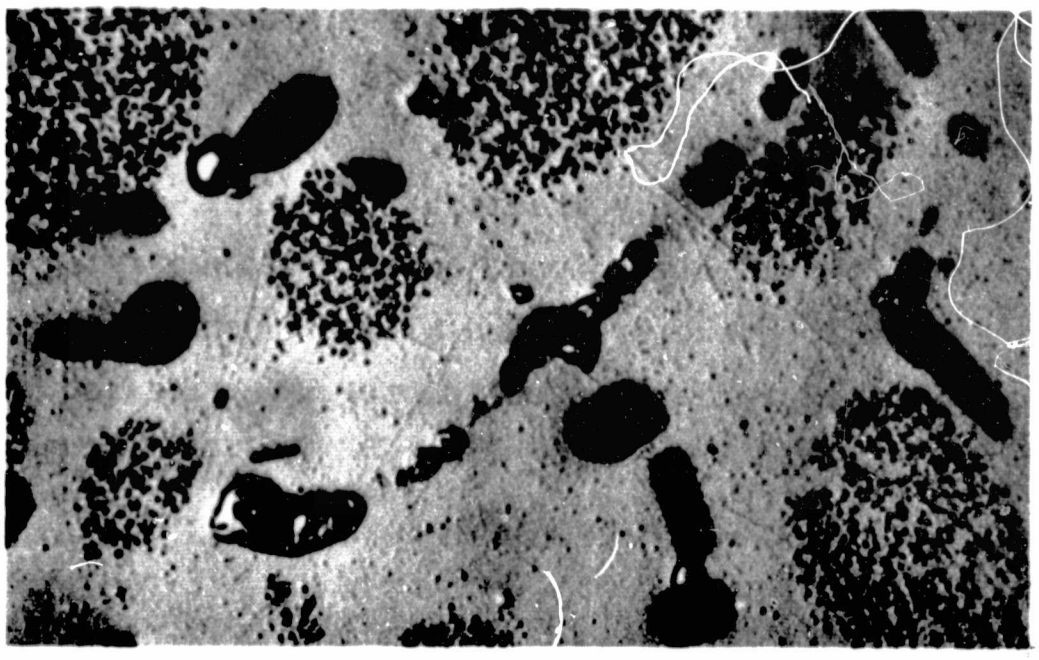

Condition: Irradiated-Strained Area

Mag: 1000X
Etchant: Keller's

Microstructure showing a solid-solution aluminum matrix, with an intermetallic Al-Si. The cored structure is typical of castings. The microstructure is representative of both the strained and unstrained areas in the irradiated material.

Condition: Irradiated-Edge Fracture

Mag: 1000X
Etchant: Keller's

Microstructure showing a solid-solution aluminum matrix, with intermetallic Al-Si. The fracture is transgranular, occurring at the solid-solution aluminum/ intermetallic Al-Si interface and through the Al-Si eutectic.

Figure 4

Aluminum A 356-T6 - Irradiated - Strained Area

1000X Magnification

c. Electron Microscopy

Electron microscopic examinations were made (at 15,000 magnifications) of samples obtained from an unstrained and strained area of tensile test coupons in the irradiated condition. Figures 5 and 6 show typical structures for those samples. The Al-Si eutectic is present in a matrix of solid solution aluminum. It is to be noted that little variation in structure occurred, with the exception of line markings both in the matrix and also adjacent to the Al-Si eutectic phase of the strained material.

Typical electron fractographs were taken from edge and center of the fracture of the irradiated tensile test coupons, Figure 7. The notched fracture displays the same characteristic as the unnotched fracture. The fractures show evidence of Al-Si eutectic extraction. It is indicated that irradiation resulted in an embrittlement of the A356 and, consequently, transgranular failure became the mode across the complete section.

Material: Aluminum A 356-T6
Form: 1/4 in. Cast Plate
Specimen No.: LU 10
Specification: QQA 601

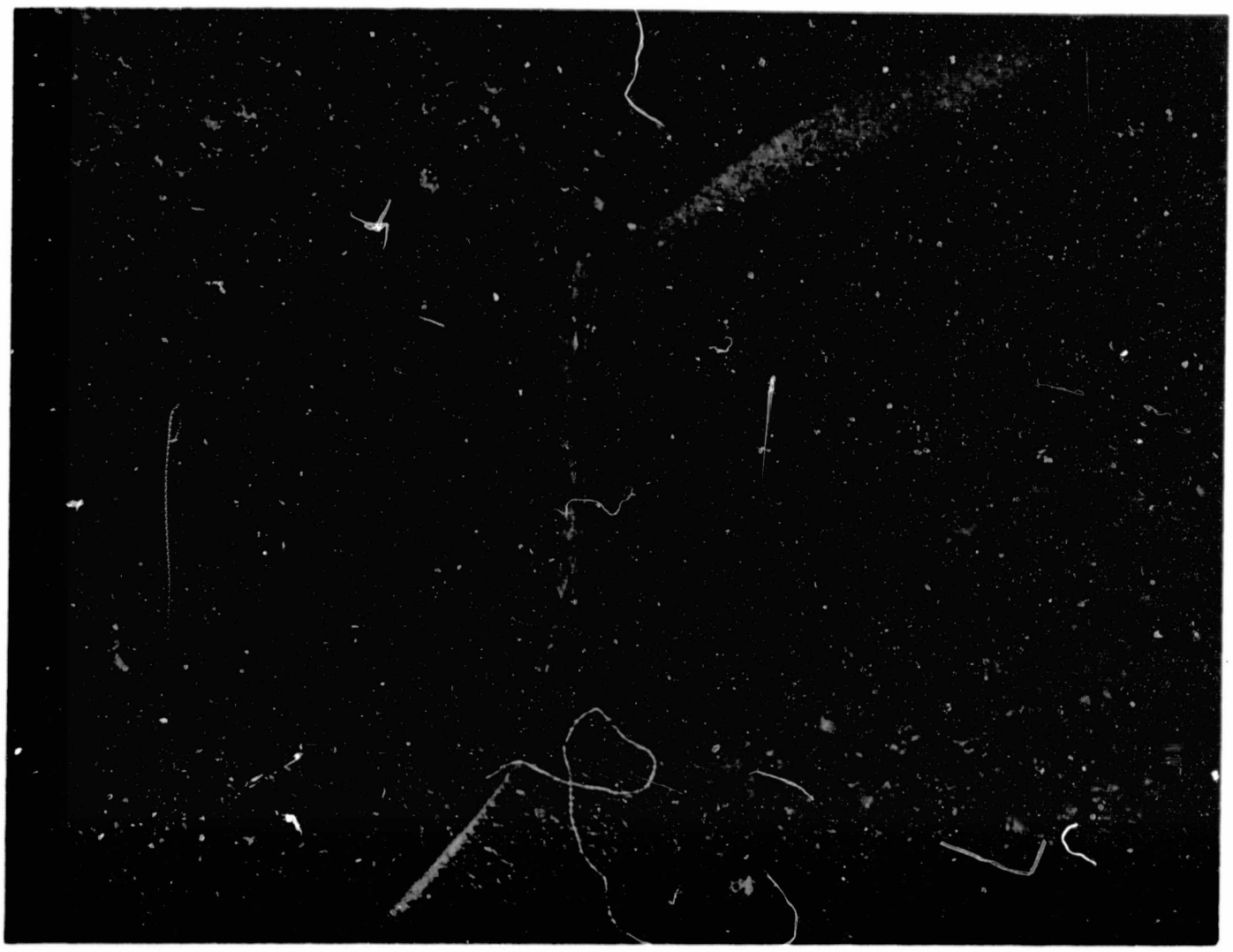

Conditions: Irradiated - Unstrained
Mag: 15000X
Etchant: Keller's

Microstructure of an unstrained portion of an irradiated sample showing the Al-Si eutectic phase on a background of solid-solution aluminum.

Figure 5

Electron Micrograph, Aluminum A 356-T6 - Irradiated - Unstrained - 15000X

Material: Aluminum A356-T6
Form: 1/4 in. Cast Plate
Specimen No.: LU 10
Specification: QQA 601

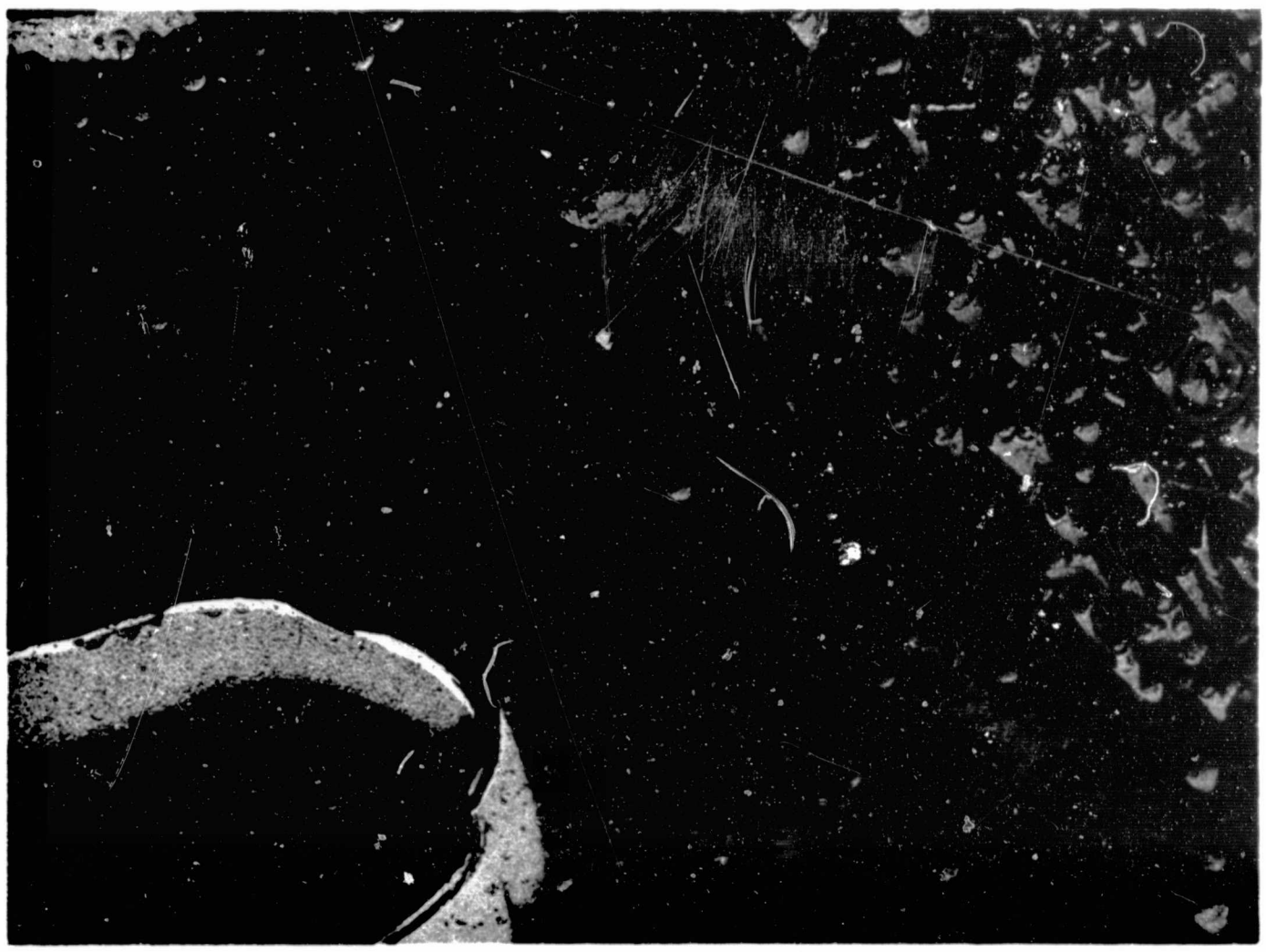

Condition: Irradiated Strained
Mag: 15000X
Etchant: Keller's

Microstructure of a strained portion of an irradiated sample showing the Al-Si eutectic (lower left) and solid-solution aluminum with insolubles (right). Note strain lines between the eutectic and the insolubles.

Figure 6

Aluminum A-356-T6 - Irradiated Strained Electron Micrographs - 15000X

Material: Aluminum A356-T6
Form: 1/4 in. Cast Plate
Specimen No.: LN 18
Specification: AAQ 601

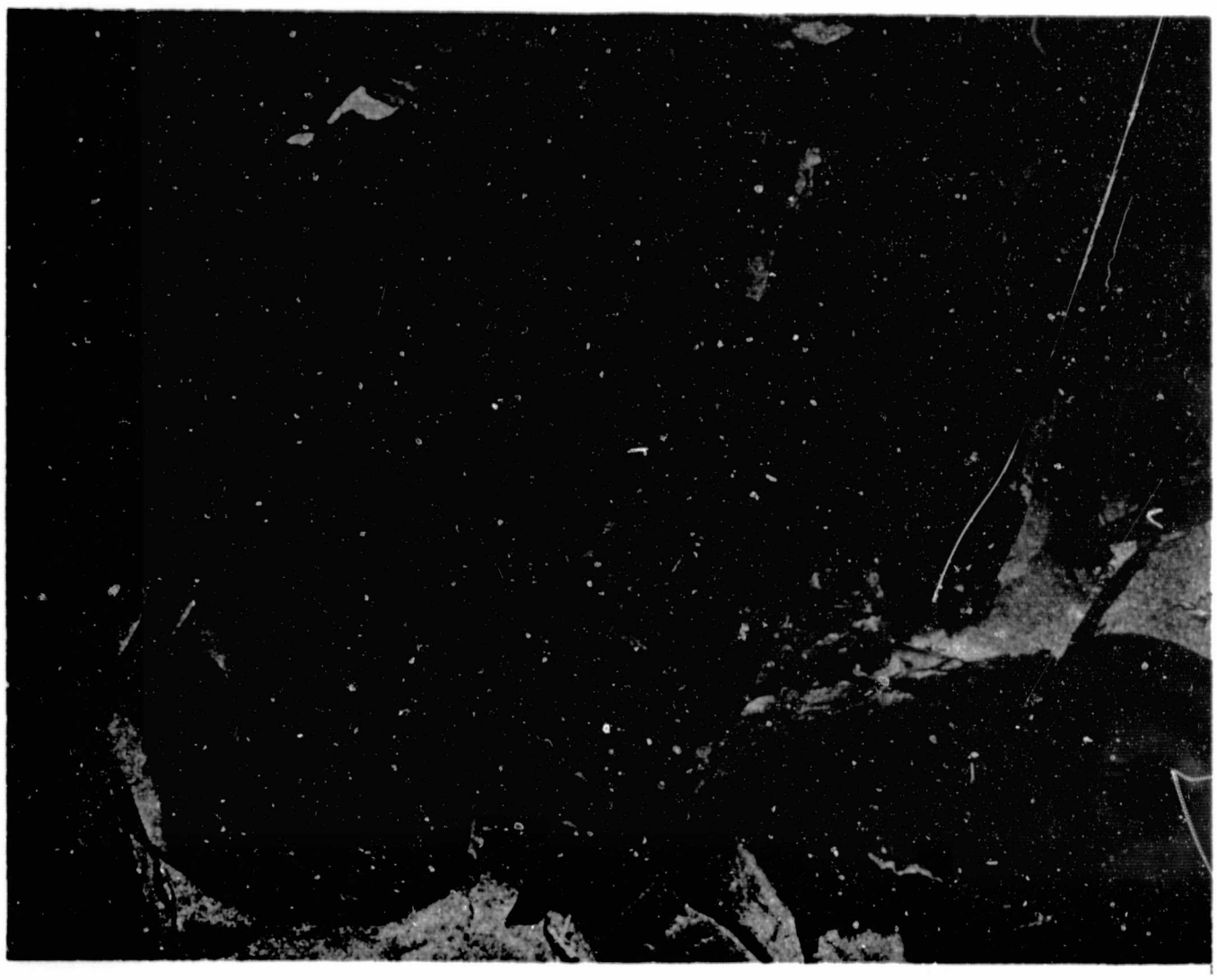

Condition: Irradiated; Center-notched
Mag: 4200K
Unetched

Notched specimen fracture from an irradiated sample displaying the same characteristics as the unnotched fractures: brittle intermetallic failure, eutectic matrix separation, and isolated areas of shallow micro-voids.

Figure 7

Aluminum A356-T6 Irradiated Notched, Electron Fractograph - 4200X

d. X-Ray Diffraction

Table 8 lists the relative intensities for different diffraction lines, the lattice parameter, and microstress for the as-received, control, and irradiated conditions.

The X-ray diffraction patterns of the as-received A356-T6 aluminum showed the face-centered cubic crystal symmetry structure of aluminum and the crystalline diamond structure of silicon.

The X-ray pattern from the control sample showed essentially the same crystal structures as the as-received sample and orientations in the unstrained region prevailed in the (311) direction. The pattern from the strained area indicated preferred orientation in the (111) and (311) directions. There was no significant change in the lattice parameter as a result of straining. There was no effect on the crystal structure that could be related to testing at cryogenic temperatures.

The microstress of the irradiated samples did not vary from that of the control material.

The changes in lattice parameters from the as-received to the irradiated specimens were within the limit of experimental error and no significant difference was noted between the parameters of the as-received and control specimens.

TABLE 8

X-RAY DIFFRACTION-A-356-T6

Miller Indices (hkl)	Pure Aluminum (1)	(2)	A356 As-Received (1)	(2)	A356 Control (Specimens 2-7) Strained (1)	(2)	Unstrained (1)	(2)	Irradiated (Specimen LU10) Strained (1)	(2)	Unstrained (1)	(2)
111	2.338	100	2.35	100	2.34	100	2.32	80	2.34	100	2.34	55
200	2.024	47	2.03	20	2.01	9	2.01	25	2.03	10	2.03	25
220	1.431	22	1.43	15	1.43	30	1.43	30	1.43	2	1.44	100
311	1.221	24	1.22	100	1.22	100	1.22	100	1.22	5	1.22	33
222	1.169	7	1.17	10	1.17	50			1.17	2	1.17	6
400	1.012	2										
331	0.929	8	0.930	10					0.93	10		
					LATTICE PARAMETER A°							
	4.0494		4.052		4.052		4.045		4.05		4.05	

					MICROSTRESS							
			0.60° (2θ = 116°)		0.40° (2θ = 78°)		0.35° (2θ = 78°)		0.50°/0.26° (2θ = 78.2°/38.35°)		0.52°/0.28° (2θ= 78.1°/38.35°)	
	Pure Silicon		As Received		Control				Pure Silicon Irradiated			
111	3.138	100	3.15	100					3.14	100	3.15	70
220	1.920	60	1.92	50	1.92	100	1.90	100	1.92	30	1.92	35
311	1.638	35	1.64	35	1.64	50	1.64	20	1.64	20	1.64	20
400	1.357	8	1.36	15	1.36	15						
331	1.246	13	1.25	20	1.25	15						
442	1.108	17	1.11	15	1.11	15	1.11	25	1.10	5	1.11	5
511	1.045	9	1.04	5	1.04	15	1.04	25				
440	0.960	5							0.94	6		
531	0.918	11							0.91	45	0.91	100
620	0.859	9										
533	0.829	5									0.85	8
					LATTICE PARAMETER A°						0.83	20
	5.4301		5.44						5.43		5.43	

NOTE: (1) "d" spacings
(2) Relative intensities, percent; Shift in "d" spacings indicates lattice expansion; Orientation change is indicated by intensity change for a given Miller Indice.

2. 6061-T6 (Wrought Al-Mg-Si-Alloy)

a. Mechanical Properties

Different specimens of this alloy were tested under various conditions which included:

(1) Sheet as-received, longitudinal to the rolling direction

(2) As-welded, longitudinal and transverse to the rolling direction

(3) Welded and heat treated after welding, longitudinal and transverse to the rolling direction

Average values and standard deviations of mechanical properties obtained at room temperature and at liquid hydrogen temperature, with and without radiation, are presented in Table 9. Detailed test results for the irradiated specimens are shown in Table 10.

(1) Parent Material

Ultimate and yield tensile strength increased from room temperature to the temperature of liquid hydrogen, and was then followed by additional increase from radiation. The percent increase of ultimate strength to liquid hydrogen temperature (45%) was followed by smaller increase from radiation (7%). The percent increase of yield strength because of radiation was higher (18%) than the increase resulting from the cryogenic temperature (15%). The threshold level of damage for this property was reached. The ductility, as measured both by elongation and area reduction, increased with the decrease of temperature. There was a small decrease in area reduction and no change in elongation resulting from radiation.

TABLE 9

AVERAGE MECHANICAL PROPERTIES TEST DATA

ALUMINUM ALLOY 6061-T6

	Room Temp.	Control -423°F	Change- Room Temp. vs Control in Percent	Irrad. -423°F	Change- Control vs Irradiated In Percent	Threshold
UNNOTCHED						
Ultimate Strength-PSI	44,500	64,700	+45	69,000	+6.7	
Std. Deviation-PSI	560	4,800		4,000		
0.2% Yield Strength-PSI	40,900	46,500	+15	55,000	+18	T
Std. Deviation-PSI	4,950	2,600		4,400		
% Elongation	11.7	24.1	+106	24.1	-0	
Std. Deviation-%	.36	2.4		3.5		
% Reduction in Area	29.8*	39.6	+33	38.0	-4.0	
Std. Deviation-%	1.6	1.9		3.3		
Ult. Shear Strength-PSI	26,700	49,800	+87	52,300	+5	
Std. Deviation	900	1100		1570		
NOTCHED Kt = 6.3						
Ultimate Strength-PSI	44,000	61,400	+39	65,800	+7.2	
Std. Deviation-PSI	1,100	4,500		5,450		
Ratio $\frac{\text{Notched Ult.}}{\text{Unnotched Ult.}}$	0.99	0.95	-4	0.95	0	
Ratio $\frac{\text{Notched Ult.}}{\text{Unnotched Yield}}$	1.08	1.32	+22	1.19	-9.9	

*Micrometer Measurements

TABLE 9 (cont.)

AVERAGE MECHANICAL PROPERTIES TEST DATA

ALUMINUM ALLOY 6061-LW - AS WELDED

	Room Temp.	**Control -423°F	Change- Room Temp. vs Control in Percent	**Irrad. -423°F	Change- Control vs Irradiated in Percent	Threshold
UNNOTCHED						
Ultimate Strength-PSI	30,800	61,500	+100	44,100	-28.3	T
Std. Deviation-PSI	600	6,300		4,750		
0.2% Yield Strength-PSI	18,800	26,900	+43	34,400	+28	T
Std. Deviation-PSI	1,500	3,000		2,300		
% Elongation	4.8	13.76	+190	*** 4.8	-65	T
Std. Deviation-%	.75	2.2		2.1		
% Reduction in Area	45.1	35.0	-22.5	11.0	-69	T
Std. Deviation-%	3.3	5.8		1.5		
Ult. Shear Strength-PSI						
Std. Deviation-PSI						
NOTCHED Kt = 6.3						
Ultimate Strength-PSI	32,100	42,100	+31	41,000	-2.6	
Std. Deviation-PSI	860	*		5,200		
Ratio $\frac{\text{Notched Ult.}}{\text{Unnotched Ult.}}$	1.04	0.68	-35	0.93	+36.8	
Ratio $\frac{\text{Notched Ult.}}{\text{Unnotched Yield}}$	1.71	1.56	-8.8	1.19	-24	

* Single specimen tested
** Different heats
***Measured between welded tabs

TABLE 9 (cont.)

AVERAGE MECHANICAL PROPERTIES TEST DATA

ALUMINUM ALLOY 6061-TW - AS WELDED

	Room Temp.	**Control -423°F	Change- Room Temp. vs Control in Percent	**Irrad. -423°F	Change- Control vs Irradiated in Percent	Threshold
UNNOTCHED						
Ultimate Strength-PSI	29,500	54,900	+86	45,900	-16.4	T
Std. Deviation-PSI	960	5,700		1,000		
0.2% Yield Strength-PSI	18,100	33,500	+85	30,600	-9	
Std. Deviation-PSI	920	5,300		2,900		
% Elongation	4.8	6.66	+39	*** 7.75	+16.4	
Std. Deviation-%	1.5	3.2		1.4		
% Reduction in Area	30.5	19.9	-35	10.9	-45	T
Std. Deviation-%	8.6	1.5		0.26		
Ult. Shear Strength-PSI						
Std. Deviation-PSI						
NOTCHED Kt = 6.3						
Ultimate Strength-PSI	27,300	31,800	+16.5	38,000	+19.5	
Std. Deviation-PSI	2,300	*		6,600		
Ratio $\frac{\text{Notched Ult.}}{\text{Unnotched Ult.}}$	0.92	0.58	-37	0.83	+43.0	
Ratio $\frac{\text{Notched Ult.}}{\text{Unnotched Yield}}$	1.51	0.95	-37	1.24	+31	

* Single specimen tested
** Different heats
***Measured between welded tabs

TABLE 9 (cont.)

AVERAGE MECHANICAL PROPERTIES TEST DATA

ALUMINUM ALLOY 6061 TW - HEAT TREATED AFTER WELDING

	Room Temp.	Control -423°F	Change- Room Temp. vs Control in Percent	Irrad. -423°F	Change- Control vs Irradiated in Percent	Threshold
UNNOTCHED						
Ultimate Strength-PSI	41,600	67,300	+62	71,700	+6.5	
Std. Deviation-PSI	1,100	3,300		4,550		
0.2% Yield Strength-PSI	36,900	47,300	+28	57,600	+22	T
Std. Deviation-PSI	750	2,400		1,200		
% Elongation	3.5	9.0	+157	9.05	+.55	
Std. Deviation-%	.7	2.		3.8		
% Reduction in Area	33.2	25.5	-23	27.3	+7	
Std. Deviation-%	4.1	2.0		6.0		
Ult. Shear Strength-PSI						
Std. Deviation-PSI						
NOTCHED Kt = 6.3						
Ultimate Strength-PSI	41,700	56,500	+35	65,100	+15.2	T
Std. Deviation-PSI	1,600	5,300		2,800		
Ratio $\frac{\text{Notched Ult.}}{\text{Unnotched Ult.}}$	1.00	0.84	-16	0.91	+8.3	
Ratio $\frac{\text{Notched Ult.}}{\text{Unnotched Yield}}$	1.13	1.19	+5	1.13	-5	

TABLE 9 (cont.)

AVERAGE MECHANICAL PROPERTIES TEST DATA

ALUMINUM ALLOY 6061 LW - HEAT TREATED AFTER WELDING

	Room Temp.	Control -423°F	Change- Room Temp. vs Control in Percent	Irrad. -423°F	Change- Control vs Irradiated in Percent	Threshold
UNNOTCHED						
Ultimate Strength-PSI	42,800	68,900	+61	70,700	+2.6	
Std. Deviation-PSI	1,400	2,200		4,700		
0.2% Yield Strength-PSI	37,400	54,300	+45	55,000	+1	
Std. Deviation-PSI	1,500	6,500		2,100		
% Elongation	3.0	6.0	+100	10.1	+68	
Std. Deviation-%	.4	2.4		3.4		
% Reduction in Area	33.4	16.6	-50	22.2	+34	
Std. Deviation-%	1.0	3.0		5.4		
Ult. Shear Strength-PSI						
Std. Deviation-PSI						
NOTCHED Kt = 6.3						
Ultimate Strength-PSI	45,200	57,300	+27	67,600	+18.0	T
Std. Deviation-PSI	2,000	8,000		1,340		
Ratio $\frac{\text{Notched Ult.}}{\text{Unnotched Ult.}}$	1.06	0.83	-22	0.96	+16	
Ratio $\frac{\text{Notched Ult.}}{\text{Unnotched Yield}}$	1.21	1.07	-12	1.23	+15	

TABLE 10

DETAILED MECHANICAL PROPERTIES DATA

ALUMINUM ALLOY 6061-T6

Specimen Number	Specimen Condition	Ultimate Strength Instron Cell (ksi)	Ultimate Strength Ram Cell (ksi)	Yield Strength 0.2% Offset(ksi)	Percent Reduction in Area	Percent Elongation
2-89	LN	75.24	62.10			
2-90	LN	75.47	71.94			
2-93	LN	72.12	60.92			
2-94	LN	72.43	68.15			
2-77	LU	78.80	64.46	49.8	34.1	26.8
2-78	LU	79.42	72.58	57.3	35.0	27.75
R-82	LU	79.36	71.63	57.0	41.9	25.0
R-83	LU	75.75	63.60	51.0	39.8	20.35
761	LU	77.00	72.80	60.0	39.4	20.75

Elongation Data

Specimen Number	Specimen Condition	Extensometer Post Irradiation (Mills)	Pull Rod Post Irradiation (Mills)	Pull Rod Control (Mills)	Bench Measurement Post Irradiation (Mills)	Bench Measurement Control (Mills)
2-77	LU	*553	626		536	
2-78	LU	-	579		555	
R-82	LU	530			500	
R-83	LU	613			407	
761	LU	-	546		415	
Average		565	584	577	483	482
% Elongation		19.9	20.6	20.4	24.1	24.1
% Damage			+1.		-	

Ultimate Shear Strength (KSI)

53.2
52.7
50.0
53.4

*Extensometer bottomed
True length is slightly more than 553 mills.

TABLE 10 (cont.)

DETAILED MECHANICAL PROPERTIES DATA

ALUMINUM ALLOY 6061, LW, AS WELDED

Specimen Number	Specimen Condition	Ultimate Strength Instron Cell (ksi)	Ultimate Strength Ram Cell (ksi)	Yield Strength 0.2% Offset(ksi)	Percent Reduction in Area	*Percent Elongation
727	LWN	38.94	35.16			
728	LWN	43.17	42.31			
3-114	LWN	53.76	45.63			
724	LWU	47.37	43.12	35.2	10.6	4.5
725	LWU	50.12	47.21	31.0	13.1	5.75
726	LWU	40.54	38.18	35.7	10.9	2.0
760	LWU	50.92	47.97	35.5	9.5	7.0

Elongation Data

Specimen Number	Specimen Condition	Extensometer Post Irradiation (Mills)	Pull Rod Post Irradiation (Mills)	Pull Rod Control (Mills)	Bench Measurement *Post Irradiation (Mills)	Bench Measurement Control (Mills)
724	LWU	76	81		90	
725	LWU	168	153		115	
726	LWU	21	40		40	
760	LWU	128	144		140	
Average		98	105	370	96	275
% Elongation		3.5	3.7	13.1	4.8	13.76
% Damage			-71.8		-65	

Ultimate Shear Strength

*Measured between welded tabs

TABLE 10 (cont.)

DETAILED MECHANICAL PROPERTIES DATA

ALUMINUM 6061-T6 - AS WELDED

Specimen Number	Specimen Condition	Ultimate Strength Instron Cell (ksi)	Ultimate Strength Ram Cell (ksi)	Yield Strength 0.2% Offset(ksi)	Percent Reduction in Area	*Percent Elongation
288	TWN	47.98	47.51			
721	TWN	43.21	36.33			
722	TWN	37.27	32.21			
723	TWN	38.45	35.85			
717	TWU	55.09	48.02	34.5	10.8	6.75
718	TWU	48.47	43.44	29.8	11.0	6.75
719	TWU	50.79	45.82	28.5	10.6	9.75
720	TWU	50.96	46.13	29.6	11.2	8.0

Elongation Data

		Extensometer	Pull Rod		Bench Measurement	
Specimen Number	Specimen Condition	Post Irradiation (Mills)	Post Irradiation (Mills)	Control (Mills)	*Post Irradiation (Mills)	Control (Mills)
717	TWU	145.7	155.3		135	
718	TWU	157.4	213.0		135	
719	TWU	176.1	252.5		190	
720	TWU	139.0	240.0		160	
Average		154.6	215.2	214.3	155	132
% Elongation		5.5	7.6	7.58	7.75	6.66
% Damage			+.02		+16.4	

*Measured between welded tabs

TABLE 10 (cont.)

DETAILED MECHANICAL PROPERTIES DATA
ALUMINUM 6061-T6, TW, HEAT TREATED AFTER WELDING

Specimen Number	Specimen Condition	Ultimate Strength Instron Cell (ksi)	Ultimate Strength Ram Cell (ksi)	Yield Strength 0.2% Offset(ksi)	Percent Reduction in Area	Percent Elongation
3-42	TWN	65.39	62.41			
3-44	TWN	71.61	68.04			
3-46	TWN	66.93	65.02			
3-31	TWU	77.71	74.46	59.0	32.1	9.25
3-32	TWU	77.84	73.32	57.8	23.4	11.85
3-35	TWU	67.36	65.10	57.0	21.0	3.4
3-36	TWU	78.35	73.81	56.5	32.8	11.7

Elongation Data

Specimen Number	Specimen Condition	Extensometer Post Irradiation (Mills)	Pull Rod Post Irradiation (Mills)	Pull Rod Control Mills	Bench Measurement Post Irradiation (Mills)	Bench Measurement Control (Mills)
3-31	TWU		257		185	
3-32	TWU	255	273		237	
3-35	TWU		119		68	
3-36	TWU		329		234	
Average		255	244	257	181	180
% Elongation		9.01	8.65	9.11	9.05	9.0
% Damage			-5.1		+.55	

TABLE 10 (cont.)

DETAILED MECHANICAL PROPERTIES DATA

ALUMINUM 6061-T6, LW, HEAT TREATED AFTER WELDING

Specimen Number	Specimen Condition	Ultimate Strength: Instron Cell (ksi)	Ultimate Strength: Ram Cell (ksi)	Yield Strength 0.2% Offset(ksi)	Percent Reduction in Area	Percent Elongation
3-90	LWN	73.00	66.59			
3-92	LWN	69.64	68.84			
3-94	LWN	71.45	68.87			
3-96	LWN	68.81	66.17			
3-78	LWU	80.07	73.94	57.1	19.4	11.25
3-80	LWU	80.27	72.84	53.0	28.4	12.75
3-82	LWU	63.39	65.32	54.9	18.7	6.25

Elongation Data

		Extensometer	Pull Rod		Bench Measurement	
Specimen Number	Specimen Condition	Post Irradiation (Mills)	Post Irradiation (Mills)	Control (Mills)	Post Irradiation (Mills)	Control (Mills)
3-78	LWU	246	328		225	
3-80	LWU	280	314		255	
3-82	LWU	119	151		125	
Average		215	264	177.5	202	120
% Elongation		7.6	9.3	6.28	10.1	6.0
% Damage			+43		+68	

The initial, large, increase in shear strength from room to liquid hydrogen temperature (87%) was followed by a small increase (5%) from radiation.

An increase in notched strength because of temperature decrease (39%) and radiation (7.2%) was obtained. The notched-to-unnotched strength ratio, however, showed decrease at liquid hydrogen temperature and no change from radiation, which indicates that the rate-of-change for notched strength is lower than that for unnotched. It should be noted that the ratio of notched-to-yield strength increased initially (22%) and then decreased by 9.9%. Since yield strength is usually used in the design, consideration should be given to this ratio. Stress-strain curves of all radiated specimen including average of irradiated, control, and room temperature data are presented in Figure 8.

(2) As Welded, Longitudinal

Caution should be exercised in evaluating this condition since the control and irradiated specimens were made from two different batches.

The ultimate tensile strength of 30.8 ksi at room temperature increased to 61.5 ksi (almost 100%) at liquid hydrogen temperature, and then decreased to 44.1 ksi (-28%). A continuous increase in yield strength was obtained. Notched strength was practically unaffected by radiation. Because of radiation, considerable loss in ductility, measured both in elongation and area reduction, was obtained (65% and 69% respectively). Additional testing of this alloy is suggested.

Also, while the notched strength was unaffected by radiation, notched-to-unnotched ratio increased by 36.8%. This effect is attributed to loss in ultimate strength rather than decrease in notch sensitivity. Notched-ultimate-to-unnotched-yield ratio decreased by 24%, which has more practical design value.

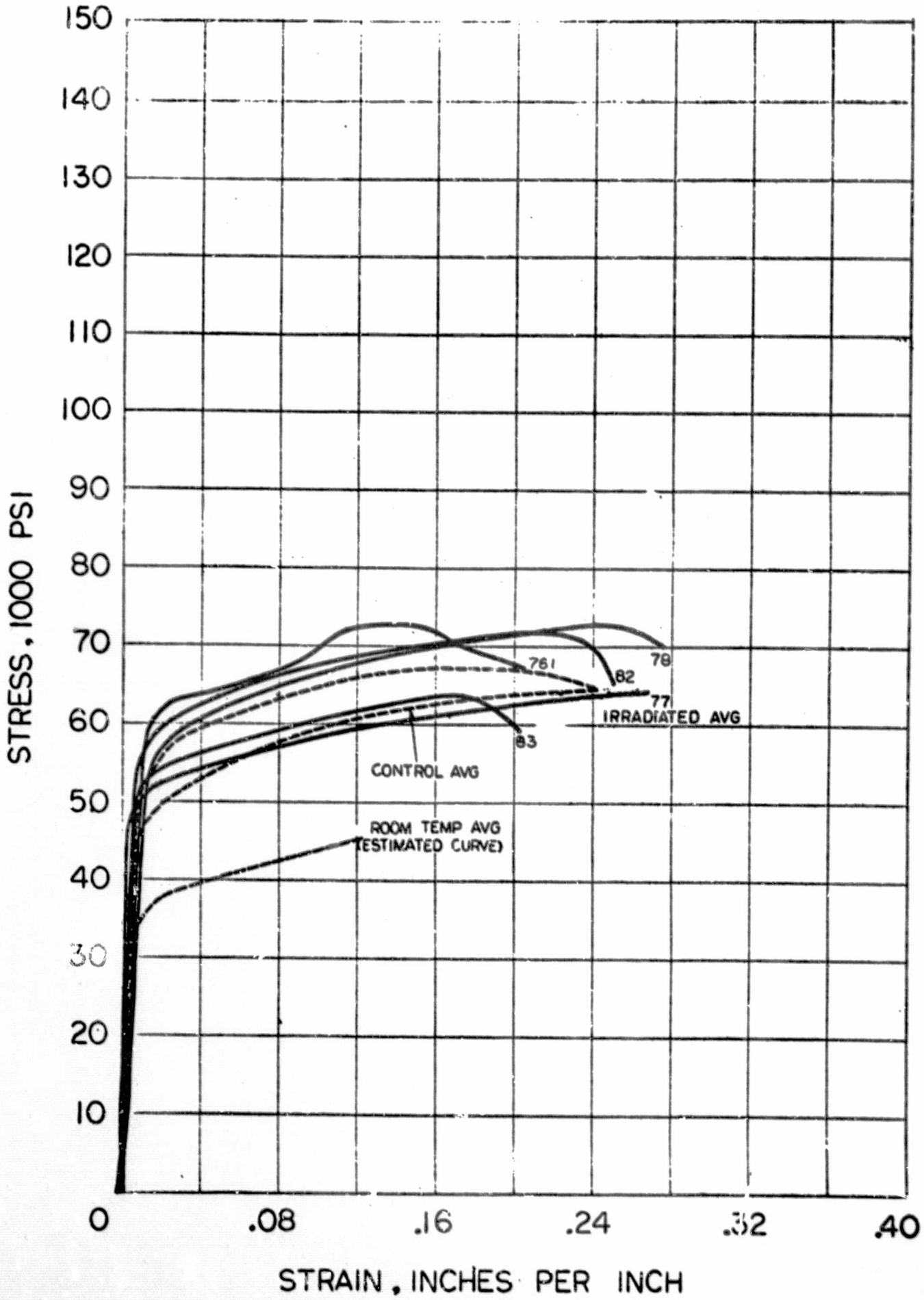

Figure 8

Stress - Strain Curves for 6061-T6 Aluminum - Parent Metal

Average stress-strain curves at room temperature liquid hydrogen temperature, and after radiation (together with individual stress-strain curves for irradiated specimens) are shown in Figure 9. (Strain data in Figure 9 is from extensometer).

Threshold level of damage was obtained for ultimate and yield strength, elongation, and area reduction.

(3) As-Welded, Transverse

Similar to the previous condition, specimens for control and irradiated material were made from two different batches. Changes in the mechanical properties of this alloy, at this condition, were similar to the property changes of the longitudinal as-welded condition. A sharp increase in ultimate (86%) and yield (85%) tensile strength from room temperature to liquid hydrogen temperature was followed by a decrease (16.4% and 9%, respectivelv) resulting from radiation. The ductility, as measured by area reduction, decreased by 35% because of liquid hydrogen temperature and was followed by additional decrease of 45% because of radiation. It is interesting to note that elongation increased as a result of both temperature decrease (39%) and radiation (16.4%). A continuous increase in notched ultimate strength was found similar to the parent and the welded heat-treated material. An increase of notched-to-unnotched ratio of 43% after radiation indicates reduction in notch sensitivity as compared to this value at liquid hydrogen temperature. This ratio increase is caused mainly by the drop in strength, and may not be valid measure of decreased notch sensitivity. Of more practical value, however, is the 31% increase in notched ultimate-to-yield strength ratio. This indicates that some annealing may take place during radiation.

Stress-strain curves for all irradiated specimens including their average, the average at room and liquid hydrogen temperature are shown in Figure 10. (Strain data in Figure 10 is from extensometer).

Threshold level of damage was reached for the ultimate tensile strength and area reduction.

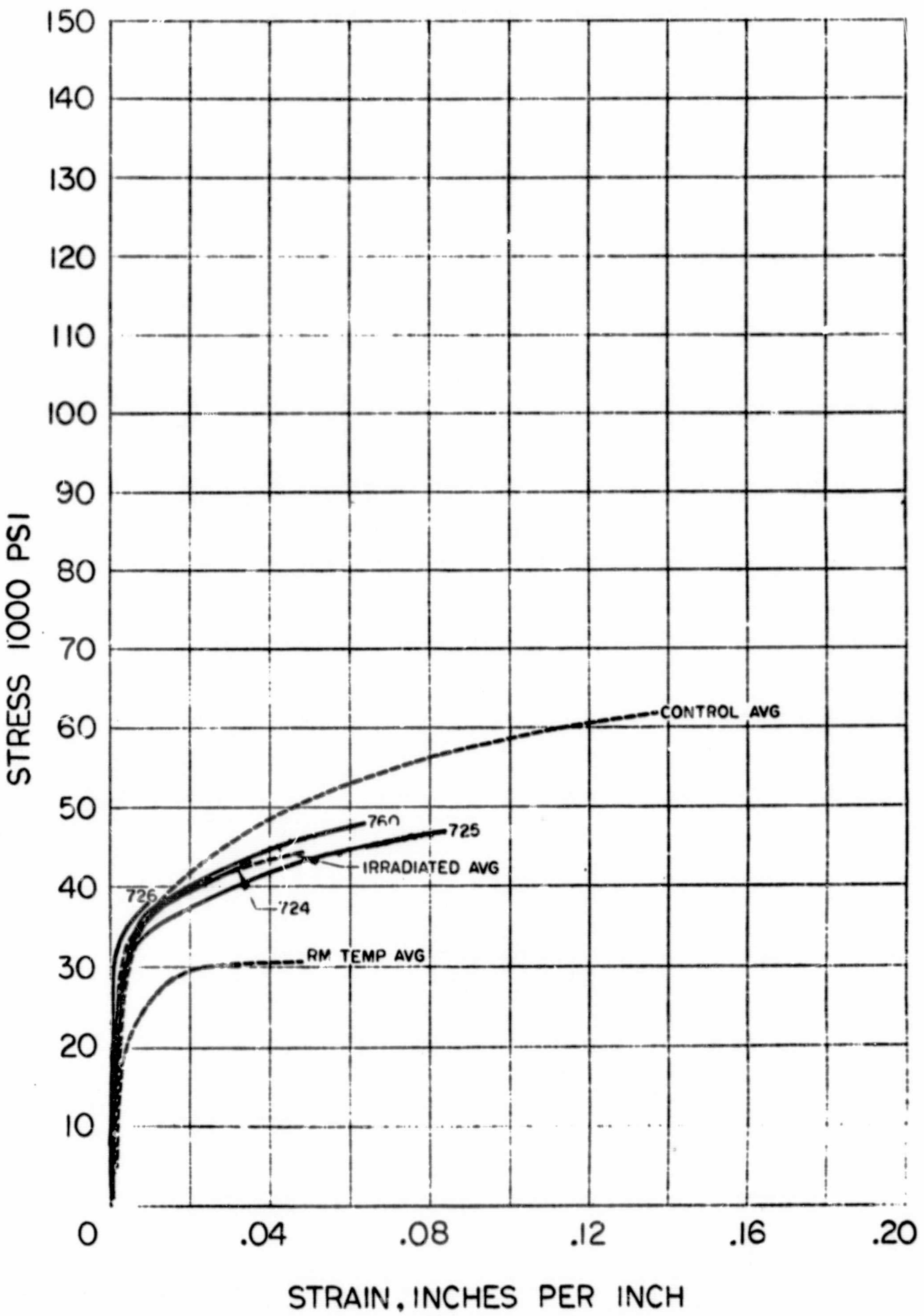

Figure 9

Stress - Strain Curve for 6061-T6 Aluminum - as-Welded, Longitudinal

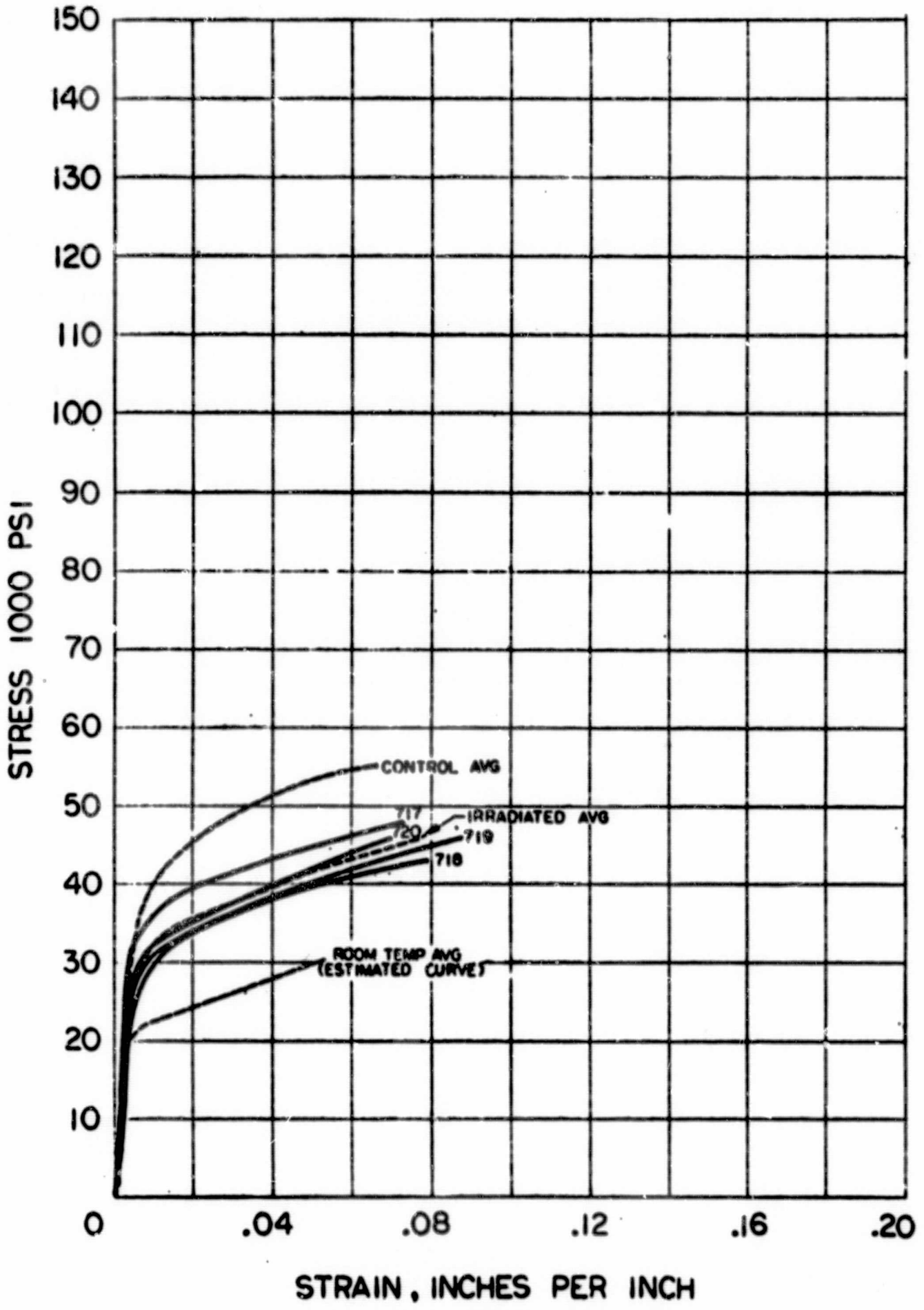

Figure 10

Stress - Strain Curves for 6061-T6 Aluminum - as-Welded, Transverse

(4) Heat Treated After Welding, Transverse

Data on properties at room temperature, and at liquid hydrogen temperature, both before and after radiation, were obtained from the same batch of material. Strength properties data (ultimate, yield and notched) continuously increased. The percent change caused by radiation is similar to the changes of parent metal, with percent change of yield strength (22%) being higher than the other. Notched-to-unnotched strength ratio increased, thus indicating slight decrease in notched sensitivity. A small decrease of the ratio notched-to-yield strength was obtained. The ductility behavior of this weldment is interesting. The elongation increased sharply by 157% from room to liquid hydrogen test temperature, then was practically unaffected by radiation, while the area reduction decreased initially by 23% and then was followed by 7% increase from radiation. Threshold level of damage was obtained for yield and notched strength.

Stress-strain curves for this condition at room temperature, in liquid hydrogen with and without radiation, including individual stress-strain curves for irradiated specimens are shown in Figure 11.

(5) Heat Treated After Welding, Longitudinal

Ultimate and yield tensile strength of this alloy was increased by radiation, however, at a much smaller rate than parent metal. The increase from room to liquid hydrogen temperature was larger, as compared to parent metal, and was closer to the percent increase of the longitudinal, as-welded, condition.

Notched tensile strength as well as notched-to-unnotched strength ratios increased. Compared with the preceding test conditions for 6061-T6 the ductility was greatly increased by radiation, 68% for elongation and 34% for reduction of area. The effect of lowering the temperature on this property was characterized with increase in elongation (100%) and decrease in area reduction (50%) similar to the transverse welded and heat treated condition. This indicates that heat treated joints as far as the radiation effect on ductility is concerned are not adversely affected.

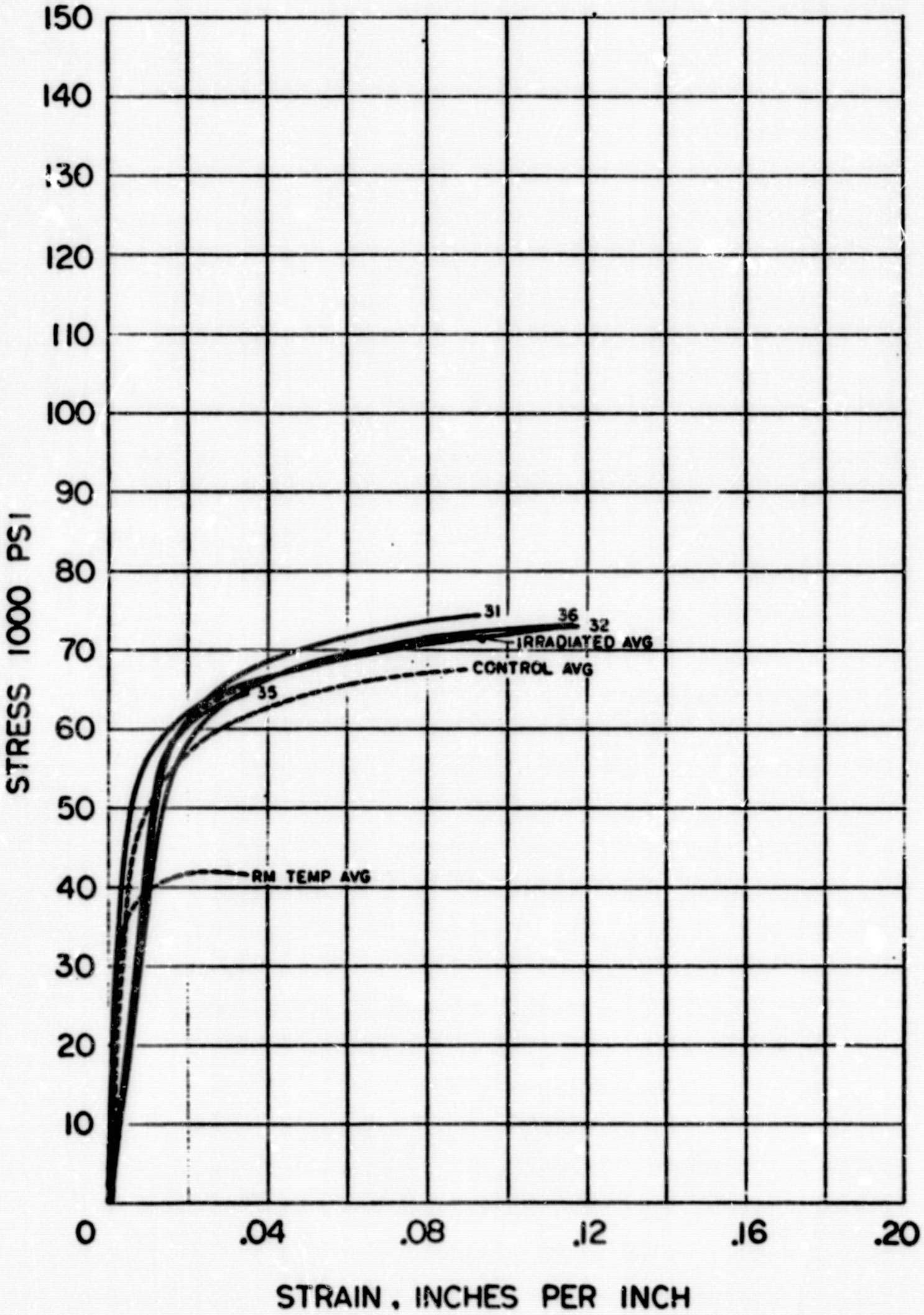

Figure 11

Stress - Strain Curves for 6061-T6 Aluminum - Welded and Heat Treated, Transverse

These conditions are evidenced in the stress-strain curves shown in Figure 12. In addition to the individual stress-strain curves for each irradiated specimen, average plots are shown for room temperature, control at LH_2 and irradiated.

Threshold level of damage for this condition was reached only for the notched strength.

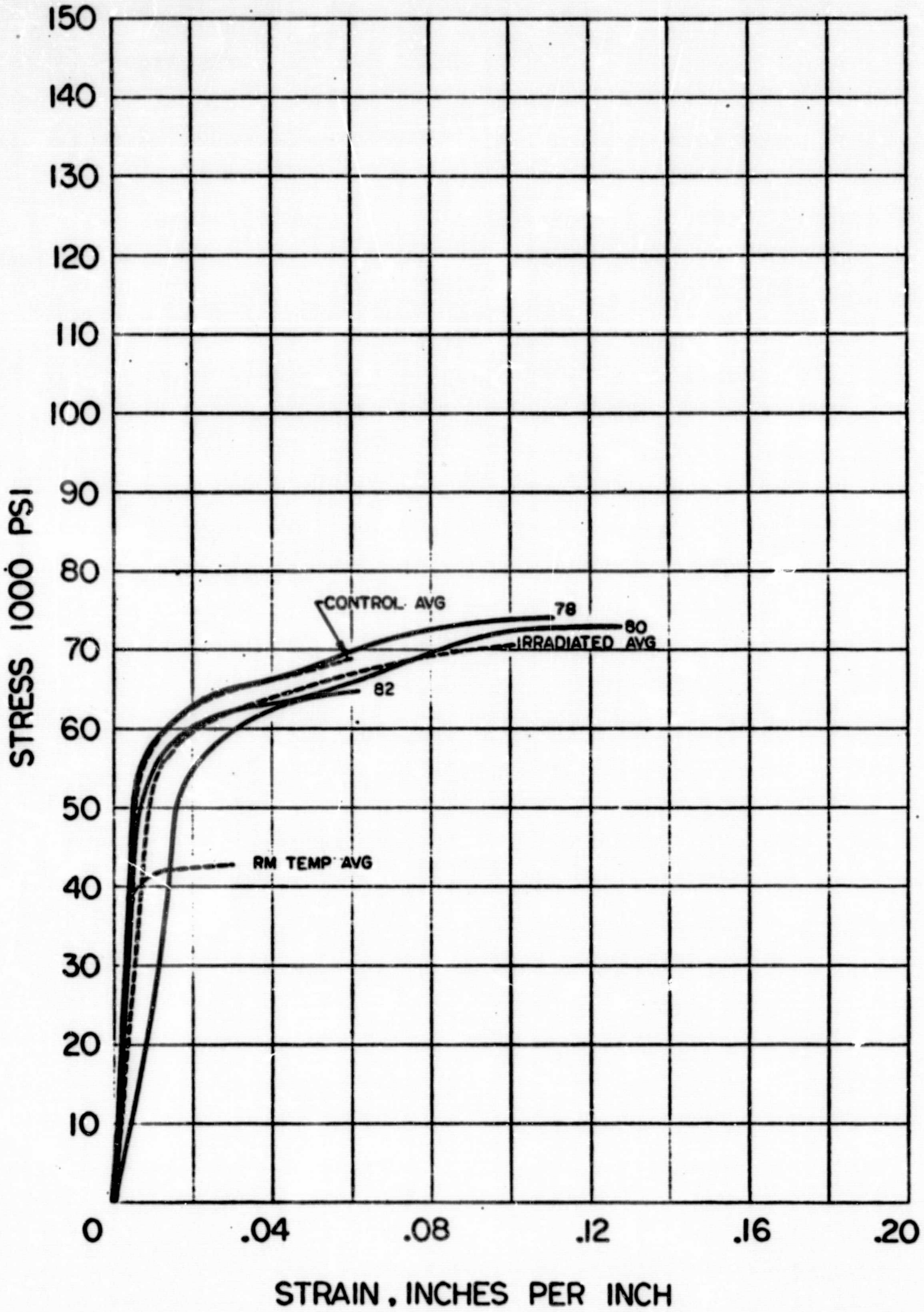

Figure 12

Stress - Strain Curves for 6061-T6 Aluminum - Welded and Heat Treated, Longitudinal

b. Metallography

Photomicrographs were made to illustrate pertinent features of the microstructure observed during examination of the strained fracture area and the unstrained area at one end of the specimen.

Microstructure of the 6061 alloy in the irradiated condition was compared with the control. Microphotographs are not included here, since the structure was not visibly altered by irradiation. The fracture was transgranular.

Figures 13, 14, 15 and 16 illustrate the microstructures of the as-welded and welded-and-heat-treated samples. The microstructures show the parent-metal to weld-metal interface and fracture surfaces with the grain boundaries accented in the heat affected zone of the matrix. The eutectic is more abundant in the weld-metal than in the base-metal because of the higher silicon content of the weld material. It was also noted that the dendritic pattern, typical of the weld metal in the control specimens and the welded-and-heat-treated, irradiated specimen, is not evident in the as-welded irradiated specimen. No explanation is available other than that the pattern is caused by a mode of solidification rather than as a result of the test and its environment. The fractures of the welded and heat treated samples were transgranular; those of the as-welded, transverse, specimens were primarily intergranular. The fractures of the as-welded, longitudinal, samples were partly intergranular and transgranular. Because the weld metal should be similar in all cases, the differences in mode of failure between the two as-welded directions were again attributed to solidification rather than test conditions.

Material: Aluminum 6061-T6

Form: 1/4" Plate

Specimen No.: TWU-3-36, LWU 3-80

Specification: QQA-327B, Cond T

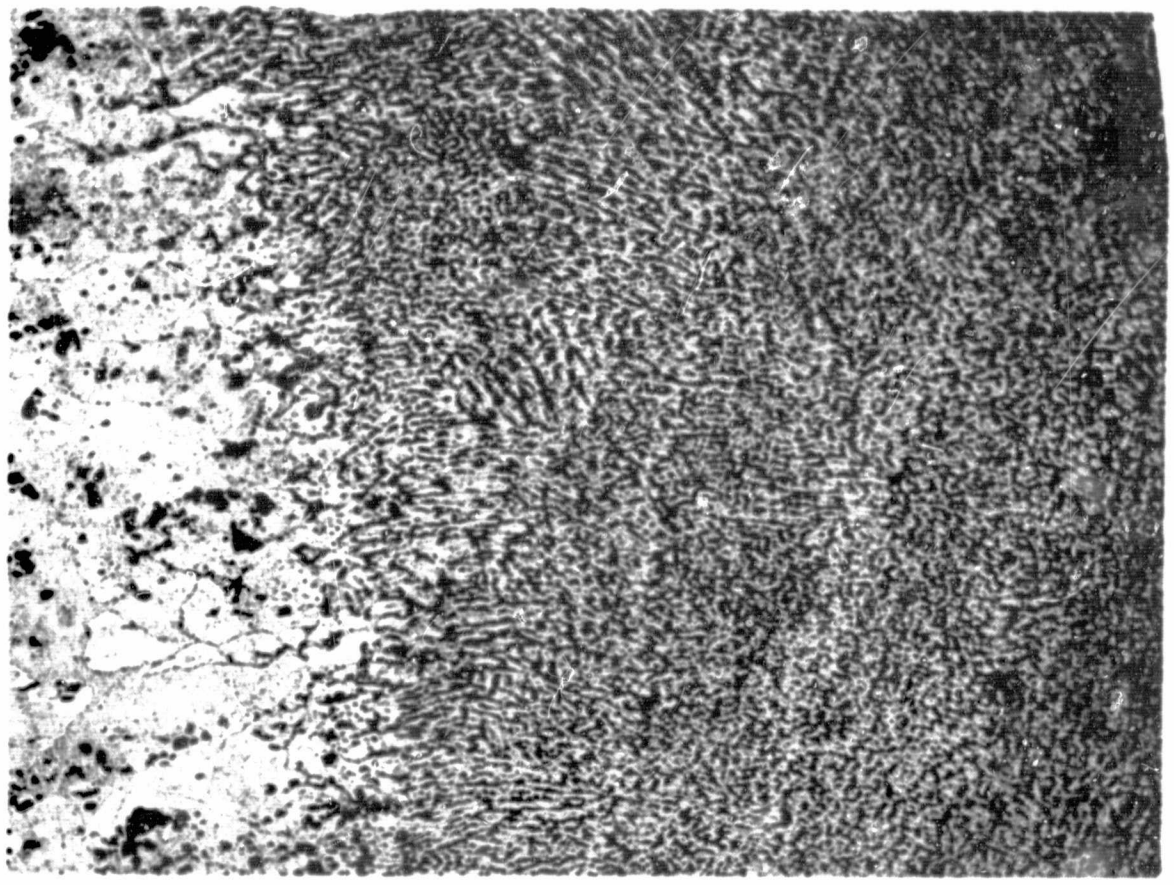

Condition: Irradiated-Welded-Heat Treated

Mag: 100X
Etchant: Keller's

The microstructure shows the parent metal (left) and the weld metal (right) interface. Note the pronounced grain boundaries of the heat affected zone in the matrix. (LWU-3-80)

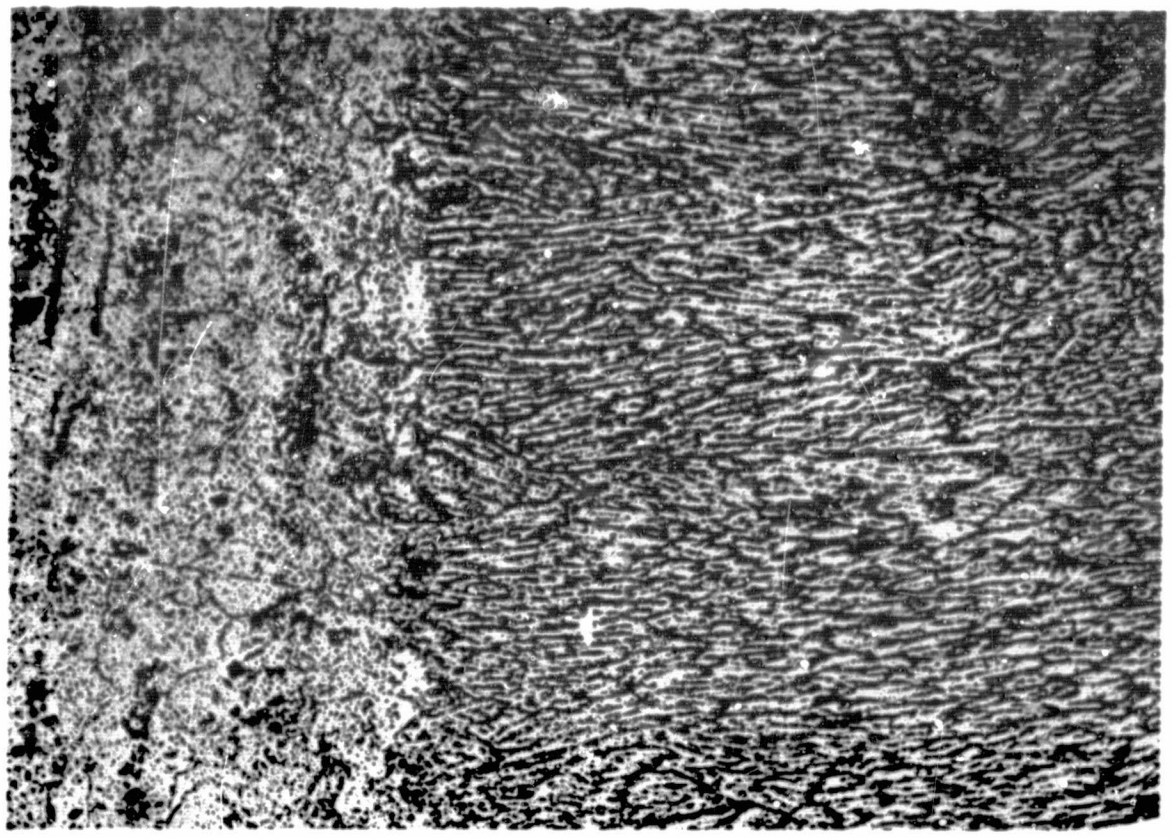

Condition: Irradiated-Welded-Heat Treated

Mag: 100X
Etchant: Keller's

The microstructure shows the parent metal (left) and the weld metal (right) interface of a sample welded transverse to the rolling direction. The grain boundaries are accented in the heat-affected zone of the matrix. (TWU 3-36)

Figure 13

Aluminum 6061 T6 - Irradiated-Condition TW and LW-Welded-Heat Treated Parent Metal-Weld Metal Interface -100X

Material: Aluminum 6061-T6
Form: 1/4 in. Plate
Identification: Specimen LWU 726
Specification: QQA-327B, Cond. T

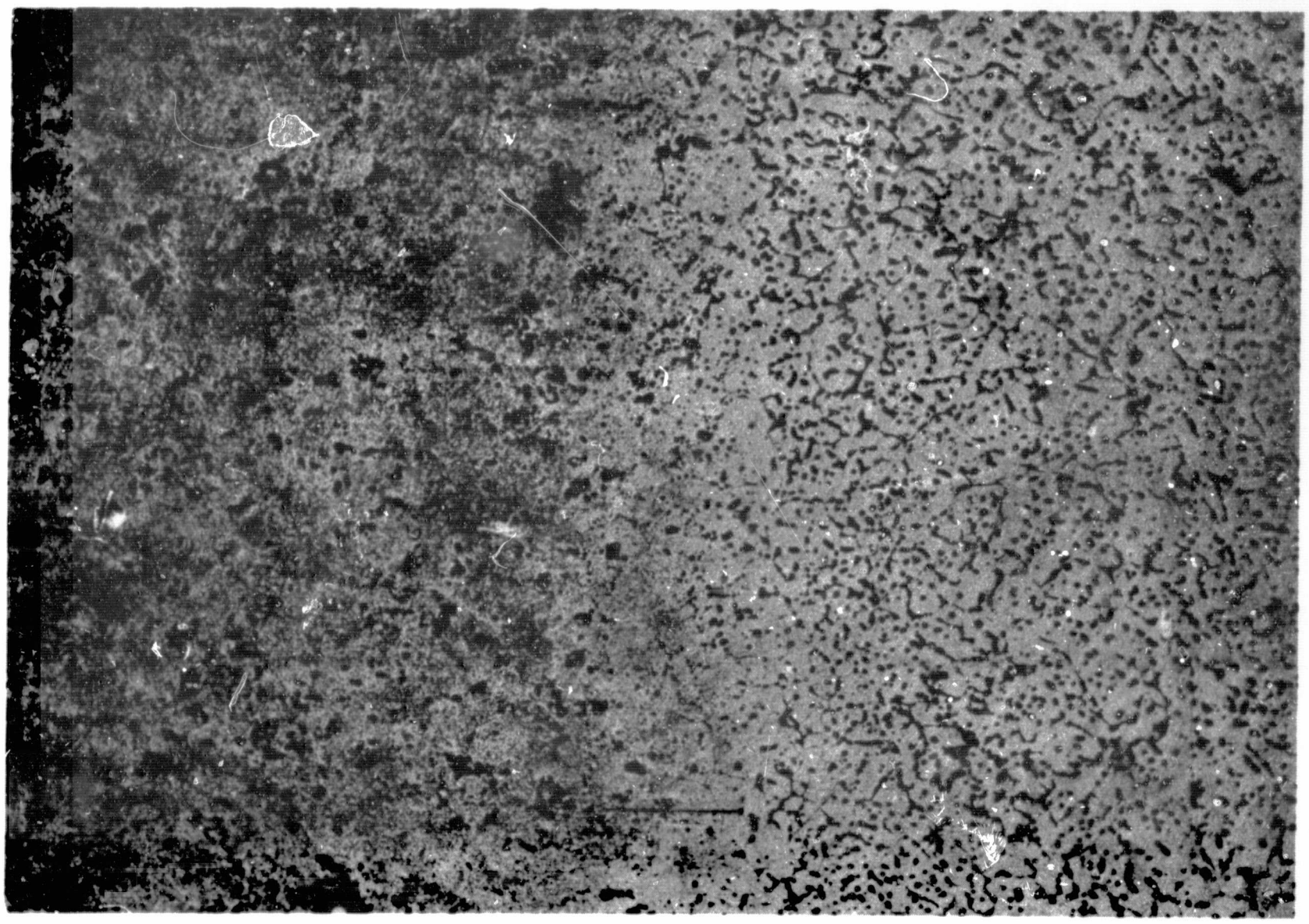

Condition: Irradiated - Welded
Mag: 100X
Etchant: Keller's

The microstructure shows the structure of the as-welded material, the heat-affected zone and the base metal.

Figure 14

Aluminum 6061-T6 - Irradiated - Condition LW - Irradiated - Weld Metal Interface - 100X

Material: Aluminum 6061 T6

Form: 1/4" Plate

Specimen No.: LWU 3-80, LWU 726

Specification: QQA 327B, Cond T

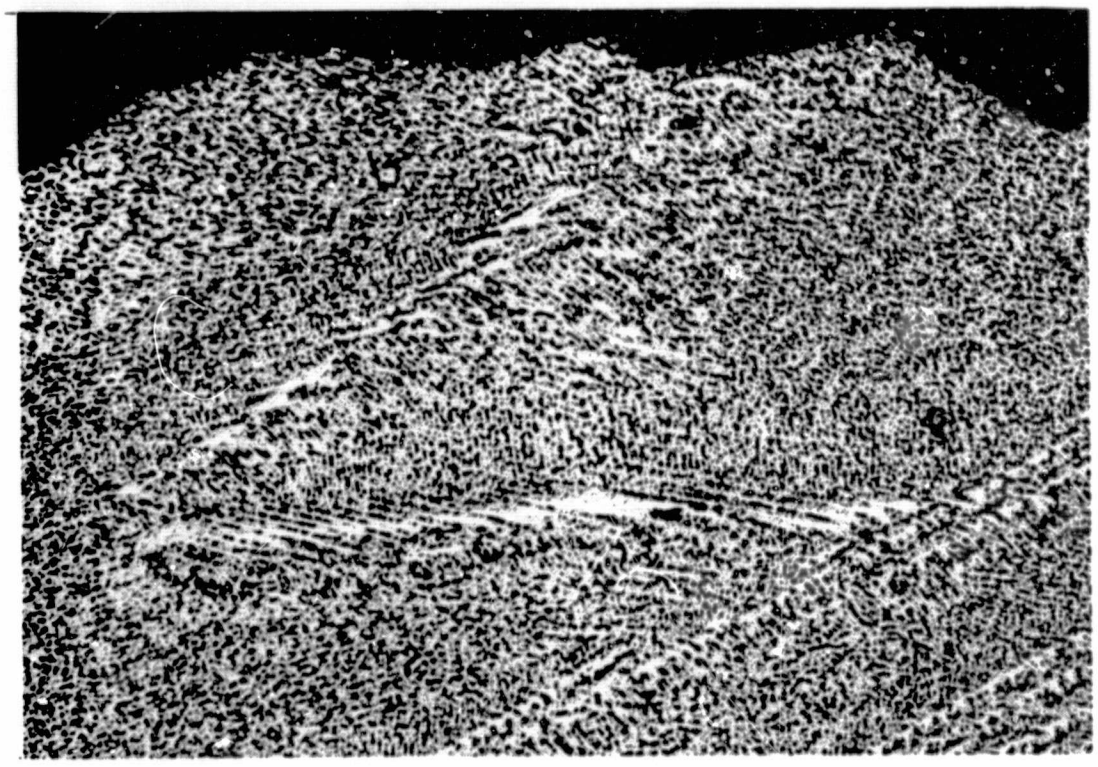

Condition: Irradiated-Welded-Heat Treated Weld Zone-Fracture

Mag: 100X
Etchant: Keller's

The microstructure shows the dendritic pattern in the weld zone and the transgranular nature of the fracture through the weld. This type of fracture is typical of both the longitudinal and transverse test specimens (LWU 3-80)

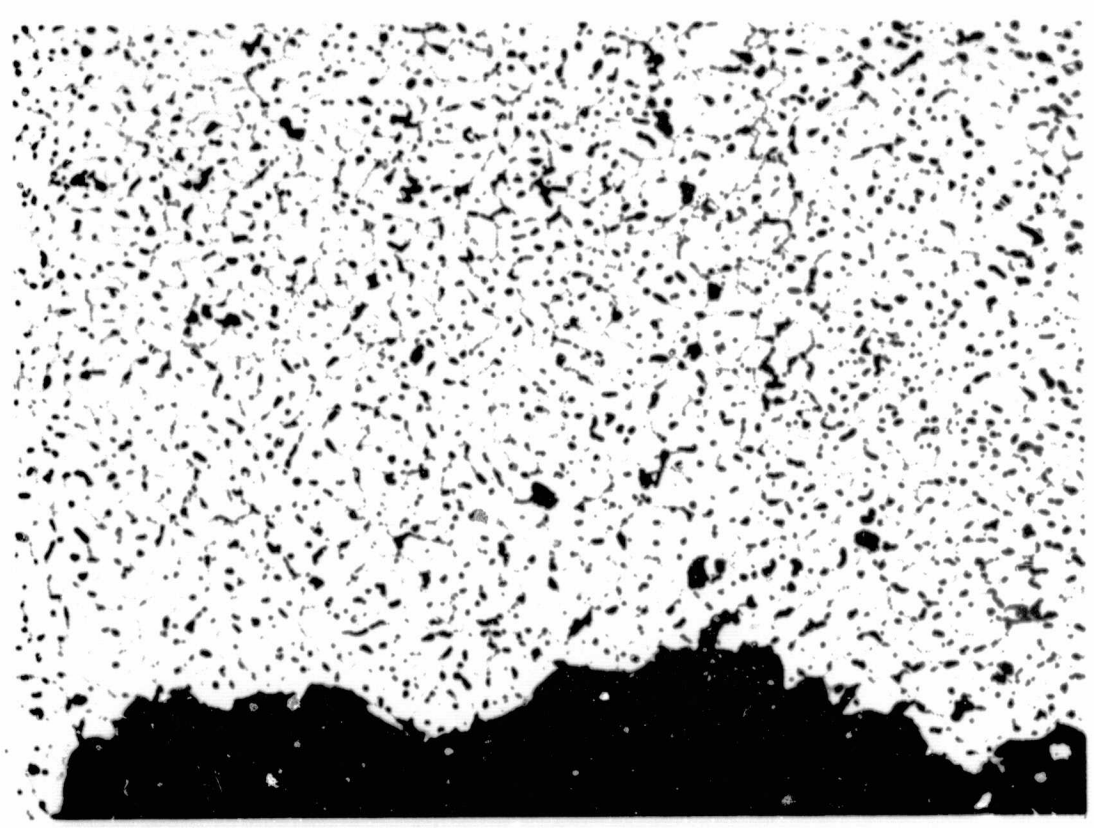

Condition: Irradiated Welded-Weld Zone-Fracture

Mag: 100X
Etchant: Keller's

The microstructure shows the structure of the untreated weld material. The fracture path appears to be partly intergranular and partly transgranular (LWU 726)

Figure 15

Aluminum 6061-T6 - Irradiated-Condition LW-Weld Zone Fracture Edge
100X Magnification

Material: Aluminum 6061-T6
Form: 1/4 in. Plate
Identification: Specimen TWU 717

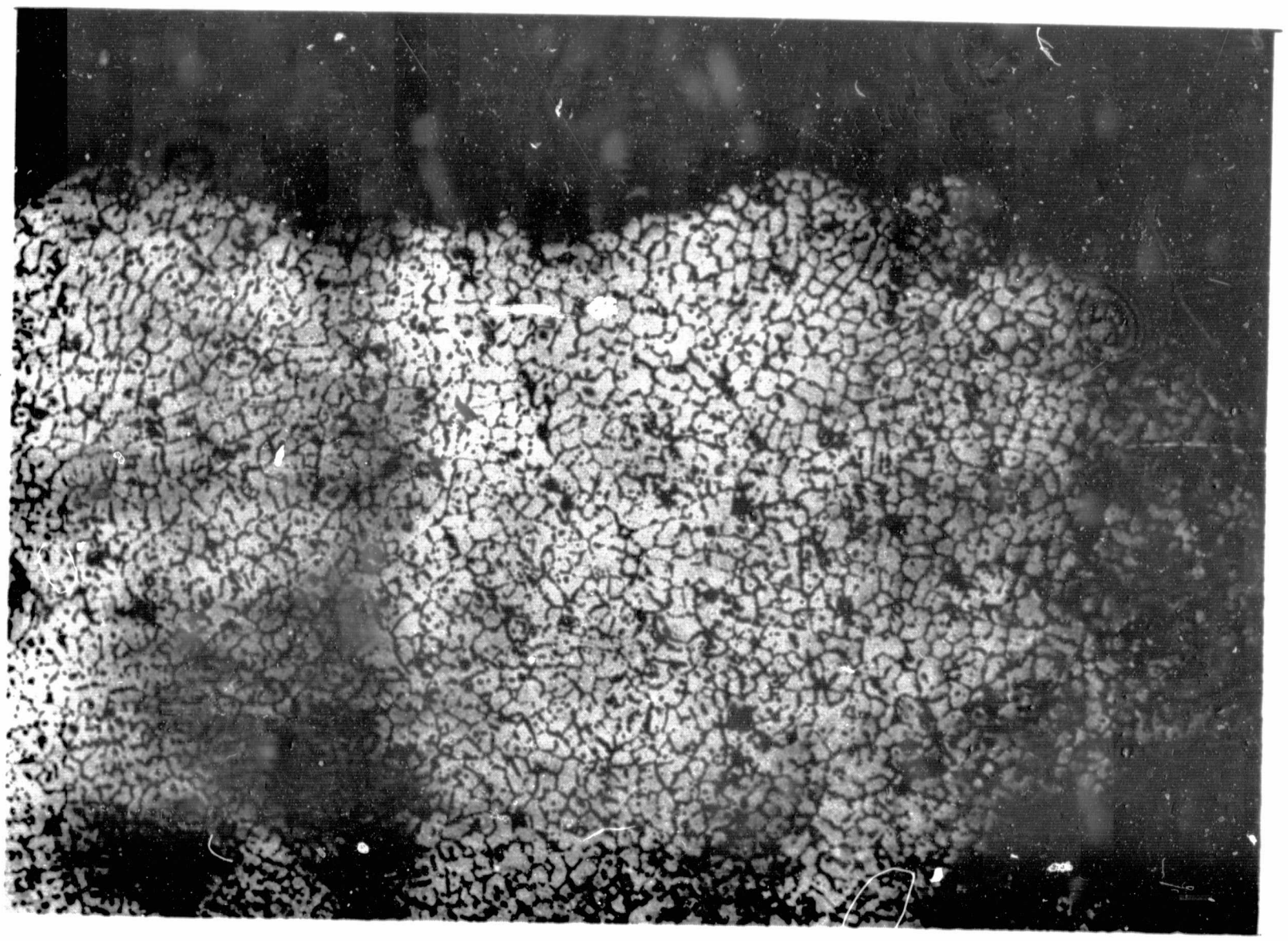

Condition: Irradiated - Welded
Mag: 100X
Etchant: Keller's

The fracture profile shows a failure that is primarily intergranular through and along the brittle eutectic.

Figure 16

Aluminum 6061-T6 - Irradiated - Condition TW - As-welded
100X Fracture Edge

c. Electron Microscopy

A typical electron micrograph of the irradiated specimen in the aged condition as well as in the welded and welded-and-heat treated condition is found in Reference 7. The microstructure is typical of a solid solution aluminum alloy with insolubles and no effects were noted as a result of irradiation.

Electron fractographs of the irradiated 6061 alloy in the T6 condition are shown in Figure 17 (top). The fracture mode consists of a series of dimples and is basically ductile. The failure mechanism is essentially the same for both the notched and unnotched irradiated and unirradiated specimens.

The fracture mode of the 6061 alloy welded in the longitudinal direction and heat treated is shown in Figure 17 (bottom). The fracture at center and edge is made up of dimples and in areas appears to follow the eutectic/matrix interface.

The fractographs of the 6061 alloy welded in the transverse direction and heat treated are shown in Figure 18 (top). The fracture surface of both the unnotched and notched samples show a dimple structure typical of ductile failure. In some areas, the fracture appears to follow the eutectic/matrix interface. Variation in dimple form is a result of inclusion, sites and consequently domain origins; no difference was noted between the control or irradiated samples which could be associated with irradiation effects.

The fracture surfaces of the 6061 alloy tested in the notched and unnotched condition and in the as-welded condition, are shown in Figure 18 (bottom). The fracture at the center of the unnotched specimen was mixed brittle and ductile, while the fracture at the edge was primarily brittle. The fracture mechanism of the notched specimen was identical to the edge of the unnotched specimen and was essentially brittle. The mixed failure mode of the center section was probably from the segregated structure of the weld. The fracture is mainly through the brittle eutectic and along the eutectic/matrix interface.

Material: Aluminum 6061 T651

Form: 1/4" Plate

Specimen No.: LU R-83, LWU 3-80

Specification:

Condition: Irradiated-Unnotched-Fractograph-Center, LU-R-83

Mag: 4200X

The fracture surface at the center of the specimen is made up almost entirely of oriented dimples formed by microvoid coalescence. The flat area in the lower left-hand corner represents the fracture of a brittle intermetallic compound.

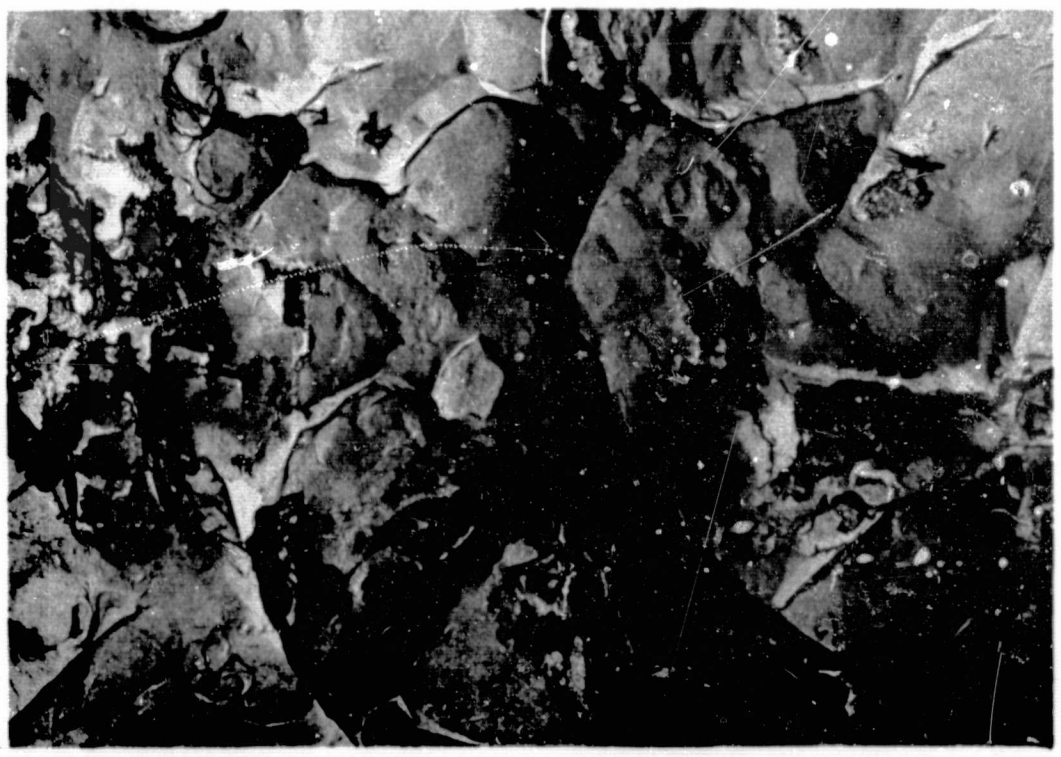

Condition: Irradiated-Welded-Treated-Unnotched-Fractograph-Center-LWU3-80

Mag: 4200X

The topography of the fracture has the characteristics of a dimple rupture. Failure occurred along the eutectic matrix interface and through the eutectic.

Figure 17

Aluminum 6061-T6 - Irradiated-Condition L and LW Heat Treated-Unnotched-Fractograph-4200X

Material: Aluminum 6061-T6

Form: 1/4" Plate

Specimen No.: TWU 3-36, LWU 726

Specification:

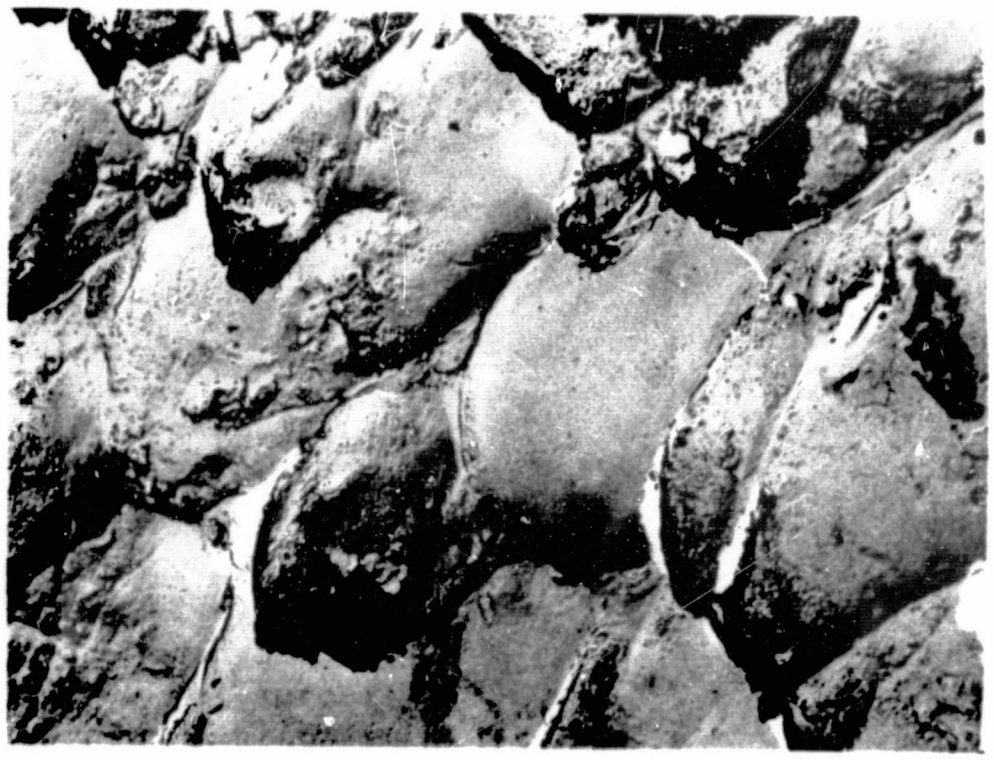

Condition: Irradiated-Welded, Heat Treated-Unnotched Fractograph-Edge (TWU 3-36)

Mag: 4200X

The surface near the edge of the fracture shows an oriented dimple rupture. There is evidence of failure through and around the eutectic. That surface condition is thought to be oxidation.

Condition: Irradiated-"As-Welded"-Unnotched Fractograph-Center (LWU 726)

Mag: 4200X

The fractograph of the center area shows a dimple rupture. Certain areas show the failure through the brittle eutectic; the fracture was transgranular within this area.

Figure 18

Aluminum 6061-T6 - Irradiated-Condition TW-Welded, Heat Treated- and LW-As Welded. Fractograph 4200X

d. X-ray Diffraction

The X-ray diffraction data are shown in Table 11. The X-ray diffraction pattern of the as-received, 6061 aluminum showed the typical face-centered-cube structure. The orientation was found to be in the (111) - (200) directions.

The 6061-T6 specimen was examined both in the area adjacent to the tensile fracture and in the grip (unstrained) area. The crystallographic orientation was found to be in the (100) direction for both areas. The lattice parameter of the unstrained area was essentially the same as the as-received material. The lattice parameters and microstress levels of the irradiated specimens were consistent with those of the control specimens but were slightly changed, however, within the experimental error.

TABLE 11

Material: Aluminum 6061-T6

X-RAY DIFFRACTION DATA-6061-T6
CONTROL

	Pure Aluminum		As-Received		6061T6 Specimen LU-2-81 Strained		6061T6 Specimen LU-2-81 Unstrained		6061L Specimen LWU-105 Strained		6061T Specimen TWU-2-273 Strained		6061T Specimen TWU-2-273 Unstrained		6061T6L Specimen LWU-3-81 Strained		6061T6L Specimen LWU-3-81 Unstrained		6061T6T Specimen TWU-2-271 Strained		6061T6T Specimen TWU-2-271 Unstrained	
	1	2	1	2	1	2	1	2	1	2	1	2	1	2	1	2	1	2	1	2	1	2
111	2.338	100	2.34	100	--	--	2.32	29	2.32	64	2.33	62	2.34	82	2.32	38	2.34	66	2.33	46	2.34	82
200	2.024	47	2.03	100	2.01	100	2.02	100	2.02	100	2.02	100	2.03	100	2.03	100	2.03	100	2.02	100	2.03	100
220	1.431	22	1.43	10	1.48	20	1.43	67	1.43	74	1.43	80	1.41	85	1.43	72	1.43	43	1.43	80	1.41	85
311	1.221	24	1.22	8	1.21	85	1.22	34	1.22	40	1.22	40	1.20	29	1.22	54	1.22	19	1.22	35	1.20	29
222	1.169	7	1.17	2					1.17	7	1.17	7	--	--	1.17	7	1.17	10	--		--	
400	1.012	2	1.01	4	1.03	18	1.01	14	1.01	17	1.01	14	1.00	43	1.01	17	1.01	36	1.01	19	1.00	43
331	0.929	8	--	--					0.929	9	0.929	10	--	--	0.929	10	0.930	17	--		--	
LATTICE PARAMETERS (A°)																						
	4.0494		4.054		4.054		4.056		4.049		4.054		4.041		4.054		4.057		4.050		4.041	
MICROSTRESS, Δ 2θ																						
			0.63° (2θ = 117°)		0.48° (2θ = 78°)		0.36° (2θ = 78°)		0.51° (2θ = 78°)		0.44° (2θ = 78°)		0.39° (2θ = 78°)		0.43° (2θ = 78°)		0.33° (2θ = 78°)		0.45° (2θ = 78)		0.39° (2θ = 78°)	

TABLE 11 (cont.)
IRRADIATED

	6061T6				6061L				6061T				6061T6L				6061T6T			
	Specimen LUR-83				Specimen LWU 726				Specimen TWU 717				Specimen LWU 3-80				Specimen TWU 3-36			
	Strained		Unstrained		Strained		Unstrained		Strained		Unstrained		Strained		Unstrained		Strained		Unstrained	
	1	2	1	2	1	2	1	2	1	2	1	2	1	2	1	2	1	2	1	2
111	2.34	20	2.34	60	2.34	30	2.34	50	2.34	20	2.35	65	2.34	21	2.35	7	2.34	25	2.35	35
200	2.03	100	2.03	100	2.03	100	2.03	100	2.03	100	2.03	100	2.03	100	2.03	100	2.03	100	2.03	100
220	1.40	30	1.40	55	1.43	8	1.43	35	1.43	15	1.43	55	1.43	14	1.44	25	1.43	30	1.44	20
311	1.20	15	1.20	30	1.22	10	1.22	18	1.22	10	1.22	30	1.22	9	1.22	4	1.22	10	1.22	78
222					1.17	3	1.17	2			1.17	4					1.17	1	1.17	2
400	1.00	5	1.00	3	1.01	7	1.01	6	1.01	4	1.01	5	1.01	3	1.01	8	1.01	4	1.01	5
331	0.92	2	0.92	6	0.93	3	0.93	6	0.93	3	0.93	6	0.93	2	0.91	2	0.93	3	0.93	2

LATTICE PARAMETERS (A°)

4.037	4.036	4.043	4.042	4.049	4.035	4.040	4.039	4.038	4.041

MICROSTRESS, $\Delta 2\theta$

0.60°/0.38° (2θ= 80.2°/ 44.7°)	0.46°/0.32° (2θ = 80.0°/ 44.65°)	0.42°/0.30° (2θ = 78.15°/ 44.7°)	0.46°/0.34° (2θ = 78.1°/ 44.6°)	0.46°/0.32° (2θ = 78.0°/ 44.6°)	0.46°/0.32° (2θ = 78.05°/ 44.55°)	0.56°/0.40° (2θ = 78°/ 44.6°)	0.46°/0.30° (2θ = 78°/ 44.6°)	0.54°/0.36° (2θ = 78.2°/ 44.7°)	0.36°/0.26° (2θ = 78°/ 44.5°)

3. 7075-T6- (Al - Zn Wrought Alloy)

a. Mechanical Properties

Table 12 presents the average values and standard deviations of mechanical properties obtained at room temperature, at the temperature of liquid hydrogen as control, and at liquid hydrogen temperature in a nuclear radiation environment. Detailed test results for the irradiated material without warmup are shown in Table 13.

The general trend of increase in strength property from room temperature to liquid hydrogen temperature without, and then with, radiation, was found for ultimate and yield tensile strength. The percent increase in strength because of liquid hydrogen temperature (34% and 25%) was much larger than that caused by radiation (3% and 10%). After a rather substantial (81%) initial increase in shear strength from room to liquid hydrogen temperature, a 15.7% decrease was obtained because of radiation. A reversed trend was observed for the notched strength: initial decrease of 13% caused by the cryogenic temperature was followed by 6.9% increase from radiation. A similar trend was obtained for the notched-to-unnotched strength ratio.

The substantial decrease in ductility resulting from the liquid hydrogen temperature (measured both by elongation (49%) and area reduction (48%) was followed by an additional decrease in elongation (9.4%) caused by radiation and a small increase in area reduction (11.6%).

Stress-strain curves obtained with the extensometer are shown in Figure 19.

The threshold level of damage for this alloy was obtained for shear strength.

TABLE 12

AVERAGE MECHANICAL PROPERTIES TENSILE TEST DATA

ALUMINUM ALLOY, 7075-T6 -

	Room Temp.	Control -423°F	Change Room Temp. vs Control in Percent	Irrad. -423°F	Change Control vs Irradiated in Percent	Threshold
UNNOTCHED						
Ultimate Strength-PSI	82,400	110,400	+34	113,400	+2.7	
Std. Deviation-PSI	1,000	7,700		2,400		
0.2% Yield Strength-PSI	76,000	94,900	+25	104,300	+10	
Std. Deviation-PSI	550	8,600		1,850		
% Elongation	12.6	6.4	-49	5.8	-9.4	
Std. Deviation-%	.75	1.1		1.1		
% Reduction in Area	25.0	12.9	-48	14.4	+11.6	
Std. Deviation-%	1.3	1.7		0.9		
Ult. Shear Strength-PSI	52,500	95,200	+81	80,300	-15.7	T
Std. Deviation-PSI	390	5,300		3,530		
NOTCHED Kt 6.3						
Ultimate Strength-PSI	81,000	70,600	-13	75,500	+6.9	
Std. Deviation-PSI	1,600	8,400		4,800		
Ratio $\frac{\text{Notched Ult.}}{\text{Unnotched Ult.}}$	0.98	0.64	-35	0.67	+4.7	
Ratio $\frac{\text{Notched Ult.}}{\text{Unnotched Yield}}$	1.06	0.74	-30	0.72	-3	

TABLE 13

DETAILED MECHANICAL PROPERTIES DATA

ALUMINUM ALLOY, 7075-T6

Specimen Number	Specimen Condition	Ultimate Strength: Instron Cell (KSI)	Ultimate Strength: Ram Cell(KSI)	Yield Strength 0.2% Offset(ksi)	Percent Reduction in Area	Percent Elongation
113	LN	70.79	69.0			
114	LN	81.85	77.59			
117	LN	81.44	80.15			
118	LN	80.68	75.27			
101	LU	121.94	111.13	102.0	14.2	7.0
102	LU	118.1	111.6	104.0	15.7	5.0
105	LU	120.1	115.4	104.5	13.5	4.75
106	LU	119.8	115.5	106.5	14.3	6.5

ELONGATION DATA

		Extensometer	Pull Rod		Bench Measurement	
Specimen Number	Specimen Condition	Post Irradiation (Mills)	Post Irradiation (Mills)	Control (Mills)	Post Irradiation	Control (Mills)
101	LU	202			140	
102	LU		204		100	
105	LU	144	227		95	
106	LU		246		130	
Average		173	226	274	116	128
% Elongation		6.1	8.0	9.7	5.8	6.4
% Damage			-17.6		-9.4	

Ultimate Shear Strength (KSI)

83.1

83.1

79.1

75.8

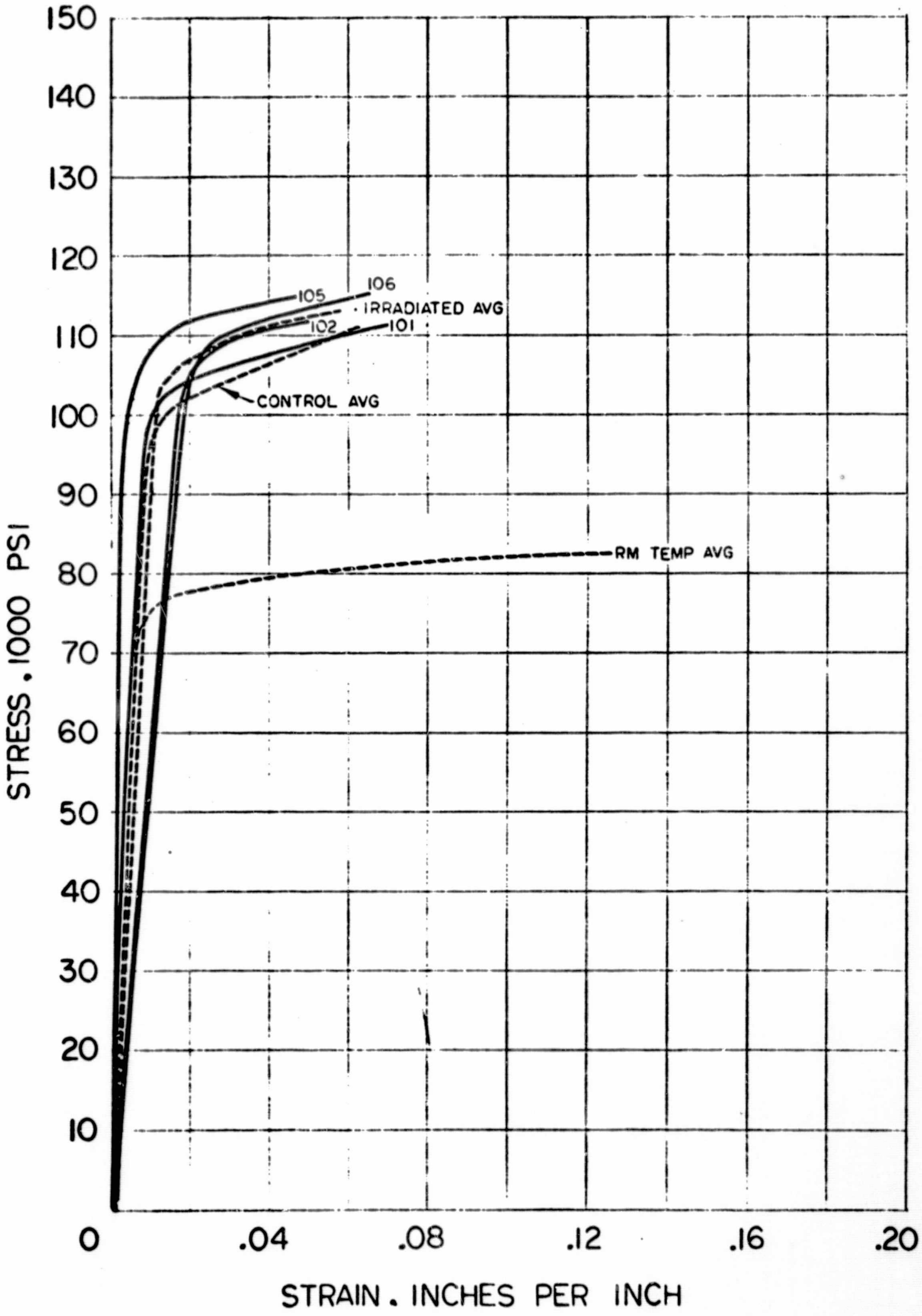

Figure 19

Stress - Strain Curves for 7075-T6 Aluminum

b. Metallography

Photomicrographs were made to illustrate the pertinent features of the microstructure observed during examination of the strained fracture area and of an unstrained area at one end of the specimen.

The microstructure of the irradiated material was unchanged from that of the as-received or control material. It was a solid solution of aluminum containing a fine precipitate and non-metallic inclusions. No variation was evident between strained or unstrained regions, and fracture remained typically transgranular. Photomicrographs may be found in References 2 and 7 and are not included in this report.

c. Electron Microscopy

Electron photomicrographs were taken (at 15000X) to illustrate typical microstructures at high magnifications. Both strained and unstrained areas from the irradiated specimens were examined.

The electron micrographs of the irradiated 7075-T6 material were not typical of those shown for the control samples. It is felt that the difference was caused by the metallographic procedure. Consequently, it should be noted that the electron micrographs of the irradiated material cannot be compared with those of the as-received or control materials. The micrographs of the strained and unstrained areas were identical; hence, only the unstrained structure was shown (see Figure 20).

Fractographs of the irradiated material in the unwelded condition are shown in Figure 21. The microstructures of the unnotched sample (top) is typical of center and edge locations, showing a glide-plane decohesion fracture mode with some intergranular fracture. The fractograph of the notched specimen shows small microvoid regions and some intergranular fracture.

Material: Aluminum 7075-T6
Form: 1/4 in. Plate
Identification: Specimen No. LU 106
Specification: QQA 283A, Cond. T

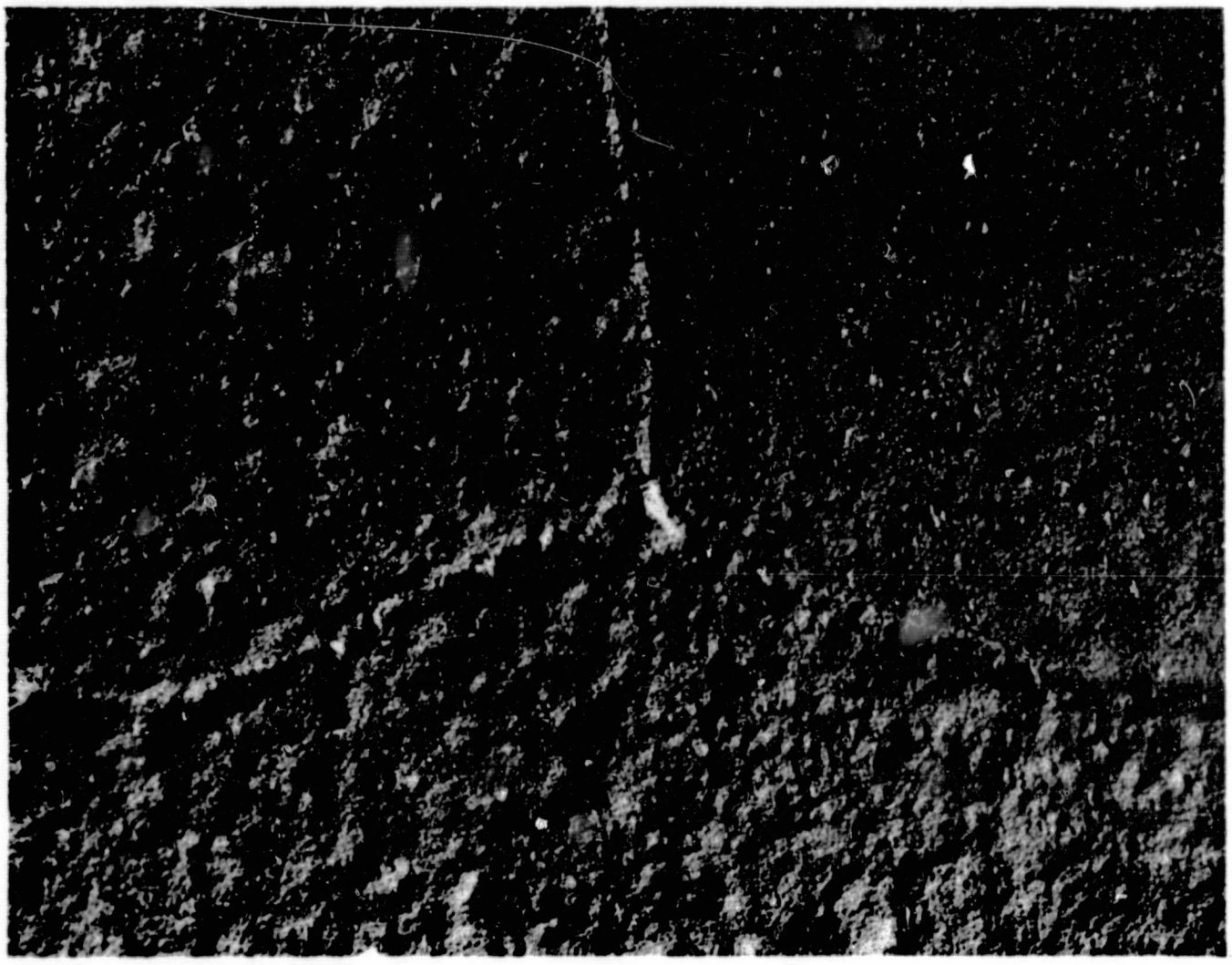

Condition: Irradiated - Unstrained
Mag: 15000X
Etchant: Keller's

The electron micrograph shows the solid-solution aluminum matrix with a grain boundary interaction and fine insolubles. The structure is typical for the strained and unstrained conditions.

Figure 20

Aluminum 7057-T6 - Condition L - Electron Micrograph - 15000X

Material: Aluminum 7075-T6

Form: 1/4" Plate

Specimen No.: LU 106, LN 113

Specification: QQA 283A Cond T

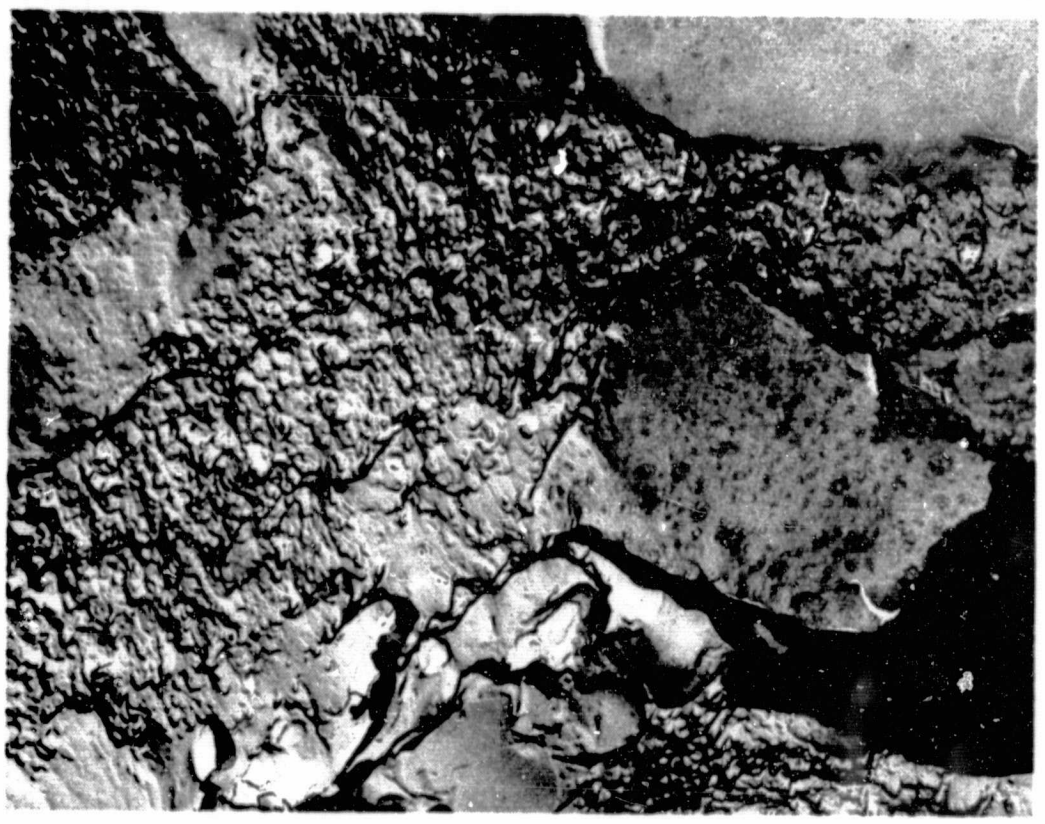

Condition: Irradiated
Fracture
Unnotched (LU 106)

The fracture near edge of specimen is made up of glide-plane decoheuion, small oriented microvoids and some intergranular fracture.

Condition: Irradiated
Fracture
Notched (LN 113)

The fractograph of the notched specimen shows small microvoid regions and some intergranular fracture.

Figure 21

Aluminum 7075-T6, Irradiated Fracture - Notched and Unnotched, Fractograph - 4200X

d. X-Ray Diffraction

The X-ray diffraction pattern of the as-received and control material showed the typical face-centered cubic crystal structure of aluminum. Orientation was found to be in the (200) direction.

There was no apparent change in crystallographic properties associated with the cryogenic test environment.

The X-ray diffraction data for the irradiation study (in Table 14) shows a preferred orientation in the (200) direction. The observed small microstress level increase for the strained condition and lattice parameter decrease are within the limit of experimental error from that of the control specimen. No significant difference is evident between the strained and unstrained areas.

TABLE 14

X-RAY DIFFRACTIONS FOR ALUMINUM ALLOY, 7075-T6

Miller Indice (hkl)	Pure Aluminum (1)	Pure Aluminum (2)	As Received (1)	As Received (2)	Control 7075-T6 Strained (1)	Control 7075-T6 Strained (2)	Control 7075-T6 Unstrained (1)	Control 7075-T6 Unstrained (2)	Irradiated 7075-T6 Strained (1)	Irradiated 7075-T6 Strained (2)	Irradiated 7075-T6 Unstrained (1)	Irradiated 7075-T6 Unstrained (2)
111	2.338	100	2.34	50	2.33	26	2.33	90	2.34	27	2.35	29
200	2.024	47	2.03	100	2.02	100	2.02	100	2.03	100	2.03	100
220	1.431	22	1.43	25	1.43	89	1.43	70	1.43	48	1.44	49
311	1.221	24	1.22	10	1.22	28	1.22	13	1.22	14	1.23	2
222	1.169	7	1.17	5	-	-	1.17	11	-	-	1.17	2
400	1.012	2	1.01	9	1.01	7	1.01	11	1.02	3	1.01	5
331	0.929	8	-	-	0.927	7	0.93	3	0.93	3	0.93	1
Lattice Parameter A°	4.049		4.057		4.051		4.056		4.049		4.047	
Microstress			0.73° (2θ = 116°)		0.50° (2θ = 78°)		0.35° (2θ = 78°)		0.60/0.40 (2θ = 78.0/44.6)		0.50°/0.32° (2θ = 78.0°/44.55°)	

Notes: (1) "d" spacings
(2) Relative intensities percent shift in "d" spacing indicates lattice expansion. Orientation change is indicated by intensity change for a given Miller Indice.
(3) Welded and heat treated to a T6 condition.

C. TITANIUM ALLOYS

1. A-110-AT-(ELI) (5Al - 2.5 Sn)

a. Mechanical Properties

An extra low interstitial grade (ELI) of this alloy was used because of its greater ductility at -423°F. Average values and standard deviations of mechanical properties obtained at room temperature, liquid hydrogen temperature as control, and at liquid hydrogen temperature after nuclear radiation are presented in Table 15. Detailed test data for the irradiated specimens are shown in Table 16. Parent material and weldments (transverse to the rolling direction) were investigated. Stress concentration factor for the notched specimen of the parent material was specially selected as K_t = 17.0. The notched strength of this alloy at K_t = 6.3, stress concentration factor, was previously evaluated (Reference 1). Since this alloy is a strong contender for pressure vessel material, it was subjected to more vigorous notch-test criteria than the remaining alloys. Extra low interstitial weld-wire was used for automatic welding in controlled atmosphere.

For parent material the general trend of increase in strength (ultimate, yield, and shear including notched tensile strength), with a decrease of temperature, was followed by additional increase in strength from radiation. An exception to this rule was a decrease in notched strength for the sharp notches because of radiation. For parent metal, the substantial increase in strength because of the cryogenic temperature (76.6% for ultimate, 74% for yield, and 52% for shear) was followed by a rather small increase from the low dose level of nuclear radiation (5%, 3% and 9% correspondingly). The rather modest increase in notch strength (20%) for the sharp notch (K_t = 17.0) because of cryogenic temperature was followed by a 10% decrease in this property caused by radiation. A constant decrease in notch-to-unnotched strength/ratio was obtained with a rather low value of 0.68 after radiation. Change in ductility from room temperature to liquid hydrogen temperature was more pronounced in the reduction

TABLE 15

AVERAGE MECHANICAL PROPERTIES TENSILE TEST DATA

TITANIUM ALLOY A-110-AT ELI

	Room Temp.	Control -423°F	Change- Room Temp. vs. Control in Percent	Irrad. -423°F	Change - Control vs Irradiation in Percent	Threshold
UNNOTCHED						
Ultimate Strength-PSI	122,500	216,400	+76.6	226,500	+4.7	
Std. Deviation-PSI	*	7,300		4,600		
0.2% Yield Strength-PSI	114,800	199,500	+74	205,100	+3	
Std. Deviation-PSI	*	9,900		2,500		
% Elongation	15.5	17.1	+10	18.6	+8.8	
Std. Deviation-%	*	1.4		.45		
% Reduction in Area**	40.0	17.8	-55	16.8	-6	
Std. Deviation-%		1.2		1.3		
Ult. Shear Strength-PSI	86,100	130,600	+52	142,500	+9.1	
Std. Deviation-PSI	7,000	4,300		8,850		
NOTCHED Kt = 17						
Ultimate Strength-PSI	142,800	171,000	+20	153,700	-10.1	
Std. Deviation-PSI	960	5,200		13,850		
Ratio Notched Ult. / Unnotched Ult.	1.16	0.79	-32	0.68	-14.0	
Ratio Notched Ult. / Unnotched Yield	1.24	0.86	-31	0.75	-13	

* One Specimen Noted

** Micrometer Measurement

TABLE 15 (cont.)

AVERAGE MECHANICAL PROPERTIES TENSILE TEST DATA

TITANIUM ALLOY A-110-AT-ELI

	Room Temp.	Control -423°F	Change- Room Temp. vs Control in Percent	Irrad. -423°F	Change- Control vs Irradiated in Percent	Threshold
UNNOTCHED						
Ultimate Strength-PSI	114,200	214,600	+88	217,100	+1.17	
Std. Deviation-PSI	2,240	5,200		8,600		
0.2% Yield Strength-PSI	109,800	198,000	+81	204,200	+3	
Std. Deviation-PSI	1,400	5,300		8,500		
% Elongation	12.5	5.9	-53	5.95	+.85	
Std. Deviation-%	14	1.4		1.8		
% Reduction in Area*	39.5	9.4	-76	11.4	+21	
Std. Deviation-%	1.6	2.5		2.4		
Ult. Shear Strength-PSI						
Std. Deviation-PSI						
NOTCHED Kt = 6.3						
Ultimate Strength-PSI	130,700	118,100	-10	121,200	+2.6	
Std. Deviation-PSI	1,700	11,000		12,100		
Ratio Notched Ult. / Unnotched Ult.	1.14	0.55	-52	0.56	+1.8	
Ratio Notched Ult. / Unnotched Yield	1.19	0.59	-50	0.59	0	

* Micrometer measurement

TABLE 16

DETAILED MECHANICAL PROPERTIES DATA

TITANIUM A-110-AT-ELI

Specimen Number	Specimen Condition	Ultimate Strength Instron Cell(KSI)	Ultimate Strength Ram Cell(KSI)	Yield Strength 0.2% Offset(ksi)	Percent Reduction in Area	Percent Elongation
329	TN	175.4	146.1			
330	TN	181.28	170.94			
333	TN	164.8	139.5			
334	TN	166.42	158.11			
281	TU	242.5	220.1	202.0	17.9	18.0
282	TU	239.7	230.9	208.0	16.8	18.1
285	TU	241.3	227.37	205.0	17.5	19.5
286	TU	236.2	227.7	205.5	15.0	19.0

Elongation Data

Specimen Number	Specimen Condition	Extensometer Post Irradiation (Mills)	Pull Rod Post Irradiation (Mills)	Pull Rod Control (Mills)	Bench Measurement Post Irradiation (Mills)	Bench Measurement Control (Mills)
281	TU	380	506		360	
282	TU	428	537		362	
285	TU	441			390	
286	TU	434	533		380	
Average		421	525.3	505	373	342
% Elongation		14.9	18.6	17.9	18.6	17.1
% Damage			+4		+8.8	

Ultimate Shear Strength (KSI)

133.1

154.4

140.0

142.6

TABLE 16 (cont.)

DETAILED MECHANICAL PROPERTIES DATA

TITANIUM A-110-AT-ELI TW

Specimen Number	Specimen Condition	Ultimate Strength Instron Cell(KSI)	Ultimate Strength Ram Cell(KSI)	Yield Strength 0.2% Offset(ksi)	Percent Reduction in Area	Percent Elongation
341	TWN	114.82	108.16			
342	TWN	144.4	135.98			
345	TWN	133.8	125.34			
346	TWN	122.3	115.22			
293	TWU	231.1			15.0	7.85
294	TWU	223.7	210.7	198.5	7.4	3.5
297	TWU	227.9	226.9	214	11.1	5.75
298	TWU	226.9	213.8	200	12.2	6.7

Elongation Data

Specimen Number	Specimen Condition	Extensometer Post Irradiation (Mills)	Pull Rod Post Irradiation (Mills)	Pull Rod Control (Mills)	Bench Measurement Post Irradiation (Mills)	Bench Measurement Control (Mills)
293	TWU				157	
294	TWU	122	202		70	
297	TWU	158	222		115	
298	TWU	152	224		134	
Average		144	216	269.3	119	118
% Elongation		5.1	7.64	9.5	5.95	5.9
% Damage			-19.7		.85	

of area (decrease from 40.0% to 17.8%). Decrease from radiation was much less (from 17.8 to 16.8%). Elongation showed an increase both from temperature and radiation.

Welded material exhibited room temperature data almost identical to the unwelded material. Increase in strength because of cryogenic temperature was in the same order of magnitude as for the parent material. Percent increase in strength from radiation was negligible, and close to the increase observed in the parent material.

Although the stress concentration factor for the welded, notched, specimens was $K_t = 6.3$, a decrease in notched strength was obtained at cryogenic temperature, followed by a negligible increase from radiation. The notched-to-unnotched strength ratios dropped to a very low level, 0.55 and 0.56 respectively. Decrease in ductility as a result of the cryogenic temperature, measured by both parameters (area reduction and elongation) was followed by an increase in area reduction and no change in elongation. This is again a case in which the properties are not consistently affected.

Stress-strain curves (obtained with an extensometer) for all irradiated specimens including average data at room temperature, liquid hydrogen temperature, with and without radiation, are shown in Figures 22 and 23.

No threshold level of damage for any property of this material was obtained.

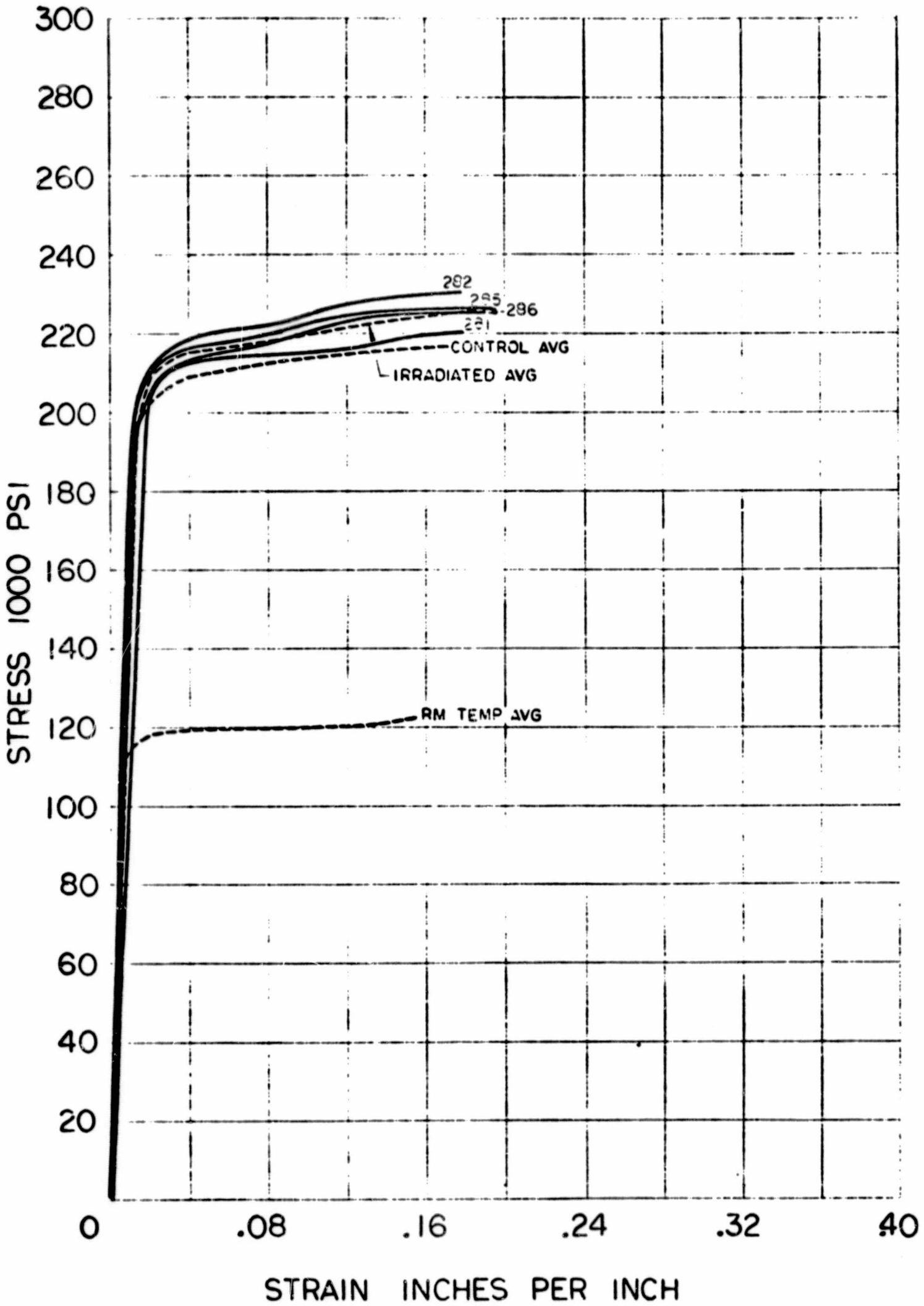

Figure 22

Stress - Strain Curves for A-110-AT Titanium, Parent Metal

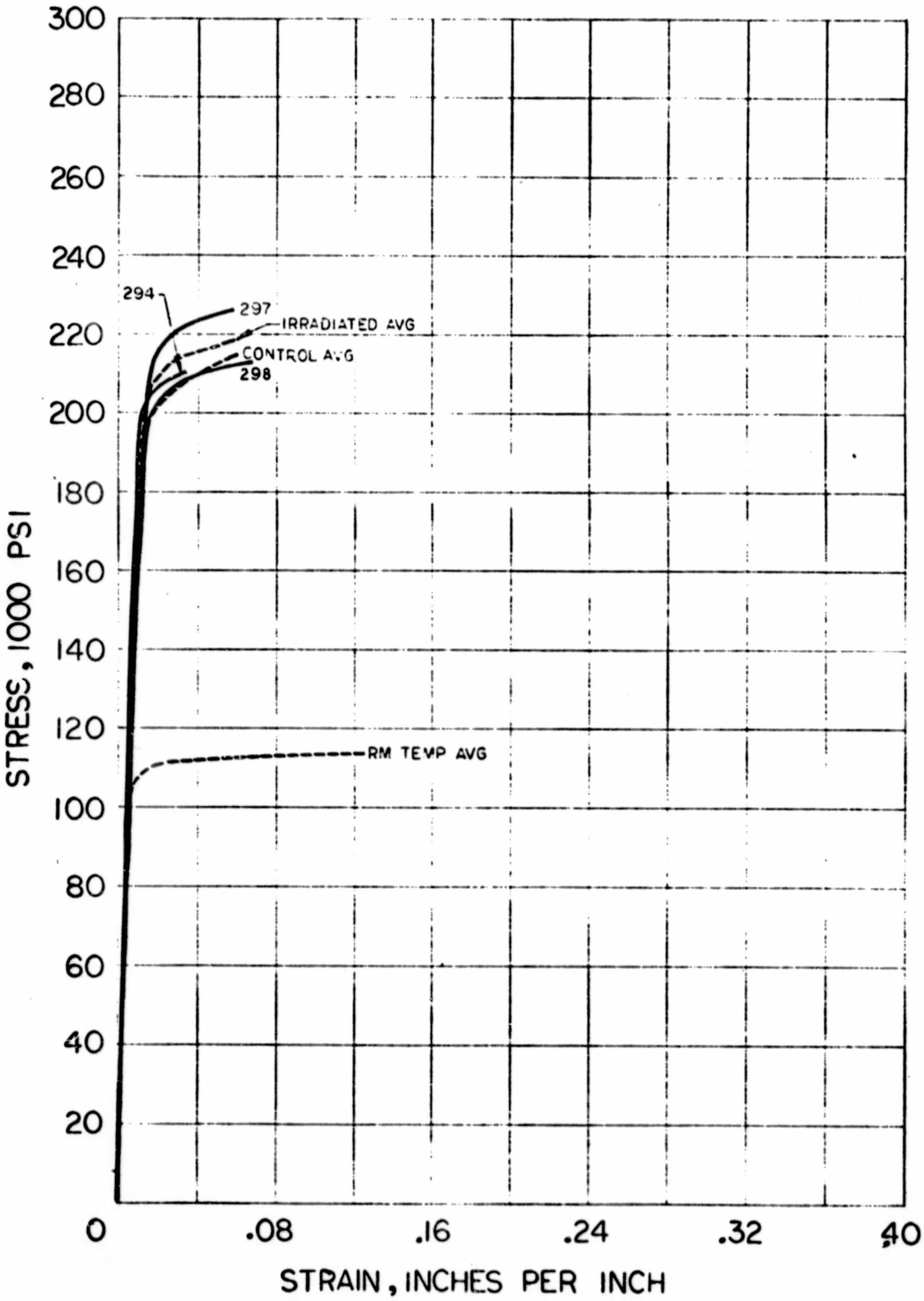

Figure 23

Stress - Strain Curves for A-110-AT Titanium, Weldments

b. Metallography

Photomicrographs were made to illustrate the pertinent features of the microstructure observed during examination of the strained fracture area and of an unstrained area at one end of the irradiated specimen.

The microstructures of the irradiated samples are normal for this alloy and are unchanged from those of the control specimens. The photographs of the structure vary slightly, but this is thought to be caused by etching procedures. The photographs can be found in References 2 and 7.

In the unwelded condition, the irradiated metal suffered a transgranular failure. The microstructure was similar to that of the control specimens, consisting of a typical titanium matrix with grain orientation depicted by the contoured effect of etchant attack.

The microstructure of the welded material was identical to that of the unwelded condition. The weld zone, however, shows an acicular titanium which has a larger grain size than the parent-metal titanium. The microstructures show the mode of fracture to be transgranular through the titanium matrix, not through the weld or heat-affected zone.

c. Electron Microscopy

Electron micrographs (at 15000X) were taken of the representative areas of the irradiated specimens.

The microstructure of the irradiated samples - in the parent metal and welded conditions - are presented in Figure 24. This illustration shows an acicular titanium weld structure, with what appears to be mechanical twins in the acicular titanium grains. The twins were not visible in the unirradiated specimens.

Fractographs of the irradiated specimens (see Figure 25) show a ductile failure mode. In the welded specimen, the fracture surface at the center was made up of large areas of shallow dimples connected by large dimples, indicating discontinuous ductile fracture. This was a minor deviation. However, the shallow dimples follow a cleavage pattern, indicating that cleavage cracks initiated the failure.

Material: Titanium A110 AT, ELI

Form: 1/4" Plate

Specimen No.: TU 285, TWU 298

Specification: MIL T9046C, Class 3, Grade ELI

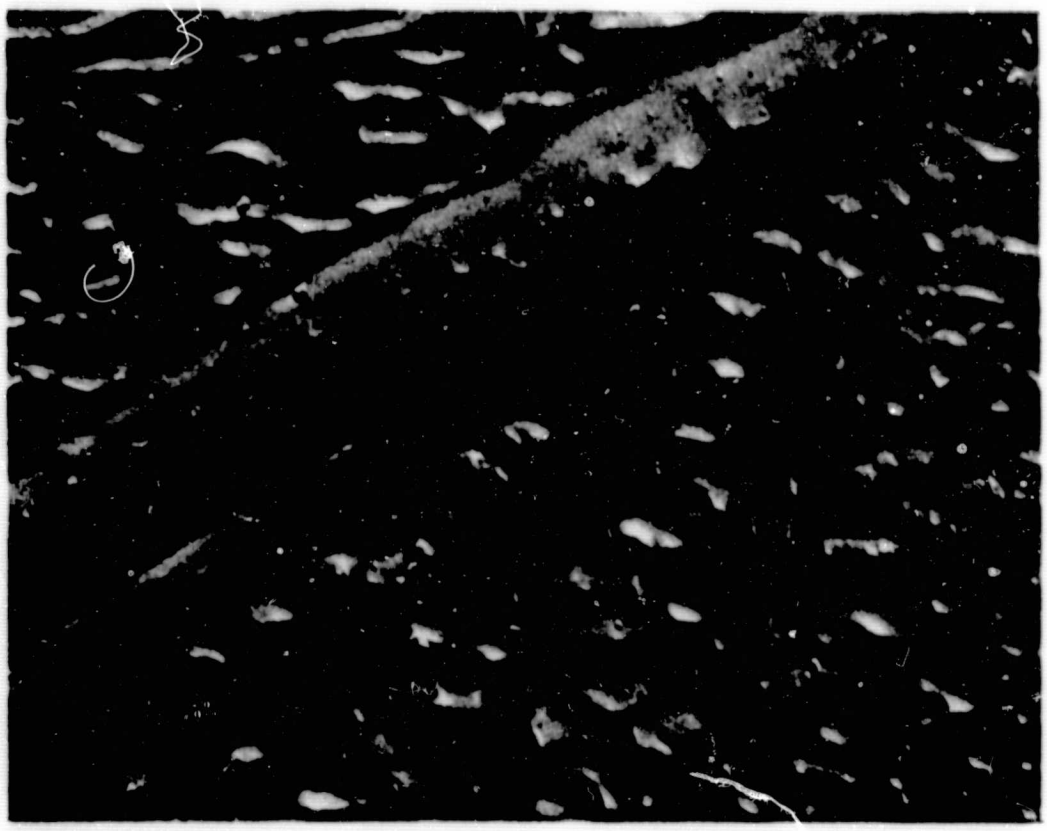

Condition: Irradiated-Unstrained (TU 285)

Mag: 15000X

The microstructure shows the α titanium grains with different orientations.

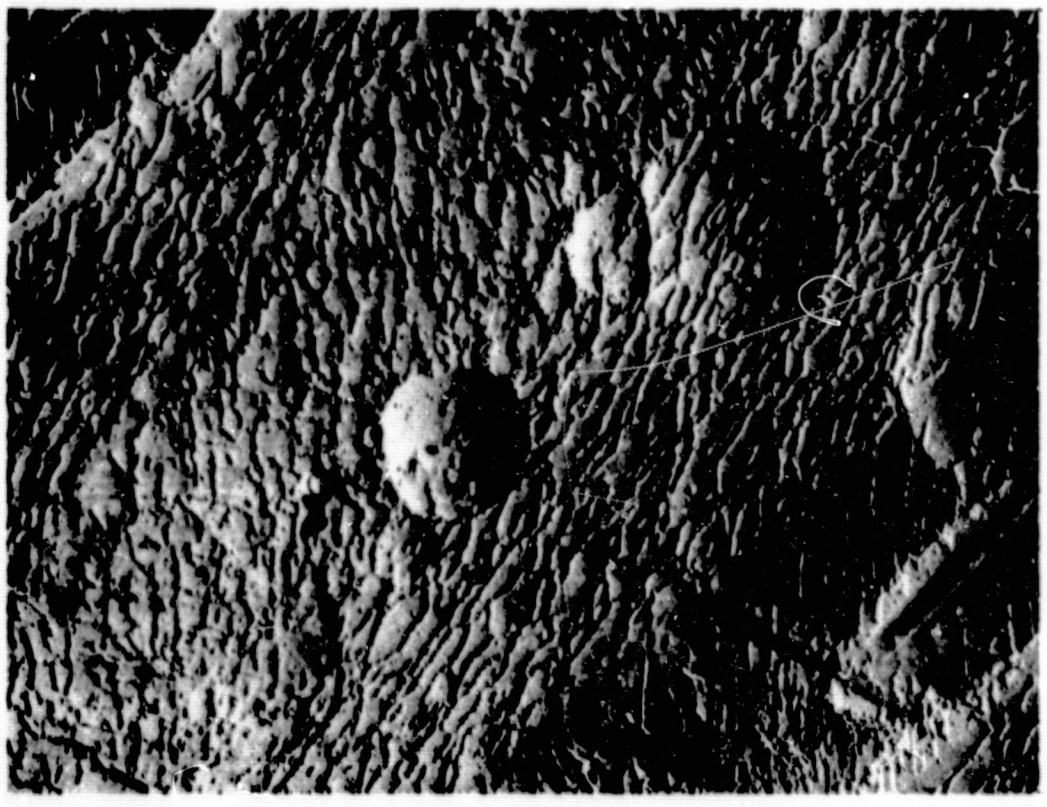

Condition: Irradiated-Welded-Strained (TWU 298)

Mag: 15000X

The microstructure is an acicular α titanium weld structure. Note the various orientations present and what appear to be mechanical twins in the acicular α titanium grains. The large globular areas represent inclusions removed during polishing.

Figure 24

Titanium A110 AT, ELI - Irradiated Condition T and TW-Strained-Unstrained - 15000X

Material: Titanium A110 AT, ELI

Form: 1/4" Plate

Specimen No.: TU 285, TWU 298

Specification: MIL T9046C, Class 3, Grade ELI

Condition: Irradiated-Fractograph-Fracture Center (TU 285)

Mag: 4200X

The fracture consists mainly of ductile microvoid; however, the shallow dimple pattern on the right is possibly the result of cleavage cracking.

Condition: Irradiated-Welded Fractograph-Fracture Center (TWU 298)

Mag: 4200X

The fracture at the center is made up of large areas of shallow dimples connected by large dimples, indicating a discontinuous ductile fracture. The shallow dimples follow a cleavage pattern, indicating that cleavage cracks initiated the failure.

Figure 25

Titanium A110 AT, ELI - Irradiated-Condition T and TW-Fractograph-4200X

d. X-Ray Diffraction

The X-ray diffraction data (presented in Table 17) show the typical hexagonal close-packed structure of titanium. The orientation was found to be in the (002) direction. The diffraction pattern from the transverse unwelded specimens, unstrained area, was essentially the same as that in the as-received pattern. No appreciable change in microstress level occurred in the strained sample.

The diffraction pattern from the strained area of the transverse welded specimen showed no crystallographic changes. There was no effect which could be related to cryogenic environment.

The diffraction pattern of the irradiated samples showed no change in preferred orientation. The unwelded strained specimen, however, exhibited a change in preferred orientation to the (011) direction. No change occurred in lattice parameter between the control and irradiated material, but a small reduction in microstress was noted, which is still within the limit of the experimental error.

TABLE 17

X-RAY DIFFRACTION DATA A110 AT TITANIUM

hkl	Theoretical Titanium (1)	Theoretical Titanium (2)	As Received (1)	As Received (2)	Unwelded-Control Strained Area (1)	Unwelded-Control Strained Area (2)	Unwelded-Control Unstrained Area (1)	Unwelded-Control Unstrained Area (2)	Welded Strained Area (Welded) (1)	Welded Strained Area (Welded) (2)	Welded Unstrained (1)	Welded Unstrained (2)	Irradiated Unwelded Strained (1)	Irradiated Unwelded Strained (2)	Irradiated Unwelded Unstrained (1)	Irradiated Unwelded Unstrained (2)	Welded Strained (1)	Welded Strained (2)
010	2.557	30	2.54	3	2.56	3												
002	2.34	26	2.34	100	2.32	100	2.32	100	2.32	100	2.35	100	2.34	15	2.35	100	2.35	100
011	2.24	100	2.23	14	2.22	25	2.22	25	2.22	50	2.24	24	2.23	100	2.24	28	2.24	35
																	1.92	10
012	1.726	19	1.72	7	1.71	14	1.71	15	1.72	25	1.73	10	1.72	8	1.73	15	1.73	40
110	1.475	17							1.46	10			1.47	5			1.47	8
103	1.332	16	1.33	18	1.33	25	1.32	30	1.33	25	1.33	20	1.33	11	1.33	25	1.33	80
112	1.247	16			1.24	5					1.25	4	1.24	7			1.24	8
004	1.171	2	1.17	6	1.17	5	1.17	15	1.17	10	1.17	5	1.23	6	1.17	7		
014	1.065	3	1.06	3	1.06	5	1.06	7	1.06	10	1.06	2			1.06	7	1.06	8
									Lattice Parameters (Å°)									
a	2.95		2.94		2.95		2.94		2.94		2.95		2.95		2.95		2.95	
c	4.69		4.68		4.678		4.674		4.672		4.68		4.68		4.68		4.68	
									Microstress, Δ θ									
			0.25°		0.58° (2θ = 82°)		0.40° (2θ = 82°)		0.34° (2θ = 82°)		0.23° (2θ = 82.2°)		No Peak (2θ = 82°)		0.34° (2θ = 82.2°)		No Peak (2θ = 82°)	
											0.24° (2θ = 38.3°)		0.24° (2θ = 28.4°)		0.26° (2θ = 38.25°)		0.30° (2θ = 38.25°)	

NOTES: (1) "d" Spacings
(2) Relative intensities, percent.
Shift in "d" spacings indicates lattice expansion.

D. STAINLESS STEELS

1. 347 Wrought Alloy and Casting

a. Mechanical Properties

Specimens of this alloy were tested in a variety of conditions which included:

(1) Wrought alloy in sheet form as received
(2) Wrought weldments
(3) Casting in the annealed condition

Average values and standard deviations of mechanical properties obtained for these conditions at room temperature, at liquid hydrogen temperature without radiation (control), and with radiation are presented in Tables 18 and 19. Detailed test results for the irradiated specimens are shown in Table 20. It should be noted that control and irradiated specimens for the unwelded sheet material are from two different batches.

Parent Material

This condition was previously evaluated and detailed data are reported in Reference 1. The test was performed at liquid hydrogen temperature, after a 30-day intermediate warmup to room temperature. The test results are included here for comparison and to discover any possible annealing effect.

Comparison of strength properties at room temperature with those at liquid hydrogen temperature shows that yield and shear strength approximately double, the ultimate strength almost triples, and the notched strength increases more than 50%.

TABLE 18

AVERAGE MECHANICAL PROPERTIES TEST DATA
STAINLESS STEEL, 347 WROUGHT ALLOY

	Room Temp	Control -423°F	Change Room Temp. vs Control in Percent	Irrad. Plus Warmup (30 days) Pulled @-423°F	Irrad. -423°F	Change Control vs Irradiated in Percent	Threshold
UNNOTCHED							
Ultimate Strength - psi	91,175	259,900	+185	236,300	227,100	-12.6	T*
Standard Deviation - psi	2,000	500		16,200	17,900		
0.2% Yield Strength -psi	44,700	87,350	+ 95	92,400	84,500	- 3	
Standard Deviation - psi	5,300	2,650		3,700	7,600		
% Elongation	44.8	40.2	- 10	32.7	40.9	+ 1.7	
Standard Deviation - %	3.9	2.25		8.2	3.0		
% Reduction in Area**	53.4	28.0	- 48	24.2	27.9	- 3.5	
Standard Deviation - %	2.6	1.7		5.2	2.4		
Ultimate Shear Strength - psi	77,000	152,400	+ 97		150,200	-14	
Standard Deviation	3,500	5,300			3,800		
NOTCHED Kt = 6.3							
Ultimate Strength - psi	83,600	139,400	+ 69	138,000	135,100	- 3.1	
Standard Deviation - psi	2,900	4,600		2,000	3,950		

* Threshold level for irradiated material at -423°F and tested without warmup.
** Micormeter measurements.

TABLE 18 (cont.)

AVERAGE MECHANICAL PROPERTIES TEST DATA
STAINLESS STEEL, 347 WROUGHT ALLOY

	Room Temp	Control -423°F	Change Room Temp. vs Control in Percent	Irrad. Plus Warmup (30 days) Pulled @-423°F	Irrad. -423°F	Change Control vs Irradiated in Percent	Threshold
Ratio $\frac{\text{Notched Ultimate}}{\text{Unnotched Ultimate}}$	.91	.54	-41	0.58	.595	+10.2	
Ratio $\frac{\text{Notched Ultimate}}{\text{Unnotched Yield}}$	1.9	1.6	-16	1.50	1.6	0	

AVERAGE MECHANICAL PROPERTIES TEST DATA STAINLESS
STEEL 347 WELDED:

UNNOTCHED							
Ultimate Strength - psi	92,700*	224,200*	+124	195,700	226,700	+1.1	
Standard Deviation - psi	2,200	18,300		40,400	10,100		
0.2% Yield Strength - psi	52,400	97,000	+85	97,700	63,000	-35.0	T
Standard Deviation - psi	2,200	9,300		150	8,800		
% Elongation	43.9	27.1	-38	21.5	40.9	+51	
Standard Deviation - %	4.2	4.2		5.0	8.7		

TABLE 18 (cont.)

AVERAGE MECHANICAL PROPERTIES TEST DATA
STAINLESS STEEL, 347 WELDED

	Room Temp	Control -423°F	Change Room Temp. vs Control in Percent	Irrad. Plus Warmup (30 days) Pulled @ -423°F	Irrad. -423°F	Change Control vs Irradiated in Percent	Threshold
% Reduction in Area	61.2	31.3	-49	14.9**	30.7	-1.9	T***
Standard Deviation - %	4.5	11.8		3.7	9.9		
Ultimate Shear Strength - psi							
Standard Deviation							
NOTCHED Kt = 6.3							
Ultimate Strength - psi	96,000	136,500*	+42	125,100	126,900	-7.0	T
Standard Deviation - psi	0	5,300		3,200	3,200		
Ratio $\frac{\text{Notched Ultimate}}{\text{Unnotched Ultimate}}$	1.03	0.61	-42	0.64	0.55	-10.0	
Ratio $\frac{\text{Notched Ultimate}}{\text{Unnotched Yield}}$	1.83	1.41	-23	1.28	2.01	+43	

* Broke in Weld Material.
** Micrometer Measurement.
*** Threshold level for irradiated material at -423°F and tested with warmup.

TABLE 19

AVERAGE TENSILE TEST DATA

STAINLESS STEEL, 347 CAST

	Room Temp.	Control -423°F	Change- Room Temp. vs Control in Percent	Irrad. -423°F	Change, Control vs Irradiated in Percent	Threshold
UNNOTCHED						
Ultimate Strength-PSI	85,600	117,300	+38	115,400	-1.62	
Std. Deviation-PSI	1,200	4,700		4,400		
0.2% Yield Strength-PSI	39,900	93,300	+134	80,300	-14	
Std. Deviation-PSI	2,200	7,400		11,000		
% Elongation	30.9	7.7	-75	8.5	+10.4	
Std. Deviation-%	3.6	1.4		One Specimen		
% Reduction in Area	33.6	11.5	-66	13.3	+16	
Std. Deviation-%	3.9	3.7		1.4		
Ult. Shear Strength-PSI	74,500	163,400	+120			
Std. Deviation-PSI	2,900	5,300				
NOTCHED Kt = 6.3						
Ultimate Strength-PSI	71,400	99,200	+34	102,300	+3.1	
Std. Deviation-PSI	3,800	4,700		4,500		
Ratio Notched Ult. / Unnotched Ult.	0.83	0.85	+2	0.885	+4.1	
Ratio Notched Ult. / Unnotched Yield	1.79	1.20	-33	1.28	+7	

Spe
Num
705
706
707
708
701
702
703
704

Spec
Numb
701
702
703
704
Ave
% El
% De

*Ext

TABLE 20

DETAILED MECHANICAL PROPERTIES DATA

SS 347 WROUGHT

Ultimate Strength

Specimen Number	Specimen Condition	Instron Cell (KSI)	Ram Cell (KSI)	Yield Strength 0.2% Offset(KSI)	Percent Reduction in Area	Percent Elong-ation
705	LN	141.6	130.79			
706	LN	142.6	134.3			
707	LN	144.8	140.4			
708	LN	143.4	135.1			
701	LU	250.9	235.64	91.0	29.1	41.15
702	LU	254.8	246.5	74.0	28.5	42.90
703	LU	255.4	220.85	89.0	30.0	43.10
704	LU	231.6	205.34	84.0	23.9	36.65

Elongation Data

		Extensometer	Pull Rod		Bench Measurement	
Specimen Number	Specimen Condition	Post Irradiation (Mills)	Post Irradiation (Mills)	Control (Mills)	Post Irradiation (Mills)	Control (Mills)
701	LU	*929	1129		823	
702	LU	*1136	1194		858	
703	LU		1187		862	
704	LU		986		733	
Average		1032	1124		819	804
% Elongation		36.5	39.8		40.9	40.2
% Damage					+1.7	

Ultimate Shear Strength (KSI)

*Extrapolated from rod movement

151.8
146.4
154.7
147.9

TABLE 20 (cont.)

DETAILED MECHANICAL PROPERTIES DATA
SS 347 LW - WELDED

Specimen Number	Specimen Condition	Ultimate Strength: Instron Cell(KSI)	Ultimate Strength: Ram Cell(KSI)	Yield Strength 0.2% Offset(KSI)	Percent Reduction in Area	Percent Elongation
210	LWN	132.6	125.25			
212	LWN	130.7	124.8			
214	LWN	142.4	130.5			
198	LWU	241.0	215.8	60.0	45.5	30.0
200	LWU	237.2	226.5	63.0	25.4	37.6
202	LWU	242.7	224.3	54.0	25.5	37.5
204	LWU	250.1	240.1	75.0	26.5	40.0

Elongation Data

Specimen Number	Specimen Condition	Extensometer: Post Irradiation (Mills)	Pull Rod: Post Irradiation (Mills)	Pull Rod: Control (Mills)	Bench Measurement: Post Irradiation (Mills)	Bench Measurement: Control (Mills)
198	LWU	728	834		600	
200	LWU				752	
202	LWU		936		750	
204	LWU	810	981		800	
Average		769	917	800	725	542
% Elongation		28.2	31.8	28.3	36.3	27.1
% Damage			+12.4		+34.0	

TABLE 20 (cont.)

DETAILED MECHANICAL PROPERTIES DATA

SS 347 CAST

Specimen Number	Specimen Condition	Ultimate Strength Instron Cell(KSI)	Ultimate Strength Ram Cell(KSI)	Yield Strength 0.2% Offset(KSI)	Percent Reduction in Area	Percent Elongation
185	LN	103.99	97.96			
186	LN	108.54	102.2			
189	LN	106.5	100.4			
190	LN	115.1	108.5			
173	LU	125.8	109.94	94.0	14.2	
174	LU	126.8	119.47	76.0	12.6	
177	LU	130.69	118.54	83.0	14.7	8.5
178	LU	120.66	113.65	68.0	11.8	

Elongation Data

Specimen Number	Specimen Condition	Extensometer Post Irradiation (Mills)	Pull Rod Post Irradiation (Mills)	Pull Rod Control (Mills)	Bench Measurement Post Irradiation (Mills)	Bench Measurement Control (Mills)
173	LU	164	215			
174	LU	204	218			
177	LU	217	270		170	
178	LU	110	128			
Average		174	208	225	170	154
% Elongation		6.15	7.35	7.95	8.5	7.7
% Damage			-7.6		+10.4	

This material exhibited an unusual trend in strength properties. After radiation and without warmup strengths generally decreased, with the exception of yield strength after warmup which increased. Comparison of the strength data for the irradiated material with and without warmup is not conclusive since the specimens for both conditions are from two different batches. Percent change to these properties is significant at these dose levels.

Ductility of this material was decreased by the cryogenic environment. The ductility of the irradiated specimens, pulled without warmup, was practically unchanged and the ductility of the irradiated specimens, pulled at -423°F after warmup, decreased.

Notched-to-unnotched strength ratio was relatively low. However, at cryogenic temperature, with and without radiation and warmup the notched-to-unrotched yield strength ratio was above unity.

Threshold levels of damage were obtained for ultimate tensile strength (under both test conditions). It should be pointed out again that material used for both test conditions was from different batches, and so the preceding conclusions may be doubtful.

Weldments

Welded specimens, joined with Type 349 weld wire, exhibited almost the same strength properties at room and cryogenic temperatures as did unwelded material.

Radiation effects on welded specimen tested at the temperature of liquid hydrogen resulted in a relatively small (1.1%) increase in ultimate strength and considerable (35%) decrease in yield strength. Notched strength decreased by 7% and notched-to-unnotched strength ratio by 10%. A substantial increase in ductility as measured by elongation and a negligible decrease in area reduction because of radiation was obtained, indicating that some annealing may

have taken place in the weld material or the heat-affected zone. Notched ultimate strength was appreciably higher than yield strength for all three test conditions (room temperature, and liquid hydrogen temperature with and without radiation). The ratio of these strengths (notched-to-yield) have more significant design value than comparison of the notched/unnotched ultimate strength ratio.

Threshold levels of damage were obtained for ultimate notched strength and 0.2% yield strength in both test conditions. A threshold level was obtained for area reduction of the specimens with warmup.

Castings

Changes in mechanical properties of the 347 cast material, from room to liquid hydrogen temperature, are a typical example of all metals for this test condition. The changes are characterized by a large increase in ultimate, yield, notched and shear strength, accompanied by a large decrease in ductility, measured both in elongation and reduction of area.

The radiation effect on this alloy at this dose level (5×10^{16} nvt) and test condition (LH_2) resulted in an increase in ductility (10.4% elongation and 16% in reduction of area) and substantially no change in strength. Notched-to-unnotched strength ratio for ultimate and yield strength is practically unchanged.

Stress-strain curves as obtained by the extensometer are shown in Figures 26, 27, and 28.

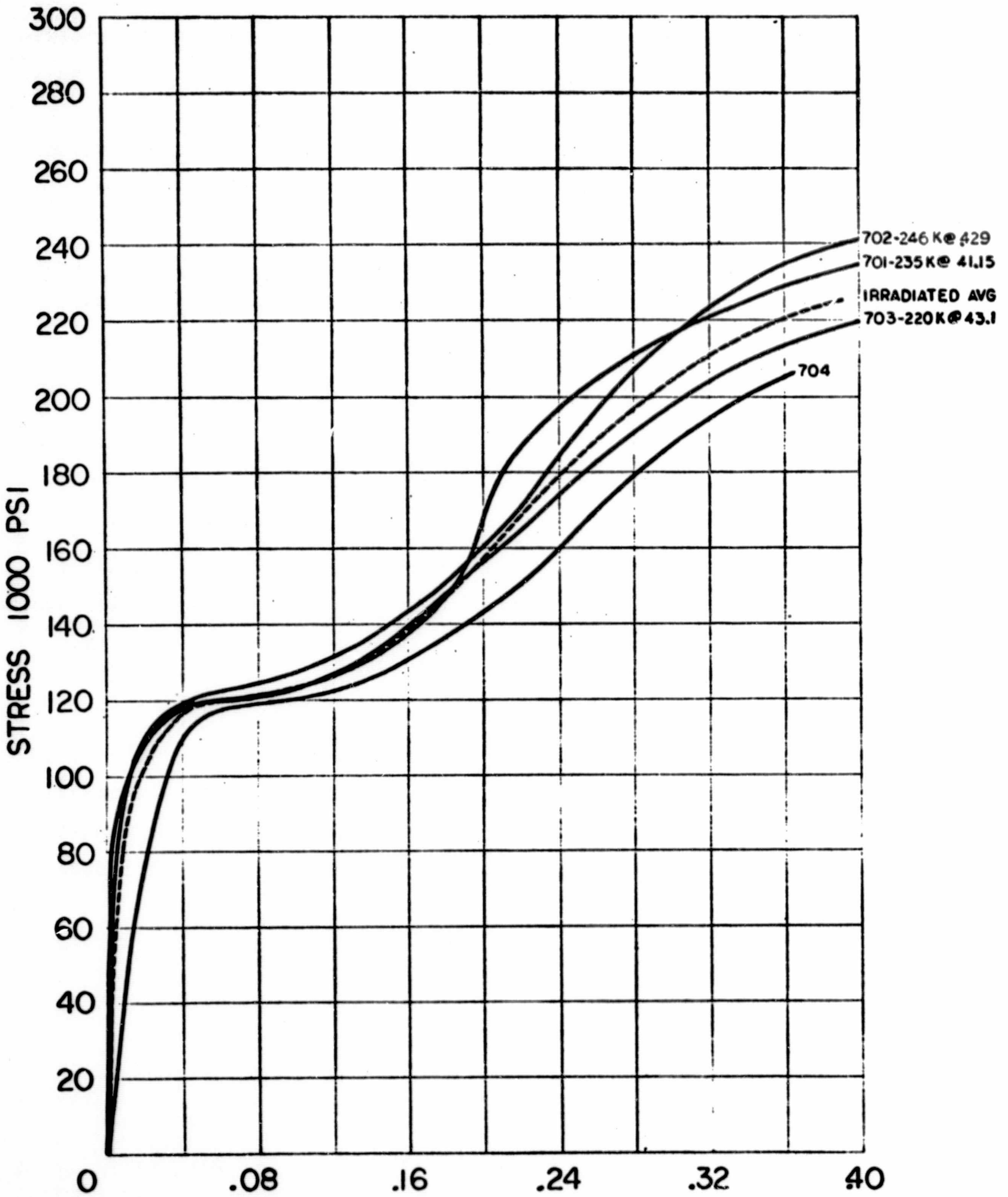

Figure 26

Stress - Strain Curves for 347 Parent Metal

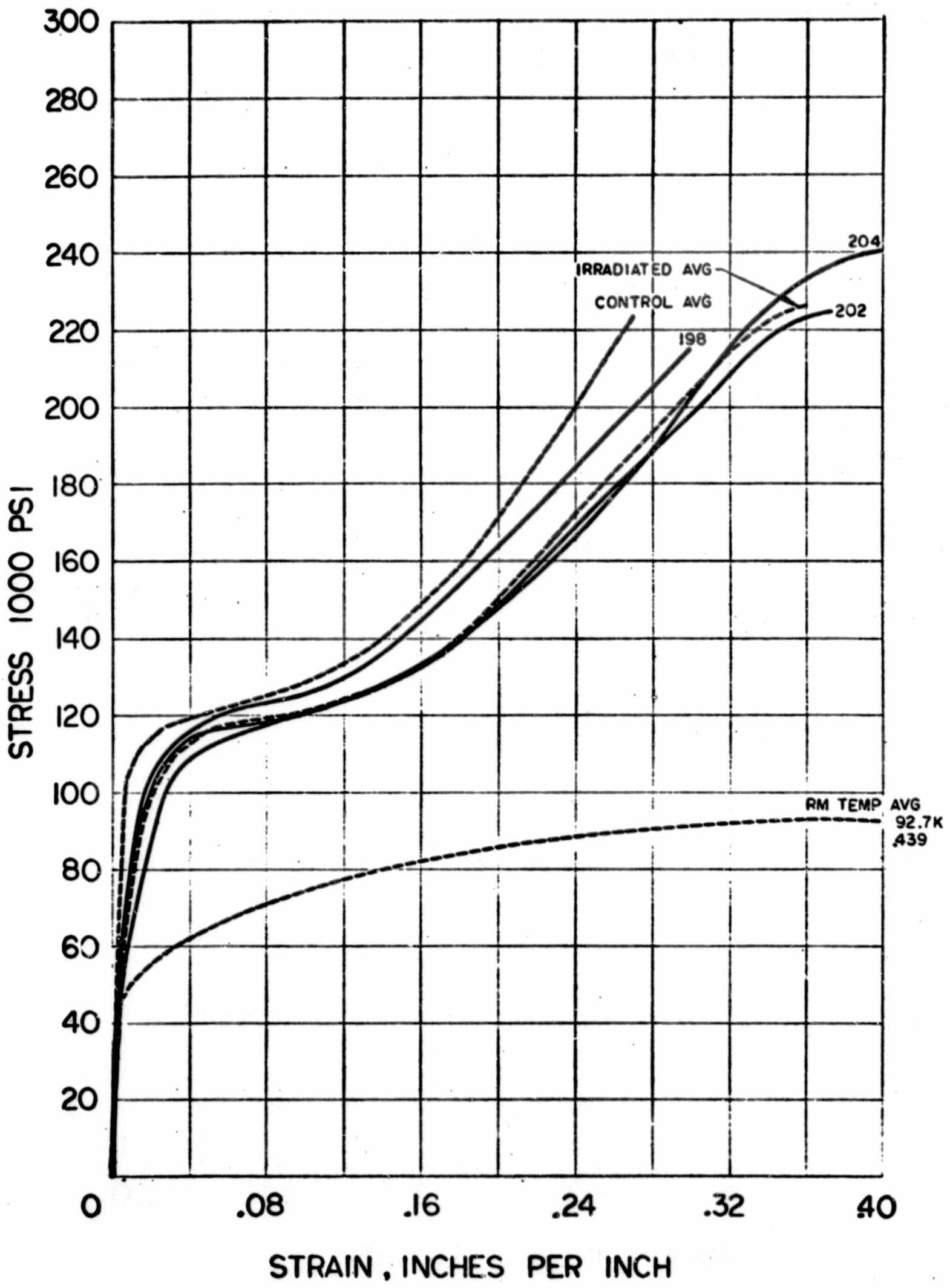

Figure 27

Stress - Strain Curves for 347 LW Welded

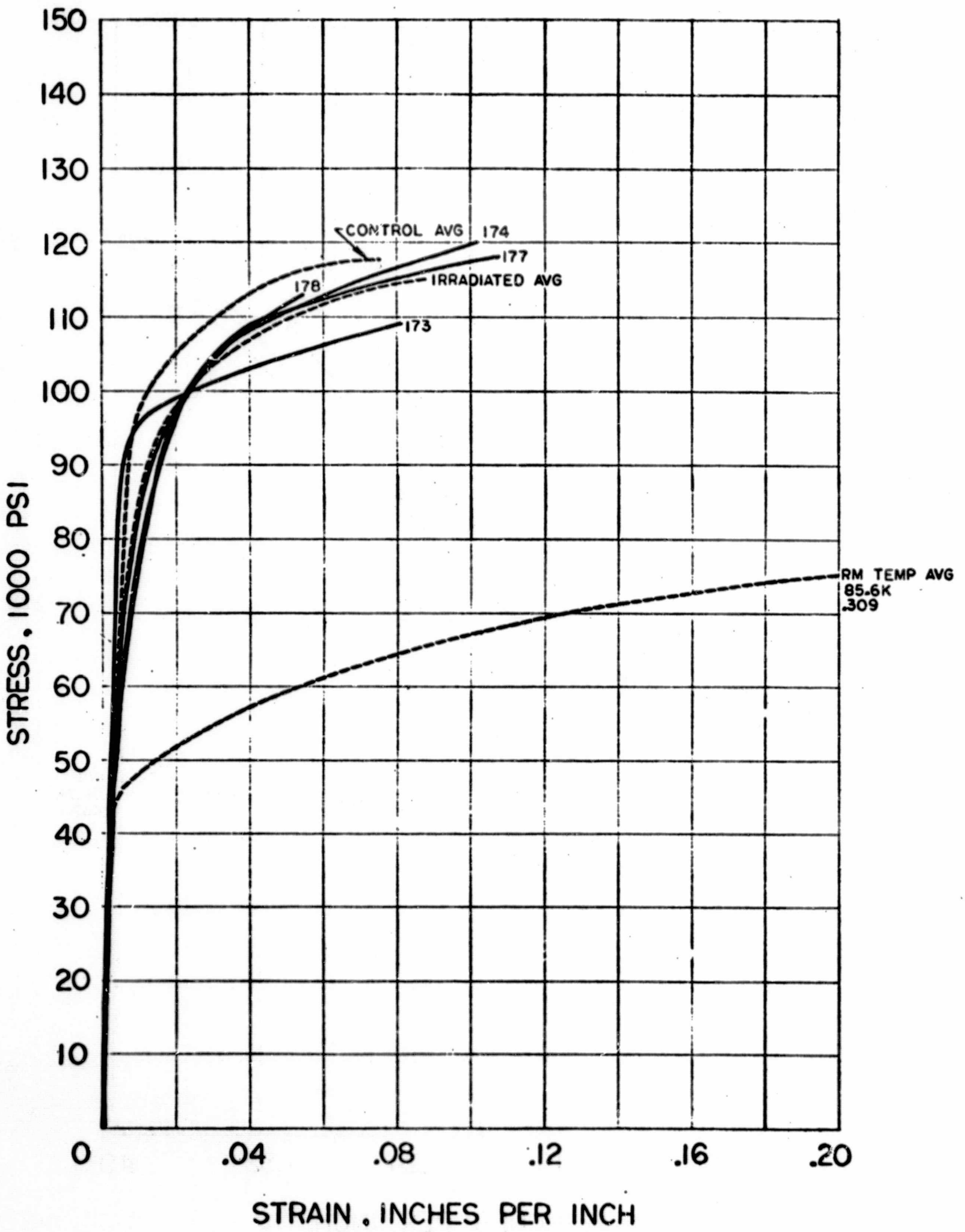

Figure 28

Stress - Strain Curves for 347 Cast

Photomicrographs (at 100X and 1000X) were made to illustrate the pertinent features of the microstructure observed during examination of the strained and unstrained areas of the test specimens.

The microstructures of irradiated 347 plate are shown (at 100X and 1000X) in Figure 29. The microstructures are typical of both the strained and unstrained conditions. No variation was noted between the unstrained, irradiated, sample and the control sample. Photomicrographs of these conditions are found in References 2 and 7. The micrograph of the irradiated, strained, area shows large areas of non-metallic inclusions, not detected in the control specimens. Since the presence of the inclusions is indicated by increasing etching sensitivity, it is difficult to state whether or not there is a weld zone of austenite and high chromium ferrite. The ferrite is finer and more evenly dispersed than in the cast structure. Changes in texture of the austenite matrix could be a result of a transformation of the austenite to martensite. This phase change would be a result of the straining in a cryogenic environment.

Figure 30 shows the microstructure of the welded 347 plate in the irradiated condition. The microstructure of the parent metal shows an austenite matrix with fine carbides. An area of austenite grain growth is noted prior to the weld zone which is composed of an austenite-ferrite matrix. Note the strain lines in the transformed austenite.

The microstructure of the strained area of the welded sample shows the result of an austenite to martensite transformation. There was no particular change in the microstructure as a result of the welding operation.

Fracture of the welded material occurred through the weld metal. The high Cr-Fe phase lies at the grain boundaries. The microstructure shows a transgranular fracture of the matrix.

Material: Stainless Steel, 347

Form: 1/4" Plate

Specimen No.: LU 702

Specification:

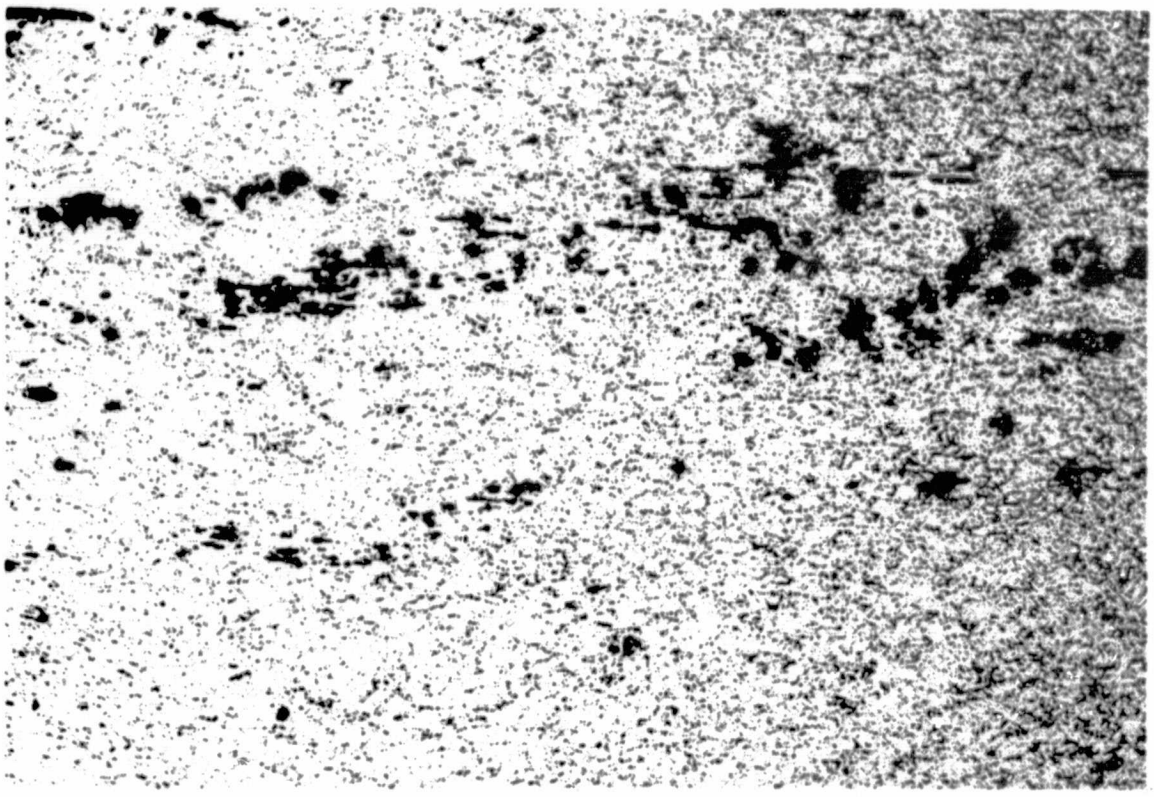

Condition: Irradiated-Strained

Mag: 100X
Etchant: 10% Ammonium Persulfate

The austentitic microstructure of a strained area shows large areas of non-metallic inclusions.

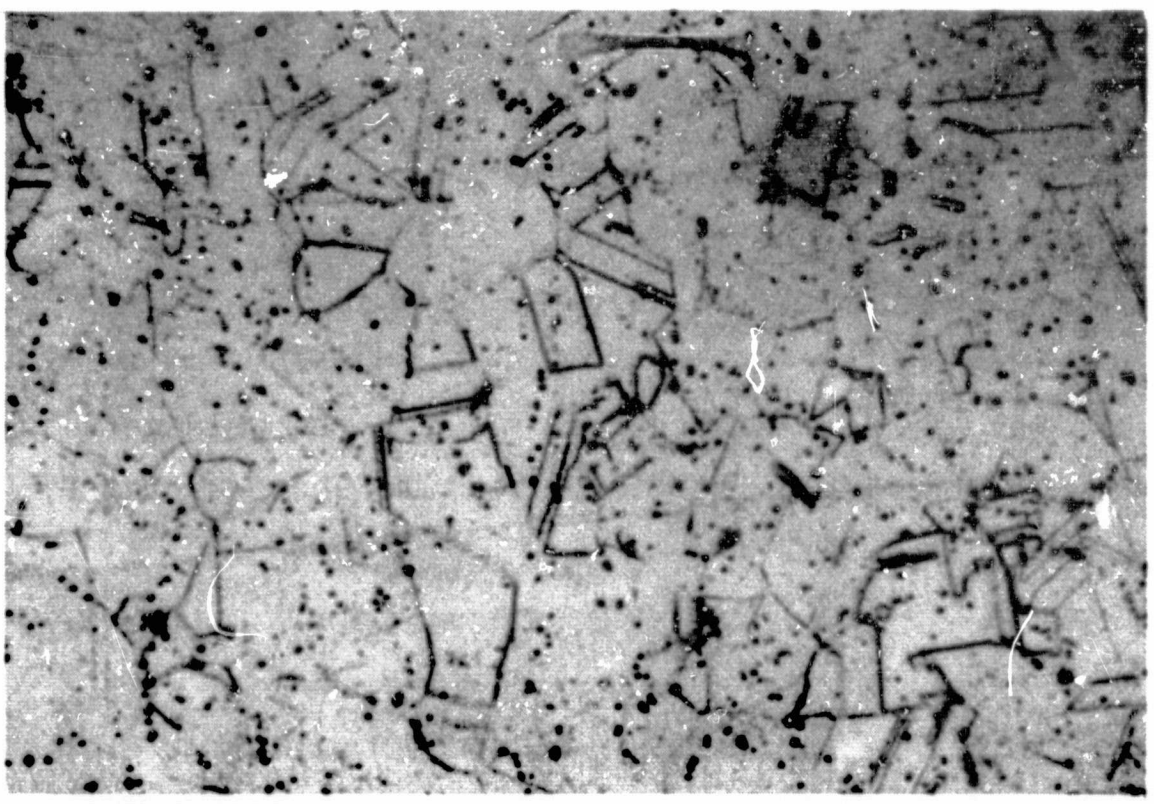

Condition: Irradiated-Unstrained

Mag: 1000X
Etchant: 10% Ammonium Persulfate

The austenitic microstructure shows the original annealing twins and carbide dispersion.

Figure 29

Stainless Steel 347, -Irradiated - Condition L - Strained - 100X and Unstrained 1000X Magnification

Material: Stainless Steel, 347

Form: 1/4" Plate

Specimen No.: LWU 204

Specification:

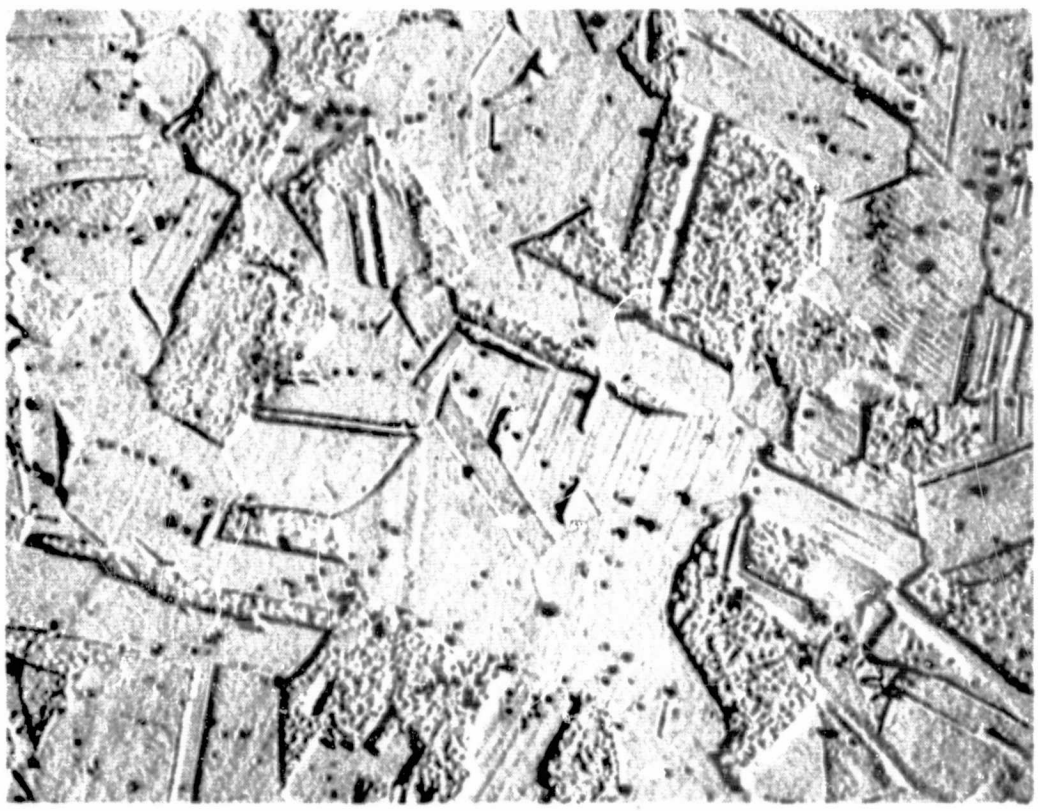

Condition: Irradiated-
Welded-
Unstrained

Mag: 1000X
Etchant: 10% Ammonium
Persulfate

The microstructure shows an austenitic matrix with fine carbides. Annealing twins are seen through the austenite grain.

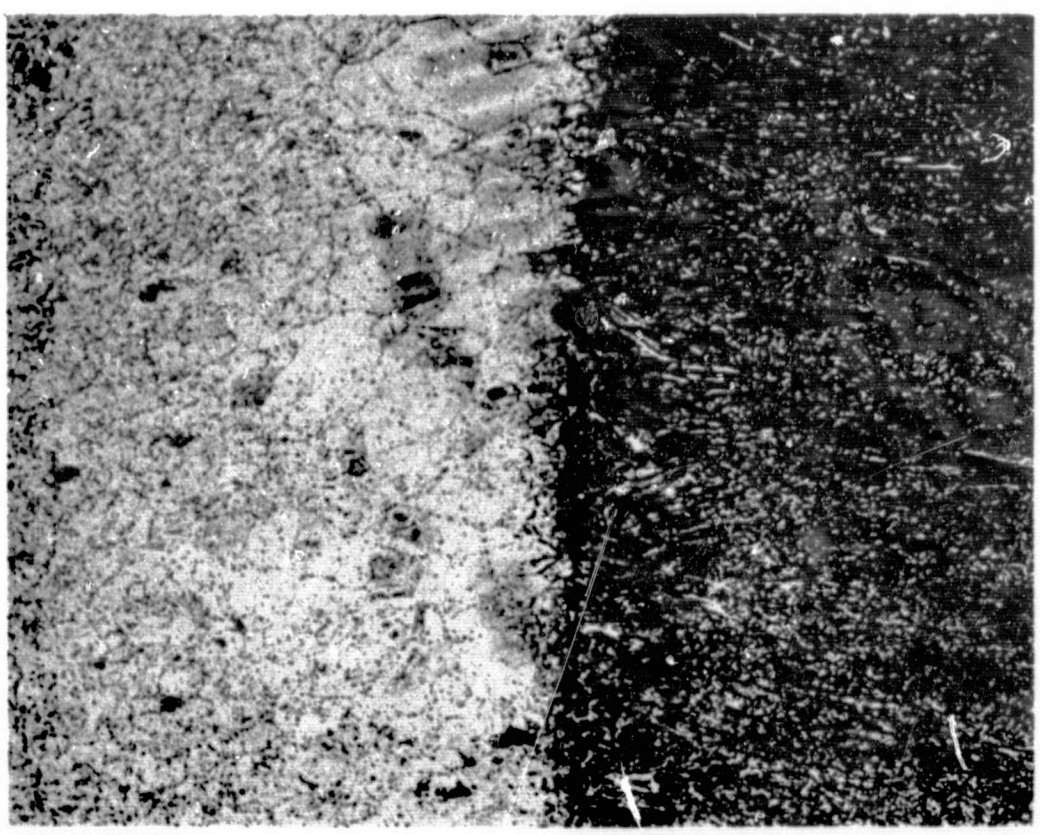

Condition: Irradiated-
Weld-Parent
Metal Interface

Mag: 100X
Etchant: 10% Ammonium
Persulfate

The microstructure represents an austenite-ferrite matrix in the weld area, transition zone of austenite grain growth and the austenite parent metal matrix with fine carbide plus non-metallic inclusions.

Figure 30

Stainless Steel, 347 - Irradiated - Welded - Condition LW -
100X, 1000X

Microstructures of the irradiated casting material (Figure 31) are essentially the same as the control sample, exhibiting a dendritic pattern of high chromium ferrite islands in a matrix of austenite. Areas of high stress exhibited a general darkening due to preferential etching.

In its microstructure, the fracture surface of the irradiated sample shows a partially transformed austenite matrix with a high chromium grain boundary phase. The fracture is both intergranular and transgranular; however, the transformation occurs only on the austenitic slip planes. The austenite shows high strain while the grain boundary material is essentially unaffected.

Material: Stainless Steel, 347C

Form: Sand Casting

Specimen No.: LU 178

Specification:

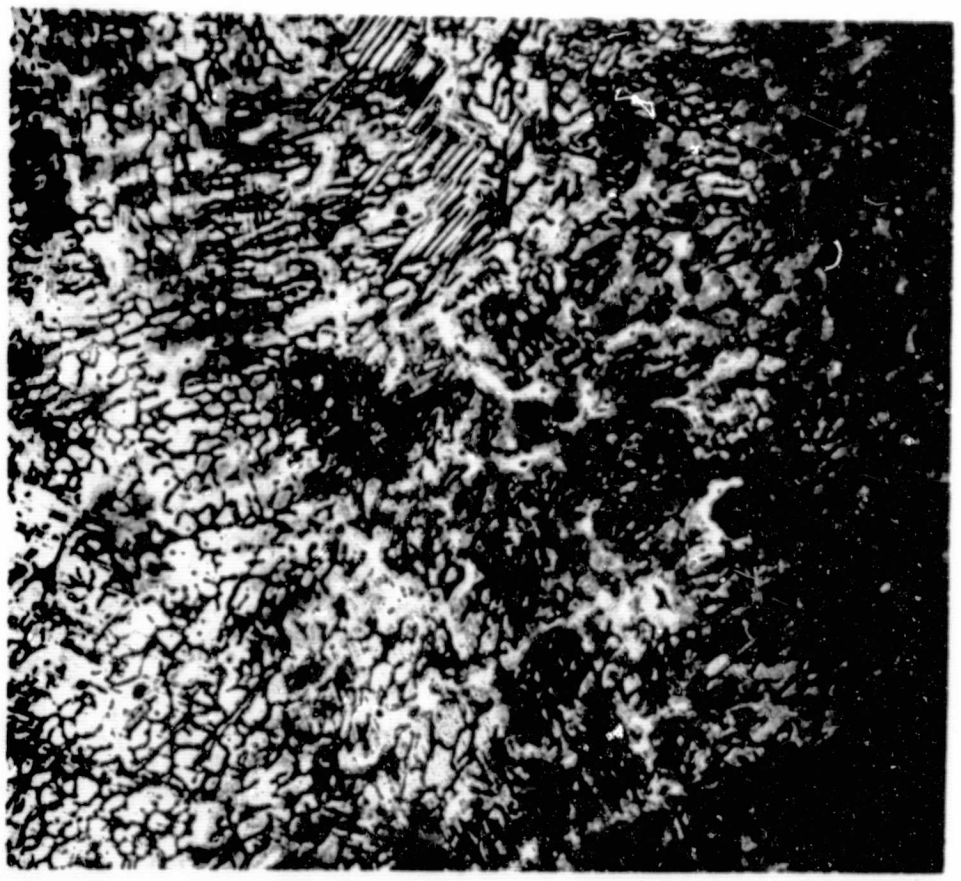

Condition: Irradiated - Strained

Mag: 100X
Etchant: 10% Ammonium Persulfate

The microstructure consists of a high Cr-Fe phase (dark) - carbides (black) in a matrix of austenite (light).

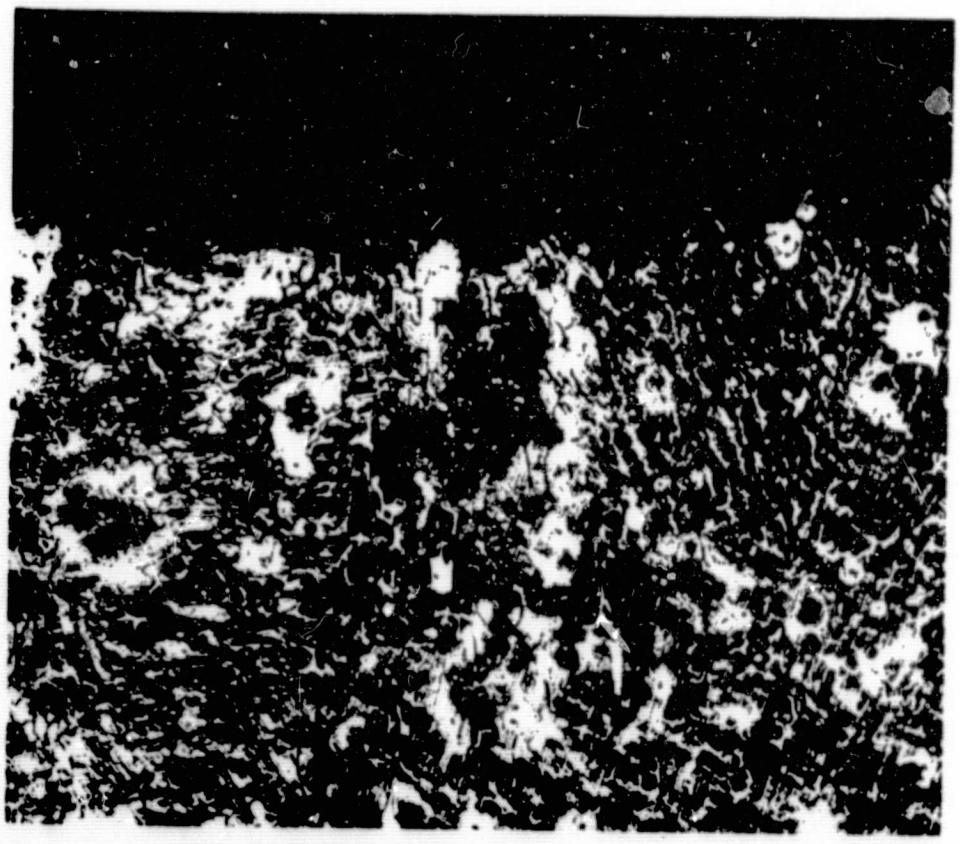

Condition: Irradiated - Strained, Fracture

Mag: 100X
Etchant: 10% Ammonium Persulfate

The areas of high strain exhibit general darkening due to preferential etching.

Figure 31

Stainless Steel, 347 - Irradiated - Sand Casting - Annealed - Condition L - Strained - Fracture - 100X

c. Electron Microscopy

Electron microscopy examinations were performed on specimens of 347 in the cast, wrought, and welded conditions. Representatative photomicrographs were taken (at 15000X).

The irradiated samples were reviewed in the as-received and welded conditions; representative electron micrographs are shown in Figure 32. The microstructure of the irradiated, unstrained material is essentially identical to that of the control samples, an austenite matrix with chromium rich ferrite. Micrographs for this condition are included in References 2 and 7. A rather complex microstructure was shown for the casting in the strained sample. It consisted of chromium rich ferrite and austenite with partially transformed areas. Bands running through the sustenite grains are reported as (111) planes thought to be epsilon martensite (or hcp). The structure is probably affected more by the straining at cryogenic temperatures than by the results of irradiation.

The welded sample was typical of control material in the unstrained and strained conditions. In the strained structures, the chromium rich ferrite phase appears in the grain boundaries of the transformed austenite. No effects of irradiation were noted.

Electron fracrographs of the fractured surface of tensile specimens were taken after testing. Representative photographs were taken of the edge and center of the fracture (at 4200X) on irradiated samples.

Examination of the fractographs of the fractured surface of the irradiated 347 plate test sample (found in References 2 and 7) shows non-oriented dimples of random size. The fracture at the edge is composed of oriented dimples typical of a ductile shear failure. Many of the dimples contain particles, probably carbides. The fracture is typically ductile with differences in inclusion content, or in just etching procedures between the two conditions. In either case, no effect of irradiation was noted. The fracture was primarily transgranular.

Material: Stainless Steel 347

Form: 1/4" Plate

Specimen No.: LWU 204, LU 178

Specification:

Condition: Irradiated - Strained

Mag: 15000X
Etchant: 10% Ammonium Persulfate

The microstructure consists of the chromium rich ferrite and austenite with partially transformed areas. The bands running through the austenite grains are (111) planes thought to be made up of (hcp) or epsilon martensite. Alpha martensite is also present. It is felt that the different textured area near the ferrite austenite interface is alpha martensite. (LU-178)

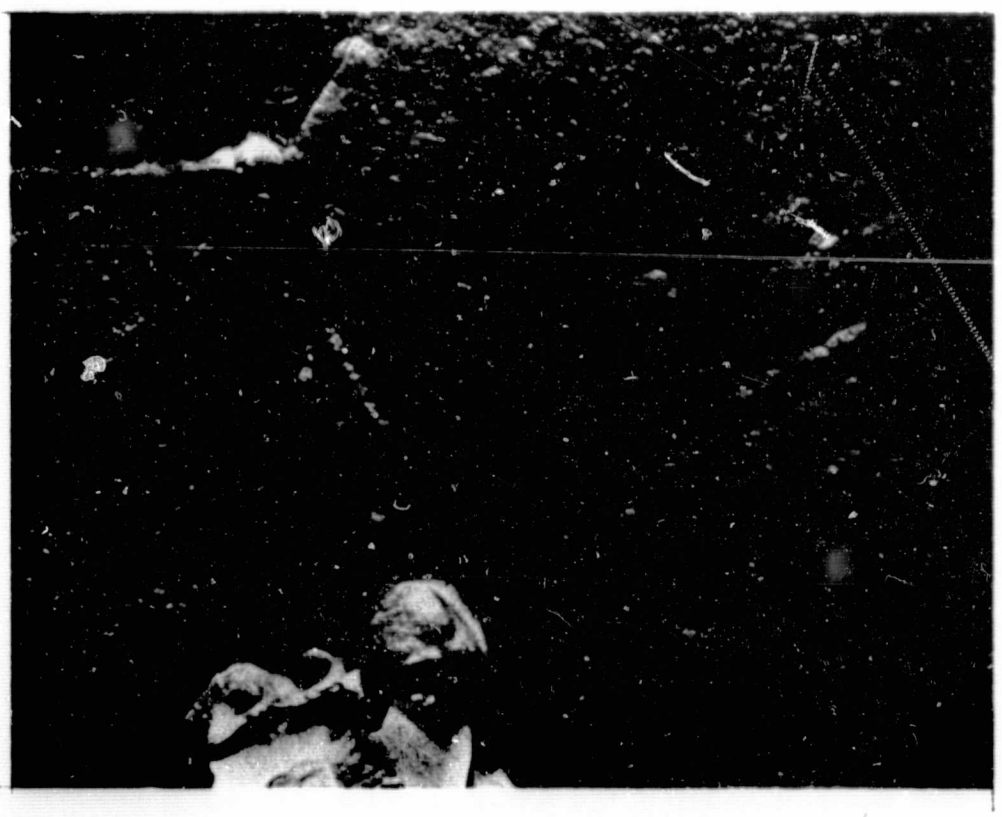

Condition: Irradiated - Welded - Strained LWU 204

Mag: 15000X
Etchant: 10% Ammonium Persulfate

The chromium-rich ferrite phase appears in the grain boundaries of the transformed austenite phase.

Figure 32

Stainless Steel 347 - Irradiated - Condition L and LW - Strained - 15000X

Figure 33 (top) exhibits the fracture surface of the welded and irradiated specimens as tested in the unnotched condition. The fracture at the edge is made up of large and small oriented dimples, typical of a shear-type of fracture. The fracture at the center (not indicated) is made up of microvoid and intergranular fractures.

Figure 33 (bottom) exhibits the fracture surface of the welded and irradiated specimens as tested in the notched condition. The fracture was ductile. The fracture at the edge is composed mainly of quasi-cleavage facets, however, some dimples are present. The overall fracture mode is irregular and semibrittle. It is thought that localized segregation, which occurred during welding, dictates the localized fracture pattern.

Figure 34 shows fractographs taken from the edge and center of the fracture of the cast 347. The microstructure at the center exhibited the same characteristics as at the edge. The control specimen exhibited ductile domains while the irradiated specimen showed large quasi-cleavage facets and some intergranular fracture at the austenite-ferrite interface.

Material: Stainless Steel 347

Form: 1/4" Plate

Specimen No.: LWU 204 and LWN 210

Specification:

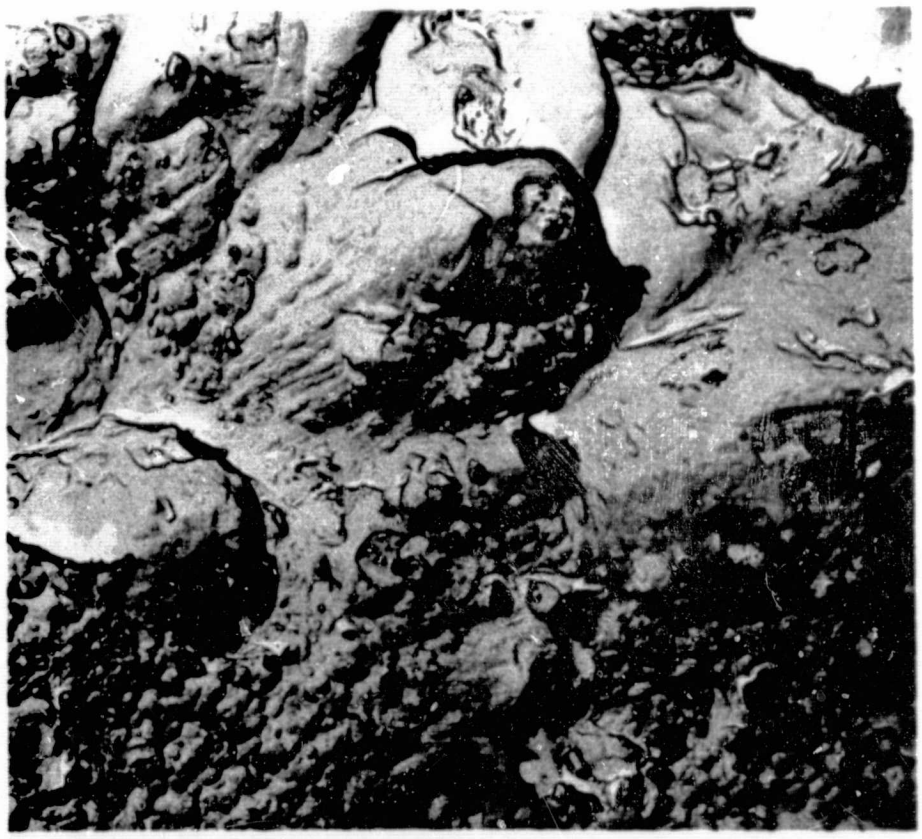

Condition: Irradiated - Welded - Unnotched - Fractograph - Edge (LWU 204)

Mag: 4200X

The fracture at the edge of the specimen is made up of large and small oriented dimples, typical of a shear-type of fracture. Some of the large dimples at the top of the photo have fractured ferrites at the tip.

Condition: Irradiated - Welded - Notched - Fractograph (LWN 210)

Mag: 4200X

The fracture is composed mainly of large dimples, indicating that the fracture was ductile in this local area. Near the upper right corner is an area that indicates localized segregation during welding and the fracture follows the cast structure produced. The pitted appearance that is present in isolated areas is oxidation.

Figure 33

Stainless Steel 347 - Irradiated-Condition LW-Welded Plate-Notched Unnotched Fractograph - 4200X

Material: Stainless Steel 347
Form: Sand Casting
Identification: Specimen No. LU 178

Condition: Irradiated - Unnotched Fractograph - LU 178
Mag: 4200X

The fracture surface at the edge of the specimen exhibited the same characteristics as at the center; large quasi-cleavage facets, some intergranular fracture at the austenite ferrite interface, and isolated areas of microvoid fracture.

Figure 34

Stainless Steel 347 - Irradiated - Sand Casting - Annealed
Unnotched - Fractograph - 4200X

d. X-Ray Diffraction

The X-ray diffraction data are shown in Table 21.

Diffractograms from the welded conditions of the unstrained area of the wrought 347 grip specimen showed the austenite phase only. Lattice parameters and microstress levels were essentially unchanged. The pattern from the strained areas showed only the martensite phase. No austenite was detected. The combination of straining and cryogenic environment had brought about the complete transformation from the face-centered cubic austenite to the body-centered cubic martensite phase. Comparisons of lattice parameter and microstress level were not valid, since a new phase was present.

The X-ray diffraction pattern for the cast 347 exhibited no significant variation between the strained and the unstrained conditions. A variation was noted between the control cast-metal and the irradiated, in that - in the unstrained condition - a basic austenite system was detected in the control sample. It is probable that the diffraction pattern of the unstrained control sample was in error and was a result of positioning in the X-ray set-up analysis.

The X-ray diffraction patterns of the irradiated plate stock and welded samples were similar to those of the control samples. A phase change occurred in the transformation of austenite to martensite while straining at cryogenic temperatures. No effect of irradiation was noted other than a small reduction in microstress level. No significant variation in lattice parameter was noted.

TABLE 21

X-RAY DIFFRACTION DATA - 347 STAINLESS STEEL

hkl	b.c.c. Martensite Alpha-Iron		f.c.c. Austenite Gamma-Iron		As-Received Plate (Sheet Stock)		CONTROL Cast Strained		CONTROL Cast Unstrained		CONTROL Welded Strained		CONTROL Welded Unstrained	
	(1)	(2)	(1)	(2)	(1)	(2)	(1)	(2)	(1)	(2)	(1)	(2)	(1)	(2)
111			2.08	100	2.09	100	2.07	100	2.08	11			2.07	100
110	2.027	100			2.04	50	2.03	12			2.02	100		
200	1.433	19	1.80	69	1.80	24	1.79	12	1.80	20			1.80	33
220			1.27	9	1.27	9	1.27	10	1.27	100			1.27	45
211	1.170	30												
	LATTICE PARAMETER, Å													
	2.87		3.60		3.60		3.595		3.595		2.861		3.593	
	MICROSTRESS, Δθ													
					1.0° (2θ=128°)		0.53° (2θ=128°)		0.60° (2θ=128°)		0.62° (2θ=69°)		0.60° (2θ=128°)	

IRRADIATED-COBALT X-RAY TARGET

hkl	Cast Strained		Cast Unstrained		Plate Strained		Plate Unstrained		Welded Strained		Welded Unstrained	
	(1)	(2)	(1)	(2)	(1)	(2)	(1)	(2)	(1)	(2)	(1)	(2)
111	2.09	100	2.08	100			2.08	100			2.07	100
110	2.03	21	2.03	10	2.03	100			2.03	100		
200	1.80	50	1.44	5			1.80	55	1.44	25	1.80	60
220			1.25	5			1.27	9			1.27	15
211	1.17	26			1.15	87	1.08	20	1.17	40	1.08	20
	MICROSTRESS, Δθ											
	0.30° (2θ=50.8°)		0.26° (2θ=51.0°)		0.66° (2θ=52.4°)		0.28° (2θ=52.4°)		0.64° (2θ= 52.4°)		0.30° (2θ= 51.1°)	
	No Peak (2θ=129°)		No Peak (2θ=129°)		No Peak (2θ=129°)		No Peak (2θ=129°)		No Peak (2θ=129°)		No Peak (2θ=129°)	
	LATTICE PARAMETER, A											
	3.533 FCC 2.857 BCC		3.414 FCC 2.868 BCC		2.815 BCC		3.570 FCC		2.865 BCC		3.578 FCC	

NOTES: (1) "d" spacings

(2) Relative intensities, percent-shift in "d" spacings indicates lattice expansion orientation change is indicated by intensity change for A given hkl

2. 440-C (Martensitic Stainless Steel)

a. Mechanical Properties

Evaluation of this alloy is not possible. All control specimens broke in such a way that tensile properties could not be measured satisfactorily. All unnotched, irradiated specimens failed in the grips as well as in the gage length.

Figure 35 shows an example of a typical fracture for an unnotched specimen of this alloy.

The average tensile strength for control and irradiated specimens are included. These data, however, should not be considered to be valid.

The average room temperature data is presented in Table 22. Detailed data, of the notched and unnotched specimens after radiation, are also included.

Additional testing and caution for use of the alloy in this environment is recommended.

TABLE 22

AVERAGE AND DETAILED MECHANICAL PROPERTIES DATA

STAINLESS STEEL 440-C

	Room Temp.	Control -423°F	Change Room Temp. vs Control in Percent	Irrad. -423°F	Change Control vs Irrad. in Percent	Threshold
Unnotched Ultimate tensile strength psi	620300	204000*	-21.7	213050*	+ 4.4	
Std. deviation - psi				3650		
0.2% Yield strength psi	243300					
% Elongation	0.2					
% Reduction in area	0.8					
Unnotched K_t = 6.3						
Ultimate strength- psi	-	-		50700		
Std deviation				6500		

DETAILED DATA

UNNOTCHED SPECIMEN*

Specimen No.	Condition	Ultimate Strength
197	LU	224200
198	LU	229500
201	LU	202000
202	LU	196500
Average		213050
Std. Deviation		3650

NOTCHED SPECIMEN

Specimen No.	Condition	Ultimate Strength
604	LN	51.400
606	LN	58900
608	LN	49300
610	LN	43100
		50700
		6500

* All unnotched specimen broke in such a manner that no satisfactory value for tensile properties could be obtained.

Material: Stainless Steel 440C R_c = 58-60
Form: 1/4 in. x 2 in. Bar
No.: 2-198
Identification: Specimen No. LN 604

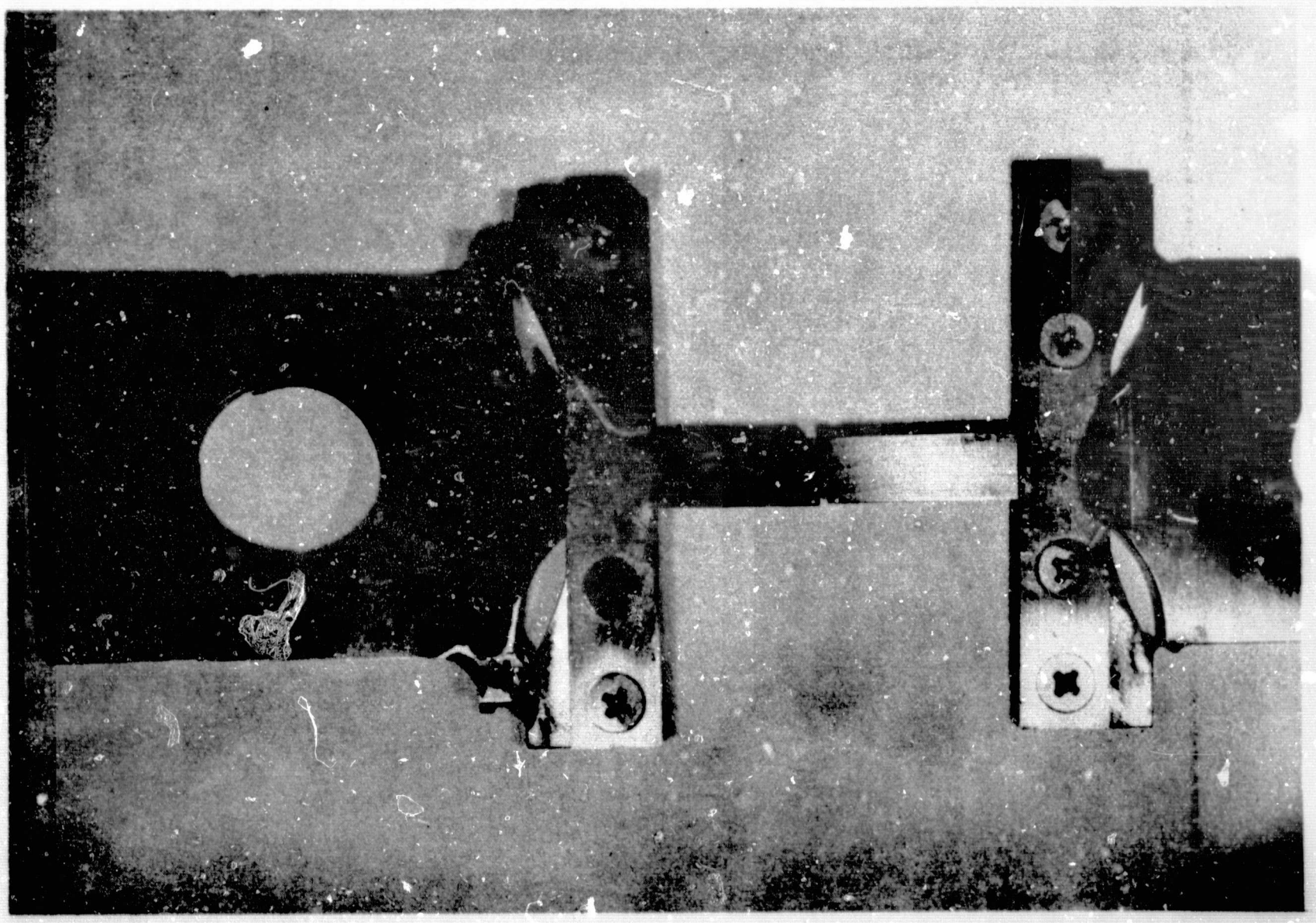

Figure 35
Typical Fracture of 440C Stainless Steel

b. Metallography

Metallographic examination of this alloy after radiation was limited to electron fractography and X-ray diffraction.

c. Electron Microscopy

Figure 36 is a fractograph at 4200X of an irradiated notched specimen. The fracture surface indicates a failure through and around the brittle carbides and a low ductility fracture at the prefix.

Material: Stainless Steel 440C R_c 58-60
Form: 1/4 in. x 2 in. Bar
Identification: Specimen No. LN 604

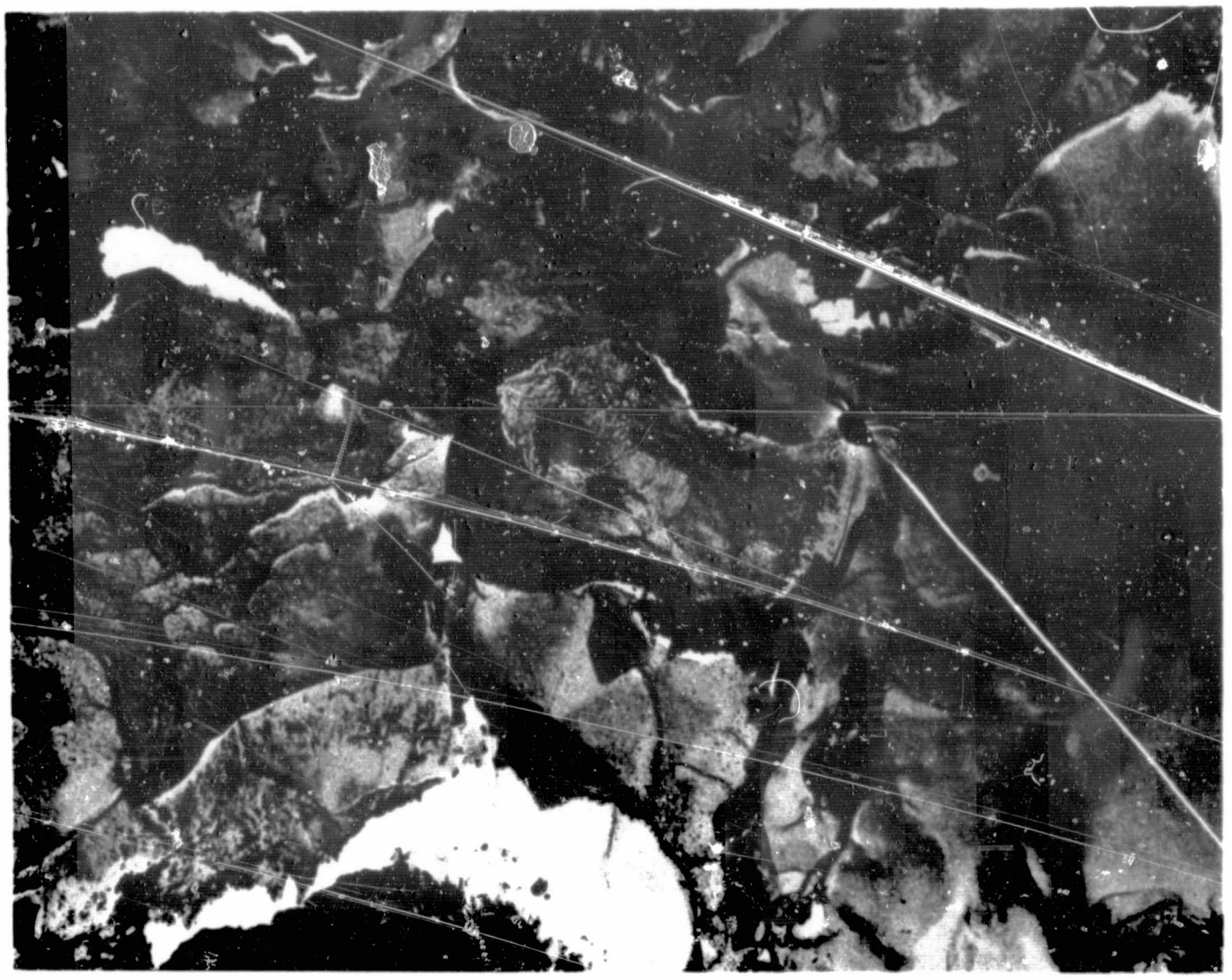

Condition: Irradiated-Fractograph
Mag: 4200X

The fracture surface indicates a failure through and around the brittle carbides and allow ductility fracture at the matrix. The area adjacent to the black extracted carbide is oxidize probably as a result of depletion of the chromium during the carbide formation.

Figure 36

Stainless Steel 440C-Irradiated-Heat Treated to R_c 58-60 Fractograph 4200X

3

d. X-Ray Diffraction

Table 23 shows a tabulation of the X-ray parameters for the control specimens. The X-ray diffraction pattern of the as-received material indicated the normal body-centered cubic structure of tempered martensite and one weak line giving evidence of some retained austenitic phase. There was no preferred orientation. The microstress level of 6.2° in 2θ, at 2θ, = 156°, indicated extreme internal micro-strains.

The diffractograms from the unstrained portion of the tensile specimen showed only one martensite diffraction line (110) which was relatively broad for such a low angle line 2θ = 68°. A weak austenite line was also present.

TABLE 23

X-RAY DIFFRACTION DATA - 440C STAINLESS STEEL

	f.c.c. Gamma-Iron Austenite		b.c.c. Alpha-Iron Martensite		As Received		Strained		Control (3) Unstrained	
hkl	(1)	(2)	(1)	(2)	(1)	(2)	(1)	(2)	(1)	(2)
111	2.08	100					2.08	10	2.08	10
200	1.80	80			1.80	5				
220	1.27	50								
110			2.03	100	2.04	100	2.03	100	2.03	100
200			1.43	19	1.44	20	1.44	5		
211			1.17	30	1.17	35				
LATTICE PARAMETER Å										
	2.87		2.88		2.88		2.88			
MICROSTRESS $\Delta\theta$										
			6.2° (2θ=154°)		0.81° (2θ=68°)		0.93 (2θ=68°)			

NOTES: (1) "d" spacings

(2) Relative intensities, percent. Shift in "d" spacings indicates lattice expansion. Orientation change is indicated by intensity change for a given hkl.

(3) LV-200

3. Type 410 (Martensitic Stainless Steel)

Shear strength for this alloy was the only property investigated. Average value, standard deviation and detailed data at room temperature, at liquid hydrogen without radiation (control), and with radiation are presented in Table 24. An increase in shear strength from 90,800 psi at room temperature, to 149,300 psi at liquid hydrogen without radiation, to 160,700 psi at liquid hydrogen with nuclear radiation (5×10^{16} nvt dose level) was obtained.

The threshold level of damage, however, was not achieved at this dose level.

TABLE 24

AVERAGE AND DETAILED SHEAR STRENGTH DATA FOR 410 S.S.

	Room Temp.	Control -423°F	Change-Room Temp. vs Control in Percent	Irrad. -423°F	Change-Control vs Irradiated in Percent	Threshold
Ultimate Shear Strength-PSI	90,800	149,300	+60	160,700	+8	
Standard Deviation PSI	940	4,100		8,480		

DETAILED SHEAR STRENGTH-KSI

168.9
167.1
150.5
166.3

E. HIGH TEMPERATURE ALLOYS

1. A-286 (Iron Base Alloy)

a. Mechanical Properties

Average values and standard deviations of mechanical properties obtained at room temperature, at liquid hydrogen temperature without radiation (control) and at liquid hydrogen temperature with nuclear radiation are presented in Table 25. Detailed test results for the irradiated specimens tested at liquid hydrogen temperature without warmup, are shown in Table 26.

The initial increase i tensile properties (ultimate, yield and notched) from room to liquid hydrogen tempe.. ..es is practically unchanged because of the radiation exposure of 5×10^{16} nvt total dose level. The initial increase of shear strength from 100,900 psi at room temperature to 168,200 psi at liquid hydrogen temperature was followed by a 7% decrease to 157,100 psi. The ratios of notched-to-unnotched ultimate and notched-to-yield strength, as affected by radiation, were for all practical purposes, unchanged. A comparison of ductility (elongation and reduction of area) at room and cryogenic temperatures shows a 95% increase in elongation, while reduction of area was decreased by 10%. This increase in percent elongation is normal behavior for the alloy; however, this large percent change has not been reported by other experimenters. The attainment of this advantageous increase in elongation resulted from the heat treating procedure used for this material. The alloy is sensitive both to heat treating temperature and to titanium content. Although maximum attainable strength depends on titanium content, considerable variation in properties may be achieved by varying the solution and aging temperature as well as time of treatment. The specimens for this test were solution heat treated at 800°F for 90 minutes (30-60 minutes longer than standard practice), air cooled and aged for 16 hours at 1350°F (1325°F usual practice).

Radiation effects on ductility was reversed as shown by a 13% decrease in elongation and 5% increase in reduction of area. Stress-strain curves obtained with extensometer are shown in Figure 37. Threshold level of damage from radiation was not obtained for any property.

TABLE 25

AVERAGE MECHANICAL PROPERTIES TEST DATA FOR A-286

	Room Temp.	Control -423°F	Change- Room Temp. vs Control in Percent	Irrad. -423°F	Change- Control vs Irradiated in Percent	Threshold
UNNOTCHED						
Ultimate Strength-PSI	154,300	223,700	+45	219,800	-1.7	
Std. Deviation-PSI	1,100	4,400		3,500		
0.2% Yield Strength-PSI	99,100	135,900	+37	137,000	+1	
Std. Deviation-PSI	600	6,000		5,700		
% Elongation	19.2	37.5	+95	32.25	-13.1	
Std. Deviation-%	5.2	1.2		7.8		
% Reduction in Area	39.1	35.2	-10	37.0	+5.1	
Std. Deviation-%	3.0	5.4		1.6		
Ult. Shear Strength-PSI	100,900	168,200	+62	157,100	-6.6	
Std. Deviation-PSI	2,100	12,000		5,100		
NOTCHED Kt = 6.3						
Ultimate Strength-PSI	152,900	185,800	+22	188,600	+1.5	
Std. Deviation-PSI	2,000	4,000		1,500		
Ratio $\frac{\text{Notched Ult.}}{\text{Unnotched Ult.}}$	0.99	0.83	-16	0.86	+3.6	
Ratio $\frac{\text{Notched Ult.}}{\text{Unnotched Yield}}$	1.54	1.37	-11	1.38	+1	

TABLE 26

DETAILED MECHANICAL PROPERTIES DATA FOR A-286

Specimen Number	Specimen Condition	Ultimate Strength: Instron Cell(KSI)	Ultimate Strength: Ram Cell(KSI)	Yield Strength 0.2% Offset(KSI)	Percent Reduction in Area	Percent Elongation
221	LN	201.8	190.61			
222	LN	200.2	188.6			
225	LN	194.4	186.91			
226	LN	199.8	188.2			
210	LU	230.9	222.2	129.0	37.4	23.75
211	LU	227.8	214.6	142.0	34.8	27.50
213	LU	233.6	221.8	137.0	37.2	38.25
214	LU	234.0	220.44	140.0	38.6	39.5

Elongation Data

Specimen Number	Specimen Condition	Extensometer: Post Irradiation (Mills)	Pull Rod: Post Irradiation (Mills)	Pull Rod: Control (Mills)	Bench Measurement: Post Irradiation (Mills)	Bench Measurement: Control (Mills)
210	LU	*570	637		475	
211	LU	*680	715		550	
213	LU	*970	994		765	
214	LU	*945	992		790	
Average		791	835	982.5	645	750
% Elongation		28.0	29.5	34.8	32.25	37.5
% Damage			-15.1		-13.1	

Ultimate Shear Strength (KSI)

162.8
152.9
155.6

*Extrapolated from rod movement

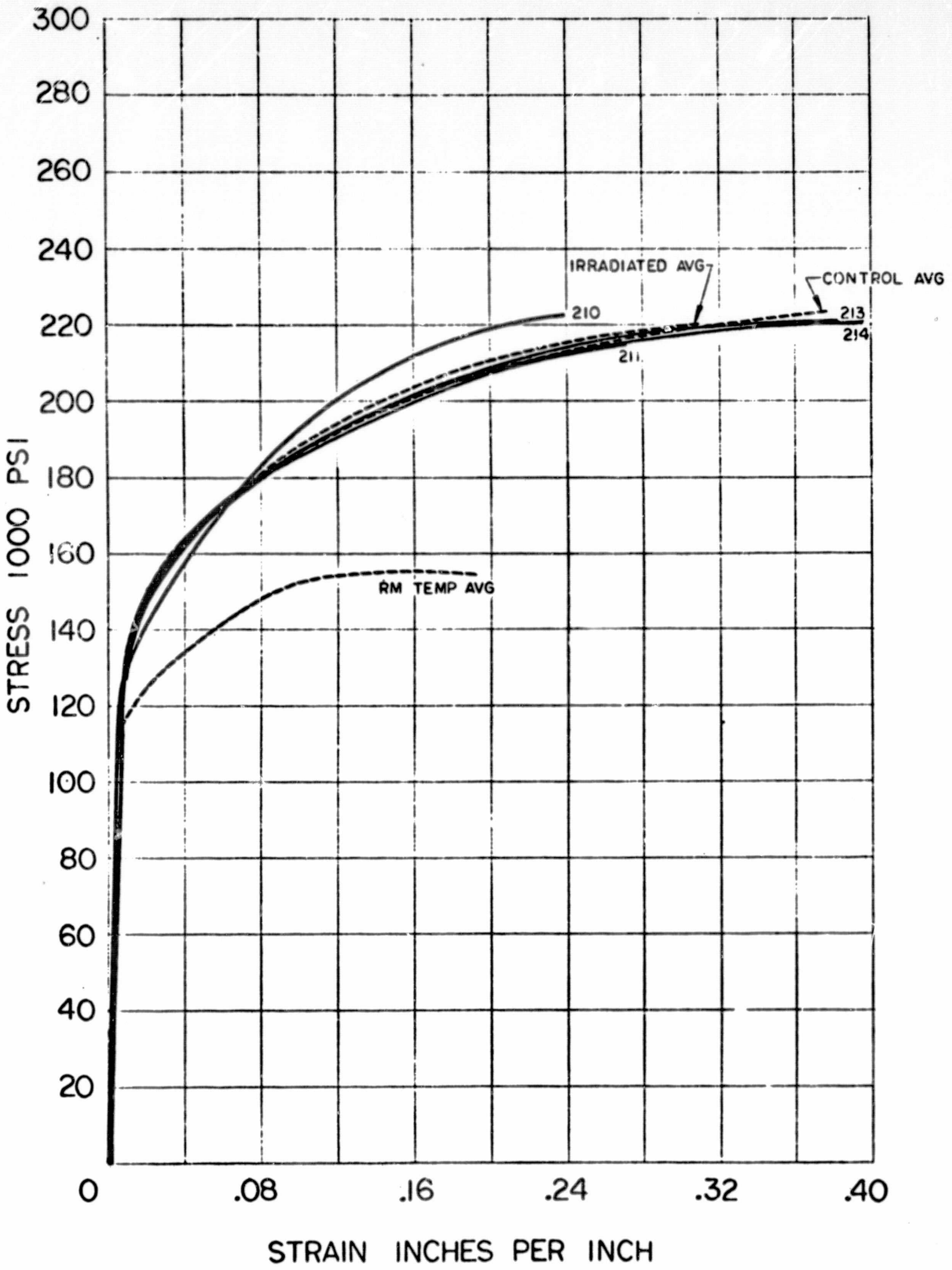

Figure 37

Stress - Strain Curves for A-286

b. Metallography

Photomicrographs of general structure of the irradiated specimens are shown in Figure 38. The general structure consists of austenite with numerous annealing twins and is speckled with titanium carbide (TiC). The grain size is ASTM No. 7. The fracture is transgranular, and fracture areas show both strain lines and elongated grains. The microstructures of the irradiated specimens are essentially the same as the control specimens.

Material: A286
Form: 1/4 in. Plate
Identification: Specimen LU 214
Specification: AMS 5525

Condition: Irradiated-Unstrained
Mag: 1000X
Etchant: 10% Oxalic Acid (Electrolytic)

The microstructure shows an austenitic matrix and dispersed carbides. Note the annealing twins.

Figure 38
A286 - Irradiated - Condition L - Unstrained - 1000X

c. Electron Microscopy

The electron micrographs of the irradiated specimens were examined. The structure is comparable to that of the control specimens and photomicrographs are not produced here. Precipitate sites were observed, and faint strain lines were evident in the strained specimen.

Figure 39 contains fractographs of the irradiated, notched and unnotched specimens and illustrates the varying size duplex dimple structures. Current theory describes the origin of each dimple to a void, nucleated at an inclusion. The relative size of dimples is dependent upon size, nature, and distribution of inclusions. Materials containing particles of two different sizes show duplex dimple sizes. Failure was typically ductile. The structure for notched and unnotched material is slightly different, but the mode of fracture is still typically ductile. No significant structural variations exist which might indicate the influence of irradiation effects.

Material: A286

Form: 1/4" Plate

Specimen No.: LU 214 and LN 221

Specification: AMS 5525

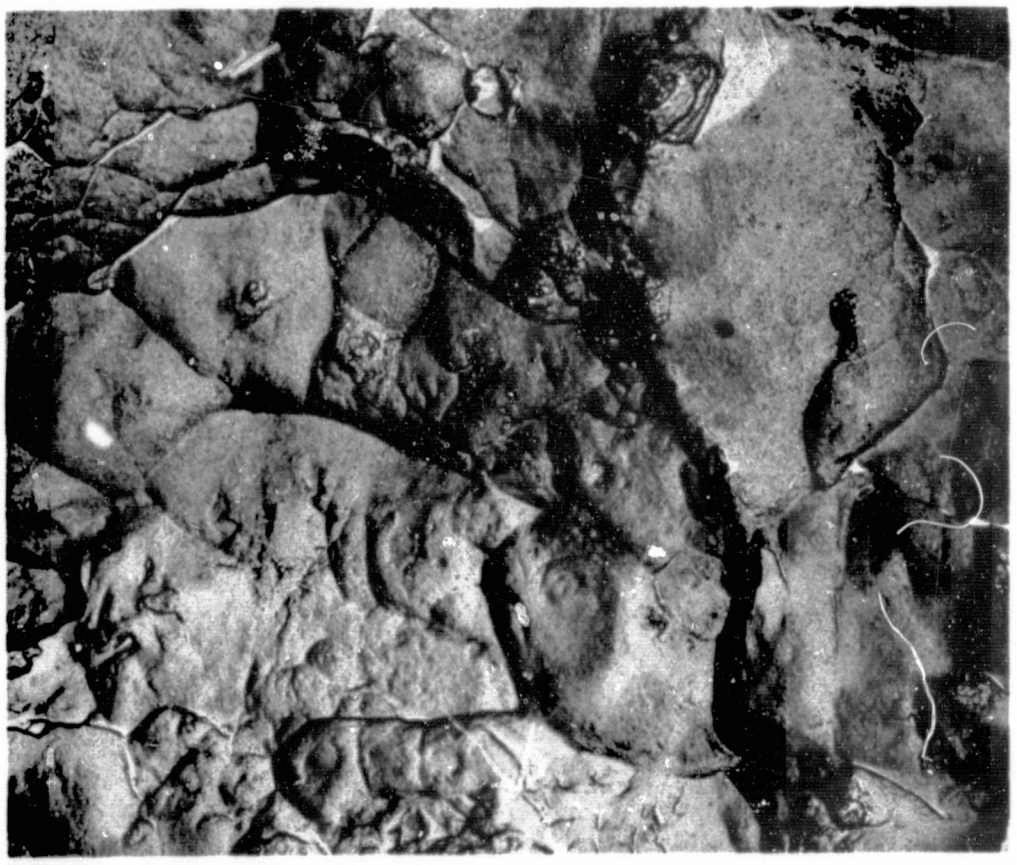

Condition: Irradiated-Fractograph-Fracture Center, Unnotched (LU 214)

Mag: 4700X

The fractograph of the center area shows a microvoid fracture mode, which is indicative of a ductile failure. Both small and large equiaxed dimples are present.

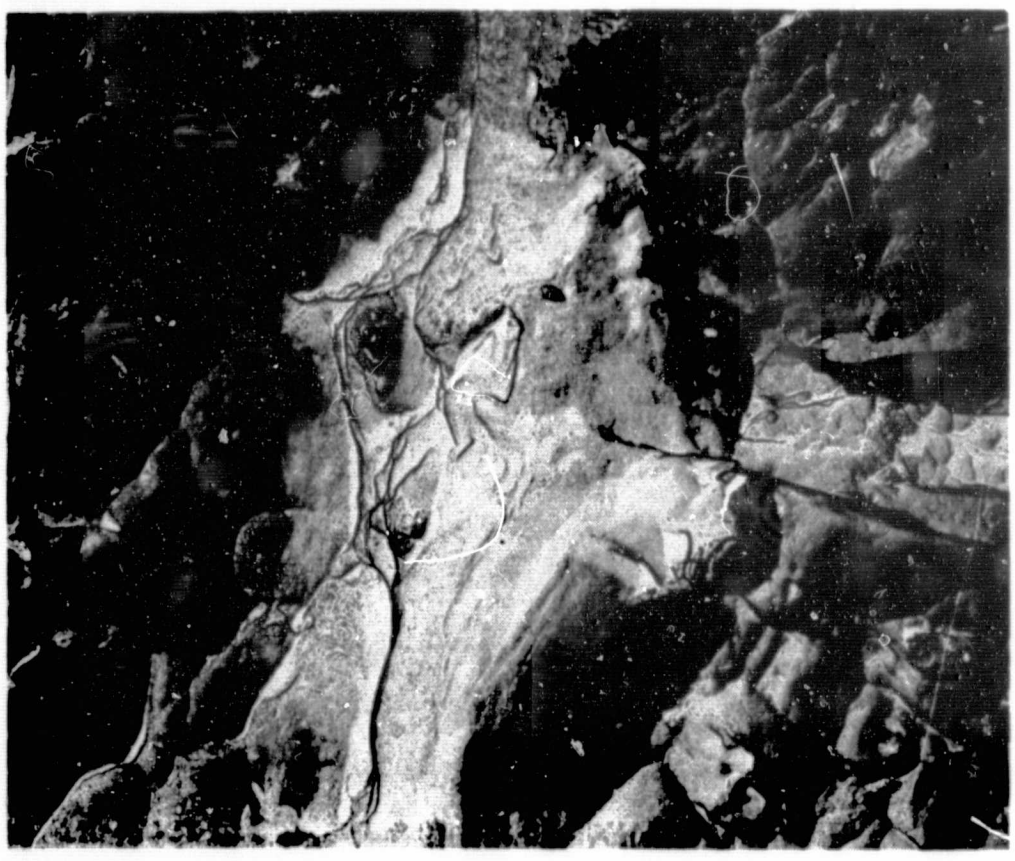

Condition: Irradiated-Fractograph-Fracture, Notched (LN-221)

Mag: 4200X

The fracture surface consists of dimples. Some of the dimples have brittle particles at the tips.

Figure 39

A286 - Irradiated - Condition L - Notched-Unnotched Fracture - Fractograph 4200X

d. X-Ray Diffraction

Table 27 shows the X-ray diffraction data. X-ray diffraction patterns were not obtained from the as-received material. Diffractograms from the strained and unstrained areas of a control specimen showed the face-centered cubic structure of austenite. The orientation of the unstrained specimen was in the (111) direction as compared to (110) for the strained area.

The X-ray diffraction data for the irradiated samples indicated the strained and unstrained material to have the same preferred orientation as the control specimen. The data shows no significant change in lattice constant either with straining or with radiation. The changes observed in the microstress level are within the experimental error and cannot be attributed to the radiation effects.

TABLE 27

X-RAY DIFFRACTION DATA - A-286 IRON BASE HIGH TEMPERATURE ALLOY

	f.c.c. Austenite Gamma-Iron				Control				Irradiated			
					Strained		Unstrained		Strained		Unstrained	
hkl	(1)	(2)	As Received (1)	(2)	(1)	(2)	(1)	(2)	(1)	(2)	(1)	(2)
111	2.08	100			2.08	30	2.07	100	2.08	65	2.08	100
110												
200	1.80	80			1.80	25	1.80	40	1.79	65	1.80	50
220	1.27	50			1.27	100	1.27	80	1.27	100	1.27	43
211											1.08	40
LATTICE PARAMETER (Å)												
	3.60				3.594		3.592		3.575		3.588	
MICRO STRESS,												
					1.67° (2θ = 129°)		0.65° (2θ = 129°)		1.08° (2θ = 21.1°) No Peak (2θ = 129°)		0.28° (2θ = 51.0°) No Peak (2θ = 129°)	

NOTES: (1) "d" spacings
(2) Relative intensities, percent.
Shifting in "d" spacings indicates lattice expansion
Orientation change is indicated by intensity change for a given hkl.

2. Hastelloy C

a. Mechanical Properties

Average values and standard deviation of mechanical properties obtained at room temperature, at liquid hydrogen temperature without radiation (control) and at liquid hydrogen temperature with nuclear radiation (5×10^{16} nvt total dose) are presented in Table 28. Detailed test results for the irradiated specimens tested at liquid hydrogen without warmup are shown in Table 29.

A comparison of tensile properties at room temperature with those obtained at -423°F showed a 56.5% increase in ultimate and 87% increase in yield strengths. A comparison of these properties obtained at -423°F with and without radiation showed no change. Because of large elongation of the unnotched specimen, which permitted pick up of the notched specimen prior to fracture, control data for notched specimens are not available for comparison.

A comparison of the shear strength obtained for the three test conditions showed an increase from 92,600 psi at room temperature to 153,400 psi at 423°F (61%), and a decrease to 139,200 psi (9.2%) because of radiation.

A comparison of the ductility of this material as measured by elongation and reduction of area for all three test conditons showed a large decrease from room to -423°F test temperatures (22% and 28%) followed by a small increase (8.5% to 0.5%) because of radiation for both papameters. Stress-strain curves obtained with extensometer are shown in Figure 40.

Threshold level of damage from radiation was obtained for shear strength.

TABLE 28

AVERAGE MECHANICAL PROPERTIES TEST DATA FOR HASTELLOY C

	Room Temp.	Control -423°F	Change- Room Temp. vs Control in Percent	Irrad. -423°F	Change- Control vs Irrad. in Percent	Threshold
UNNOTCHED						
Ultimate Strength-PSI	118,700	185,700	+56.5	187,300	+.86	
Std. Deviation-PSI	1,500	One Specimen Tested		3,800		
o.2% Yield Strength-PSI	59,300	111,000	+87	111,500	+.45	
Std. Deviation-PSI	800	1,000		2,500		
% Elongation	50.4	39.2	-22.2	42.5	+8.5	
Std. Deviation-%	.9	1.8		10.2		
% Reduction in Area	51.3	37.1	-28	37.3	+0.5	
Std. Deviation-%	3.4	2.0		6.5		
Ult. Shear Strength-PSI	92,600	153,400**	+61	139,200	-9.2	T
Std. Deviation-PSI	2,600	3,400*		1,680		
NOTCHED Kt - 6.3						
Ultimate Strength-PSI	99,700	No Data		156,800		
Std. Deviation-PSI	6,500			2,500		
Ratio $\frac{\text{Notched Ult.}}{\text{Unnotched Ult.}}$	0.84			0.835		
Ratio $\frac{\text{Notched Ult.}}{\text{Unnotched Yield}}$				1.40		

* Instron Data

** Calculated from instron data

TABLE 29

DETAILED MECHANICAL PROPERTIES TEST DATA FOR HASTELLOY C

Specimen Number	Specimen Condition	Ultimate Strength Instron Cell(KSI)	Ultimate Strength Ram Cell(KSI)	Yield Strength 0.2% Offset(KSI)	Percent Reduction in Area	Percent Elongation
365	LN	162.58	158.8			
370	LN	163.3	153.8			
353	LU	194.32	183.0	112.0	32.9	35.2
354	LU	197.3	185.9	112.0	42.9	48.5
357	LU	203.83	192.0	108.0	42.8	54.2
358	LU	180.6	188.2	114.0	30.6	38.2

Elongation Data

Specimen Number	Specimen Condition	Extensometer Post Irradiation (Mills)	Pull Rod Post Irradiation (Mills)	Pull Rod Control (Mills)	Bench Measurement Post Irradiation (Mills)	Bench Measurement Control (Mills)
353	LU	946	973		704	
354	LU	1266	1313		969	
357	LU	*1435	1435		1084	
358	LU	943	966		764	
Average		1150	1179		851	784
% Elongation		40.6	41.6		42.5	39.2
% Damage					+8.5	

Ultimate Shear Strength (KSI)

140.6
140.6
137.7
137.7

* Extrapolated from rod movement

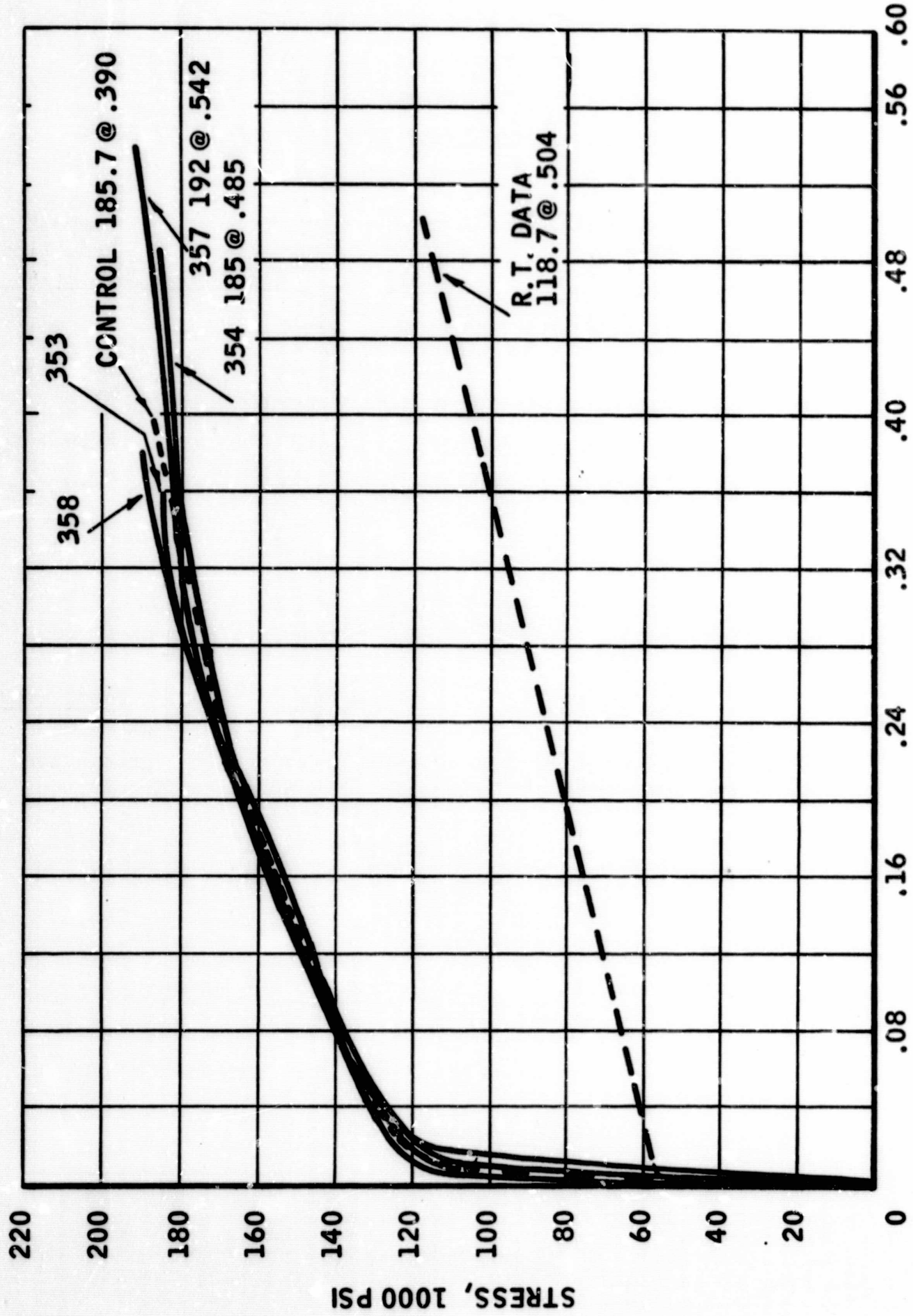

Figure 40

...s - Strain Curves for Hastelloy C

b. Metallography

Photomicrographs (at 100X and 1000X) were examined to evaluate any pertinent changes of the microstructure of the strained and unstrained areas of the irradiated specimens.

There is no evident variation of the structure of the irradiated specimens from the control. The irradiated samples appear to be deeply etched, hence, strain orientation and annealing twins are more readily evident. The microstructure from the unstrained irradiated specimen shows equiaxed grains of nickel rich matrix. Twinning is again prominent within the grains. Carbide inclusions are evident. The fracture mode is transgranular with normal grain elongation during straining.

c. Electron Microscopy

Electron microscopic examinations were performed on strained and unstrained areas of the irradiated specimens.

Figure 41 shows a typical microstructure (at 15000X) of the irradiated material in the strained condition. The structure is typical of the strained and unstrained regions of the irradiated sample and within the allowable degree of comparison (although limited in scope) is the same as that of the control specimens: nickel rich matrix and spherical carbides.

Electron fractographs were taken from the edge and center of tensile fractures of irradiated specimens. Representative photomicrographs are shown in Figure 42. The fractographs of the irradiated samples exhibited large microvoids and decohesion glide markings. The fracture is typically ductile at both center and edge areas. The structure is unaffected by either notched or unnotched testing.

Material: Hastelloy C
Form: 1/4 in. Plate
Identification: Specimen No. LU 354
Specification: AMS 5530C

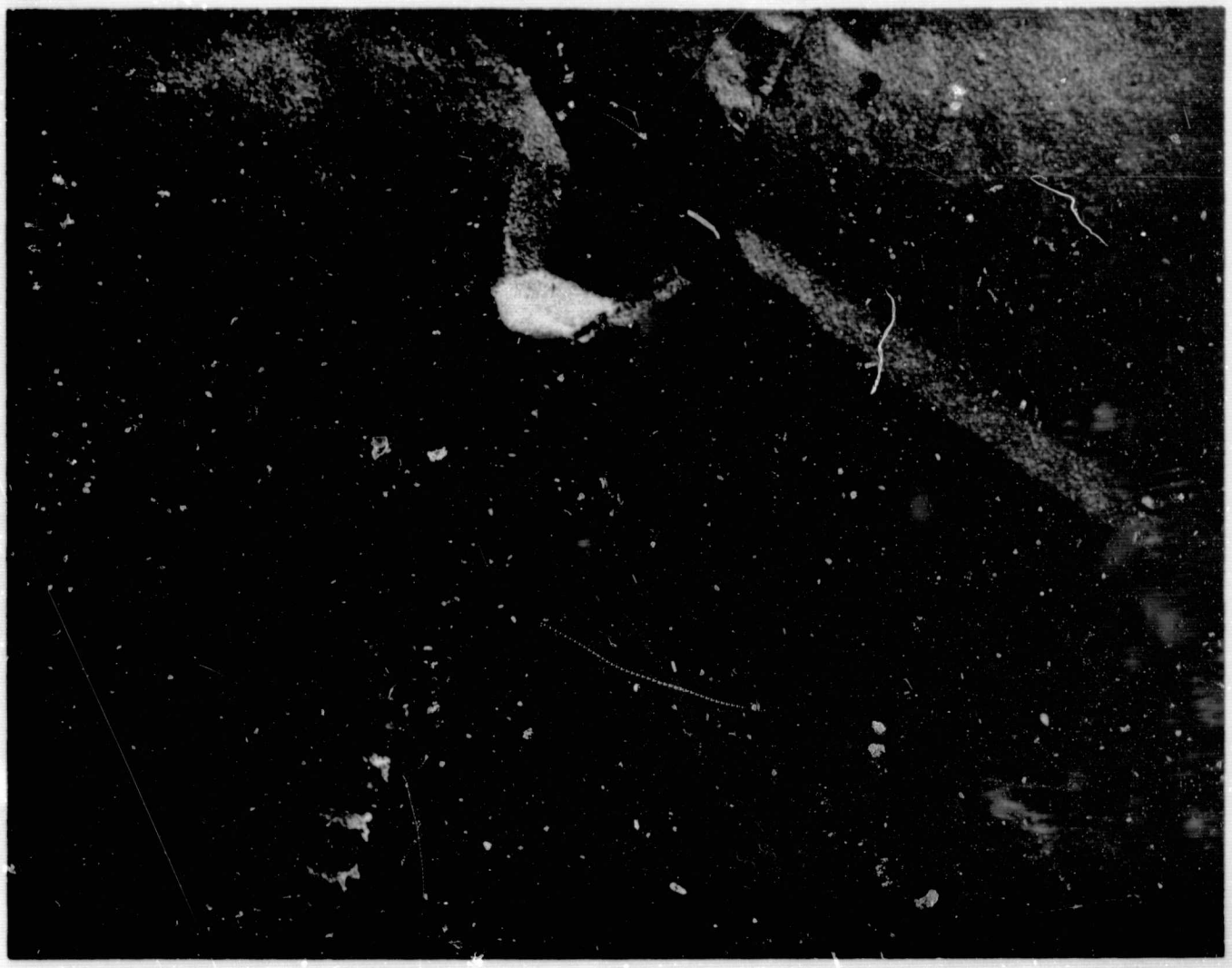

Condition: Irradiated-Strained
Mag: 15000X

The microstructure shows an annealing twin, a grain boundary with fine precipitate and austenitic matrix. The strain lines visible at lower magnifications are evident here as shallow troughs. The rectangular site is an etch pit of a carbide.

Figure 41

Hastelloy C-Irradiated-Condition L-Strained-15000X

Material: Hastelloy C

Form: 1/4" Plate

Specimen No.: LU 354

Specification: MMS 354

Condition: Irradiated and Fractograph-Fracture Center

Mag: 4200X

A grain boundary runs diagonally across. Fine carbide network appears on the boundary. The structure on the right is decohesion glide on large microvoids. Large carbides have fractured in a brittle manner, probably ahead of the main crack front initiating the free surface necessary for serpentive glide.

Condition: Irradiated-Fractograph-Fracture Edge

Mag: 4200X

This area taken near the edge exhibits a ductile failure mode, as evidenced by the large microvoids and decohesion glide marking.

Figure 42

Hastelloy C-Irradiated-Fractograph 4200X

d. X-Ray Diffraction

The X-ray diffraction data are shown in Table 30. The X-ray diffraction pattern from the solution annealed as-received material showed the face-centered cubic structure of nickel.

Diffractograms from the strained and unstrained areas of a tensile specimen test at -423°F showed lattice parameters of both areas to be identical with the as-received material. The microstress level of the strained area increased because of straining. The strained specimen had preferred orientation in the (220) direction.

Diffractograms from the strained and unstrained areas of the irradiated tensile specimen showed lattice parameters comparable to the control specimens. The microstress level decreased; and, even though the strained area had a higher microstress level than the unstrained, no significant difference was noted. The lattice parameter of the unstrained areas was essentially the same as the control specimens, but a decrease in lattice parameter was noted for the strained area. The spread of data, however, is within the limit of the experimental error and these changes may not be considered as a result of the radiation.

TABLE 30

X-RAY DIFFRACTION DATA - HASTELLOY C

	Pure Nickel		Control						Irradiated			
			As Received		Strained		Unstrained		Strained		Unstrained	
hkl	(1)	(2)	(1)	(2)	(1)	(2)	(1)	(2)	(1)	(2)	(1)	(2)
111	2.034	100	2.08	100	2.09	85	2.09	100	2.09	75	2.09	100
200	1.762	42	1.80	40	1.81	30	1.81	65	1.81	55	1.81	69
220	1.246	21	1.28	30	1.28	100	1.28	60	1.28	100	1.28	55
311									1.09	35	1.09	25
LATTICE PARAMETER, Å	3.524		3.61		3.61		3.61		3.581		3.605	
MICROSTRESS			0.53° (2θ = 129°)		1.10° (2θ = 129°)		0.64° (2θ = 129°)		0.32° (2θ = 74.2°) No Peak (2θ = 129°)		0.22° (2θ = 74.0°) No Peak (2θ = 129°)	

NOTES: (1) "d" Spacings

(2) Relative intensities, percent shift in "d" spacings indicates lattice expansion.

Orientation change is indicated by intensity change for a given hkl

3. Inconel X-750 (Precipitation Hardened Alloy)

a. Mechanical Properties

Average values and standard deviations of mechanical properties obtained at room temperature, liquid hydrogen temperature without radiation (control), and liquid hydrogen temperature with nuclear radiation (5×10^{16} nvt total dose) are presented in Table 31. Detailed test results for the irradiated specimens tested at -423°F without warmup are shown in Table 32.

A comparison of room temperature properties with those obtained at -423°F showed an increase in strength properties (ultimate, yield, notched and shear) and a decrease in area reduction. Elongation increased by 25%. The notched sensitivity as measured by notched-to-unnotched ultimate strength ratio decreased. however, the notched sensitivity of this material as measured by the notched ultimate to yield strength ratio decreased, which is more significant for design purposes. A material with higher notched-to-unnotched strength ratio is less notch-sensitive.

The radiation effect on the mechanical properties of this alloy is demonstrated by: (a) decrease in ultimate tensile strength (by 10%), and (b) increase in yield tensile strength, (8%) notched ultimate strength, (2.9%) shear strength (6%), and ductility (6.1% in elongation and 4% in reduction of area). The ratio of notched-to-unnotched tensile strength increased from 0.76 to 0.87%, and notched-to-unnotched yield strength decreased from 1.41 to 1.34 which is still above unity. Stress-strain curves as obtained by the extensometer are shown in Figure 43.

Threshold level of damage from radiation was reached for shear strength.

TABLE 31

AVERAGE MECHANICAL PROPERTIES TEST DATA FOR INCONEL X-750

	Room Temp.	Control -423°F	Change- Room Temp. vs Control in Percent	Irrad. -423°F	Change- Control vs Irradiated in Percent	Threshold
UNNOTCHED						
Ultimate Strength-PSI	175,100	253,300	+45	227,700	-10.1	
Std. Deviation-PSI	500	28,200		12,600		
0.2% Yield Strength-PSI	117,800	135,800	+15	146,800	+8	
Std. Deviation-PSI	5,700	13,700		700		
% Elongation	25.0	31.2	+25	33.1	+6.1	
Std. Deviation-%	2.7	2.1		1.85		
% Reduction in Area	40.8	32.0	-22	33.3	+4	
Std. Deviation-%	1.4	0.46		2.6		
Ult. Shear Strength-PSI	118,000	152,800	+30	162,000	+6.0	T
Std. Deviation-PSI	2,300	1,500		4,960		
NOTCHED Kt = 6.3						
Ultimate Strength-PSI	163,300	191,600	+17	197,200	+2.9	
Std. Deviation-PSI	6,600	5,100		5,100		
Ratio $\frac{\text{Notched Ult.}}{\text{Unnotched Ult.}}$	0.93	0.76	-18	0.87	+14.5	
Ratio $\frac{\text{Notched Ult.}}{\text{Unnotched Yield}}$	1.38	1.41	+2	1.34	-5	

TABLE 32

DETAILED MECHANICAL PROPERTIES DATA FOR INCONEL X-750

Specimen Number	Specimen Condition	Ultimate Strength: Instron Cell(KSI)	Ultimate Strength: Ram Cell(KSI)	Yield Strength 0.2% Offset(KSI)	Percent Reduction in Area	Percent Elongation
389	LN	209.5	191.7			
390	LN	211.1	194.2			
391	LN	203.6	200.6			
392	LN	203.3	202.4			
381	LU	250.6	224.8	146	35.5	35.75
382	LU	260.6	246.2	147.5	31.7	32.75
377	LU	245.0	220.5	147	30.4	31.4
378	LU	238.8	219.1	146.5	35.4	32.6

Elongation Data

Specimen Number	Specimen Condition	Extensometer: Post Irradiation (Mills)	Pull Rod: Post Irradiation (Mills)	Pull Rod: Control (Mills)	Bench Measurement: Post Irradiation (Mills)	Bench Measurement: Control (Mills)
381	LU	776	891		715	
382	LU	741	874		655	
377	LU	817	836		628	
378	LU	826	829		652	
Average		790	857	972.5	662	624
% Elongation		27.9	30.3	34.4	33.1	31.2
% Damage			-11.8		+6.1	

Ultimate Shear Strength (KSI)

168.9
162.3
158.4
158.4

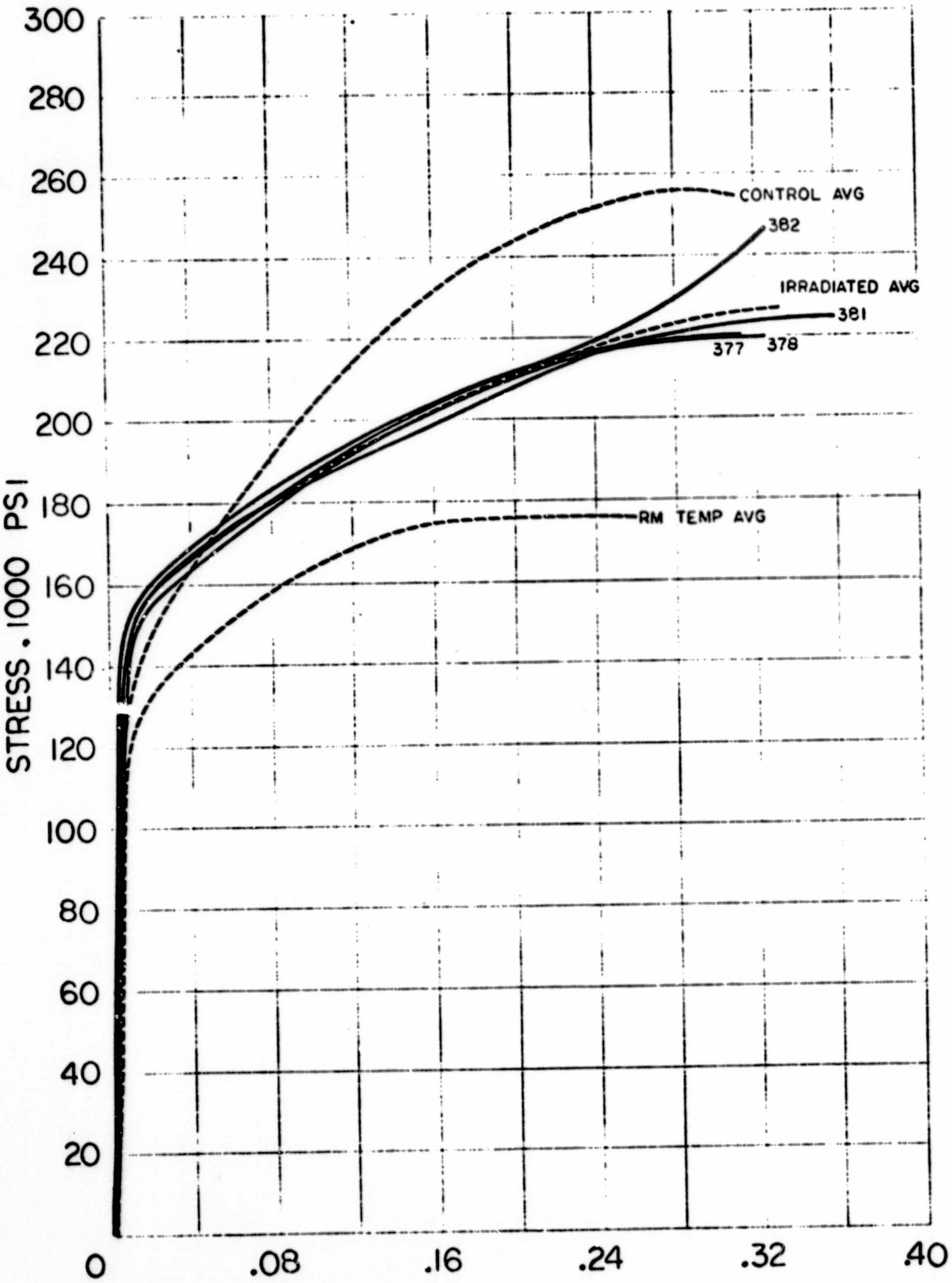

Figure 43

Stress - Strain Curves for Inconel X750

b. Metallography

Metallurgical examinations were made on representative samples of the irradiated material. Photomicrographs were taken (at 100X and 1000X) of typical areas.

The microstructures exhibited no effects of irradiation and are essentially the same as the control specimens. The strained areas exhibit elongated grains. Strain line orientation was observed within the grains. The fracture was transgranular. Representative photomicrographs may be found in References 2 and 7 and are not included in this report.

c. Electron Microscopy

Electron microscopic examination was performed on strained-unstrained areas of irradiated samples. Typical microstructures were taken at 15000X.

Figure 44 exhibits the microstructure of the irradiated sample. The microstructure shows austenite with grain boundary precipitation. The strain lines present on the optical micrographs do not show in this photograph. The structure is typical of that noted for the unstrained areas.

Electron fractographs were taken from the edge and center of a fracture of a typical tensile specimen tested in the irradiated condition.

Figure 45 shows fractographs (at 4200X) taken from the center of notched and unnotched specimens. No significant variation was observed between the fractographs of edge or center locations. The fracture surfaces were composed of multiple dimples and glide-plane decohesion. The fractures were primarily ductile and similar to the control specimen.

Material: Inconel X750
Form: 1/5 in. Plate
Identification: Specimen No. LU 382
Specification: AMS 5542F

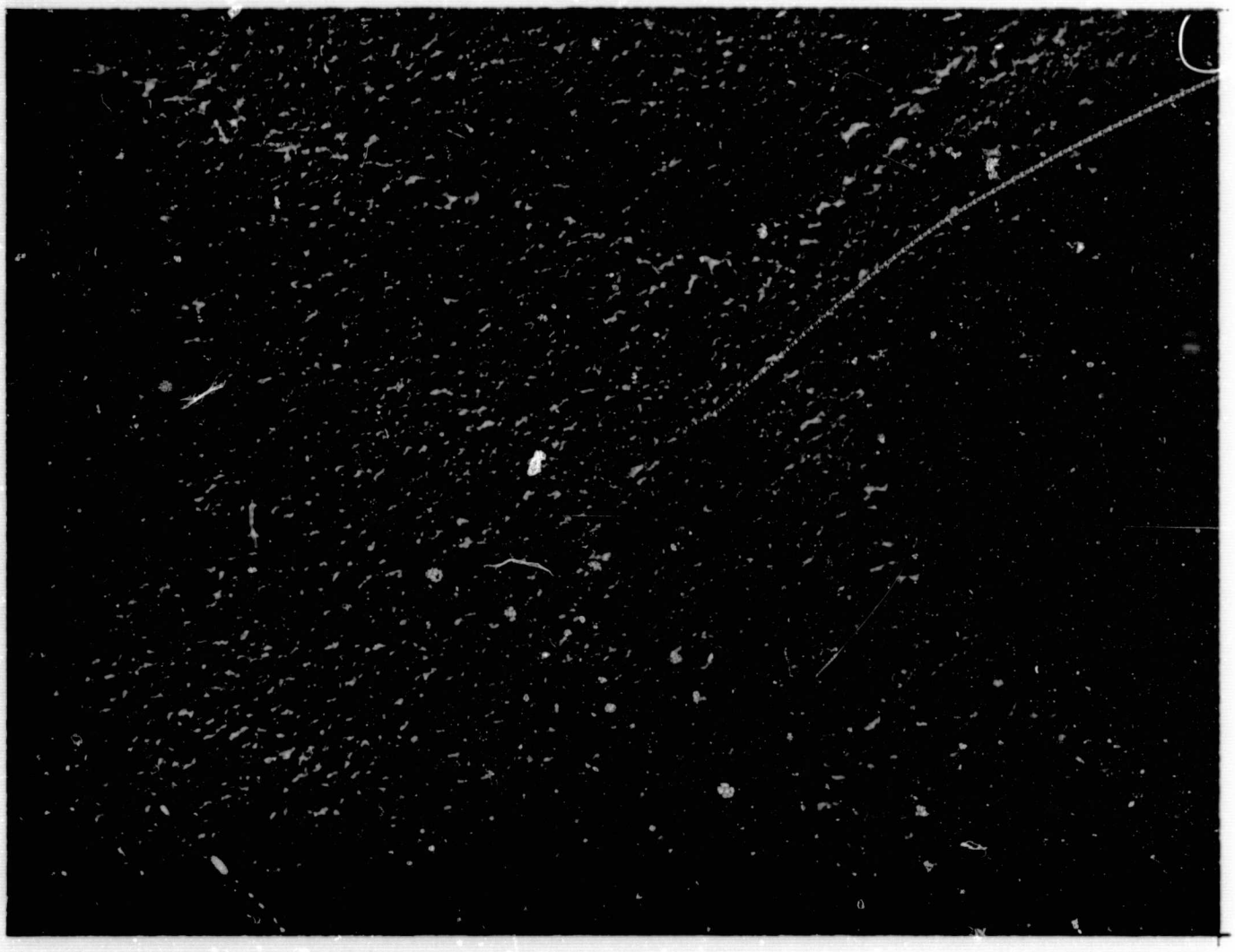

Condition: Irradiated-Strained
Mag: 15000X

The microstructure shows austenite with grain boundary precipitation. The strain lines present on the optical micrographs do not show in this photograph. Structure shown is typical of unstrained area.

Figure 44

Inconel, X750 - Irradiated - Aged 1350°F for 20 Hours
Condition L. Strained - 15000X

Material: Inconel X750
Form: 1/4 in. Plate
Identification: Specimen LU 382
Specification: AMS 5542F

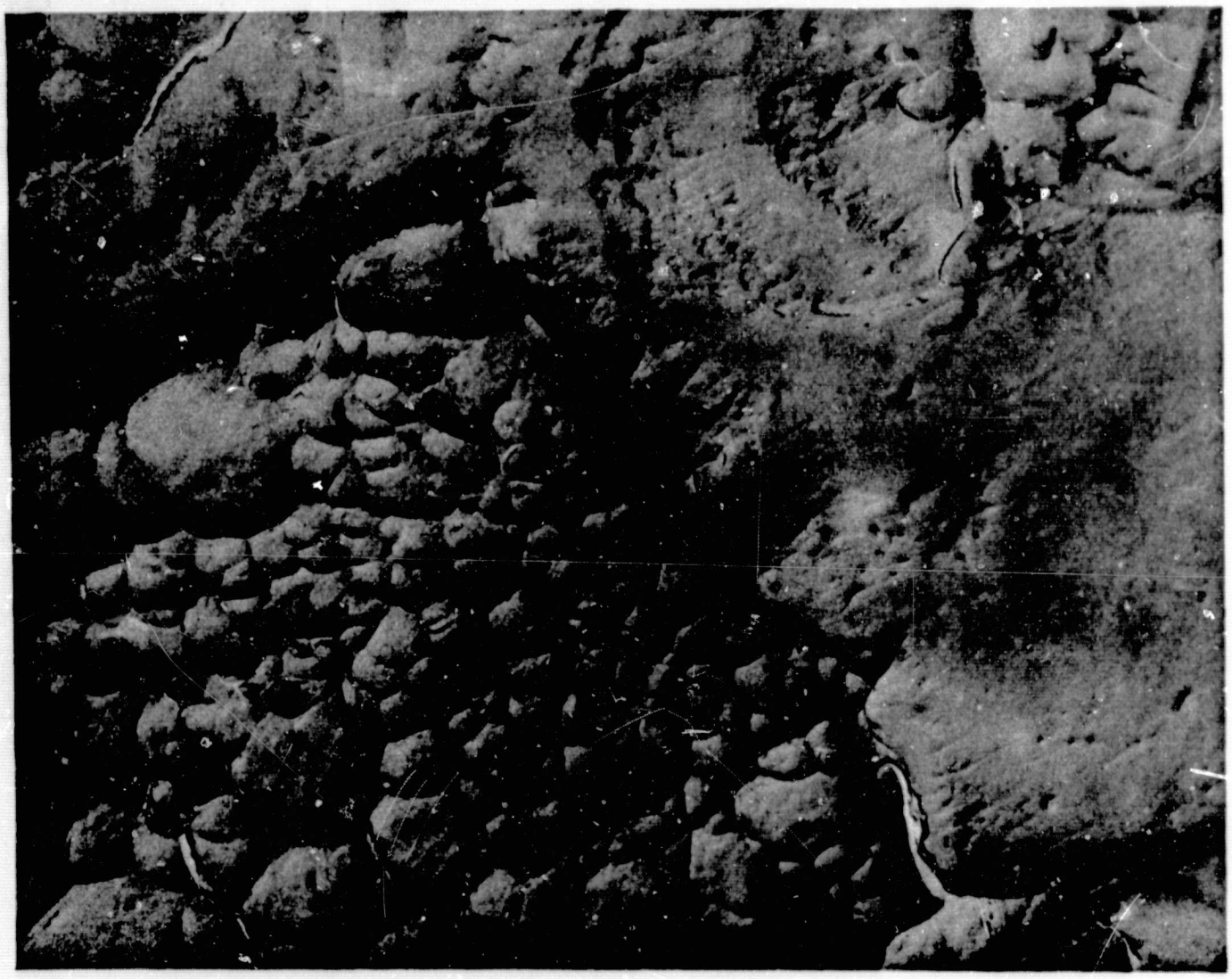

Condition: Irradiated-Fractograph-Fracture Center
Mag: 4200X

The fracture at the central area of the specimen is similar to that of the edge and is made up of oriented dimples and glide plane decohesion. The boundary in the center of the photograph is, in all probability, a grain boundary. In the grain on the right, a glide or slip plane is lined up with the shearing stresses and the failure is by glide plane decohesion. In the area on the left, the plane of easy glide is not lined up and the failure is by microvoid formation and lineup. This type of fracture is associated with ductile failure.

Figure 45, Sheet 1 of 2

Inconel X750 - Irradiated-Aged 1350°F for 20 Hours -
Condition L Fractograph-Center - 4200X

Material: Inconel X750
Form: 1/4 in. Plate
Identification: Specimen LN 389
Specification: AMS 5542F

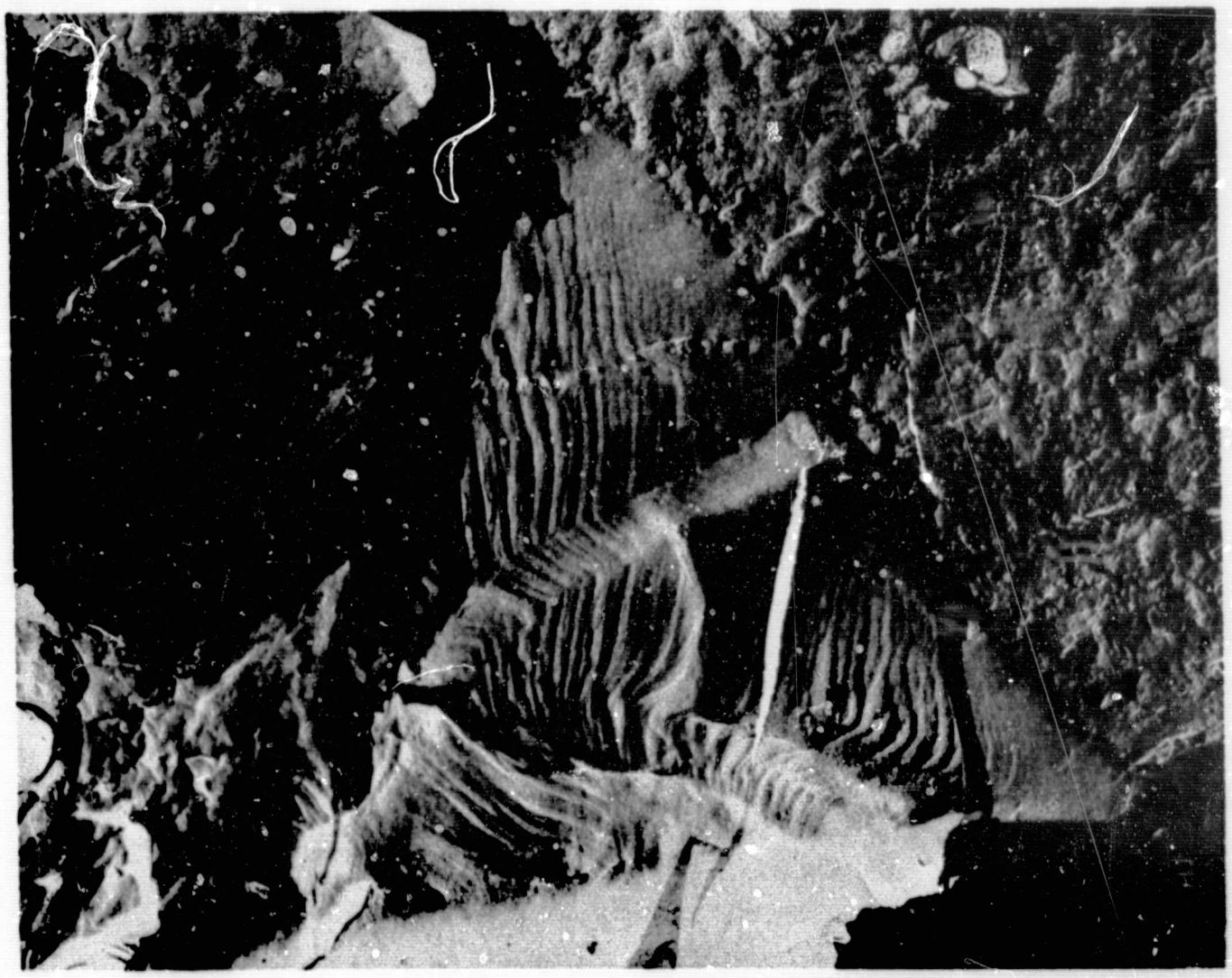

Condition: Irradiated-Fractograph-Fracture Center

The fracture is typical of both center and edge locations and is made up of an area of serpentine glide striations in the triangular area at the center of the photograph, a semi-ductile microvoid area on the left, and glideplane decohesion and a shear microvoid on the right. The serpentine glide striations are a result of a local fracture giving a free surface ahead of the main crack. The material below this arc surface is subsequently deformed as the main crack front advances, giving rise to slip-hard striations or serpentine glide on the free surface. It is thought that the band across the middle of the serpentine glide zone represents a twin.

Figure 45, Sheet 2 of 2

Inconel X750 - Irradiated-Aged 1350°F for 20 Hours -
Condition L Fractograph-Center - 4200X

d. X-Ray Diffraction

Table 33 presents the X-ray diffraction data. X-ray diffraction patterns from the as-received material showed the face-centered cubic structure of nickel. The lattice parameter was expanded as a result of solid solution alloying effects. The microstress level was indicative of the wrought condition.

The diffractogram of the unstrained area of a control sample showed essentially the same characteristics found in the as-received sample. The preferred orientation is in the (111) direction.

The diffractograms from the strained and unstrained areas of the irradiated material exhibited a preferred orientation in the (111) direction. This preferred orientation is the same as for the as-received and unstrained control samples. The lattice parameters of the strained and unstrained areas were essentially the same and were only slightly lower than those of the control specimens.

TABLE 33

X-RAY DIFFRACTION DATA - INCONEL X-750

	Pure Nickel		Control						Irradiated			
			As-Received		Strained		Unstrained		Strained		Unstrained	
hkl	(1)	(2)	(1)	(2)	(1)	(2)	(1)	(2)	(1)	(2)	(1)	(2)
111	2.034	100	2.06	100	2.06	80	2.06	100	2.06	100	2.07	100
200	1.762	42	1.78	60	1.78	30	1.79	30	1.78	32	1.79	35
220	1.246	21	1.26	60	1.26	100	1.26	30	1.26	66	1.26	7
311	1.062	20							1.08	20	1.08	5
222	1.017	7										
LATTICE PARAMETERS (Å)												
	3.524		3.57		3.57		3.57		3.57		3.57	
MICROSTRESS, Δ θ												
			0.65° (2θ = 130°)		1.69° (2θ = 130°)		0.96° (2θ = 130°)		0.42° (2θ = 43.8°) No Peak (2θ = 130°)		0.30° (2θ = 43.8°) No Peak (2θ = 130°)	

NOTES: (1) "d" Spacings
(2) Relative Intensities, percent.
Shift in "d" spacings indicates lattice expansions.
Orientation change is indicated by intensity change for a given hkl.

4. Inconel 713-C (Casting)

a. Mechanical Properties

Average values and standard deviations of mechanical properties obtained at room temperature, liquid hydrogen temperature as control, and at liquid hydrogen temperature after nuclear radiation (5×10^{16} nvt total dose) are presented in Table 34. Detailed test results for the irradiated material tested at -423°F without intermediate warmup are shown in Table 35.

This alloy showed an unusual behavior. A comparison of average properties at -423°F with those at room temperature showed no noticeable change in tensile strength properties or in ultimate, yield and notched. There was no noticeable decrease in elongation or reduction of area as a result of the cryogenic temperature. The slight increase in yield strength decreased the gap between ultimate and yield strength from 5500 psi at room temperature to about 2400 at -423°F. Shear strength increased appreciably from 121,900 to 144,500 psi. The notched-to-unnotched ultimate strength ratio increased from approximately 1.0 at room temperature to 1.14 at -423°F, thus indicating a tendency toward notch toughness.

The radiation effect on mechanical properties is demonstrated by a substantial increase in ultimate as well as yield tensile strength to a point where both values are almost equal, and by a substantial decrease in ductility both in elongation (39%) and area reduction (48%). Ultimate notched strength was equal to the ultimate tensile strength. Effect of radiation on shear strength was not evaluated.

Notched-to-unnotched ratio for ultimate and yield strength was about 1.0. Stress-strain curves, as obtained by the extensometer, are shown in Figure 46. Threshold level of damage was reached for ultimate and yield tensile strength, and reduction of area.

TABLE 34

AVERAGE MECHANICAL PROPERTIES TEST DATA FOR INCONEL 713-C

	Room Temp.	Control -423°F	Change- Room Temp. vs. Control in Percent	Irrad. -423°F	Change- Control vs Irradiated In Percent	Threshold
UNNOTCHED						
Ultimate Strength-PSI	110,400	111,600	+1	133,400	19.5	T
Std. Deviation-PSI	4,000	10,400		6,100		
0.2% Yield Strength-PSI	104,900	108,000	+3	133,200	+23	T
Std. Deviation-PSI	500	10,200		3,900		
% Elongation	4.0	3.0	-25	1.8	-39	
Std. Deviation-%	.4	0.9		1.3		
% Reduction in Area	11.3	15.6	+38	9.5	-39	T
Std. Deviation-%	1.9	4.2		1.6		
Ult. Shear Strength-PSI	121,900	144,500	18.5	Not Tested		
Std. Deviation-PSI	5,700	12,900				
NOTCHED Kt = 6.3						
Ultimate Strength-PSI	116,800	127,700	+9.5	135,400	+6.0	
Std. Deviation-PSI	4,000	8,900		10,100		
Ratio $\frac{\text{Notched Ult.}}{\text{Unnotched Ult.}}$	1.05	1.14	+9	.99	-13.1	
Ratio $\frac{\text{Notched Ult.}}{\text{Unnotched Yield}}$	1.11	1.18	+6	1.02	-13.6	

TABLE 35

DETAILED MECHANICAL PROPERTIES DATA FOR INCONEL 713-C

Specimen Number	Specimen Condition	Ultimate Strength Instron Cell (KSI)	Ultimate Strength Ram Cell(KSI)	Yield Strength 0.2% Offset(KSI)	Percent Reduction in Area	*Percent Elongation
413	LN	140.2	127.1			
414	LN	145.7	141.5			
417	LN	157.2	146.5			
418	LN	131.5	126.5			
401	LU	142.6	130.5	130.0	10.5	.3
402	LU	144.3	137.5	132.0	8.0	2.75
405	LU	134.3	126.2		11.1	1.25
406	LU	142.9	139.4	137.5	8.3	3.0

Elongation Data

Specimen Number	Specimen Condition	Extensometer Post Irradiation (Mills)	Pull Rod Post Irradiation (Mills)	Pull Rod Control (Mills)	Bench Measurement *Post Irradiation (Mills)	Bench Measurement Control (Mills)
401	LU	24	70		6	
402	LU	30	105		55	
405	LU	21	54		25	
406	LU	22	76		60	
Average		24	76.25	93.5	36.5	60
% Elongation		0.85	2.7	3.3	1.8	3.0
% Damage			-18.5		-39	

Ultimate Shear Strength (KSI)

Data not obtained.

*Measured between welded tabs.

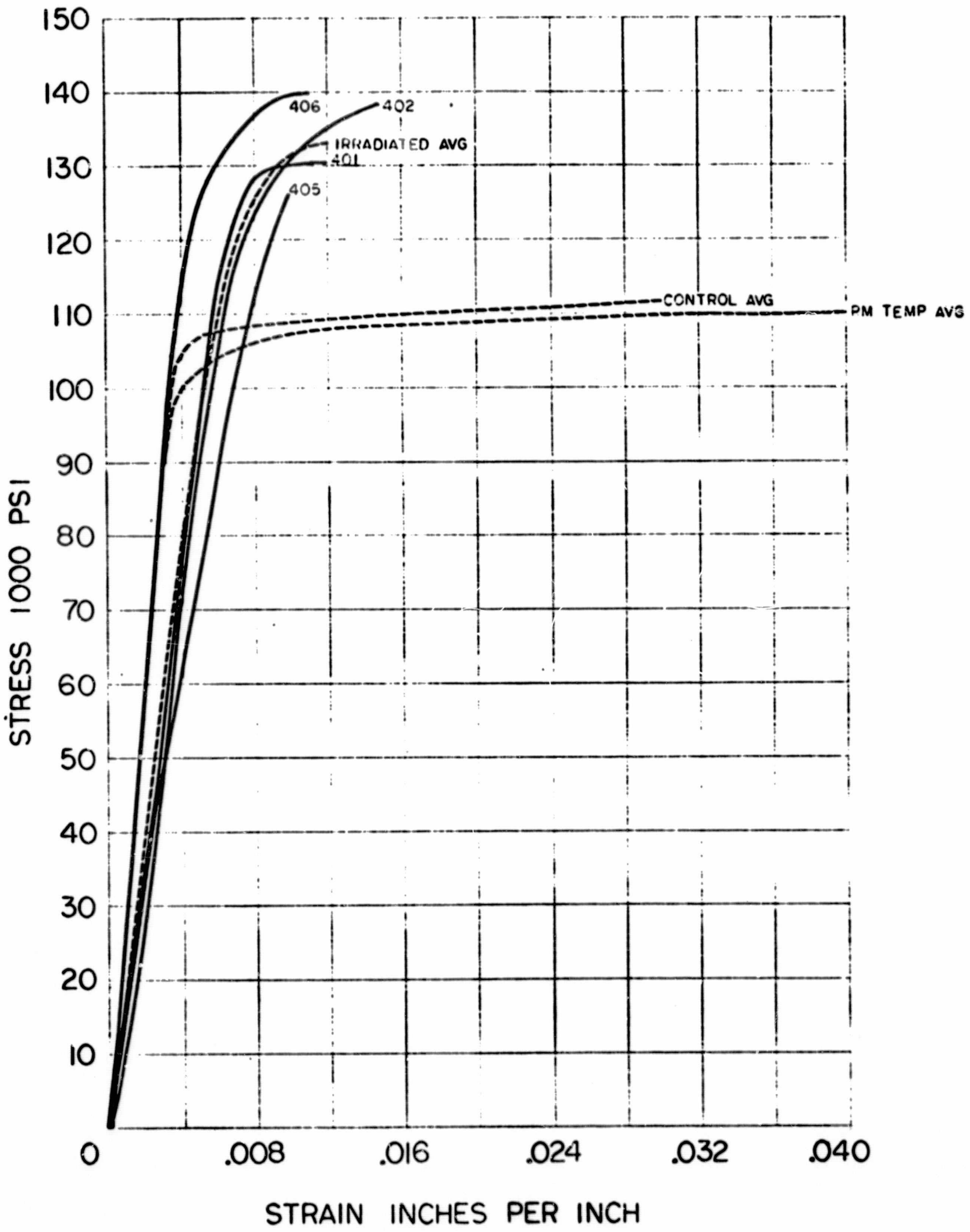

Figure 46

Stress - Strain Curves for Inconel 713C

b. Metallography

Photomicrographs (taken at 100X and 1000X) of irradiated material were compared to control specimens both for general structure and fracture area. The dendritic structure, characteristic of castings, was unchanged. The grain-composition matrix was probably Ni-Cr (alpha and beta) eutectic, and may have contained some Ni-Al (epsilon-zeta) peritectic. Carbide-type particles were observed in the grain boundaries. The fracture was duplex in nature, following a transgranular path at some points and an interdendritic path at others. The cast grain size was large and, since the fracture path did not preferentially appear to follow it, the term "generally transgranular" is applicable. There was no apparent difference (either in the microstructures or the fracture mode) between the control and the irradiated material.

c. Electron Microstructure

Figure 47 (top) is the typical microstructure of the Inconel 713C alloy in the irradiated condition. The microstructure is representative both for the strained and unstrained areas of the test specimens. The microstructure is in a high state of resolution, hence, the presence of the gamma prime precipitate is more noticeable. It is to be noted that the structure does not exhibit any irregularities as a result of irradiation.

Figure 47 (bottom) is a representative fractograph of the irradiated condition, depicting the fracture surface of both the notched and unnotched specimens. The notched specimens displayed the same fracture characteristics as the unnotched specimens: large areas of brittle cleavage and partially-formed dimples. The mechanism of fracture is typical of this material.

Material: Inconel 713C

Form: Sand Casting

Specimen No.: LU 401

Specification:

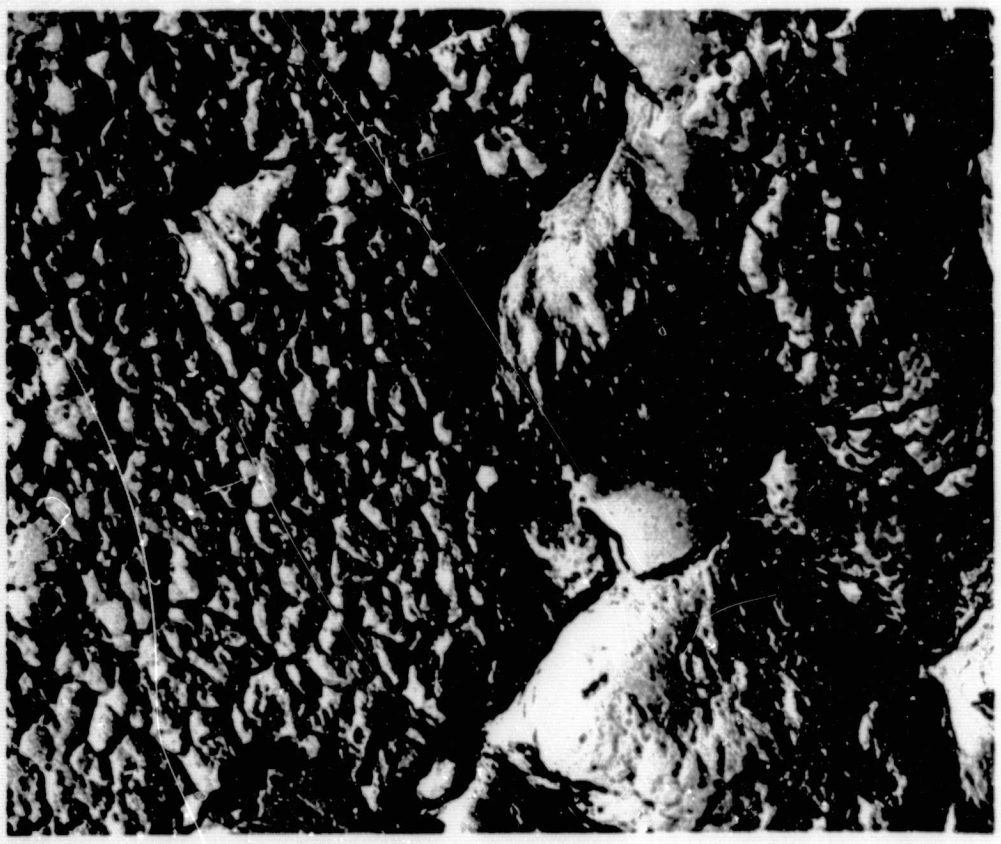

Condition: Irradiated-Strained

Mag: 15000X
Etchant: 10% Oxalic Acid Electrolytic

Microstructure showing the Ni-Cr matrix with the gamma prime precipitate. The microstructure of the unstrained area is similar.

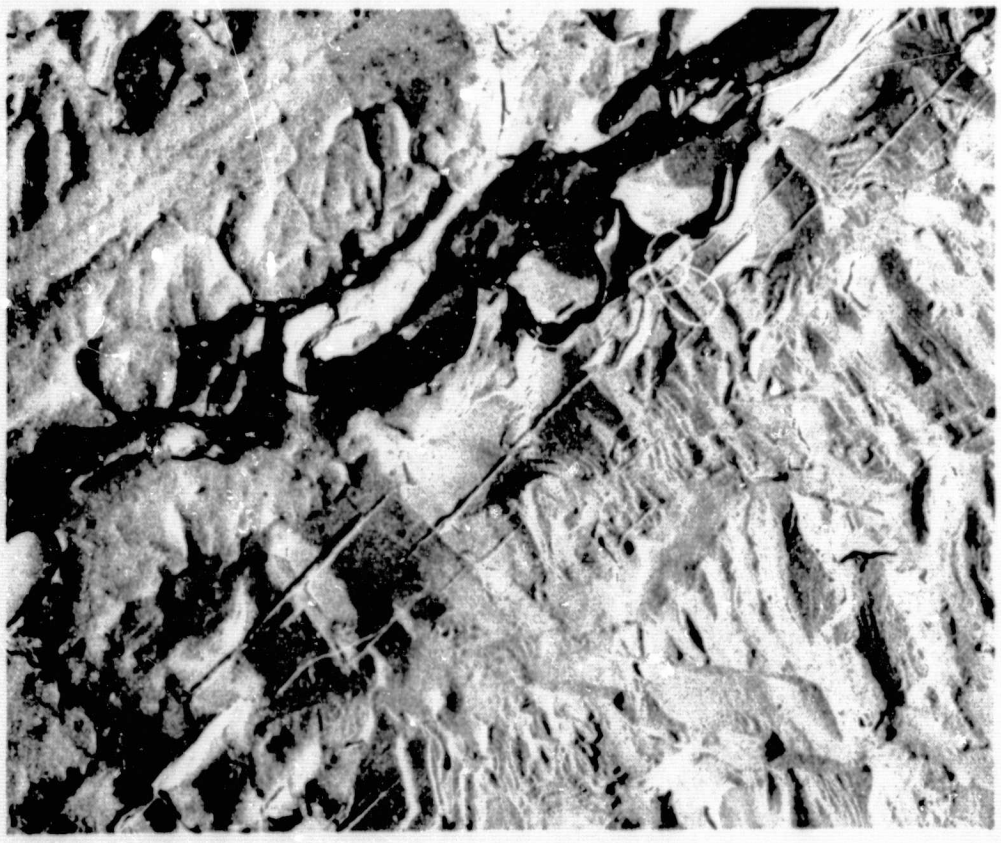

Condition: Irradiated-Fracture

Mag: 4200X
Etchant: None

Microstructure of the fracture showing a large area of brittle cleavage (lower right) and an area of shallow partially formed microvoids (upper left). These shallow microvoids are often present on brittle failures. The fracture topography at the edge was the same as that found at the center.

Figure 47

Inconel 713C - Irradiated - Electron Micrograph and Fractograph
4200X, 15000X Magnifications

d. X-Ray Diffraction

Table 36 presents X-ray diffraction data of the as-received, control, and irradiated specimens. The as-received diffractogram showed the face-centered cubic structure of nickel. The unstrained control specimen showed no diffraction lines because of the large grains. The strained specimen showed only a weak (111) reflection presumably caused by large grain size. The same reflection characteristic was evident for the irradiated material.

TABLE 36

X-RAY DIFFRACTION

Material: Inconel 713C

	Pure Nickel		As-received		Control				Irradiated			
					Strained		Unstrained		Strained		Unstrained	
hkl	(1)	(2)	(1)	(2)	(1)	(2)	(1)	(2)	(1)	(2)	(1)	(2)
111	2.034	100	2.07	100	2.07	100	(5)		No Peaks Observable		2.07	100
200	1.762	42	1.79	12								
220	1.246	21	1.27	20								
300	1.062	20										
222	1.017	7										
LATTICE PARAMETER, Å												
	3.524		3.58		3.59						3.59	
MICROSTRESS,												
			2.50° (2θ = 129°)		0.40° (2θ = 69°)				No Peak (2θ = 69°) No Peak (2θ = 129°)		0.22° (2θ = 43 No Peak (2θ = 69°) No Peak (2θ = 129°)	

Notes: (1) "d" Spacings
(2) Relative intensities, percent
Shift in "d" spacings indicates lattice expansion
Orientation change is indicated by intensity change for a given hkl
(3) X-ray diffraction pattern not observable because of large-grained structure.

5. D-979

a. Mechanical Properties

Shear strength was the only property evaluated for this alloy.

Average values and standard deviations for shear strength at room temperature, at the temperature of liquid hydrogen, (control), at the temperature of liquid hydrogen with nuclear radiation (5×10^{16} nvt total dose), are presented in Table 37. Included in this table are detailed data for the irradiated specimens.

A comparison of these data shows a typical increase in strength from 115,000 psi at room temperature to 152,500 psi at -423°F and 160,000 psi because of radiation.

Threshold level of damage was not reached at this dose level.

TABLE 37

AVERAGE AND DETAILED SHEAR STRENGTH TEST DATA

	Room Temp.	Control 423°F	Change- Room Temp. vs Control in Percent	Irrad -423°F	Change Control vs Irradiated in Percent	Threshold
Ultimate Strength-PSI	196,500					
0.2% Yield Strength-PSI	148,800					
% Elongation	15					
% Reduction in Area	15.6					
Ultimate Shear Strength PSI	114,900	152,500	+34	160,100	+5	
Std. Deviation-PSI	2,200	5,900		4,370		

Detailed Shear Strength KSI

165.3
158.8
156.1

F. TEST EQUIPMENT

The equipment used included two pulling assemblies, two cryostats, pneumatic and hydraulic systems, liquid hydrogen supply and exhaust system and instrumentation. It is essentially the same equipment used during the first radiation test on structural materials (Reference 1); however, considerable improvements and modifications were made to increase the safety of operation and accuracy of the data acquisition. These improvements included: two shrouds with provisions for inert atmosphere, automatic liquid level control system and an improved extensometer system.

1. Cryostat

The liquid-hydrogen dewar consists of two concentric cylinders with 2:1 eliptical domes connected to a common circular top-plate. The compartment enclosed between the two cylinders is evacuated to 10^{-6} mm of mercury to serve as thermal insulation.

The inner vessel contains a rectangular container or "can", which is filled with liquid hydrogen and secured to the pulling assembly. The boiled-off hydrogen gas is discharged from the dewar through a 1.25-in. exhaust line. Figure 48 shows a section through the dewar, the lower part of the pulling assembly (with extensometer), the liquid-hydrogen "can" attached to the bottom plate of the assembly, and the exhaust line. The hydrogen boil-off goes out of the "can" into the inner dewar compartment and then is picked up by the exhaust line at the bottom of the dewar. Thus, the gas is used as a heat-shield to reduce the boil-off. The dewar is connected to the pulling assembly with twenty 0.5-in.-diameter A-286 bolts, having allowable design yield strength of 140,000 psi. The joint is sealed by an 0.0625-in. asbestos gasket and silicone grease. The dewar is hydrostatically proof tested at 30 psig. Two rupture discs of 3-in. diameter and 15-psig rating are provided, for safety on both the hydrogen and vacuum chambers. The latter rupture disc is provided because of the possibility of leaks into this chamber with subsequent liquification and re-evaporation of air, gas expansion, pressure buildup and

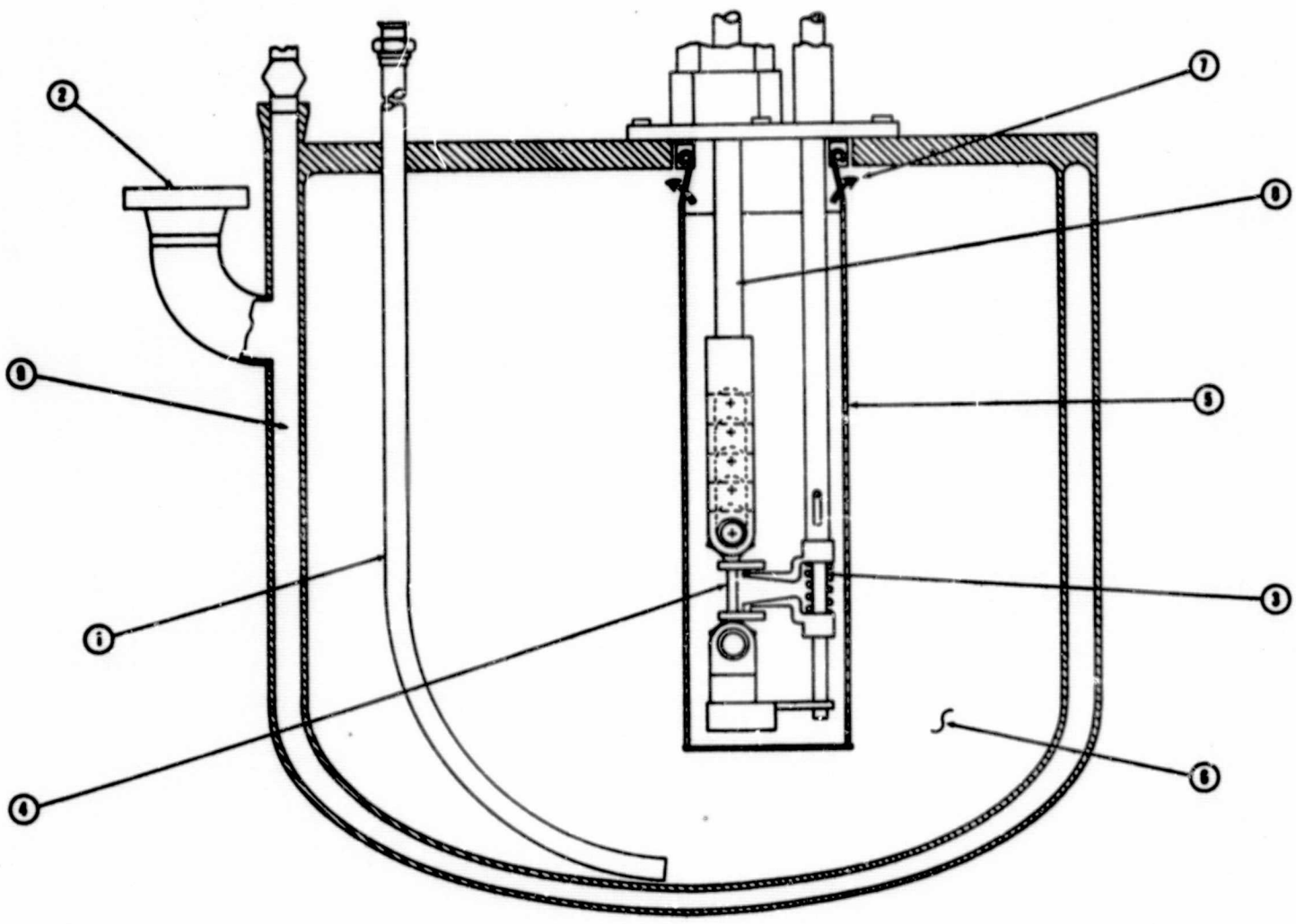

Figure 48

LH_2 Dewar Cross Section

possible rupture of the dewar walls. A bakeable valve, a rupture disc and a vacuum gage are provided for the exterior compartment to measure the vacuum during the test and permit additional vacuum pumping, if required. An additional pop-off valve, set at 8 psig, is provided through the dewar cover plate. The cryostat is made of 6061-T6 aluminum.

2. Pulling Assembly

Each pulling assembly consists of four selectively-actuated, identical systems built to fit a single dewar. An individual system includes a hydraulic cylinder and piston, a heavy cross-member, two pull rods, and two clevises.

All items, except the hydraulic piston rod, are made from Type 316 stainless steel because of its high strength and high ductility at -423°F. Figure 49 shows that the liquid-hydrogen "can" attached to the pulling assembly (which contains various types of openings and seals to the cryogenic chamber for the pull rods, extensometers and instrumentation) is completely enclosed in an aluminum shroud. Gaseous helium is supplied to this compartment to provide inert atmosphere during the radiation run and to minimize the possibilities of hydrogen fire. Another small shroud is provided on the top of the cryostat around the rupture disc and vacuum valve. Both shrouds are connected and exhausted independent of the hydrogen boil-off.

The piston rod is screwed into a necked-down section which is instrumented with strain gages that are calibrated to measure tensile loading. The necked-down section is screwed into a strong cross-member called the "pull-bar" actuator.

The cross member divides the loading between two 1.375-in. pull rods. These pull rods pass through the cryostat cover plate and are threaded into the upper movable clevis. Maximum allowable pull-rod travel is 10-in. from the

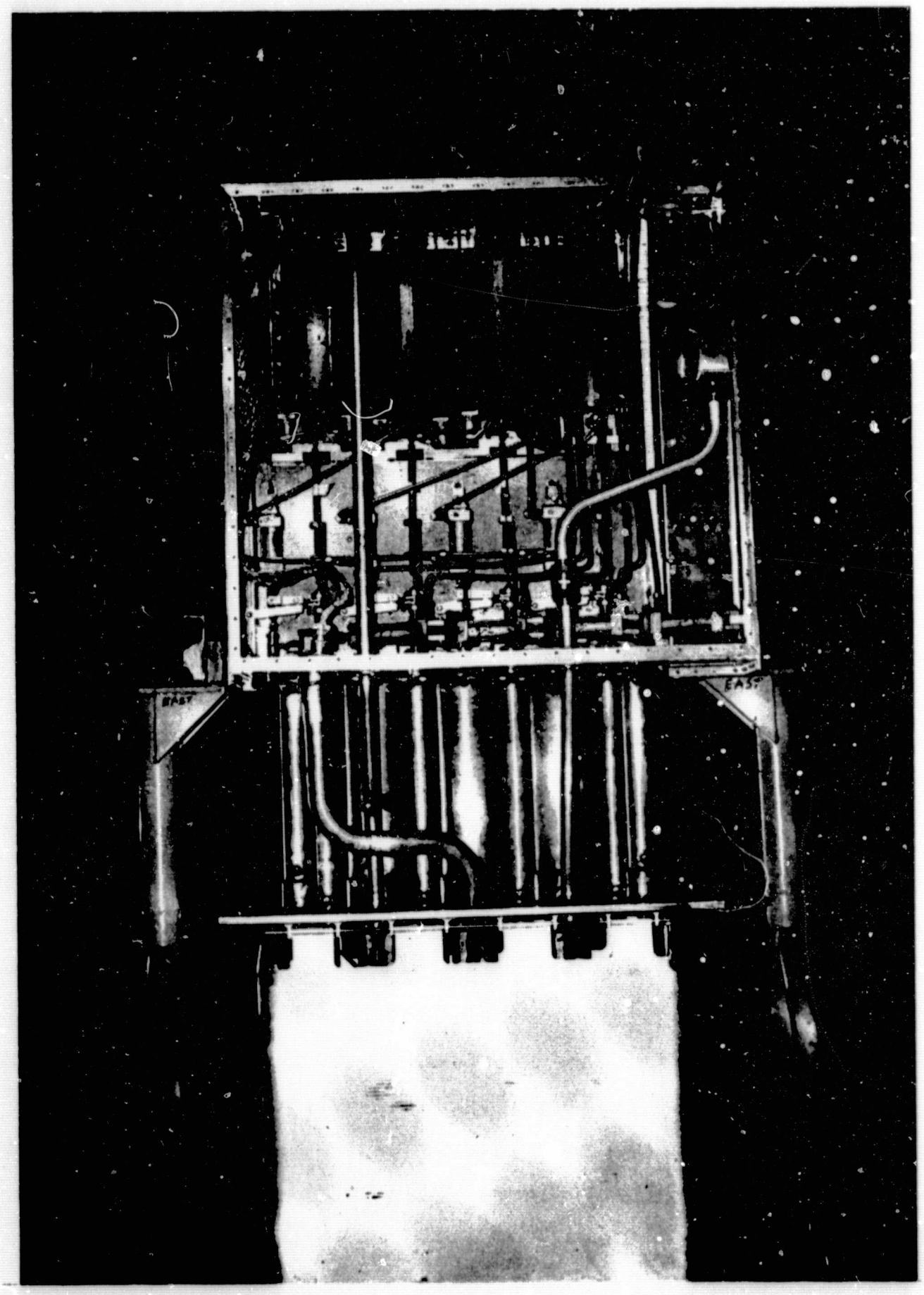

Figure 49

Pulling Assembly (Detailed View)

lowest specimen position. The stationary clevises are bolted to a box-shaped base plate, which transmits the load to the cylinder mounting assembly through five compressive members. Exterior members are of circular sections for maximum buckling resistance in all directions. The interior members are I-shaped.

Specific attention is given to the elimination of bending moments from the specimens in the design of the pulling clevises (which hold the specimens). Each clevis is divided into two, 2.06-in. sections, each capable of accommodating a maximum of eight specimens (0.25-in. thick at the grip-end). Thus, each pull rod permits tensile testing of 16 specimens. Bending is avoided by pulling the specimens concentrically on two sides. Specimen orientation during irradiation is such that specimen edges are perpendicular to the reactor-closet wall with only a single row of specimens, reducing the possibility of total flux differences between specimens, which would have occurred from self-shielding if the pull rod had been rotated 90°, as in the GD/A equipment. Special aluminum stands are used to support these assemblies in the reactor area.

3. Extensometer

The units consist of tube-in-tube design and are mounted one for each pulling position. The extensometer measures the specimen elongation within the 2-in. gage length. Tabs are clamped and then spot-welded on the edges of the unnotched specimen. The extensometers can be rotated in an arc to contact each of the specimens mounted in the clevises. Extensometer fingers are connected to the concentric tubes, which in turn are secured to the transducers. The transducers have a $\pm$ 1.00 in. range. Sealing between the tubes is achieved with Teflon Balseals. The fingers are indexed from one specimen to the other by using pneumatic cylinders for contracting the fingers, and hydraulic cylinders for horizontal positioning. A 10-lb. spring forces the fingers apart to maintain contact with the metal tabs attached to the specimens. Figure 50 shows the lower part of the extensometer system.

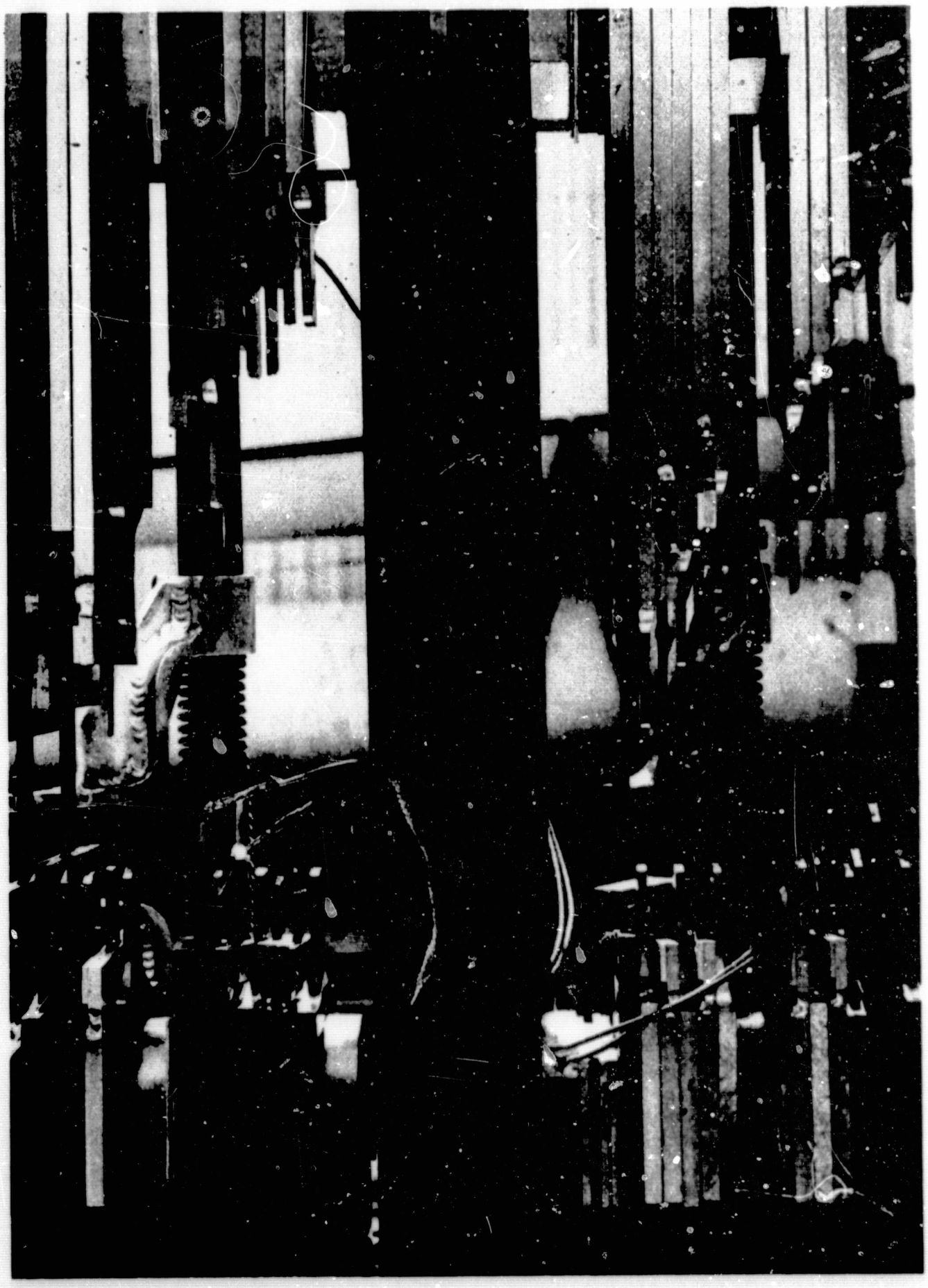

Figure 50

Extensometer Assembly

The pneumatic system is pressurized by a compressed-air cylinder regulated to deliver a pressure of 100 psi. The hydraulic cylinders have a 1.5-in. bore and a 3-in. stroke. Each pulling assembly is equipped with four pairs of cylinders. A series of indicator lights inform the pump operator of the extensometer position.

4. Pneumatic and Hydraulic Systems

Tensile loading is applied by a hydraulic system consisting of the following:

a. A master cylinder, mounted between the upper and lower crosshead of the Instron testing machine, which engages the load cell.

b. Four slave cylinders, located at each pull rod position, for each assembly.

c. Pressure and return manifolds.

d. Supply reservoir.

e. Pressure pump.

f. Copper lines, fittings and valves.

The master hydraulic cylinder of the Instron testing machine is located in the control room and is connected port-to-port with the slave cylinders through a system of pressure and return manifolds. The hydraulic oil used is Oronite Chemical Company, No. 8515. Slave cylinders, being part of the cryostat assembly, are located in the reactor irradiation chamber. Control manifolds, and the master cylinder, are located in the reactor control room. Figure 51 shows the main control panel.

Auxiliary hydraulic and pneumatic systems are used for positioning the extensometers and are operated through manifolds located in the lower half of the control panel.

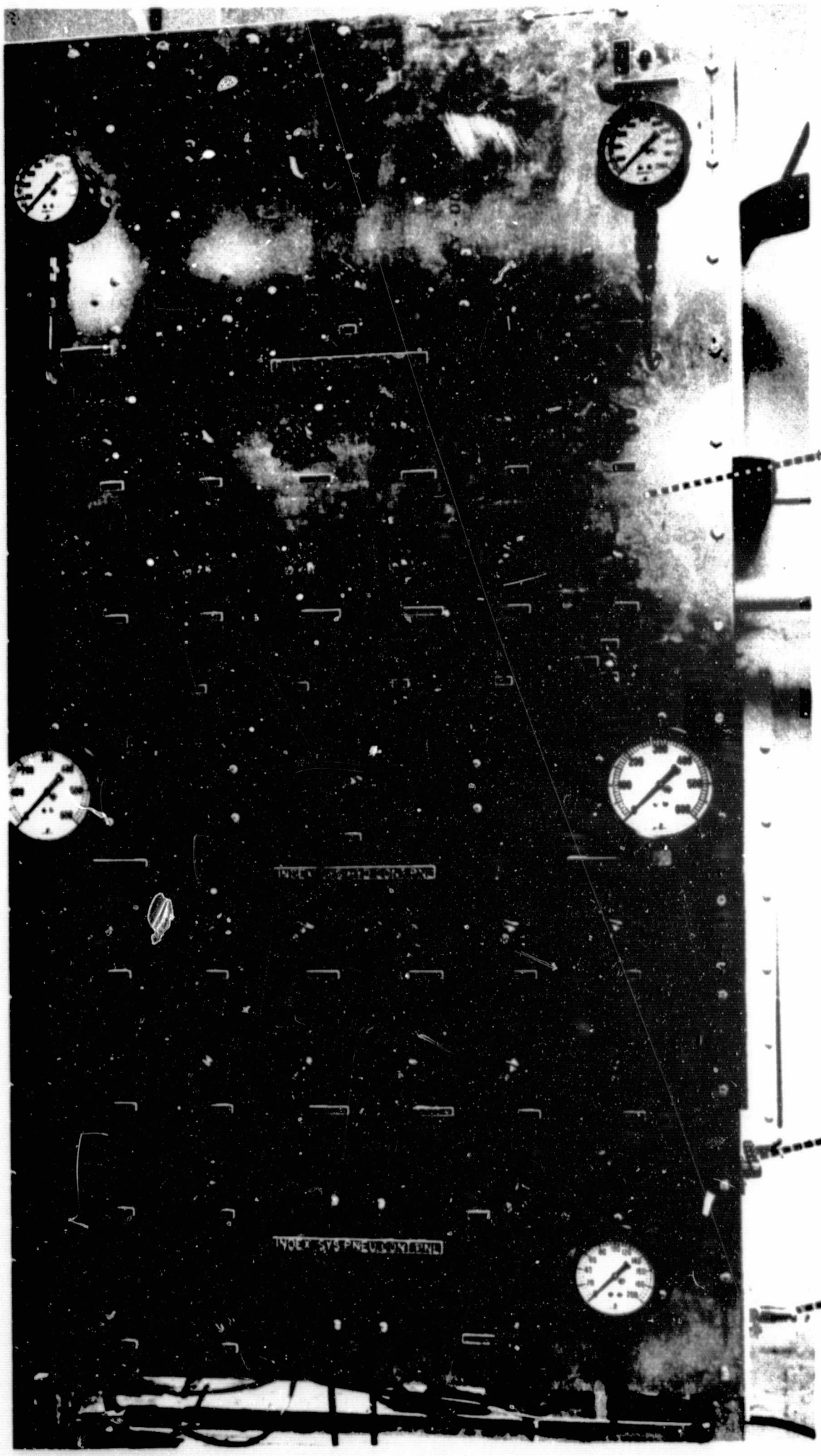

Figure 51

Main Control Panel

5. Liquid Hydrogen Supply and Transfer System

Liquid hydrogen is supplied to each dewar by a 0.75-in., flexible, vacuum-insulated line from a liquid-hydrogen transfer trailer located adjacent to the reactor pool. A liquid-hydrogen supply manifold, equipped with remotely operated supply valves, is located outside the facility shield. Each valve is equipped with a pneumatically controlled positioner to permit proportional control of the liquid-hydrogen flow. Each test assembly is connected to the manifold with 90 foot lines. The manifold is equipped with two inlet valves to permit changeover of LH_2 trailers without interrupting flow to the test assemblies.

6. Exhaust System

The gaseous hydrogen is vented through a combination of flexible and rigid 1.5-in. lines, manifolded into a 5 in., and then through an 8-in., rigid line, and burned in the hydrogen stack. The exhaust system is equipped with gate and check valves located between the 1.5 in. line and the manifold, and is capable of vacuum purging the pulling assemblies. The purge system consists of a valve network, a mechanical vacuum gage, a pressure vacuum gage and vacuum pump. Individual pulling assemblies can be purged independently; or all test units can be purged in parallel.

7. Instrumentation

The instrumentation consists of equipment to monitor Instron load and crosshead travel, the tensile load applied to the specimen by each hydraulic ram, the temperature of selected specimens and of the liquid hydrogen, the level of the liquid and the pressure within the dewar, and strain-gage output for selected specimens. The dewar pressure level is maintained near local ambient at all times.

a. Load Measurement

The load applied to the specimens is measured by the load applied to the hydraulic system with the Instron load cell and by a strain-gage-bridge

load cell on each hydraulic slave cylinder pull rod. The former is recorded on the Instron recorder and the latter is recorded on an Offner Dynograph Millivolt Recorder with a 150-1100 carrier preamplifier. Both systems are calibrated to 15,000 pounds.

b. Strain Measurement

The strain measurements are made by:

(1) Extensometers - one for each pull rod
(2) Helipot potentiometers - one for each pull rod
(3) Strain gages welded to selected specimens - at least one strain gage for each pull rod.

A helipot potentiometer with gear arrangements is installed on each pull rod to indicate crosshead travel. This potentiometer is of the 360° rotation type with equally spaced taps so arranged that for 0.050 in. of travel one sweep of the recorder pen is obtained.

Microdot weldable strain gages are used with cermaic bonding which provides maximum radiation resistance.

Means for selecting the appropriate gage are provided on the control panel. The Offner Recorder is used to record the strain gage output.

c. Temperature Measurement

Copper-constantan thermocouples referenced to liquid nitrogen are used to monitor the temperatures. Thermocouples are located 12 and 24 in. below the dewar flange plate, as a cross check on the liquid level system. A continuous record is kept of the readings of these thermocouples.

d. Liquid-Level Measurement and Control

The liquid-level indicator system consists of seven-1000 ohm, 0.5 watt carbon resistors mounted in a rake and connected to a monitor panel. The resistors are spaced 4.12, 6.25, 9.00, 11.00, 19.00, 21.75, and 29.50 inches below the dewar flange. The monitor panel contains a power supply, balancing network, level indicating lights, and a warning horn. The level indicating system is adjusted to warn on immersion or withdrawal of the specimens from the cryogenic fluid, depending upon operating requirements.

The liquid-level control system consists of three copper-constantan thermocouples mounted in a rake and connected to a Bristol Control unit. The thermocouples, are positioned to maintain the liquid hydrogen level between 9 and 11 inches below the dewar flange. The Bristol Control unit has a +100°F to -430°F range, and it supplies the signal to the pneumatically controlled positioner on the hydrogen supply valve. During the first radiation run, the liquid level was adjusted manually, using pneumatically actuated control valves. This proved extremely tedious and an automatic system has since been installed.

e. Pressure Measurements

Pressures within the dewars and in the shrouds are monitored by the Ultradyne Pressure Transducers, and recorded by the Offner Recorder.

G. TEST PROCEDURES

Procedural activities connected with this run included: Pre-irradiation check out, irradiation period, post-irradiation testing, and removal of the test equipment. To minimize - and possibly eliminate - any potential hazard, several safety provisions were incorporated. The 400-hour radiation test was divided in two, 200-hour, irradiation periods, with 10 days re-setup period. All activities leading to the performance of this test as outlined in General Dynamics Planning Document (Reference 2) were strictly followed. Mapping runs with the actual equipment were conducted for all three access areas or, where this was not advisable, close simulations were made. A brief description of the test procedures follows:

1. Pre-Irradiation Checkout

a. Loading of Specimens

All pertinent dimensions on the tensile specimens within the gage length were measured and recorded. One Microdot weldable strain gage was used on one preselected specimen for each pull rod. Two pulling assemblies were used during the first 200-hour run, and one was used during the second. The loading schedules for the three assemblies are shown in Tables 38, 39 and 40.

The specimens are listed by type of material and condition, specimen type and number, and distance ("B") between pulling locations. Specimens are designed for individual testing by varying the slot on one side of the gage length. The following designations are used for the type of specimen:

L - Longitudinal direction - parallel to the rolling direction of the material.

T - Transversal direction - perpendicular to the rolling direction of the material.

U - Unnotched, specimen.

TABLE 38

SPECIMEN LOCATIONS IN EAST PULLING ASSEMBLY,
FIRST IRRADIATION

Pull Rod 1 (South Position)				Pull Rod 2			
Material	Condition	No.	B (in.)	Material	Condition	No.	B (in.)
347	LU	701	13.00	440C	LU	201	13.00
7075-T6	LN	117	12.625	440C	LU	197	12.625
7075-T6	LU	105	12.125	6061-T6	LWU[a]	724	12.00
7075-T6	LN	113	11.75	347	LN	707	11.50
7075-T6	LU	101	11.25				
6061-T6	LN	2-93	10.75	347	LN	705	11.00
6061-T6	LU	R-83	9.875	A-286	LN	225	10.50
6061-T6	LN[b]	2-89	9.375	A-286	LU	213	9.375
6061-T6	LU[b]	2-77	8.50	A-286	LN[b]	221	8.875
A-110-AT	TN	333	8.00	A-286	LU[b]	210	7.75
A-110-AT	TU	285	7.25	A-110-AT	TWN	345	7.375
A-110-AT	TN	329	6.75	A-110-AT	TWU	297	6.875
A-110-AT	TU	281	5.99	A-110-AT	TWN	341	6.50
				A-110-AT	TWU	293	5.99

Pull Rod 3				Pull Rod 4			
Material	Condition	No.	B (in.)	Material	Condition	No.	B (in.)
440C	LU	202	13.00	347	LU	702	13.00
440C	LU	198	12.625	7075-T6	LN	118	12.625
6061-T6	LWU[a]	725	12.00	7075-T6	LU	106	12.125
347	LN	708	11.50	7075-T6	LN	114	11.75
347	LN	706	11.00	7075-T6	LU	102	11.25
A-286	LN	226	10.50	6061-T6	LN	2-94	10.75
A-286	LU	214	9.375	6061-T6	LU	R-82	9.875
A-286	LN[b]	222	8.875	6061-T6	LN[b]	2-90	9.375
A-286	LU[b]	211	7.75	6061-T6	LU[b]	2-78	8.50
A-110-AT	TWN	346	7.375	A-110-AT	TN	334	8.00
A-110-AT	TWU	298	6.875	A-110-AT	TU	286	7.25
A-110-AT	TWN	342	6.50	A-110-AT	TN	330	6.75
A-110-AT	TWU	294	5.99	A-110-AT	TU	282	5.99

[a]Specimens tested in the "as-welded" condition (without heat treatment).

[b]Strain gage welded to specimen to measure strain in reduced cross section.

TABLE 39

SPECIMEN LOCATIONS IN WEST PULLING ASSEMBLY,
FIRST IRRADIATION

Pull Rod 4 (South Position)				Pull Rod 2			
Material	Condition	No.	B (in.)	Material	Condition	No.	B (in.)
347	LU	703	13.25	6061-T6	TWU	3-31	13.00
347	LU[a]	704	12.125	6061-T6	TWU[a]	3,35	12.50
A356-T6	LN	22	11.75	6061-T6	TWN	3-42	12.125
A356-T6	LU	10	11.25	6061-T6	TWN	3-44	11.75
A356-T6	LN	18	10.875	6061-T6	TWN	3-46	11.375
A356-T6	LU	6	10.375	6061-T6	TWN	3-48	11.00
347C	LU	177	9.937	347	LWN	216	10.75
347C	LN	185	9.562	347	LWU	204	9.75
347C	LU	173	9.125	347	LWN	214	9.50
Hastelloy C	LN	369	8.625	347	LWU	202	8.50
Hastelloy C	LU	357	7.50	347	LWN	212	8.25
Hastelloy C	LN	365	7.00	347	LWU	200	7.25
Hastelloy C	LU	353	5.99	347	LWN	210	6.875
				347	LWU[a]	198	5.99

Pull Rod 3				Pull Rod 1	
Material	Condition	No.	B (in.)	Material[b]	No.
6061-T6	TWU	3-32	13.00		
6061-T6	TWU	3-36	12.50	6061-T6	1
A356-T6	LN	21	11.75	6061-T6	2
A356-T6	LU	9	11.25	6061-T6	3
A356-T6	LN	17	10.875	6061-T6	4
A356-T6	LU[a]	5	10.375	A-286	5
347C	LU	178	9.937	Hastelloy C	6
347C	LN	186	9.562	Hastelloy C	7
347C	LU	174	9.125	Hastelloy C	8
Hastelloy C	LN	370	8.65	Hastelloy C	9
Hastelloy C	LU	358	7.50	A-286	10
Hastelloy C	LN	366	7.00	A356-T6	11
Hastelloy C	LU	354	5.99	A356-T6	12
				A356-T6	13
				A356-T6	14
				A-286	15
				7075-T6	16
				7075-T6	17
				7075-T6	18
				7075-T6	19
				A-286	20

[a]Strain gage welded to specimen to measure strain in reduced cross section.

[b]Shear specimens

TABLE 40

SPECIMEN LOCATIONS IN EAST PULLING ASSEMBLY, SECOND IRRADIATION

Pull Rod 1 (South Position)				Pull Rod 2			
Material	Condition	No.	B (in.)	Material	Condition	No.	B (in.)
Inconel X-750	LU	381	13.00	Inconel X-750	LU	382	13.00
Inconel X-750	LN[b]	389	12.50	Inconel X-750	LN	390	12.50
Inconel X-750	LU[b]	377	11.375	Inconel X-750	LU	378	11.375
6061-T6	LWN[a]	3-114	11.00	6061-T6	TWN	288	11.00
6061-T6	LWN[a]	727	10.75	6061-T6	LU	761	10.25
6061-T6	TWU[a]	720	10.25	6061-T6	LWU[a]	760	9.875
6061-T6	TWN[a]	723	9.875				
6061-T6	TWU[a]	719	9.375	6061-T6	LWN	3-92	9.00
6061-T6	TWN[a]	722	9.00	6061-T6	LWU	3-80	8.50
6061-T6	TWU[a]	718	8.50	6061-T6	LWN[b]	3-90	8.125
6061-T6	TWN[a][b]	721	8.125	6061-T6	LWU[b]	3-78	7.625
6061-T6	TWU	717	7.625	Inconel 713C	LN	418	7.25
Inconel 713C	LN	417	7.25	Inconel 713C	LU	406	6.812
Inconel 713C	LU	405	6.812	Inconel 713C	LN	414	6.437
Inconel 713C	LN	413	6.437	Inconel 713C	LU	402	5.99
Inconel 713C	LU	401	5.99				

Pull Rod 3				Pull Rod 4	
Material	Condition	No.	F (in.)	Material[c]	No.
				A-110-AT	1
Inconel X-750	LN	392	13.00	A-110-AT	2
Inconel X-750	LN	391	12.50	A-110-AT	3
6061-T6	LWU[a]	726	12.00	A-110-AT	4
347C	LN	190	11.50	D-979	5
347C	LN	189	11.00	Inconel X	6
6061-T6	LWN	3-96	10.625	Inconel X	7
6061-T6	LWU	R-84	9.75	Inconel X	8
6061-T6	LWN[b]	3-94	9.375	Inconel X	9
6061-T6	LWU[b]	3-82	8.50	D-979	10
440C	LN	610	8.00	347	11
440C	LN	608	7.50	347	12
440C	LN	606	7.00	347	13
440C	LN	604	6.50	347	14
6061-T6	LWN[a]	728	5.99	D-979	15
				410	16
				410	17
				410	18
				410	19
				D-979	20

[a]Specimens tested in the "as-welded" condition (without heat treatment).

[b]Strain gage welded to specimen to measure strain in reduced cross section.

[c]Shear specimens

N - Notched specimen.

W - Welded specimen, heat treated after welding.

Specimens not heat treated after welding are identified as being in "as-welded" condition.

The pulling assembly located at the east side of the reactor closet for the first 200-hour run contained only tensile specimens on all four pull rods. The west pulling assembly of the first run, and the east assembly of the second run, contained 20 shear specimens each on one pulling rod. Figure 52 shows schematic arrangement of the tensile specimens, and Figure 53 shows the shear specimen arrangement. Detailed description of the shear testing is presented in Reference 3.

b. Dosimetry

Neutron detector packets were installed at each pulling assembly (to the front and back of the specimens inside the liquid hydrogen "can", on the front and back outside of this "can", and inside the gas chamber of the dewar). Each packet contained phosphorus for thermal detection and nickel for threshold detection. These detectors are the only type anticipated to have the measuring capability for the 200-hour radiation runs. To obtain the desired radiation information, mapping runs were necessary for all three access areas. Foils and cobalt glass were used for these runs. To account for the reactor poisoned condition, two mapping runs were conducted. The unpoisoned core mapping run was to verify predicted exposure; the retracted core (poisoned) mapping run was made to establish neutron fluxes and spectral dependence as well as gamma dose rates. The neutron and gamma detector packets for the mapping runs consisted of indium, sulfur, and aluminum foils for obtaining the fast flux of nominal energies greater than 0.85 Mev, 2.9 Mev and 8.1 Mev. respectively. Bare and cadmium-covered copper foils were used for thermal flux. Cobalt glass enriched with boron and encapsulated was used for gamma monitoring. In addition, nine special neutron

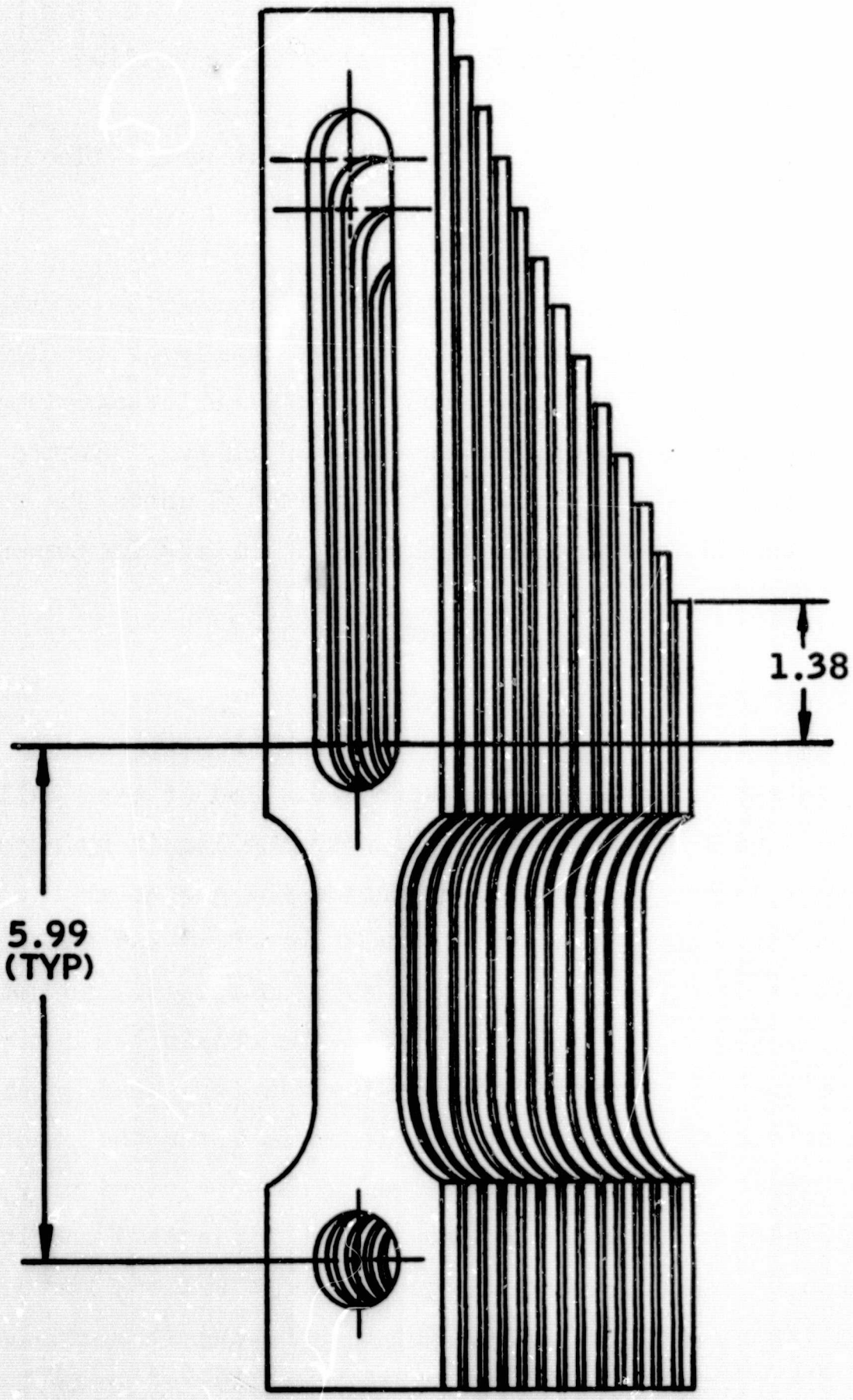

Figure 52
Specimen Bundle

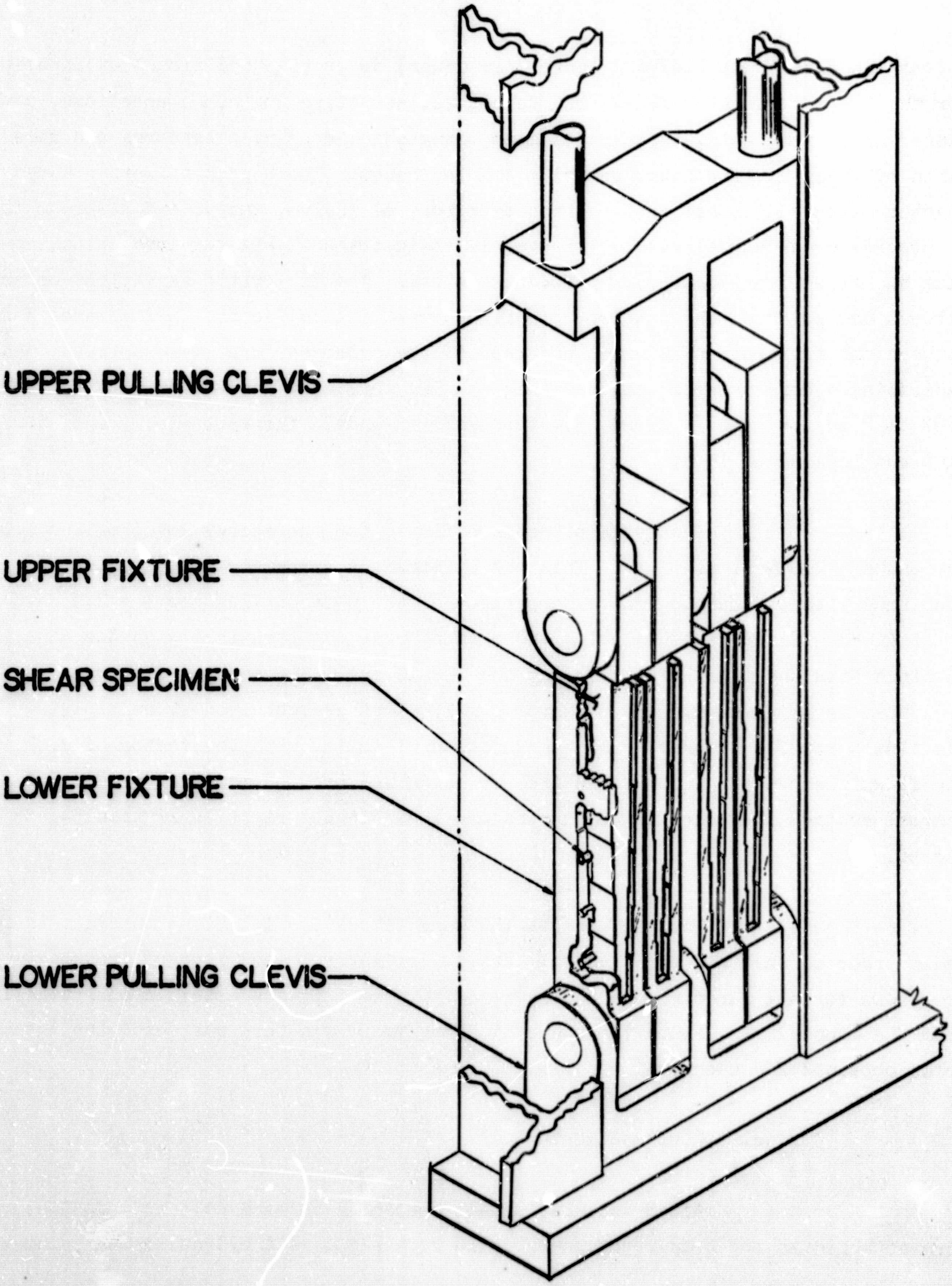

Figure 53

Fixture for Double Shear Measurements

spectral packets were included (three per dewar) to provide additional extrapolations for the 0.1 Mev. neutron flux. The detectors, sensitive to (n, γ) reactions, consisted of indium, gold, tungsten cadmium, manganese, copper, phosphorus and rare earth of lutetium, europium, samarium and lauthenum. These packets were mounted together with additional fast neutron detectors of indium, sulfur and aluminum foils to provide cross correlation. The overall dosimetry analysis required obtaining flux and/or activation of over 1500 data points. The flux ratio variations observed between the poisoned and unpoisoned map runs were insignificant. Differences however between the flux ratios in front and rear of the hydrogen "can" were noticed, thus indicating a condensing spectrum within the LH_2 barrier. The values in front were 2.97 to 2.10 for ϕ in./ϕ s and 25.4 for ϕ s/ϕ al and in the back ϕ in./ϕ s of 2.67 - 2.96 and ϕ s/ϕ Al of 19.4.

The ratio of neutron fluxes for the energy level of E > 1.0 Mev and E > 2.9 Mev. was 2.82. This ratio, obtained by previous GTR runs, was confirmed with the mapping run. Comparison of the neutron flux for E > 2.9 Mev, as obtained with the sulfur during the mapping run, was identical with the data obtained with the nickel foils during the GTR-16 run. The neutron flux maps presented in Figures 90, 91 and 92 for E > 1.0 Mev were obtained by multiplying the fluxes for E > 2.9 Mev. (as measured with Ni-foils) with the factor of 2.82. The flux is shown for location in front, inside and back of the LH_2 "can". Integrated thermal neutron flux maps for both runs are shown in the right of Figures 54, 55 and 56.

The profiles of the gamma doses for locations outside, in front, and in rear of the LH_2 "can" (as well as inside, in front and rear of the specimens) are shown for all three dewars in Figure 57. These maps are obtained analytically from the mapping run, since the range of all gamma dosimeters was below the total doses obtained for each run.

c. Equipment Setup

After assembly of all specimens on each pull rod, dosimeters were attached in front and back as shown in Figure 58. All hydraulic and pneumatic

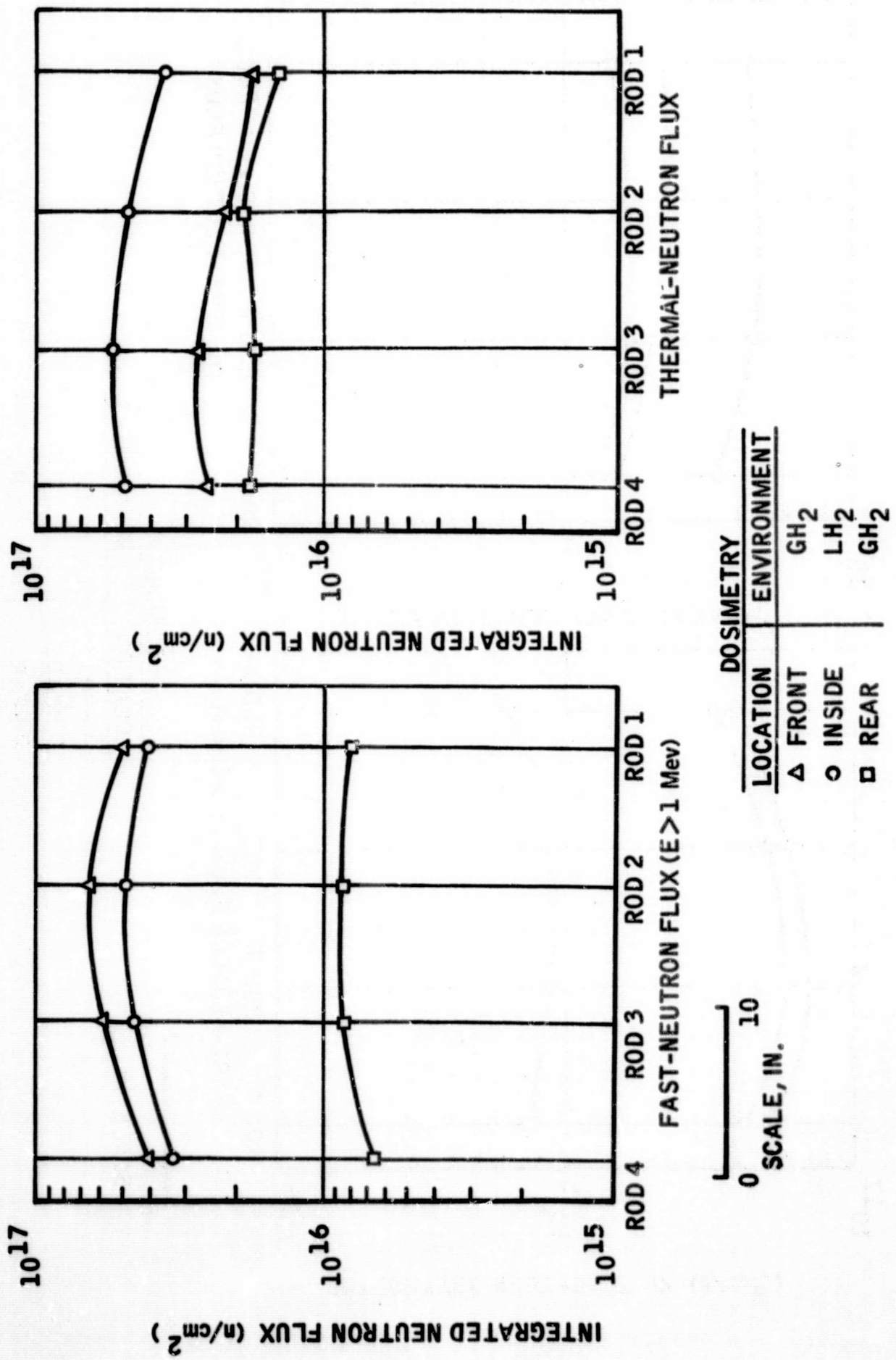

Figure 54

Measured Integrated Neutron Flux: First Irradiation, East Assembly

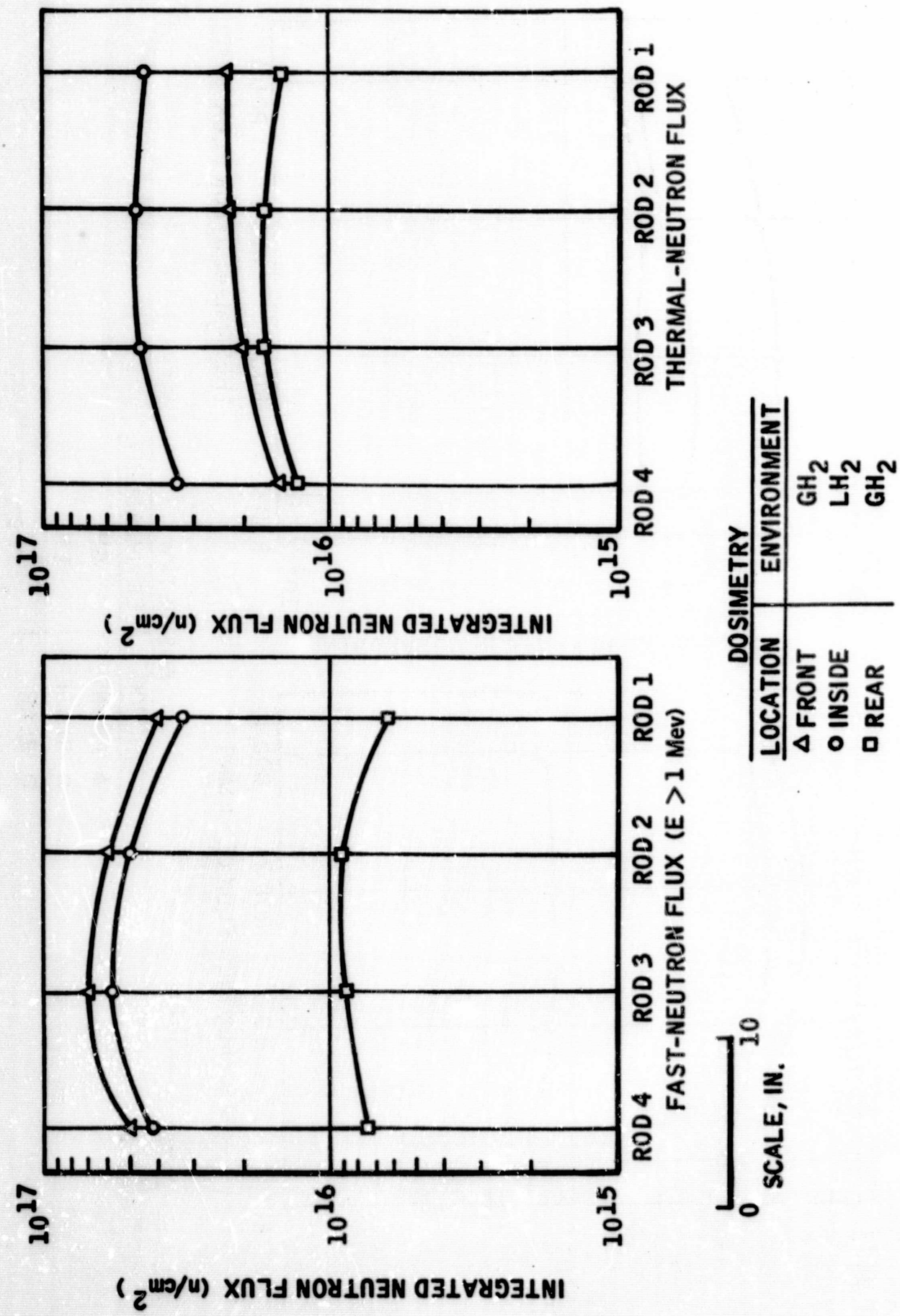

Figure 55

Measured Integrated Neutron Flux: First Irradiation, West Assembly

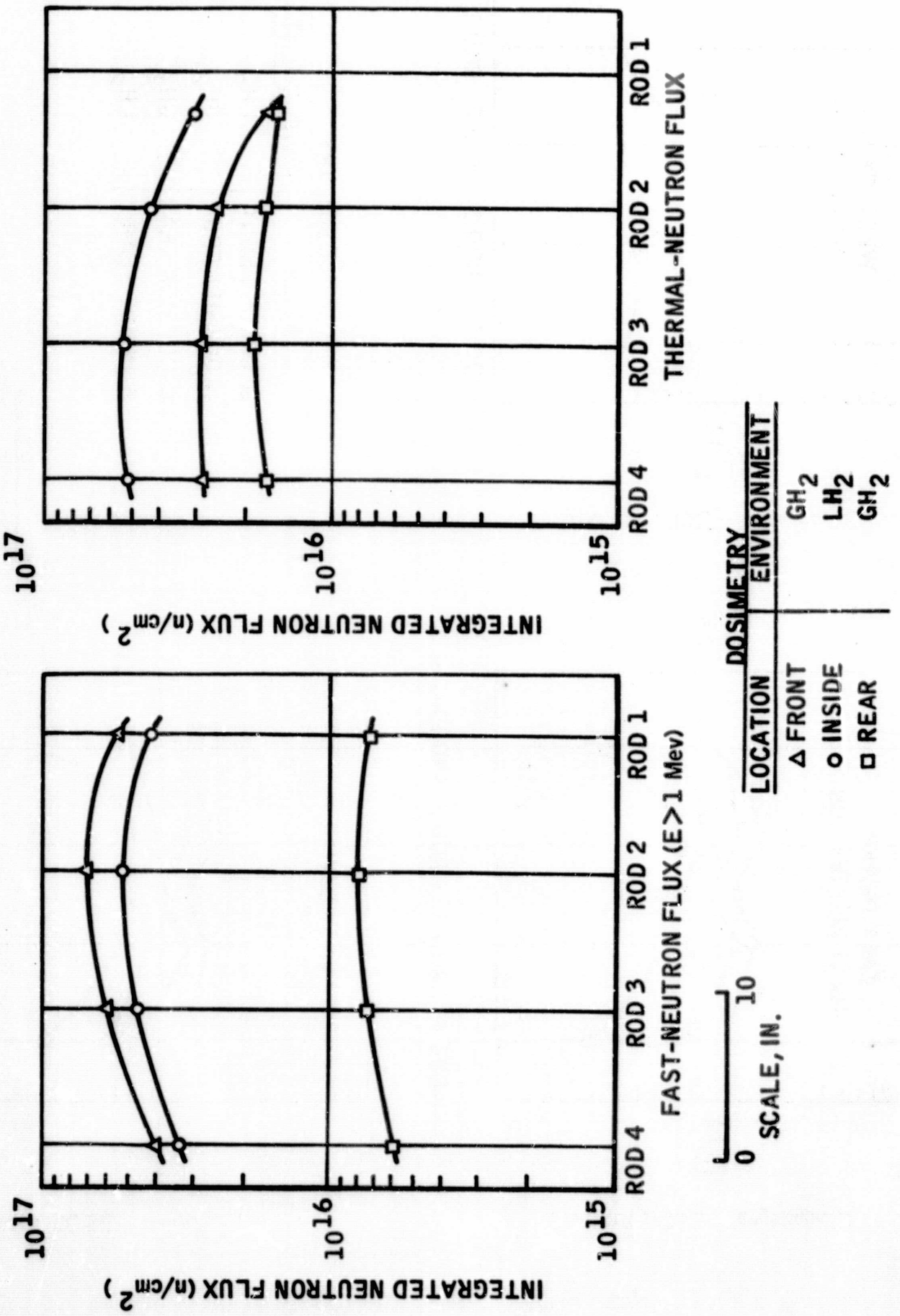

Figure 56

Measured Integrated Neutron Flux: Second Irradiation, East Assembly

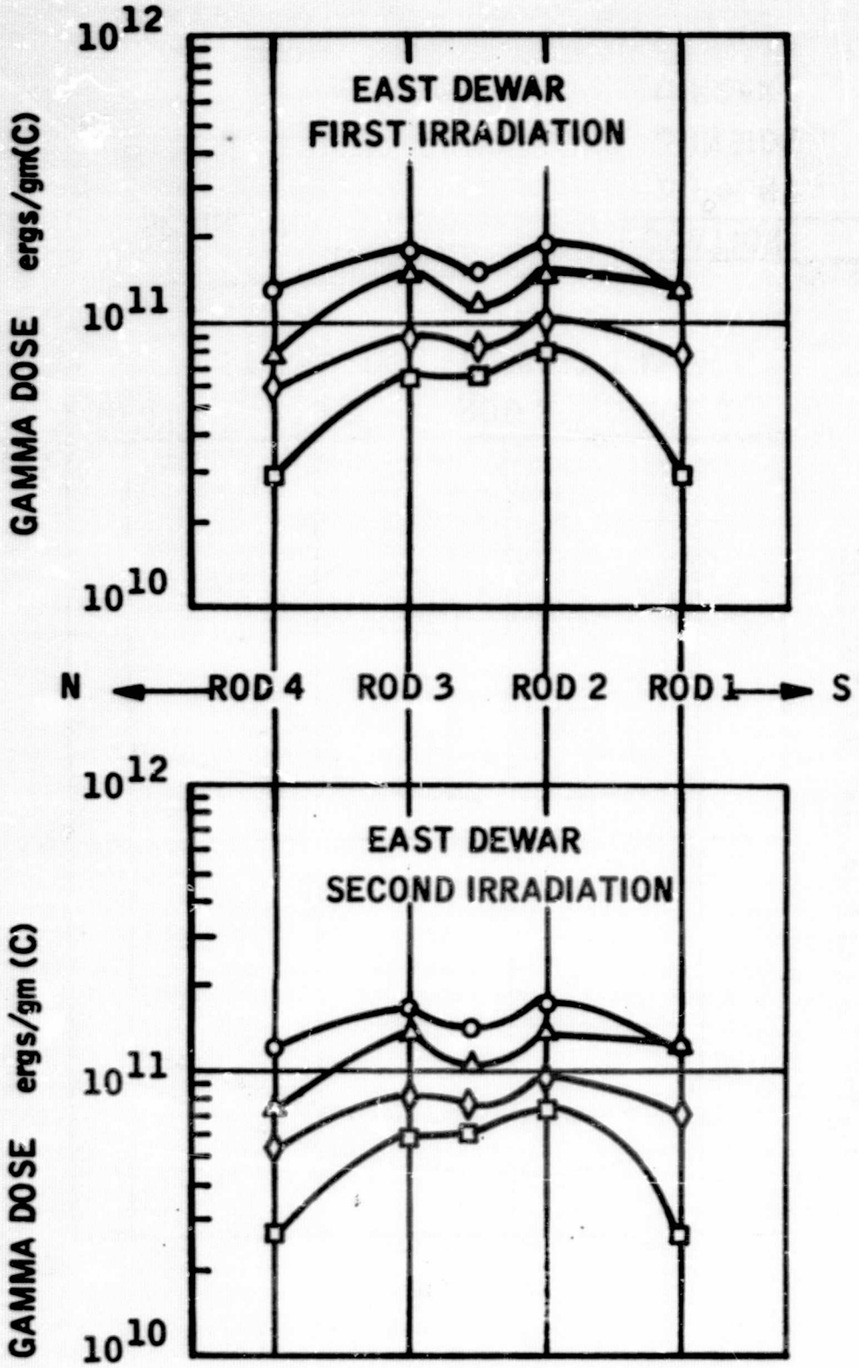

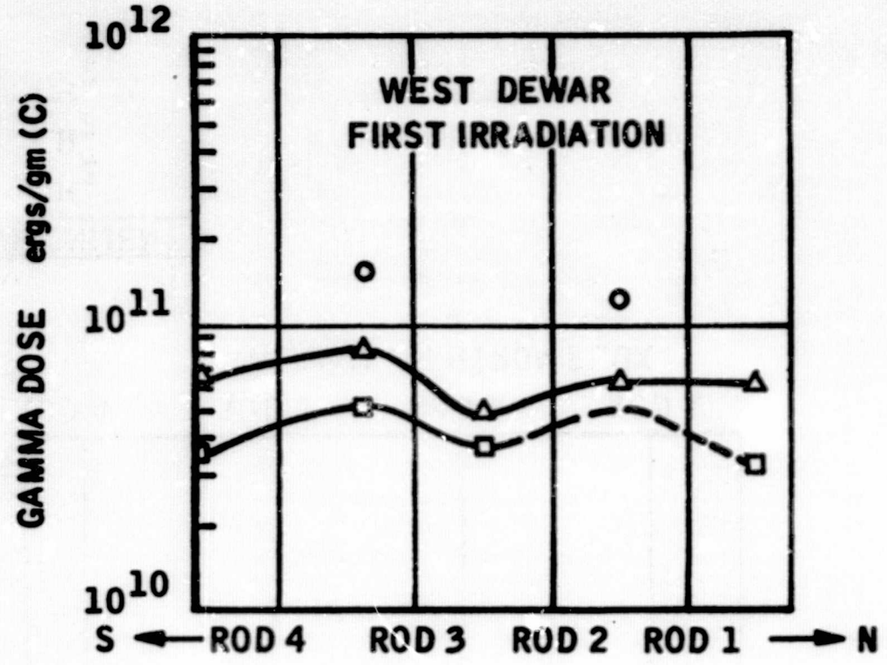

DOSIMETRY

LOCATION	ENVIRONMENT
△ INSIDE FRONT	LH_2
○ OUTSIDE FRONT	GH_2
□ OUTSIDE REAR	GH_2
◇ INSIDE REAR	LH_2

0 10
SCALE, IN.

Figure 57
Gamma Dose Mapping Profile for AGC Cryogenic Materials
Test Assembly
180

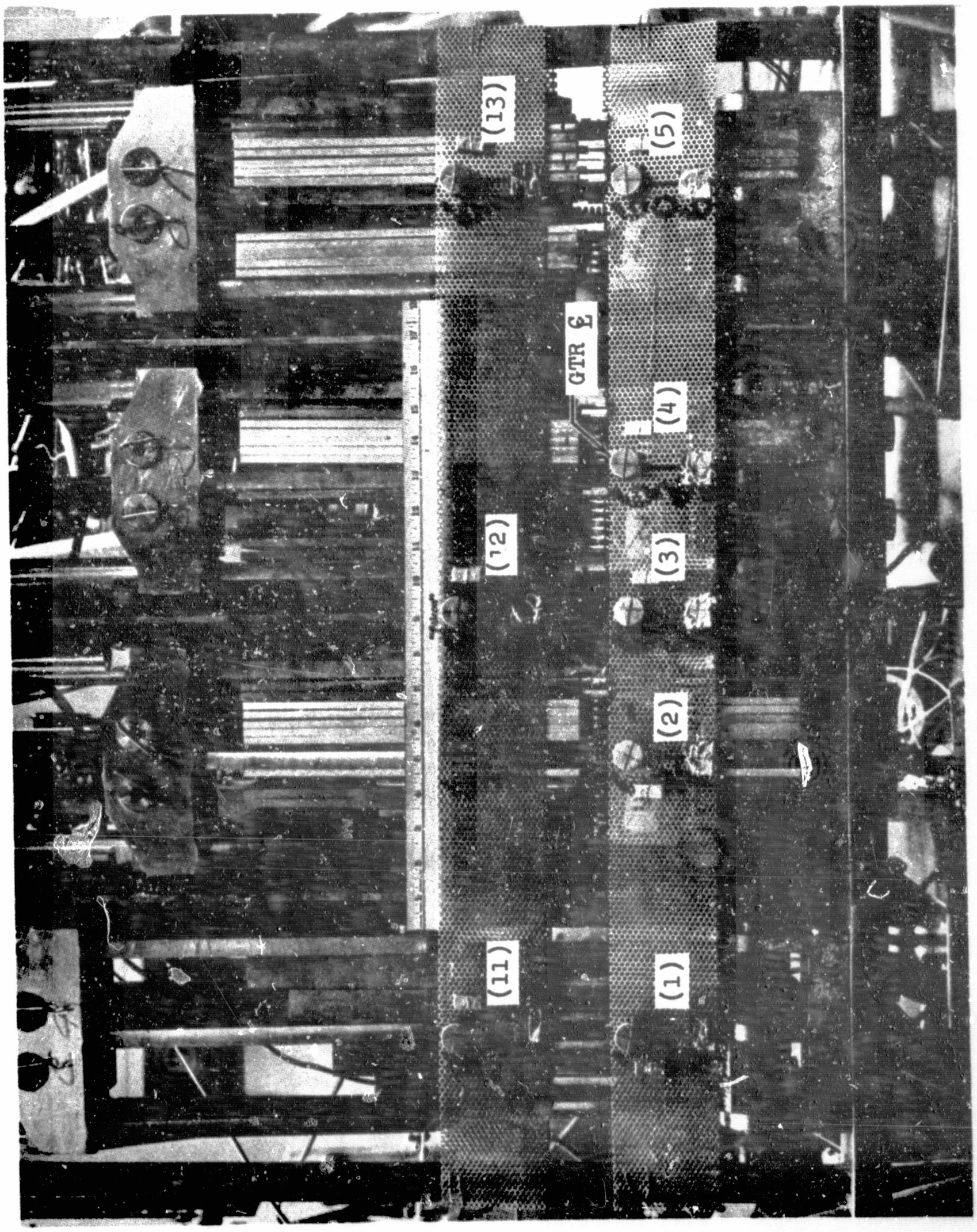

Figure 58

Equipment Setup with Dosimeters Attached
(Front View)

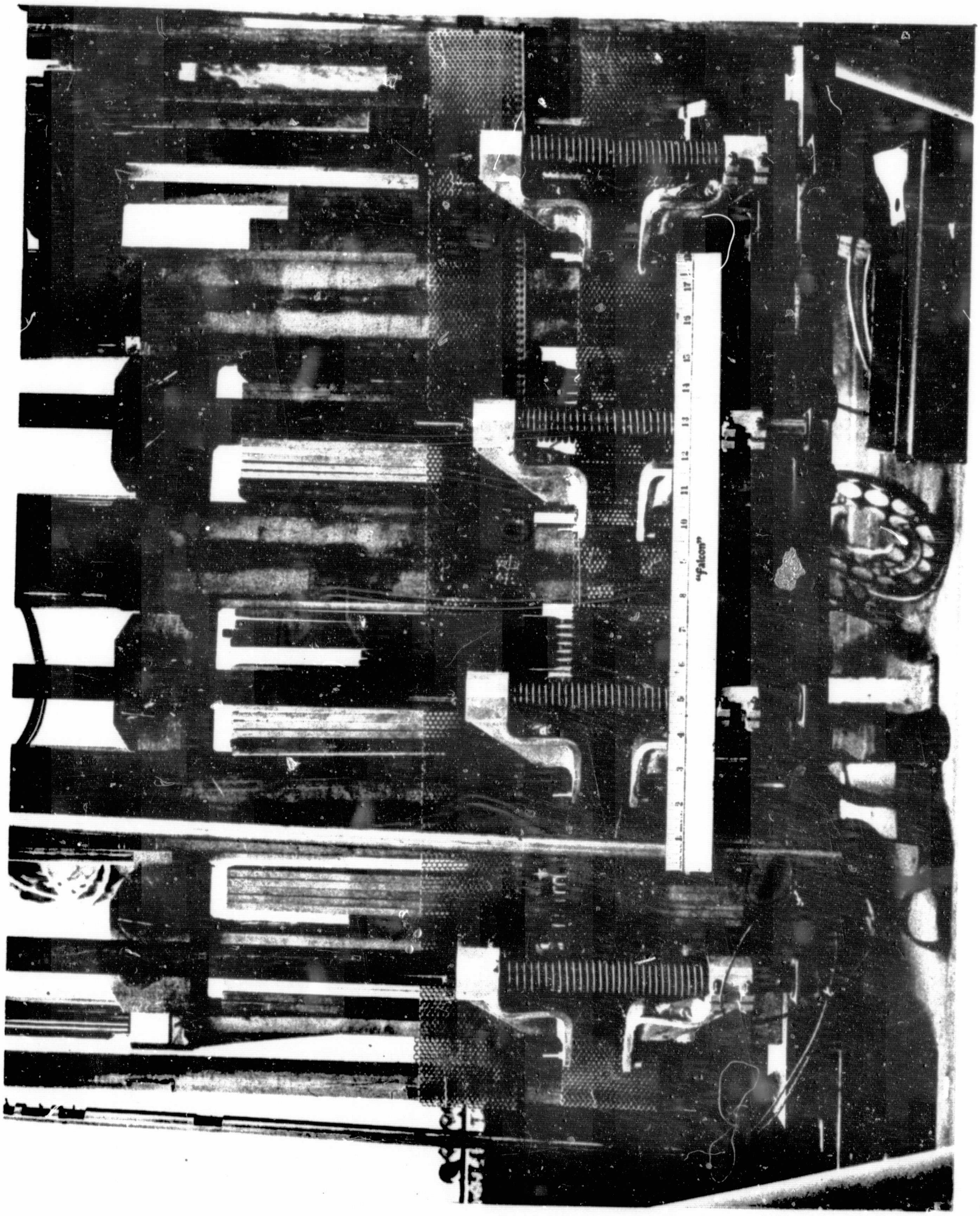

Figure 58

Equipment Setup with Dosimeters Attached
(Back View)

lines were connected, bleed and leak-checked. All instrumentation, including pressure transducers, liquid-level indicators and controls, was hooked up and checked for continuity and operational performance. Lines were connected, helium purged and checked. The liquid-hydrogen container were connected to the pulling assemblies and the pulling assemblies were then mated to the LH_2 dewars. The A-286 bolts were torqued to 500 - 600 in./lbs. The vacuum chamber of the dewar, the pop-off safety valve and the rupture discs were checked; the emergency vent lines were connected and checked.

The liquid-hydrogen supply lines were connected to the dewar and the manifold. All pneumatic valve and liquid-hydrogen control instruments were connected and checked.

d. Leak Check, Purging and Installation of the Assemblies

Each pulling assembly was cycled three times to LH_2 temperature and then leak checked. All connections, joints and seals were proof checked. The hydraulic system of the pulling assemblies was charged and bled prior to irradiation. After completion of all these operations the shroud was closed, pressure tested, and the assemblies installed in the proximity of the reactor for radiation.

The helium purge lines were then connected to the hydrogen transfer lines. This system is designed to allow purging of individual assemblies or all three assemblies in series. During the entire test each assembly was purged several times: prior and after leak check, prior to the radiation run, and upon completion of the test. The exhaust system was equipped with vacuum purging capability.

2. Irradiation Period

Immediately after the purging operations were completed, liquid-hydrogen flow was initiated. Close control was maintained over all operations.

After stabilizing the cryogen level in each assembly, one hour was allowed for reaching thermal equilibrium before the reactor was brought to power (3Mw) and traversed to the 2-in. position to the north wall.

After 192 hours of operation of the first 200-hour run, one of the sensors indicated hydrogen concentration in the pool. The reactor was scrammed to avoid possible fire and damage of the instrumentation. Post examination of this particular sniffer indicated electrical shift. After 178 hours of the second 200-hour run, a leakage on one of the pulling assemblies was noticed. Three sensors had indicated hydrogen gas concentration in the pool. It was decided to scram the reactor and start pulling the specimens. Dewar and shroud pressures were monitored constantly. The temperature of dewar and shroud were also periodically monitored.

3. Testing

Briefly, the operational sequences associated with the testing of the specimens were as follows:

a. After reactor shutdown one hour was allowed to stabilize the LH_2 flow, before starting the pulling. The Instron cross head travel was set at 0.05-in./min. After fracture of one specimen, the Instron was stopped to permit indexing the extensometer to the next unnotched specimen. The preceding procedure was repeated until all specimens were fractured.

b. After completion of the pulling procedures on the first 192-hour run, the test assembly with the suspected leak was checked on the ramp above the pool to determine whether or not an actual leak existed, and to take adequate steps to prevent such occurrences in the second 200-hour test. Similar procedure was followed for the east assembly after the second 178-hour test. The systems were pressurized to 7 psig with helium. The west assembly showed a leak indication around a damaged exhaust line but it could not be determined whether this damage occurred during or prior to the assembly removal. The east assembly showed no detectable leakage. Both assemblies were filled with LH_2 on the ramp for a period of two hours without a leak being detected.

c. During the pulling procedure also, most of the instrumentation functioned properly. The following shortcomings were recorded:

(1) A load cell on pull rod three of the first 200-hour run became unbonded after several specimens were tested.

(2) Extensometer data was lost on six specimens. Positioning of extensometer was prevented by broken specimens.

(3) Improvement of the extensometer indexing mechanism for the second 178-hour run was made by making provisions for bleeding the hydraulic fluid in the lines after radiation and replacing this fluid containing the gas evolved during the radiation exposure.

4. System Removal

Upon completion of the pulling, LH_2 flow was terminated for the particular dewar, the assembly was purged and left in the test cell for one week to allow decay of the radioactivity. The assemblies were then removed and stored in isolated areas.

5. Safety Provisions

With the objective to minimize and eliminate any possible hazard, several safety provisions have been made, as follows:

a. Provision was made for leak-tight shrouds over the upper portion of each pulling assembly. They were continuously purged with helium and separately vented out of the pool.

b. A pop-off safety valve set at 7.5 psi for overpressure was put in each dewar. It is vented in the shroud and visual and audible alarms are connected to it in the control room.

c. A 22-psi rupture disc was incorporated in the dewar closure. The rupture disk is ported to the shroud exhaust system for venting-out of the pool.

d. A separate shroud was provided above the rupture disk and vacuum valve.

e. The LH_2 supply line was terminated inside the shroud to allow any leakage to be collected and independently exhausted.

f. The electrical wiring was routed through 24 stainless steel tubes into the shroud. Hermetic connectors were used for routing the instrumentation out of the shroud.

g. Dewar and shroud pressures were monitored continuously.

REFERENCES

1. Data Obtained From The First Irradiation Test on Structural Materials, REON Report 2473, dated 15 April 1963

2. Control Specimens Data for Structural Materials Irradiation Test Program, REON Report RN-S-0128 dated 12 November 1964

3. Preliminary Report GTR-16 Materials Radiation Test at -423°F, REON Report RN-S-0237 dated August 1965

4. Final Test Specifications for GTR-15 and 16, REON Report RN-S-0184 dated December 1964

5. "Shear Strength of Several Alloys at Liquid Hydrogen Temperature," Advances in Cryogenic Engineering Vol. 10 1965 paper A-6

6. Planning Document GTR-16, REM-1355 (Revisio A), General Dynamics, Fort Worth, 6 November 1964

7. NERVA Materials Irradiation Program Vol 1 GTR-16 AGC Materials Test FZK-263-1, General Dynamics, Fort Worth, 20 October 1965

PART 2

Radiation Tests of
ARMALON BEARING RETAINERS

BLANK PAGE

I. INTRODUCTION

This part of the report covers the GTR 16 tests on Armalon bearing retainers. Armalon is a candidate material for NERVA turbopump bearing retainers and its acceptance or rejection will depend on its ability to withstand radiation.

Twenty-one bearing retainers were exposed to 10^{11} ergs/gm (C) while immersed in LH_2, and were subsequently tested at room temperature to determine the change in mechanical properties and volume fractions of teflon resin to glass filler.

BLANK PAGE

II. CONCLUSIONS

Armalon 510-128 and 405C-116 are not suitable materials in a cryogenic and nuclear environment of 10^{11} ergs/gm (C). Both types exhibited visual evidence of radiation damage in the form of free standing glass strands and areas of delamination. Both types had 75 to 95% loss of tensile and flexure properties. Armalon with F.E.P. Teflon is more sensitive to irradiation than the T.F.E. type as judged by the greater percentage loss in strength and volumetric composition.

III. TECHNICAL DISCUSSION

Samples of three NERVA I bearing retainers were tested to determine the effects of radiation on the retainer material.

The retainers were made of 405C-116 Armalon and 510-128 Armalon. The difference between these two materials are as follows: Armalon 405C-116 is a composite of 116-style glass cloth pre-impregnated with TFE Teflon resin. The cloth weave contains $\cong$ 60 warp and 58 fill yarns-per-in. Equal yarn distribution in both fill and warp direction results in approximately equal Teflon exposure to every pocket face with a glass to Teflon ratio of 2:1. Armalon 510-128 is a composite of 128-style glass cloth pre-impregnated with FEP Teflon resin. The glass cloth is a heavy grade using an open weave of $\cong$ 42 warp and 32 fill yarns per in. The resin is a higher-strength variation of the original Teflon (TFE) and is characterized by a lower softening temperature. A 3:1 ratio of glass-to-Teflon exists in the warp surface and a 2:1 ratio exists in the fill surface. The following table identifies the material and source for each type of retainer.

TABLE 41

RETAINER TYPE AND ARMALON TYPE

AGC Part Number	Type of Retainer	Type of Armalon	Vendor
290156	Roller bearing	405C-116(TFE)	Bearings Mfg. Company
290126	Thin ball bearing	405C-116(TFE)	ITI
287808	Thick ball bearing	510-128 (FEP)	Flurocarbon Corporation

Seven specimens of each type of retainers were tested. Two specimens of each type were cut in half, with one half of each used for control purposes. The two remaining halves were irradiated with the five whole specimens of each type. The specimens were submerged in LH_2 and exposed to 10^{11} ergs/gm (C) radiation for 200 hours. The control and irradiated specimens were tested at room temperature for the following mechanical properties:

A. Hoop tension
B. Flexure
C. Fill tensile (axial)
D. Warp tensile (circumferential)

In addition, volumetric analysis was performed to determine changes in material fractions.

Table 42 shows graphically the average mechanical properties of the control and irradiated specimens. Table 43 is the volumetric fractions of selected specimens before and after irradiation.

Figures 59 through 61 show the worst and best irradiated specimens of each retainer type. Figure 59A shows surface degradation in the form of free-standing glass fibers and delaminated surface area of a roller bearing retainer made of TFE Armalon. Figure 59B is a retainer of the same type and material as Figure 59A and shows no obvious damage, however, both parts retained only about 20% of their pre-irradiated warp tensile strength and about 17% of their pre-irradiated flexure strength.

Figures 60A and 60B show two ball bearing retainers made of TFE Armalon. Although the apparent damage is much less in Figure 60B, the mechanical properties of both specimens are about equal.

Figures 61A and 61B show two ball bearing retainers made of FEP Armalon. The contrast and mechanical properties pattern is similar to the TFE Armalon retainers, however, there is a higher percentage loss in strength.

TABLE 42

AVERAGE MECHANICAL PROPERTIES OF CONTROL AND IRRADIATED RETAINER SPECIMENS

Roller Retainer - 290156 Armalon 405C-116 (TFE) Fabricator - BMC

		psi x 10^3 0 1 2 3 4 5 6 7 8 9 10 11 12 13 14
Hoop Tension	Control	No Test
	Irradiated	
Flexure	Control	
	Irradiated	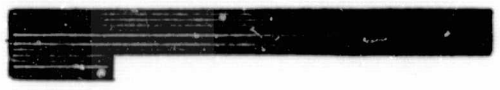
Fill Tensile	Control	No Test
	Irradiated	
Warp Tensile	Control	
	Irradiated	

Thin Ball Retainer - 290126 Armalon 405C-116 (TFE) Fabricator - ITI

		psi x 10^3 0 1 2 3 4 5 6 7 8 9 10 11 12 13 14
Hoop Tension	Control	No Test
	Irradiated	
Flexure	Control	
	Irradiated	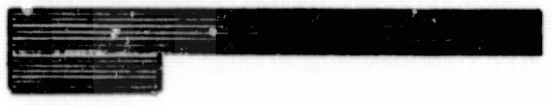
Fill Tensile	Control	No Test
	Irradiated	
Warp Tensile	Control	
	Irradiated	

Thick Ball Retainer - 287808 Armalon [illegible]-128 (FEP) Fabricator - Fluorocarbon

		psi x 10^3 0 1 2 3 4 5 6 7 8 9 10 11 12 13 14
Hoop Tension	Control	
	Irradiated	
Flexure	Control	
	Irradiated	
Fill Tensile	Control	
	Irradiated	
Warp Tensile	Control	
	Irradiated	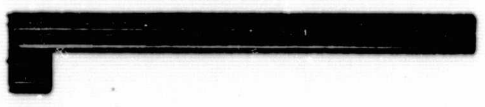

TABLE 43

TYPICAL VOLUMETRIC ANALYSIS RESULTS

	12118A		12118B	
	Control	Irrad.	Control	Irrad.
Composite density	2.18	2.21	2.19	2.21
Vol. %, Glass	32.2	33.1	35	34.8
Vol %, Teflon	61.3	60.8	57.3	60.5
Vol. %, Voids	6.5	6.1	7.7	4.7
	100.0	100.0	100.0	100.0

	0007		0013	
Composite density	2.2	2.2	2.19	2.19
Vol. %, Glass	32.9	31.1	32.8	31.8
Vol. %, Teflon	61.2	60	59.7	60.9
Vol. %, Voids	5.9	8.9	7.5	7.3
	100.0	100.0	100.0	100.0

	145		149	
Composite density	2.2	2.19	2.12	2.19
Vol. %, Glass	23.1	31.8	19.5	33.6
Vol. %, Teflon	73.4	68.2	73.3	66.4
Vol. %, Voids	3.5	0	7.2	0
	100.0	100.0	100.0	100.0

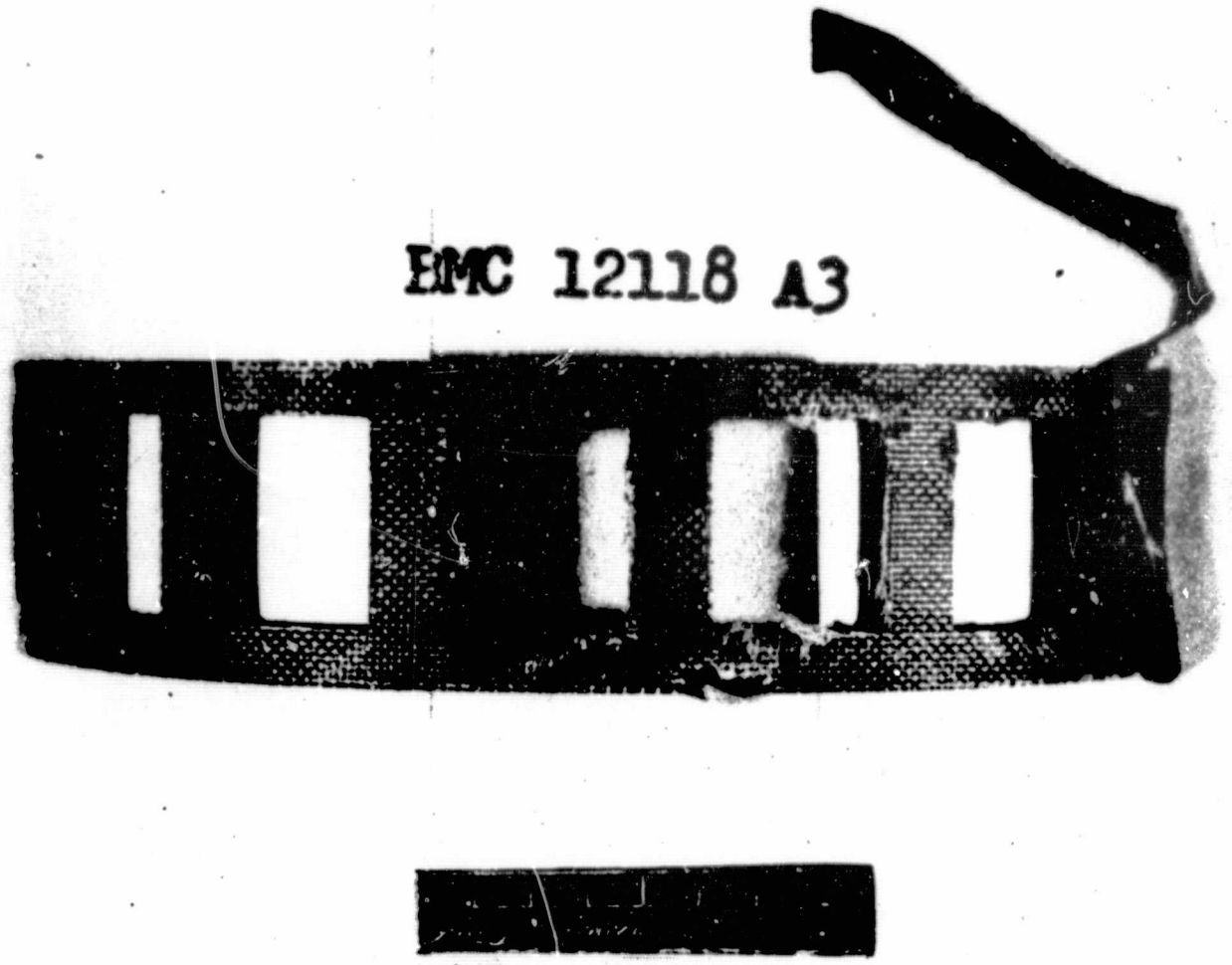

A

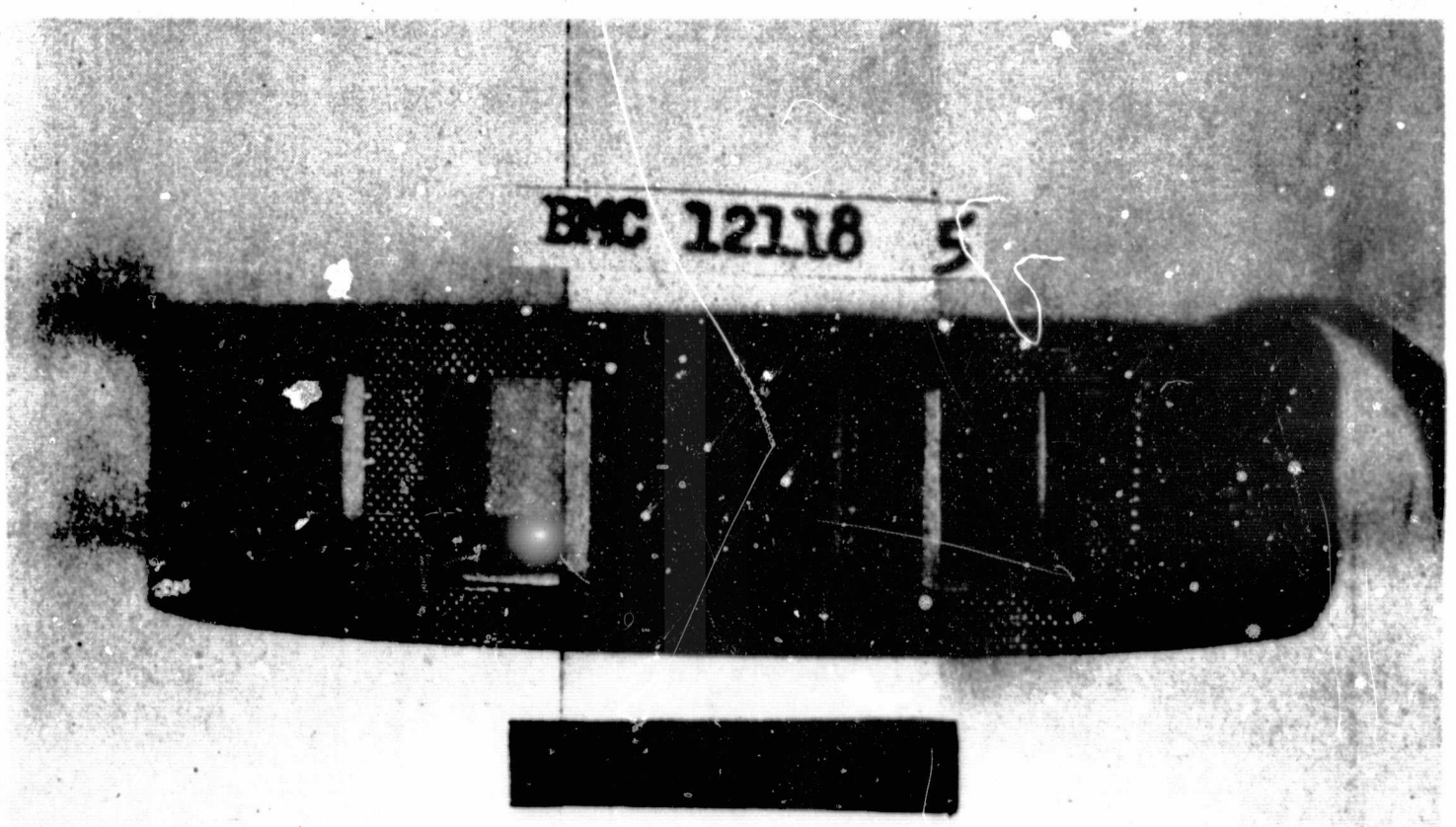

B

Figure 59

Roller Bearing Retainer - TFE Armalon

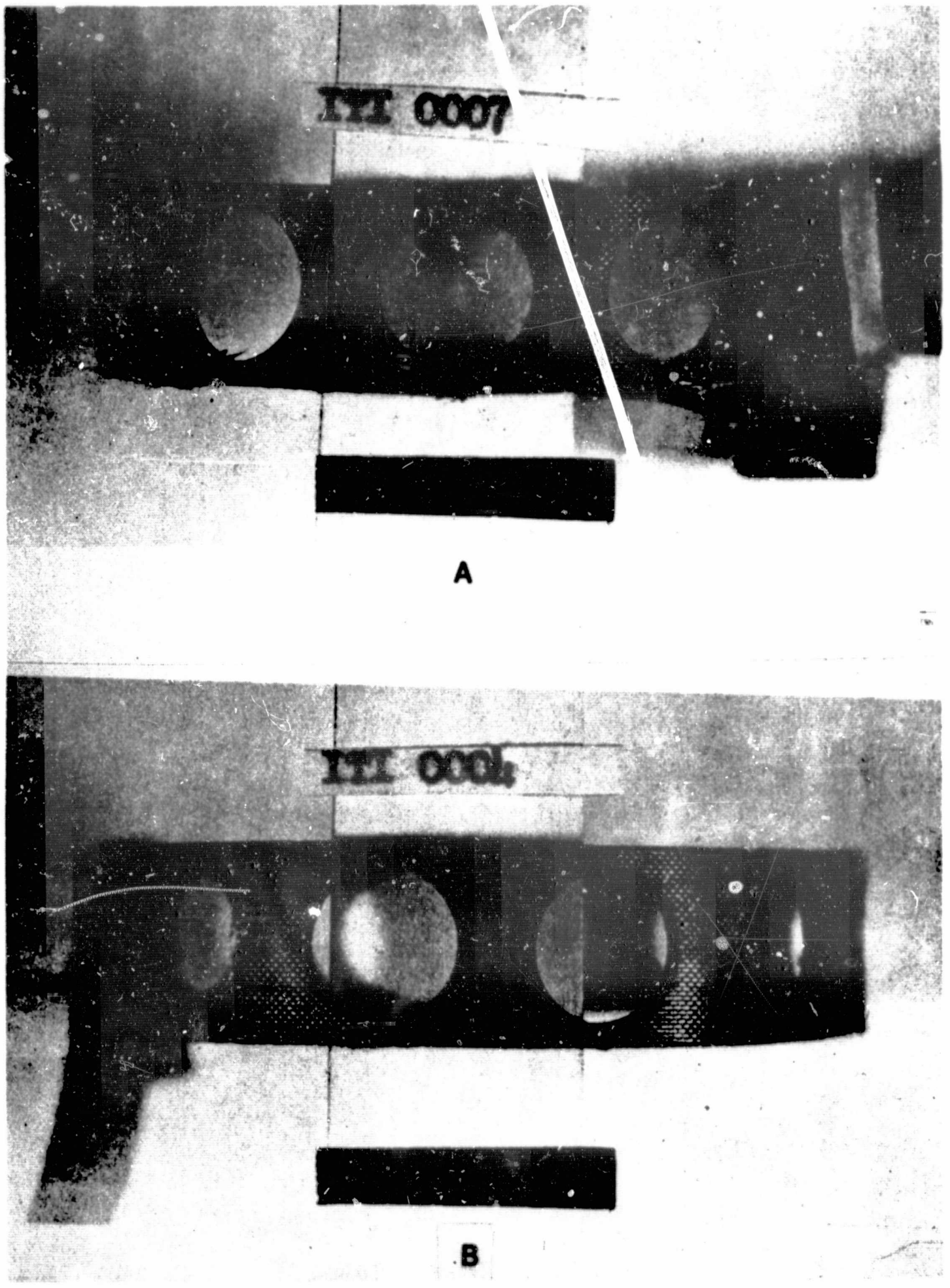

Figure 60

Ball Bearing Retainer - TFE Armalon

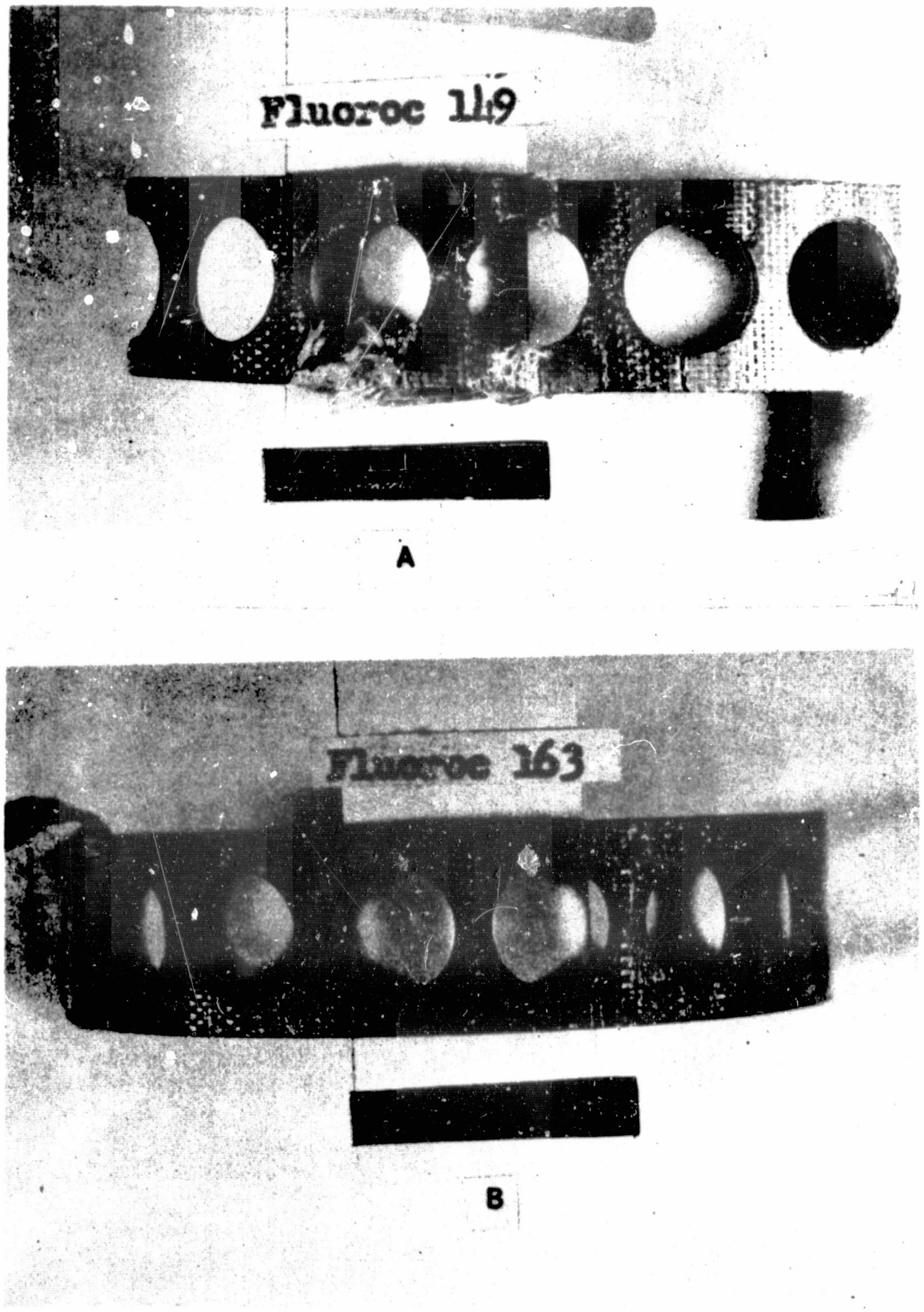

Figure 61

Ball Bearing Retainer - FEP Armalon